USGS
science for a changing world

Conditions and Processes Affecting Sand Resources at Archeological Sites in the Colorado River Corridor Below Glen Canyon Dam, Arizona

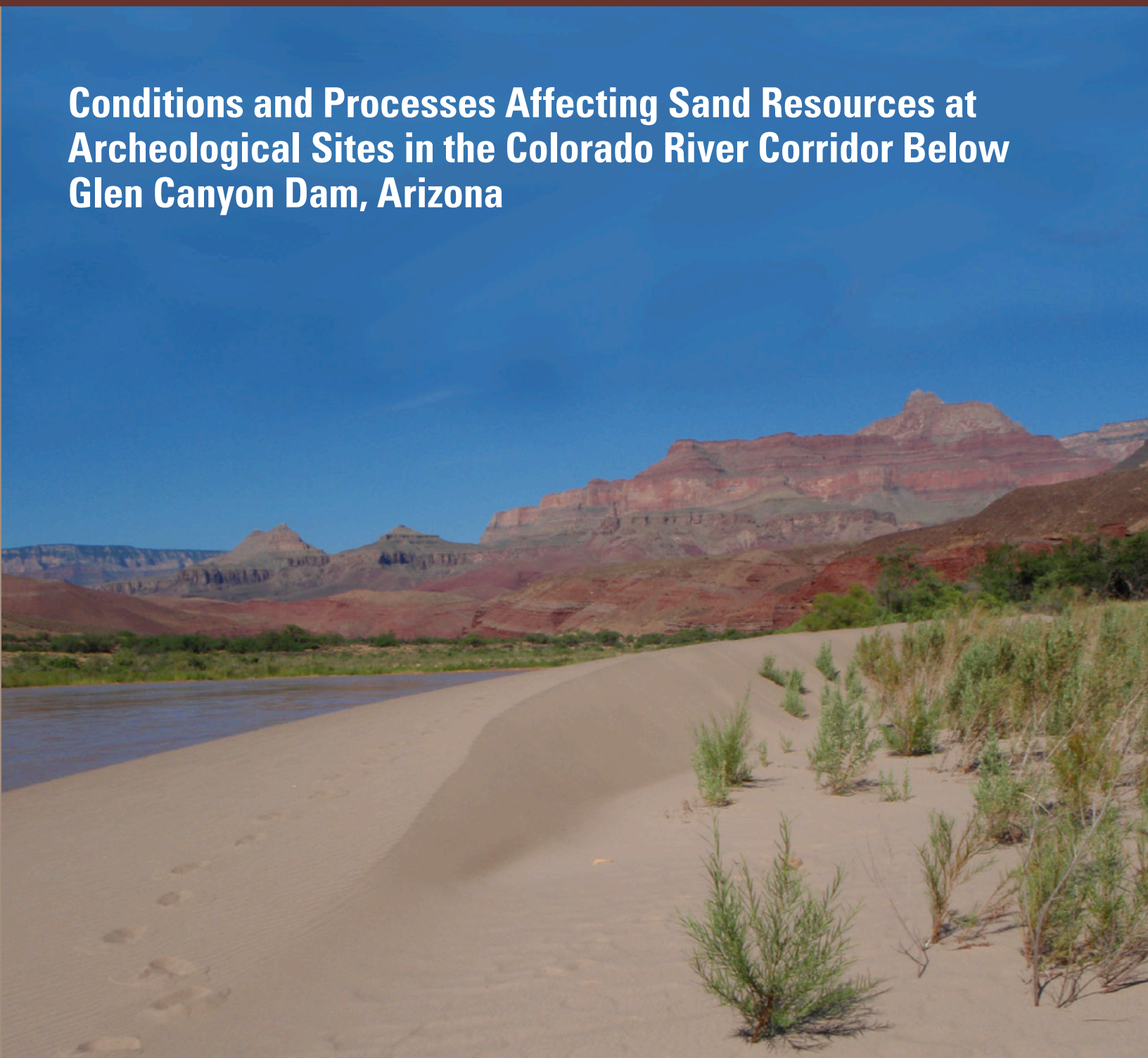

Professional Paper 1825

U.S. Department of the Interior
U.S. Geological Survey

Cover: Active source-bordering dune, approximately 1 m high, near RM 70 along the Colorado River, Grand Canyon, Arizona. Photograph taken in July 2008, several months after the upwind sandbar had enlarged substantially as a result of the March 2008 controlled flood.

Conditions and Processes Affecting Sand Resources at Archeological Sites in the Colorado River Corridor Below Glen Canyon Dam, Arizona

By Amy E. East, Brian D. Collins, Joel B. Sankey, Skye C. Corbett, Helen C. Fairley, and Joshua Caster

Professional Paper 1825

U.S. Department of the Interior
U.S. Geological Survey

U.S. Department of the Interior
SALLY JEWELL, Secretary

U.S. Geological Survey
Suzette M. Kimball, Director

U.S. Geological Survey, Reston, Virginia: 2016

For more information on the USGS—the Federal source for science about the Earth, its natural and living resources, natural hazards, and the environment—visit http://www.usgs.gov or call 1–888–ASK–USGS.

For an overview of USGS information products, including maps, imagery, and publications, visit http://www.usgs.gov/pubprod/.

Suggested citation:
East, A.E., Collins, B.D., Sankey, J.B., Corbett, S.C., Fairley, H.C., and Caster, J., 2016, Conditions and processes affecting sand resources at archeological sites in the Colorado River corridor below Glen Canyon Dam, Arizona: U.S. Geological Survey Professional Paper 1825, 104 p., http://dx.doi.org/10.3133/pp1825.

ISSN 2330-7102 (online)

Contents

Figures

Tables

Conversion Factors

Multiply	By	To obtain
	Length	
centimeter (cm)	0.3937	inch (in.)
millimeter (mm)	0.03937	inch (in.)
meter (m)	3.281	foot (ft)
kilometer (km)	0.6214	mile (mi)
meter (m)	1.094	yard (yd)
	Area	
square meter (m^2)	0.0002471	acre
square kilometer (km^2)	247.1	Acre
square meter (m^2)	10.76	square foot (ft^2)
square kilometer (km^2)	0.3861	square mile (mi^2)
	Volume	
liter (L)	33.82	ounce, fluid (fl. oz)
liter (L)	2.113	pint (pt)
liter (L)	1.057	quart (qt)
liter (L)	0.2642	gallon (gal)
cubic meter (m^3)	264.2	gallon (gal)
cubic meter (m^3)	0.0002642	million gallons (Mgal)
cubic centimeter (cm^3)	0.06102	cubic inch (in^3)
cubic decimeter (dm^3)	61.02	cubic inch (in^3)
liter (L)	61.02	cubic inch (in^3)
cubic meter (m^3)	35.31	cubic foot (ft^3)
cubic meter (m^3)	1.308	cubic yard (yd^3)
cubic meter (m^3)	0.0008107	acre-foot (acre-ft)
	Flow rate	
meter per second (m/s)	3.281	foot per second (ft/s)
meter per minute (m/min)	3.281	foot per minute (ft/min)
meter per hour (m/hr)	3.281	foot per hour (ft/hr)
meter per day (m/d)	3.281	foot per day (ft/d)
meter per year (m/yr)	3.281	foot per year ft/yr)
cubic meter per second (m^3/s)	35.31	cubic foot per second (ft^3/s)

Acronyms

DEM	digital elevation model
EmLCR	Eminence–Little Colorado River reach
FF	Furnace Flats reach
GCDAMP	Glen Canyon Dam Adaptive Management Program
GCMRC	Grand Canyon Monitoring and Research Center
GIS	geographic information system
GLCA	Glen Canyon reach
GP	Granite Park reach
RM	river mile (measured as distance downstream from Lees Ferry)
SCA	Stevens–Conquistador Aisle reach
TIN	triangulated irregular network
UGG	Upper Granite Gorge reach

Acknowledgments

This study was supported by funding from the Bureau of Reclamation through the U.S. Geological Survey (USGS) Grand Canyon Monitoring and Research Center, and was conducted in collaboration with the National Park Service (NPS; Grand Canyon National Park and Glen Canyon National Recreation Area). We thank Jennifer Dierker and Thann Baker (NPS), David Bedford (USGS), and Mary Barger (Bureau of Reclamation) for valuable discussions regarding landscape processes and archeological sites. The ideas of David Rubin, Jack Schmidt, Ted Melis, Ivo Lucchitta, Richard Hereford, and Bob Webb were instrumental to our conceptual understanding of landscape processes discussed herein. Aaron Borling, Joe Hazel, Keith Kohl, Mark Mastin, and Paul Rauss provided survey support. Carol Fritzinger coordinated field logistics; boatmen Carolyn Alvord, Don Bacco, Kirk Burnett, Seth Felder, Dave Foster, Mark Perkins, and Dom Zanzucchi contributed in numerous ways to the field operations and data collection. Jeanne DiLeo drafted two of the figures in this report. We thank Jack Schmidt and Paul Grams for their feedback and discussions of our work. Reviewers Kathleen Nicoll and Joel Pederson provided valuable comments that improved the manuscript. We thank Katherine Jacques and Jacqueline Olson for their conscientious editorial work.

David R. Bedford
1974–2016

Dave Bedford, USGS research geologist, worked on this project for many years. He contributed scientific direction and consistently provided new insights into the processes that shape the landscape and archeological record of Grand Canyon. His enthusiasm for scientific inquiry, his thoughtfulness to assist others, and his warmhearted friendship will always be remembered.

Conditions and Processes Affecting Sand Resources at Archeological Sites in the Colorado River Corridor Below Glen Canyon Dam, Arizona

By Amy E. East, Brian D. Collins, Joel B. Sankey, Skye C. Corbett, Helen C. Fairley, and Joshua Caster

Abstract

This study examined links among fluvial, aeolian, and hillslope geomorphic processes that affect archeological sites and surrounding landscapes in the Colorado River corridor downstream from Glen Canyon Dam, Arizona. We assessed the potential for Colorado River sediment to enhance the preservation of river-corridor archeological resources through aeolian sand deposition or mitigation of gully erosion. By identifying locally prevailing wind directions, locations of modern sandbars, and likely aeolian-transport barriers, we determined that relatively few archeological sites are now ideally situated to receive aeolian sand supply from sandbars deposited by recent controlled floods. Whereas three-fourths of the 358 river-corridor archeological sites we examined include Colorado River sediment as an integral component of their geomorphic context, only 32 sites currently appear to have a high degree of connectivity (coupled interactions) between modern fluvial sandbars and sand-dominated landscapes downwind. This represents a substantial decrease from past decades, as determined by aerial-photograph analysis. Thus, we infer that recent controlled floods have had a limited, and declining, influence on archeological-site preservation.

Within the study area, overland-flow (gully) erosion is less severe in sand landscapes with active aeolian sand than in landscapes that lack aeolian transport; gullies terminate more commonly in active sand (sand that is mobile by wind rather than stabilized by biologic soil crust). We infer that these characteristics largely result from aeolian sand transport being an effective gully-limiting and gully-annealing mechanism. Aeolian sand activity in the river corridor varies substantially as a function of reach morphology and dominant wind direction relative to the river-corridor orientation, factors that control accommodation space for river-derived sand and the modern sand supply to aeolian dunes. These attributes, together with an inverse correlation between aeolian sand activity and gully occurrence, define varying degrees of net long-term gully-erosion risk for sediment deposits and associated archeological sites in different regions of the river corridor. Over most of the river corridor, including some of the archeologically richest regions, sand is too inactive with respect to aeolian transport to anneal gullies effectively. At eight selected archeological sites that we studied with high-resolution terrestrial lidar scans for more than a year, sand loss by overland flow (gully erosion) and aeolian deflation generally exceeded deposition, such that erosion dominated over most monitoring intervals—even at four sites with strong connectivity to modern sand supply.

The Glen Canyon reach of the river corridor appears especially vulnerable to gully erosion. Among the sites that we monitored in detail, erosion generally dominated over deposition to a greater degree at four Glen Canyon sites with no modern sand supply than at four Marble–Grand Canyon sites with aeolian sand supply from controlled-flood sandbars. Although gross annual-scale erosion rates were similar among the Glen Canyon sites and among the Marble–Grand Canyon sites, a relative lack of depositional processes led to greater net erosion at the Glen Canyon sites. Having found no differences in weather patterns to suggest greater erosive forcing in Glen Canyon, and no conclusively influential differences in the slope or watershed area contributing to gully formation, we attribute the greater erosion at the Glen Canyon sites to a combination of inherent geomorphic context (high terraces that do not receive modern sediment supply) and pronounced effects of postdam sediment-supply limitation.

We conclude that most of the river-corridor archeological sites are at elevated risk of net erosion under present dam operations. In the present flow regime, controlled floods do not simulate the magnitude or frequency of natural floods, and are not large enough to deposit sand at elevations that were flooded at annual to decadal intervals in predam time. For archeological sites that depend upon river-derived sand, we infer elevated erosion risk owing to a combination of reduced sand supply (both fluvial and aeolian) through (1) the lower-than-natural flood magnitude, frequency, and sediment supply of the controlled-flooding protocol; (2) reduction of open, dry sand area available for wind redistribution under current normal (nonflood) dam operations, which do not include flows as low as natural seasonal low flows and do include substantial daily flow fluctuations; and (3) impeded aeolian sand entrainment and transport owing to increased riparian vegetation growth in the absence of larger, more-frequent floods. If dam operations were to increase the supply of sand available for windblown transport—for example, through larger floods, sediment augmentation, or increased fluvial sandbar exposure by low flows—and also decrease riparian vegetation, the prevalence of active aeolian sand could increase over time, and the propensity for unmitigated gully erosion could decrease. Although the evolution of river-corridor landscapes and archeological sites has

been altered fundamentally by the lack of large, sediment-rich floods (flows on the order of 5,000 m^3/s), some combination of sediment-rich flows above 1,270 m^3/s, seasonal flows below 226 m^3/s, and riparian-vegetation removal might increase the preservation potential for sand-dependent archeological resources in the Colorado River corridor.

Introduction and Background

Landscape Context of Cultural Resources in the Colorado River Corridor

The Colorado River corridor through Glen, Marble, and Grand Canyons, Arizona (fig. 1), is an iconic landscape that has drawn human interest for more than 10,000 years. Set within the large bedrock canyon incised into the surrounding Colorado Plateau, the river corridor preserves a complex geomorphic and human history (Fairley, 2003). Climatic fluctuations within the canyon region and in the Colorado River headwaters varied the flow and sediment supply in the river and controlled other landscape processes in the canyon, leading to formation of a stratigraphic and cultural record that spans thousands of years (Fairley and others, 1994; O'Connor and others, 1994; Hereford and others, 1993, 1996; Fairley and Hereford, 2002; Anderson and Neff, 2011; Pederson and O'Brien, 2014). Cultural resources along the river corridor consist of the physical evidence of past human activities, as well as places and natural resources of traditional importance to Native American cultures (Fairley, 2005). Many remnants of past human activity, including archeological sites and historical structures, are situated within or on top of fine-grained sediment deposits derived from the Colorado River[1]. These historically and culturally significant places are susceptible to degradation and erosive damage over time, owing to natural weathering and erosion and to modern anthropogenic impacts (Balsom and others, 2005; Fairley, 2005). The latter can occur as a direct effect of visitor use and, as we investigate in this report, also can include changes to the river-corridor landscape as a result of Glen Canyon Dam operations.

The Colorado River basin drains 637,000 km^2 in an arid to semi-arid (dryland) region where large dams provide water storage. Glen Canyon Dam, 216 m tall, impounds Lake Powell, the second-largest reservoir in the United States (fig. 1). After the completion of Glen Canyon Dam in 1963, the hydrology and sediment supply downstream from the dam changed substantially (Topping and others, 2000, 2003; Rubin and others, 2002; Wright and others, 2005), as is common in dam-controlled rivers (Williams and Wolman, 1984; Chien, 1985; Collier and others, 1996; Schmidt and Wilcock, 2008). Glen Canyon Dam has reduced the fluvial sediment supply to upper Marble Canyon by more than 90 percent, with all sediment inputs now supplied by tributaries downstream from the dam (Topping and others, 2000; Wright and others, 2005).

Dam-released flows generally exceed lower seasonal predam flows that previously induced sand accumulation in the river channel, and dam releases do not include the natural floods that occurred regularly before dam closure (Topping and others, 2003; Magirl and others, 2008; Wright and others, 2008). Owing to the loss of sediment supply, the reduced magnitude and frequency of floods, and to riparian vegetation growth in the absence of large floods, there has been a systemwide decrease in the size and number of subaerially exposed fluvial sand deposits since the 1960s (Turner and Karpiscak, 1980; Beus and others, 1985; Schmidt and Graf, 1987, 1990; Johnson, 1991; Kearsley and others, 1994; Hazel and others, 2010). Sandbar decline has been punctuated by episodic aggradation of some bars during occasional higher flows such as those that occurred in 1983–1985, in controlled floods released in 1996, 2004, 2008, 2012, 2013, and 2014, and by sediment input from tributary floods (Lucchitta and Leopold, 1999; Hazel and others, 2010; Topping and others, 2010). Additional, lower-magnitude experimental floods in 2000 and a natural Little Colorado River flood in winter 1993 resulted in some sandbar aggradation as well (table 1; Melis and others, 2011).

Controlled floods, involving dam releases of approximately 1,200 m^3/s over several days, can successfully increase sandbar area and volume in the Colorado River corridor (fig. 2), although sandbar response in any particular location is a complex result of sediment concentration and grain size in each flood (Webb and others, 1999; Topping and others, 2006, 2010; Wright and Kaplinski, 2011; Draut and Rubin, 2013; Grams and others, 2013, 2015). However, the typical controlled-flood magnitude (maximum 1,270 m^3/s) is approximately half of the predam mean annual flood peak (2,400 m^3/s) and only one-fifth as large as the maximum historic predam flood (5,940 m^3/s, in 1884; Topping and others, 2003). Paleoflood-deposit elevations suggest that the largest predam floods may have exceeded 8,400 m^3/s (O'Connor and others 1994; Topping and others, 2003; Greenbaum and others, 2014). Therefore, controlled floods released from Glen Canyon Dam do not simulate the magnitude or frequency of natural floods, and are not large enough to deposit sand at elevations that were flooded at annual to decadal intervals in predam time.

Wind reworks the sand in fluvial sandbars to form aeolian (windblown) sediment deposits in the Colorado River corridor, as in other dryland environments (for example, Gilbert, 1899; Lancaster, 1995; Han and others, 2007). Aeolian deposits are a common feature of the landscape (fig. 3), composed of sand supplied from predam and postdam fluvial deposits. As a result of reduced fluvial sand supply, windblown sand supply in the river corridor downstream from Glen Canyon Dam has been reduced, and, in many locations, eliminated (Draut and Rubin, 2008). The

[1]Although fine-grained sediment includes sand, silt, and clay particle sizes, the fluvial and aeolian deposits relevant to this study are dominated by sand. Therefore, this report generally uses terms such as sand supply and sand deposits except when referring specifically to sediment with abundant silt and clay.

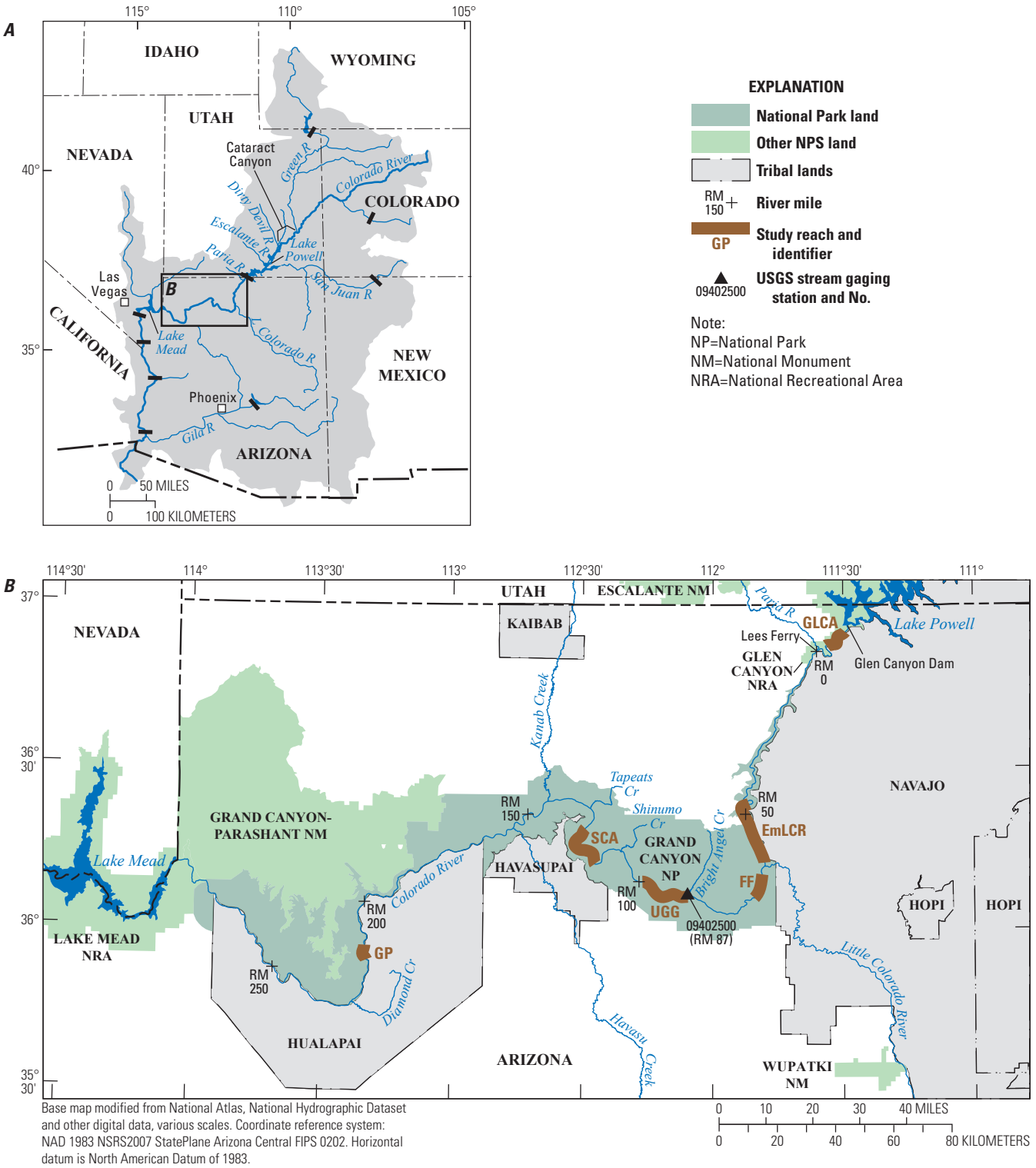

Figure 1. (*A*) The Colorado River watershed (gray shaded region). Major dams are indicated with black bars. Box outlines the area shown in (*B*). (*B*) The Colorado River corridor through Grand Canyon National Park, Ariz., and adjacent areas. River miles (RM) begin with RM 0 at Lees Ferry, 15 miles downstream from Glen Canyon Dam, and increase downstream. Glen Canyon includes the canyon region from Lake Powell downstream to Lees Ferry (RM 0). Marble Canyon extends from RM 0 to 61, and Grand Canyon from RM 61 to 277. Gray regions indicate river reaches studied in detail during this study: Glen Canyon (GLCA), Eminence to Little Colorado River (Em-LCR), Furnace Flats (FF), Upper Granite Gorge (UGG), Stevens-Conquistador Aisles (SCA), and Granite Park (GP).

Figure 2. Growth of fluvial sandbars as a result of controlled floods. (*A*) Sandbar at RM 70 at a flow of approximately 226 m^3/s, 11 days before the March 2008 controlled flood of 1,250 m^3/s. (*B*) Same sandbar as in (*A*), one month after the March 2008 controlled flood, shown at a flow of approximately 226 m^3/s. Person standing on sandbar for scale in (*B*). Arrow indicates position and orientation of photograph in figure 3*A*. (*C*) Sandbar at RM 66 shown two days before the November 2004 controlled flood of 1,190 m^3/s, shown at a flow of 226 m^3/s. (*D*) Same sandbar as in (*C*), three weeks after the November 2004 controlled flood, at a flow of 283 m^3/s. (*E*) Sandbar at RM 58 shown three days before the November 2004 flood, at a flow of 226 m^3/s. (*F*) Same sandbar as in (*E*), three weeks after the November 2004 flood, at a flow of approximately 226 m^3/s. Person standing on far end of sandbar shows scale. For reference, arrows indicate rocks in common to photographs (*E*) and (*F*).

Figure 3. Examples of aeolian sedimentary deposits in the Colorado River corridor. (*A*) Active source-bordering dune approximately 1 m high, migrating inland toward photographer's right, that formed at the landward edge of the sandbar shown in fig. 2*B*. Photograph taken in July 2008, several months after the upwind sandbar had enlarged substantially as a result of the March 2008 controlled flood. (*B*) Active source-bordering dune at RM 190, with dune crest (dashed line) indicating dune migration toward the photographer's right. This location is approximately 30 m downwind (inland) from the river margin. (*C*) Aeolian deposit (sand ramp) of light-colored Colorado River sand plastered against talus slopes well above the historic high-flow river stage. Prevailing wind direction at this location (measured at a weather station) is toward the photographer's left, approximately perpendicular to the trend of the river corridor. The main sand source for these aeolian deposits is fluvial sandbars at right, just out of view. (*D*) Dunes with mature mesquite trees as part of the vegetation cover. Color of sand in dunes indicates wind-derivation from Colorado River fluvial deposits (in this case, predam flood deposits, as there is no modern fluvial sandbar upwind), whereas red sediment in interdune swale (foreground) indicates slopewash runoff derived from local bedrock sources. (*E*) Large, partly vegetated dune field at RM 70.6. (*F*) Aeolian dunes (sunlit) atop a small debris fan. Lightest-colored areas are active aeolian sand with little to no biologic crust cover.

loss of sand supply has altered the connectivity of aeolian, fluvial, and hillslope processes—that is, the interactions among wind, river, and hillslope sedimentary and ecosystem processes—with complex geomorphic and ecological effects (Draut, 2012).

The cultural resources of Glen, Marble, and Grand Canyons are commonly situated on and within fluvial and aeolian sand deposits derived from the Colorado River (fig. 4; Hereford and others, 1993, 1996, 2000a; Fairley and others, 1994; Fairley and Hereford, 2002; Draut and others, 2008; O'Brien and Pederson, 2009a; Anderson and Neff, 2011). The stability of those sand deposits through time, and the condition of archeological material within them, largely depends upon the alternately erosive and depositional capacities of wind and water. Fluvial and aeolian sand deposits naturally erode over time as wind and rainfall runoff remove some sediment. Particularly as overland flow channelizes into gullies, rainfall runoff can erode sand and archeological sites substantially (fig. 4; Pederson and others, 2006; O'Brien and Pederson, 2009a,b; Collins and others, 2009, 2012; Pederson and O'Brien, 2014).

In a natural system, the erosive action of wind and water would be counteracted to some degree as river floods and subsequent wind action supplied new sand to the landscape. In an unregulated Colorado River, sediment-rich floods would regularly bring new sand into Glen, Marble, and Grand Canyons and deposit it on fluvial terraces, in eddies, and along the channel margins; wind would then redistribute much of that sand to

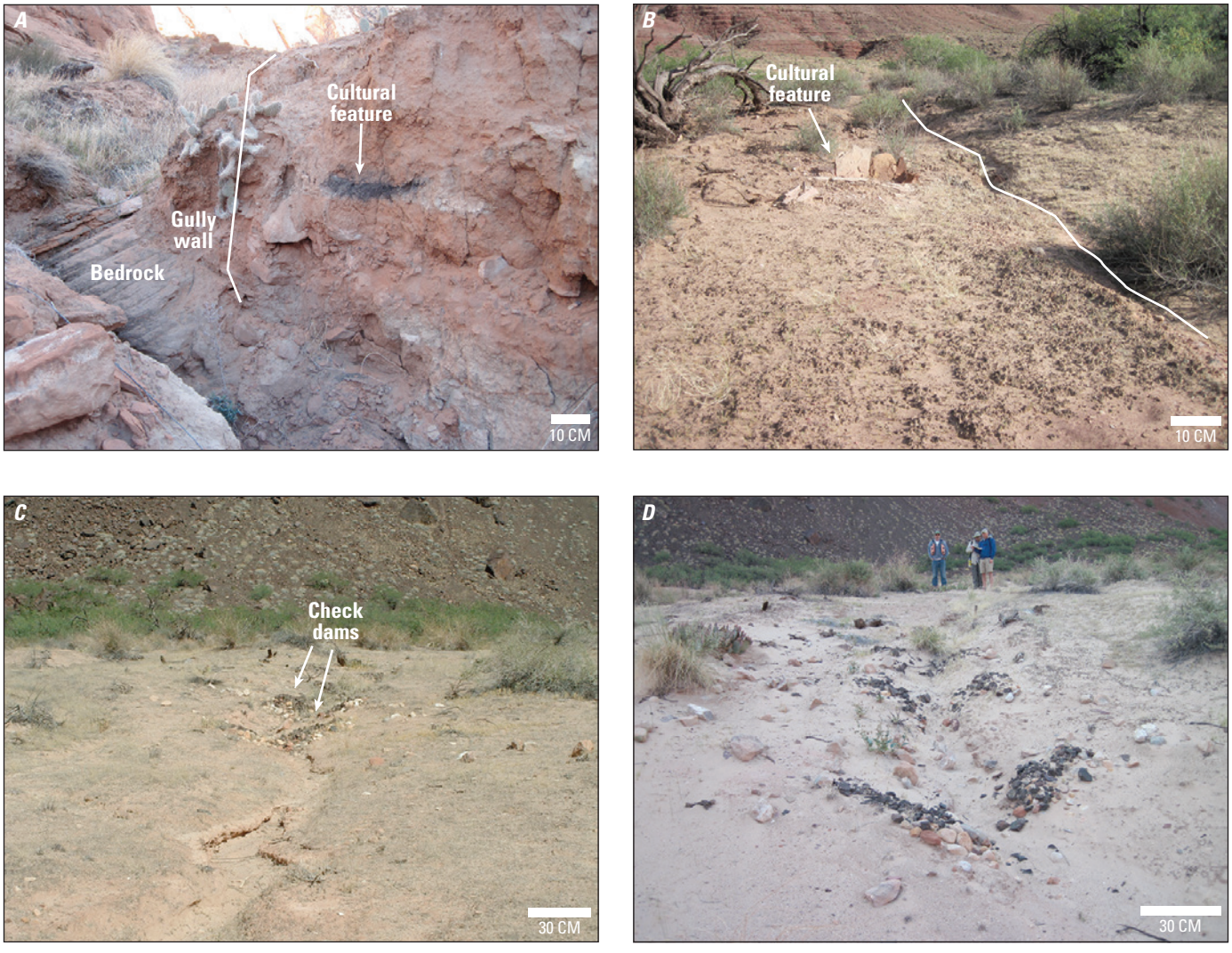

Figure 4. Gully erosion, resulting from overland flow, at river-corridor archeological sites. All photographs show gullies that incise sediment deposits composed of interbedded fluvial, colluvial, and debris-fan material, with fluvial terraces locally dominating the morphology. (*A*) Gully erosion exposes a cultural feature in Glen Canyon. (*B*) Gully incision through inactive aeolian sand dunes composed of river-derived sediment covered with dark biologic soil crust, in the Furnace Flats reach of eastern Grand Canyon. White line indicates gully flow path. Foreground shows red-colored sediment derived from local bedrock, presumably deposited by overland flow. (*C*) Gully incision through an archeological site in river-derived sand covered with biologic soil crust, Furnace Flats reach, May 2004. Rock checkdams (arrows) were built in the 1990s to mitigate gully erosion. (*D*) The same gully as in (*C*) in May 2013, with checkdams breached.

upland landscapes, replenishing sand supply to aeolian dunes (for example, Draut, 2012)[2]. Thus, wind and water both deposit and erode sand. The balance between supply (deposition) and erosion determines landscape evolution and cultural-site condition in a dryland river corridor.

The loss of sand supply to fluvial and aeolian deposits owing to the construction and subsequent operations of Glen Canyon Dam, and thus the reduced potential to counteract erosion, has consequences for the preservation of cultural sites. That dam operations may affect archeological-site preservation is of concern to the Glen Canyon Dam Adaptive Management Program (GCDAMP) stakeholders, Native American tribes, and Federal and State agencies that manage the river corridor and dam operations.

Beginning in the 1990s, concern arose that the predam sand that forms the setting of many cultural sites might have eroded more rapidly in the late 20th century than previously (Hereford and others, 1993), although little quantitative information was available to assess that possibility. Several factors were proposed to explain an apparent increase in erosion rates—increased rainfall intensity and magnitude during the late 1970s and early 1980s, reduced sand supply owing to Glen Canyon Dam operations, and impacts from visitation and recreational use of the river corridor (Hereford and others, 1993; Thompson and Potochnik, 2000; Fairley, 2005). Regarding the likely role of reduced sand supply, Hereford and others (1993) suggested that lack of sediment supply at the elevations of large predam floods had caused gully erosion to incise more deeply into predam flood deposits and to migrate farther headward (upslope), increasing the net material lost from rainfall runoff. Hereford and others (1993) postulated that whereas the predam river corridor contained many ephemerally flowing gullies graded to terrace surfaces formed and maintained by Colorado River floods, the postdam landscape included more gullies graded to the elevation of the regulated river, several meters lower than the predam flood terraces. In predam time, large sediment-rich floods filled large gullies with sand (McKee, 1938), as still occurs in the Colorado River upstream from Lake Powell (Thompson and Potochnik, 2000). Hereford and others (1993) proposed that because gully channels in postdam Marble–Grand Canyon are no longer infilled by sand during large Colorado River floods, and because gullies can incise to a lower base level now, gully erosion of predam sand deposits and associated cultural sites has increased in postdam time.

Based on qualitative field observations, researchers proposed that the reduced fluvial discharge and sand supply, as well as expansion of riparian vegetation in the regulated river had, in turn, reduced the aeolian sand supply to upland landscapes and archeological sites, further exacerbating their potential for erosion (Lucchitta, 1991; Hereford and others, 1993; Neal and others, 2000; Thompson and Potochnik, 2000). The ability of aeolian sand to infill gullies and aggrade upland sediment deposits, thus counteracting erosion processes to some degree, was known from local documentation of gullies terminating in and filled by aeolian sand (Hereford and others, 1993; Draut and Rubin, 2008) and from measurements of aeolian inflation (aggradation) at some cultural sites (Yeatts, 1996; Collins and others, 2009). However, aeolian infilling processes had not been evaluated quantitatively over large areas. Draut (2012) found that characteristics of aeolian deposits differed significantly with the availability of modern upwind sand supply—differences that suggested varying susceptibility to gully development. The suite of observations on fluvial and aeolian upland landscapes from the early 1990s through 2012, together with direct measurements of landscape change at selected sites (discussed below), formed the basis for a more quantitative, larger-scale assessment within this study.

The links among fluvial and aeolian sand movement, hillslope runoff through upland landscapes, and dam operations that control sand abundance and transport are complex and difficult to quantify, especially in a remote setting. Despite such challenges, a better understanding of these interconnected processes is essential not only to understanding fundamental principles of dryland regions, but also to optimizing the GCDAMP management goal of preserving cultural resources. In accordance with the National Historic Preservation Act (Public Law 102-575, Sections 106, 110) and the Grand Canyon Protection Act of 1992, the GCDAMP aims to mitigate the effects of dam operations on cultural resources, with the highest priority being to preserve those resources in place. Achieving this goal requires optimizing conditions that preserve the stability of upland sand deposits. One goal of dam operations, including controlled flooding, has been to increase the sandbar area that can supply windblown sand to upland aeolian deposits, potentially increasing the protective cover over archeological sites and reducing the net effects of erosional processes (Draut and others, 2010; Melis, 2011). To determine the effectiveness of such actions, it is necessary to determine more quantitatively the extent to which dam operations affect archeological sites, and to assess how effectively dam operations, without large floods, can supply sand to upland areas. Thus, we evaluated one aspect of a complex scientific and management problem—how to optimize natural- and cultural-resource conditions in the Colorado River ecosystem while meeting national needs for water supply and hydropower generation at Glen Canyon Dam.

This publication presents the findings of a two-year study under the GCDAMP biennial work plan (fiscal years 2013–14, project J) intended to refine understanding of the role of dam operations in affecting archeological-site conditions. The scale of our research ranged from high-resolution monitoring of selected individual archeological sites to landscape-wide field and remote-sensing analyses. Building on the studies mentioned above, this work addresses whether cultural sites in Glen, Marble, and Grand Canyon are eroding or changing faster or in a significantly different manner than they would if the dam were operated differently.

[2] We use *upland* to refer to areas above the recently active channel or flood zone. Presently, this implies regions above the 1,270 m^3/s controlled-flood stage, but three decades ago the active channel was the area below the largest historical dam release stage of 2,740 m^3/s, and in predam time what we now call upland areas were part of the active channel when inundated by much larger floods.

Aeolian-Fluvial-Hillslope Connectivity: Background and Previous Studies

To provide sufficient context for the findings of this study, we review some geomorphic processes that govern upland landscape evolution in the Colorado River corridor and summarize studies that led directly into the current work. Comprehensive treatment of recent geomorphic processes in the river corridor can be found in works such as Howard and Dolan (1981), Schmidt (1990), Melis and others (1995), Webb and others (2003), Magirl and others (2005), Yanites and others (2006), Grams and others (2007), Melis (2011), and Pederson (2012); we focus here on the fluvial, aeolian, and hillslope-runoff processes most relevant to sand transport around archeological sites.

Landscape evolution in dryland regions depends strongly on connectivity among fluvial, aeolian, and hillslope systems (Loope and others, 1995; Kocurek, 1998; Field and others, 2009; Telfer and others, 2014), although wind- and water-borne sediment transport are rarely studied together (Bullard and Livingstone, 2002; Bullard and McTainsh, 2003; Belnap and others, 2011). In many settings, fluvial–aeolian sedimentary and geomorphic interactions affect not only the ways in which human communities occupy a landscape, but also the preservation of their archeological record (Holliday and others, 2007; Gibling and others, 2008; Martínez and Martínez, 2011; Roskin and others, 2014). To understand the suite of factors that control sediment supply to, and loss from, river-corridor landscapes and cultural sites of Glen, Marble, and Grand Canyons requires linking the erosive and sand-replenishing roles of wind and water.

Predam floods were the dominant source of sand in the upland (sand) deposits that contain archeological sites; these floods were larger than any in the postdam era. The importance of large Colorado River terrace deposits as the major substrate in upland landscapes is readily apparently within river-corridor stratigraphy (Hereford, 1996; Hereford and others, 1996, 1998, 2000a; Burke and others, 2003; Draut and others, 2005, 2008; Anderson and Neff, 2011; Pederson and others, 2011; Neff and Anderson, 2012). Locally, flood-deposited sediment is interbedded with aeolian, debris-flow, and slopewash strata; flood deposits dominate the sedimentary record in major terraces that are relevant to many archeological-site locations (Hereford, 1996; Hereford and others, 2000a; Burke and others, 2003; Draut and others, 2005). For clarity, we refer here to Colorado River flows and sediment as fluvial and to localized slope-runoff flows and sediment as hillslope or slopewash. Several river reaches contain well developed predam fluvial terraces meters thick and tens of meters wide that include dense concentrations of cultural sites (Fairley and others, 1994; Anderson and Neff, 2011; Pederson and O'Brien, 2014), for example much of Glen Canyon (River Mile [RM] -14 to -6), the so-called Furnace Flats reach of eastern Grand Canyon (RM 66–72), and the Granite Park area (RM 208–210; fig. 1). The fluvial terraces presumably were formed by predam floods, but the paleomagnitude or recurrence interval of those floods is not known with certainty. The formation of those deposits probably was affected to some degree by changes in channel gradient, upstream sediment supply, and ponding upstream from recently active debris fans (Harvey and Pederson, 2011). In most areas that contain spatially extensive fluvial deposits and numerous archeological sites, the topography is such that today those terraces could only be overtopped by floods of 4,800 m^3/s and greater, as shown by discharge-elevation models (Magirl and others, 2008). A discharge of 4,800 m^3/s was last attained in 1921, and had an estimated return interval of 40 years in the predam Colorado River hydrology (Topping and others, 2003). Thus, over the past few centuries, the river-derived deposits forming the substrate and cover for many cultural sites resulted from large, relatively rare (decadal-scale) flood events combined with some influence of downstream debris-fan activity that altered the local hydraulic control.

Fluvial terraces are commonly overlain by, and interbedded with, aeolian sand that indicates wind reworking of surficial flood sediment between flood events (Hereford and others, 1993; Burke and others, 2003; Draut and others, 2008). The wind mobilizes fluvial sand and redeposits it adjacent to the river channel, forming dunes that are known as source-bordering dunes, in the terminology of Bullard and McTainsh (2003; see also Draut and others, 2010; Draut, 2012). Many such aeolian dune fields occur in the Colorado River corridor (fig. 3). Maximum elevations of aeolian sand vary according to local topography and wind conditions, and can be tens of meters above the base of any given aeolian deposit. Wind can reshape flood deposits substantially, turning their surfaces from near-flat terraces into aeolian dune fields (fig. 3). In some places, aeolian sand forms a thick mantle on talus slopes at the bases of bedrock canyon walls (sand ramps; fig. 3*C*). Aeolian sediment in this river corridor is derived almost entirely from Colorado River deposits of various ages, judging from the similar color and composition of aeolian and fluvial sand there; any contribution of local bedrock-derived sediment to the aeolian deposits is evidently overwhelmed by a much greater supply of buff-colored, mature, quartz-rich sand from Colorado River deposits (for example, fig. 3*D*; Hereford and others, 1998, 2000a; Draut and others, 2005).

In addition to the large dune fields (10^3–10^4 m^2) that develop atop wide, predam flood terraces (fig. 5*A*), many smaller aeolian dune complexes occur in Marble and Grand Canyons overlying tributary debris fans (fig. 5*B*). These smaller aeolian deposits (commonly 10^1–10^3 m^2) formed as the wind reworked river flood sediment in predam, and in some places also postdam, separation and reattachment sandbars in eddies at the downstream side of debris fans (the fan-eddy complex of Schmidt, 1990; Schmidt and Rubin, 1995). Large, predam floods covered small debris fans almost entirely, often leaving deposits that blanketed large parts of the fans rather than merely forming separation and reattachment bars (Magirl and others, 2008), whereas the controlled floods today are not large enough to submerge most tributary debris fans. An estimated 1,000 or more fan-eddy complexes occur throughout Marble and Grand Canyons (based on approximately 350 having been identified in Marble Canyon alone; Hazel and others, 2006); most consist of some combination of fluvial and reworked aeolian sand overlying the debris fan. Archeological sites commonly occur in and on river-derived sand in those settings, though at lower site

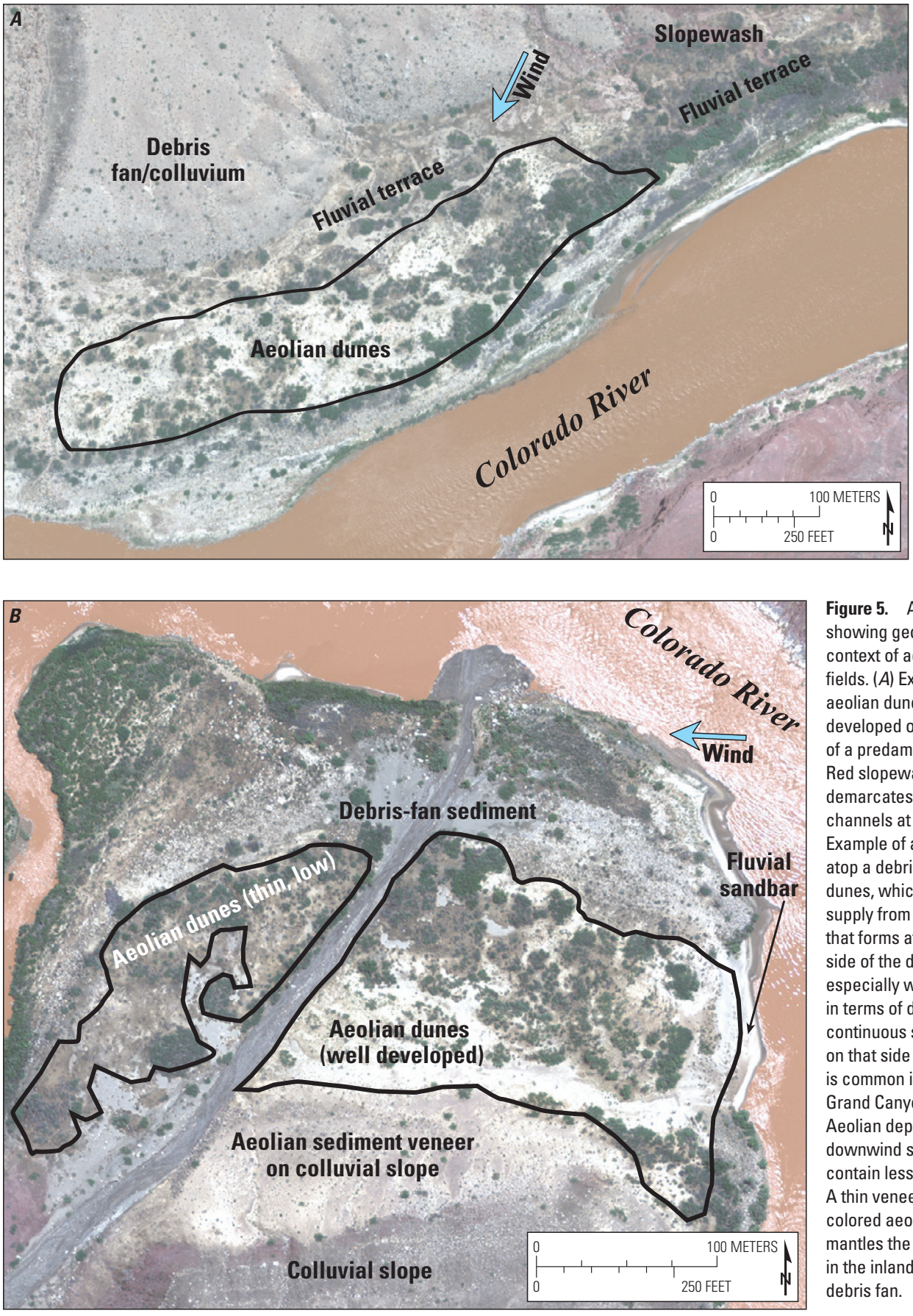

Figure 5. Aerial images showing geomorphic context of aeolian dune fields. (*A*) Example of aeolian dunes that developed on the surface of a predam fluvial terrace. Red slopewash sediment demarcates overland-flow channels at upper right. (*B*) Example of aeolian dunes atop a debris fan. The dunes, which receive sand supply from a sandbar that forms at the upwind side of the debris fan, are especially well developed in terms of dune height and continuous surface cover on that side of the fan, as is common in Marble–Grand Canyon debris fans. Aeolian deposits on the downwind side of the fan contain less sand volume. A thin veneer of light-colored aeolian sand also mantles the colluvial slope in the inland part of the debris fan.

densities than in the wider predam terraces (Fairley and others, 1994; Pederson and O'Brien, 2014).

Wind action continually modifies aeolian sand areas, whether in large dune fields atop major flood terraces or smaller deposits overlying debris fans. In many places aeolian sand entrainment and transport are impeded by vegetation or biologic soil crust (for example, Buckley, 1987; Leys and Eldridge, 1998; Okin and others, 2006; Dong and others, 2011), but where the sand is open and bare, aeolian deposition aggrades (inflates) and aeolian erosion degrades (deflates) the land surface, and aeolian dunes migrate downwind over time. Spatial patterns of inflation and deflation, and the rates and orientations of dune migration, depend upon local wind dynamics and the availability of upwind sediment supply. Thus, land surfaces in aeolian dune fields undergo frequent natural changes in elevation and local sand-cover thickness, processes that can affect the stability of archeological sites (Draut and Rubin, 2008). The greatest potential for aeolian landscape modification occurs during spring, when dry, windy weather is common and sand-transport rates generally are greater than at other times of year (Draut and Rubin, 2005, 2006, 2008; Draut and others, 2009a,b; Dealy and others, 2014); however, aeolian sand transport can occur during any time of year. Severe sandstorms were mentioned frequently in the accounts of early Colorado River runners, including some in conjunction with incoming summer monsoonal storms. For example, an autumn 1938 journal entry by river-runner Buzz Holmstrom noted, "sky so full of sand sun blotted out" (Boyer and Webb, 2007).

The locations of aeolian dune fields relative to fluvial sandbars, pre- and postdam flood elevations, and wind patterns indicate whether substantial modern, postdam sand supply reaches them. Some aeolian dunes form directly inland from modern sandbars that were deposited by controlled floods; after floods recede, in places where the dominant wind direction brings sand inland from the river, new aeolian dunes form above the flood stage (for example, fig. 3*A*). Other aeolian landscapes in the canyons have no modern, controlled-flood sandbar upwind, and thus receive little to no aeolian supply from modern sandbars, but are relict features composed of wind-reworked predam sand. Draut (2012) termed these two groups modern-fluvial-sourced (MFS) and relict-fluvial-sourced (RFS) aeolian deposits, respectively.

Glen Canyon Dam operations reduce sediment sources to aeolian landscapes not only by eliminating floods, but also by eliminating low flows (<100 m^3/s, 4 percent of the predam mean annual flood) that would have exposed additional fluvial sediment to wind, and creating conditions conducive to vegetation encroachment on channel-margin and sandbar deposits. Dam operations also involve daily flow fluctuations great enough that the lowest-elevation fluvial sand exposed typically does not have time to dry and be mobilized by wind before being submerged again by rising flows. However, the reduced aeolian sand supply resulting from lack of sustained low flows and from larger daily flow fluctuations likely affects upland sedimentary systems less than the loss of large floods and increased vegetation cover. The relatively greater importance of the loss of large floods is evident from the upland sedimentary record around archeological sites, where flood deposits form a more ubiquitous and fundamental geomorphic context than do aeolian deposits (Hereford and others, 2000a; Draut and others, 2008; Anderson and Neff, 2011).

Upland sand deposits of the Colorado River corridor are modified not only by wind, but also by rainfall runoff. As in other dryland regions worldwide, sediment deposits erode as rainfall runoff focuses into overland flow that is channelized in gullies. Flow through gullies also can include contributions from sapping or subsurface flow (for example, Faulkner and others, 2004; Pederson and others, 2006; Tebebu and others, 2010; Svoray and others, 2012). Gully development is a complex function of rainfall intensity, infiltration capacity of the sedimentary substrate, and upslope catchment area. In sand deposits of the Colorado River corridor, gullies commonly form and evolve in response to overland flow from upslope areas mantled by relatively impermeable colluvium and bedrock, even if the rainfall intensity and infiltration capacity of the sand otherwise would not have induced gully formation (Collins and others, 2016). Gully erosion has damaged numerous archeological sites in Glen, Marble, and Grand Canyons (fig. 4; Hereford and others, 1993; Pederson and others, 2003, 2006; Balsom and others, 2005; Hazel and others, 2008; O'Brien and Pederson, 2009b; Collins and others, 2009, 2014, 2016). Although overland flow is the dominant process of archeological-site degradation in this setting, more gradual hillslope processes such as creep also cause substantial erosion over time (Pederson and O'Brien, 2014).

Many previous studies have addressed gully formation and enlargement, but relatively little is known about mechanisms that may anneal gullies—that is, processes that impede or counteract gully growth (Antevs, 1952; Patton and Schumm, 1975; Ghimire and others, 2006; Le Roux and Sumner, 2012). In the Colorado River corridor, windblown sand has been observed to fill gullies on the order of 10 cm wide and 10 cm deep (fig. 6*A*, *B*). Topographic depressions capture aeolian sand—not only gullies, but also larger tributary channels oriented transverse to the dominant wind direction (fig. 6). Spatially limited stratigraphic examinations have not revealed clear examples of paleogullies filled with windblown sand (Hereford and others, 2000a; Draut and others, 2005; Anderson and Neff, 2011). However, the aeolian-sand-trapping tendency of channels, and examples in the literature of aeolian sand filling paleogullies (McIntosh and others, 2004; Xu and others, 2006; Mazaeva and others, 2011), suggest that aeolian sand may have annealed gullies in the Colorado River corridor in the past, and potentially could today, given sufficient sand supply.

The Role of Glen Canyon Dam Operations

Given the complex interactions among fluvial and aeolian sand transport and the erosive potential of wind and rain, it is not straightforward to identify how dam operations affect these processes or damage cultural sites. To assess the effects of dam-induced sand-supply limitation on upland landscapes, the most rigorous approach would be to quantify differences between predam and postdam upland landscapes—comparing site elevations, dune topography, ground cover, and degree of gully development in sand

Figure 6. Aeolian sand filling topographic depressions. (*A*) A recently formed gully (foreground) terminating in aeolian sand. (*B*) Aeolian sand, lighter-colored than its surroundings, partly fills a gully incised through biocrusted sand. Gully flow path was downslope toward the photographer. (*C*) Aeolian dune migrating into a gully, covering a cultural feature that had been exposed several years earlier by gully erosion. Dune migration direction is toward photographer's right. (*D*) Aeolian dune migrating into and partly filling a tributary channel. Dune migration direction is toward photographer's right. Dunes commonly migrate into a tributary wash but do not cross it entirely, presumably because tributary flow episodically removes dune sand. (*E*) Landscape-scale view of similar phenomenon as in (*D*), with aeolian dunes having migrated into a tributary channel. Note well developed dune complex on upwind side of tributary (right side of photograph) compared to little to no dune morphology on downwind (left) side of tributary; same location as in figure 5*B*.

deposits in the early 1960s and today. However, few of the necessary records exist for predam time periods. The first detailed geomorphic maps of the river corridor were made in the 1990s, for only a few select areas (Leschin and Schmidt, 1995; Hereford, 1996; Hereford and others, 1993, 1998, 2000a,b). Historical photographs provide some information about the size and location of fluvial sandbars, and the presence of upland gullies, in the 1960s and earlier (for example, Schmidt and Graf, 1990), but problems of exposure and resolution limit their utility for quantifying upland ground cover, dune-migration rates, or gully dimensions. However, even with few representations of predam upland geomorphic conditions, we can identify some links between dam operations and upland sand resources by analyzing upland conditions in the modern river corridor at landscape scale, and by measuring rates and processes of landscape change at site scale.

Statistically significant differences in ground cover (biologic soil crust and vegetation), open sand area, and aeolian sand-transport rates between upland sand deposits with and without modern aeolian sand supply (MFS and RFS landscapes) indicate that availability of modern sand supply plays a critical role in the geomorphic and ecosystem evolution of upland landscapes (Draut, 2012). Because upland areas no longer receive fluvial sand replenishment from floods—their primary sediment source in predam time—and because vegetation now covers most channel-margin and predam sandbar deposits, the only remaining upland sediment supply comes from aeolian sand transport from controlled-flood sandbars. Analyzing 27 upland sand areas of Marble–Grand Canyon, Draut (2012) found that landscapes with modern aeolian sand supply from controlled-flood sandbars have less biologic soil crust, less vegetation, and much greater sand-transport activity than do upland areas without modern aeolian sand supply.

With fewer, smaller modern sources of aeolian (originally fluvial) sand under dam operations, many upland areas now apparently contain less active aeolian sand than is natural. Active sand is that which shows evidence for contemporary aeolian sand transport, including wind ripples and, locally, slipfaces at the angle of repose (fig. 7; Lancaster, 1994); in the Colorado River ecosystem, active aeolian sand typically contains less than 20 percent biologic crust cover (Draut, 2012). The proportion of active aeolian river-derived sand in lower Marble Canyon (RM 44–61) is substantially less than in the geomorphically and climatically similar Cataract Canyon reach of the Colorado River upstream from Lake Powell, where sediment-rich floods occur annually; this difference is inferred to result from dam-imposed flow and sand-supply limitation (Draut, 2012). The findings of Draut (2012) indicated that further work to quantify gully extent in active and inactive aeolian sand areas could indicate whether the unnaturally low proportion of active sand area downstream from Glen Canyon Dam promoted extensive gully development. The initial, spatially limited identification of areas with and without modern sand supply (MFS and RFS landscapes; Draut, 2012) also suggested that a more refined process was needed to classify archeological sites according to their relative potential to receive aeolian sand after controlled floods.

In view of the potential for rain, wind, and the river to alter landscapes associated with cultural sites, multiple research and monitoring efforts have attempted to quantify landscape change and its causes at selected archeological sites. The largest-scale erosion assessment to date has been that of Pederson and O'Brien (2014), who developed and analyzed a geospatial database of 227 river-corridor sites throughout Marble–Grand Canyon selected for their relevance to management concerns. Pederson and O'Brien (2014) found that gully erosion was the dominant cause of severe site degradation, with 184 study sites displaying evidence for overland flow and nearly half (112 sites) having overland flow as the primary erosive process. Creep, rainsplash, and bioturbation also degraded archeological sites over time, displacing artifacts downslope or otherwise altering their context. Diffusive and creep processes were evident at 165 sites, and were the primary degradation process at 68 sites (Pederson and O'Brien, 2014). Modern aeolian erosion (deflation or scour) and visitation impacts also affected sites, but to a lesser degree—aeolian processes had some geomorphic effect at 89 of the 227 sites—and sediment deposition by wind or water was rare, occurring at only 15 sites (Pederson and O'Brien, 2014).

Researchers have documented landscape change at high spatial resolution over seasonal to annual time scales at approximately 20 archeological sites, using topographic surveys, photogrammetry, and terrestrial-lidar measurements (Pederson and others, 2003, 2006; Collins and others, 2008, 2009, 2012, 2014). These analyses complemented monitoring by the National Park Service (NPS) that has documented changes to cultural sites using direct observation, repeat oblique photography, and occasional topographic surveys of select gully segments—lower-resolution methods applied over greater spatial and temporal scales, encompassing several hundred sites over more than two decades. Together, these efforts have shown evidence for episodic erosion by rainfall-runoff gullying as well as wind deflation, and local occurrences of aeolian inflation, with erosion dominating (Collins and others, 2016).

Understanding the frequency and magnitude of landscape-altering weather events is an important aspect of analyzing the potential for dam operations to counteract erosive processes and slow the degradation of cultural resources. Measurements of landscape change, made in conjunction with high-resolution rainfall and wind measurements at 15 locations for intervals of 2–6 years each since 2003 (Draut and Rubin, 2005, 2006; Draut and others, 2009a,b; Caster and others, 2014; Dealy and others, 2014), have provided valuable information about the magnitude and frequency of weather events that affect archeological sites, and on threshold conditions for landscape change (Collins and others, 2016).

Figure 7. Active and inactive aeolian sand deposits. (*A*) and (*B*) show examples of active aeolian sand, displaying wind ripples that indicate recent sand transport, and in (*A*), sharply defined dune crests that indicate active migration. Note abundant bare, open sand with sparse vegetation and little to no biologic soil crust. (*C*) and (*D*) show aeolian dune forms that are inactive, with well developed biologic crust cover indicating lack of recent aeolian sand movement. An archeological feature is visible in the foreground of (*D*). (*E*) Inactive aeolian dunes with surface cover that includes biologic soil crust and abundant vegetation (mostly exotic brome grass, in this case). (*F*) Landscape view common in Colorado River-corridor dune fields, in which there is both active and inactive (vegetated and biocrusted) dune area.

Project Objectives

The objectives of our study (project J under the GCDAMP biennial work plan) were to better define and quantify the effects, and potential effects, of Glen Canyon Dam operations on upland archeological sites and their surrounding river-corridor landscape. Building on the findings described above, this phase of research was based upon the question:

- Are archeological sites in the Colorado River corridor eroding or changing faster or in a significantly different manner than they would if Glen Canyon Dam were operated differently than it has been?

Within the context of addressing that broad question, we investigated landscape processes that included aeolian sand transport and overland-flow erosion. Given that some archeological sites are known to receive aeolian sand supply after controlled flood flows that enlarge fluvial sandbars directly upwind (Draut and others, 2010), in Section I we addressed the question:

- What number, and what proportion, of cultural sites in the Colorado River corridor potentially receive aeolian sand supply from controlled flood flows?

One important focus was to define the extent of gully formation and annealing processes in the river-corridor landscape. To investigate the effectiveness of aeolian sand activity as a gully-annealing process, we pursued the following additional questions in Section II:

- How does the relative abundance of active and inactive aeolian sand vary in different segments of the Colorado River corridor?
- How does the degree of gully incision differ in sand deposits that are active versus inactive with respect to aeolian sand transport?
- To what extent does aeolian sand transport counteract gully erosion in Marble–Grand Canyons?

We also evaluated site-scale rates and patterns of landscape change at several upland sites known to receive aeolian sand from controlled-flood sandbars. In Section III of this report, we asked:

- Does aeolian sand supply from controlled-flood sandbars to archeological sites cause enough deposition to offset erosion, and thereby protect the archeological resources?
- In areas with modern aeolian sand supply, and with land surfaces undergoing both gully erosion and active aeolian sand transport, is there net sediment loss and topographic lowering such that cultural resources are affected?

Finally, sites in Glen Canyon have been considered potentially more susceptible to erosion linked directly to dam operations and, indirectly, to the lack of modern sandbars providing sources of windblown sand. Therefore, in Section IV we addressed the questions:

- What rates and processes of landscape change occur at Glen Canyon sites, and how do they contrast with those measured in Marble–Grand Canyon, where the modern sand supply is greater?
- Are sites in Glen Canyon more vulnerable to long-term erosion than are sites in sediment-richer Marble–Grand Canyon?

Section I - Potential Aeolian Sand Supply to River-Corridor Archeological Sites in Grand Canyon National Park

Background

For decades, researchers have recognized that many archeological sites depend on Colorado River-derived sand as a substrate, as a cover, or both—either as fluvial deposits or as aeolian reworked sand that originated in fluvial deposits (hereafter we use *river-derived sand* to signify both). Prior to our study, there had been no systematic assessment of the modern potential for wind to supply sand to each site. We evaluated the potential for wind to supply sand from recently active fluvial sand deposits to river-corridor archeological sites in Marble–Grand Canyon (Grand Canyon National Park), between Lees Ferry and Separation Canyon (RM 0 to 239.8). Our study reach ended at the confluence of Separation Canyon and the Colorado River because downstream from that confluence, sedimentary deposits of the Lake Mead reservoir delta complicate interpretation of sediment-supply effects from Glen Canyon Dam operations. We evaluated the geomorphic context of archeological sites, local wind directions, the presence of upwind fluvial sandbars, and local topography and vegetation; we used those data to assess the potential for aeolian sand to reach each of 358 river-corridor cultural sites. Our evaluations were facilitated by collaboration with the river-corridor archaeology program at Grand Canyon National Park, which provided site-monitoring data and facilitated many site visits; this study complemented the O'Brien and Pederson (2009a,b) landscape-process study of 227 river-corridor archeological sites. A similar analysis for approximately 50 river-corridor sites between Glen Canyon Dam and Lees Ferry, in Glen Canyon National Recreation Area, was completed in 2016.

Research Question

- What number and what proportion of archeological sites potentially receive aeolian sand supply from controlled-flood deposits?

Classification System and Methods

We evaluated the potential for wind to supply sand to cultural sites by using direct field observations and by examining historical aerial photographs. This analysis focused on four different time intervals (table 1): (1) 2012–14, during which time three controlled floods occurred that lasted 3 days each with discharge above 1,000 m^3/s; (2) April 1996, several weeks after a 7-day controlled flood of 1,300 m^3/s; (3) 1984–85, following a postdam flood with an instantaneous peak discharge of 2,740 m^3/s in 1983 (maximum daily average discharge was 2,610 m^3/s on June 29, 1983), and flows above 1,000 m^3/s continuously for several months each in 1983, 1984, and 1985 (table 1); and (4) June 1973. High flows preceding the June 1973 imagery included several years in which daily average discharge exceeded 1,000 m^3/s for weeks to months, and several much larger predam peaks (table 1; Topping and others, 2003; U.S. Geological Survey, 2015). Thus, for the 2012–14 interval and for April 1996, we evaluated potential aeolian sand supply resulting from sandbar growth from specific controlled floods of similar magnitude, whereas for the two earlier time periods (that is, 1984–85 and 1973) we interpreted fluvial sand sources that formed from a variety of flows that exceeded the range of normal dam operations, rather than from an isolated controlled-flood event.

For the 2012–14 (hereafter, modern) time period, we assessed the geomorphic effects of controlled floods by direct field observation shortly after the floods receded. Particularly for the November 2012 high flow, we evaluated geomorphic effects, including deposition of fluvial sandbars upwind from specific archeological sites, by using oblique photographs taken on river trips during flows of 226 m^3/s during the two weeks immediately after that flood, as well as from field observations made in May 2013 during two additional river trips on flows between 226 and 375 m^3/s. Similarly, effects of the November 2013 controlled flood were evaluated by field observations of recent sand deposits in May 2014 during a river trip on flows between 181 and 308 m^3/s.

We analyzed the effects of the 1996 controlled flood by inspecting archival photographs that were taken at a flow of 226 m^3/s approximately three weeks after the flood. We compared the presence of fluvial deposits in April 1996 after the flood to those visible in aerial photographs taken in March 1996, just before the flood. Although our analyses of the effects of the 1996 and modern controlled floods were based on different data resources (archival aerial photographs versus oblique photography and field visits), the accuracy of both assessment methods is comparable, as both analyses primarily relied on photographic evidence taken within two weeks following each flood.

The 1983 flood (2,740 m^3/s) was the largest postdam flow release. Effects of this peak flow, and the months-long high flows in 1983 and 1984 (table 1), were evaluated by examining two sets of aerial photographs—taken in October 1984 and June 1985—for the presence of fluvial sandbars upwind from each archeological site. The October 1984 aerial photographs were taken at a discharge of approximately 140 m^3/s, and we used these photographs whenever possible. To analyze 20 archeological sites for which the 1984 aerial images were missing from photographic archives (including where the original flight path missed a short section between RM 209.3 and RM 209.9, and everywhere downstream from RM 214), we used aerial photographs taken in June 1985 during discharge of 850–1,020 m^3/s. We did not distinguish among fluvial deposits formed during the peak discharge of the flood of 1983, deposits formed by the high flows of 1984 whose magnitude was nearly the same of later controlled floods, and other flows of approximately 850 m^3/s, although Schmidt and others (2004) were able to distinguish among those deposits in some reaches. Rather than trying to specify which 1980s flows had contributed more substantially to sandbar presence or sand abundance, we focused on ascertaining whether upwind fluvial sand resources existed for each archeological site at that time. Similarly, for the 1973 time interval (for which we used photographs taken in June 1973 at discharge ranging from 170 to 368 m^3/s), at most locations we did not attempt to identify which of the specific high-flow events in the preceding two decades had supplied fluvial sand—except in some cases where bright, apparently open sand deposits seemed to match the 3,540-m^3/s shoreline modeled by Magirl and others (2008) that represented the 1958 flood peak. Instead we simply assessed whether fluvial sand deposits existed in 1973 that could have supplied aeolian sand to archeological sites downwind. For each time interval, we assumed that a subaerially exposed, open, unvegetated fluvial sandbar potentially could serve as a source from which wind could transport sand.

Table 1. Time intervals used in archeological-site-classification analysis and Colorado River high flows preceding each interval. Data indicate daily average discharge measured at U.S. Geological Survey gaging station 09402500 (fig. 1).

Time interval analyzed	Recent preceding high flows	
	Discharge (m^3/s)	Dates
2012–2014	1,080	November 12–14, 2014
	1,060	November 13–15, 2013
	1,270	November 20–22, 2012
	1,250	March 6–8, 2008
	1,190	November 22–24, 2004
	910	September 6–8, 2000
	900	May 4–6, 2000
1996	1,300	March 27–April 2, 1996
	760–860	January and February 1993
1984–1985	1,000–1,320	May 18–June 28, 1985
	1,000–1,260	May 7–July 18, 1984
	1,000–2,610	June 4–August 11, 1983
1973	1,000–1,580	April 24–June 26, 1965
	1,000–2,400	April 19–July 11, 1962*
	1,000–1,300	June 6–26, 1960*
	1,000–3,030	April 21–June 24, 1958*
	1,000–3,510	May 8–August 11, 1957*

We classified each of the 358 river-corridor archeological sites for each of the four time intervals (2012–14 or modern, 1996, 1984–85, and 1973) based on the degree to which each site potentially received windblown sand from adjacent, upwind active fluvial sand deposits. Our evaluation of each site included documenting (1) geomorphic and sedimentary context (whether fluvial, aeolian, or other, as assessed in this analysis and by any previous research at each site), (2) site elevation relative to inundation potential for historic flood flows (based on flood stages modeled by Magirl and others, 2008), (3) dominant wind direction, (4) the presence of a recent fluvial sand deposit upwind of the site, assessed for each time step independently, and (5) the presence of any vegetation or topographic barriers between the fluvial deposit and downwind archeological site. These metrics were used to define five categories, or types, of archeological sites. Types 1–4 are those whose geomorphic context includes river-derived sand as an integral component—fluvial, aeolian, or both. Type 5 sites are those at which river-derived sand is absent or, if present, is merely incidental to site context. The site-type definitions are as follows:

- Type 1: Sites with an adjacent, upwind, recent subaerial fluvial sand deposit, and where there are no substantial barriers to impede aeolian sand transport from the flood deposit toward the archeological site.
- Type 2: Sites with an adjacent, upwind, recent subaerial fluvial sand deposit, but with a barrier separating the flood deposit from the archeological site. Barriers were interpreted to limit potential aeolian sand transport from the fluvial deposit toward the archeological site, but may not eliminate sand movement entirely from sandbar to archeological site. We defined three subtypes:
  - Type 2a: Vegetation barrier present (may be riparian vegetation or higher-elevation, nonriparian upland vegetation).
  - Type 2b: Topographic barrier present (most commonly a tributary channel, but in several cases a steep bedrock cliff or large boulder deposit).
  - Type 2c: Both vegetation and topographic barriers present.
- Type 3: Sites at which an upwind shoreline exists for a recent high flow, but where the recent high flow resulted in no open, unvegetated sandbar along the river margin.
- Type 4: Sites at which there is no upwind shoreline corresponding to a recent high flow, but whose geomorphic context does involve river-derived sand.
- Type 5: Sites in the river corridor at which Colorado River-derived sand is absent or is only incidental to site context, such as sites entirely on bedrock or talus.

Where possible, we assessed locally dominant wind directions from direct measurements at weather stations operated in the river corridor by GCMRC (Draut and Rubin, 2005, 2006, 2008; Draut and others, 2009a,b, 2010; Caster and others, 2014; Dealy and others, 2014). If no weather station operated near a particular area of interest, we inferred the locally prevailing wind direction from orientations of aeolian dune crests and slip faces, sand shadows in the lee of rocks and vegetation, and wind ripples (fig. 8). These features, if clearly visible in the field, reliably indicate the dominant directions of recent sand-transporting winds. Field observations of geomorphic wind indicators were made during the 2013 and 2014 river trips; we assumed that the locally dominant wind directions inferred in 2013–14 were the same in the three earlier time intervals we considered. This assumption is reasonable because dune crests, slipfaces, and large sand shadows are persistent features that tend to form over time scales longer than one or several wind events or seasons. Our observations at many of these sites over many years indicate that dune and sand-shadow orientations commonly persist over timeframes of at least a decade. Wind ripples, being much smaller features than dunes or sand shadows (fig. 8), are more transient and may be less representative of the long-term locally dominant wind direction. For this reason, we inferred wind direction from wind ripples only if neither well-defined dunes nor sand shadows were available. Similarly, if sand shadows of various sizes were present, we inferred wind direction from the largest available sand shadows, based on the assumption that those would reflect the dominant wind direction. However, at no sites did we observe large and small sand shadows that differed markedly in their orientations. This suggests that variable competing wind directions are not a major factor affecting river-corridor geomorphology in Marble–Grand Canyon, an assumption generally corroborated by weather-station data.

Thus, we defined type 1 archeological sites as having the greatest potential to receive windblown sand supply from recently deposited fluvial sandbars, with the potential for aeolian sand supply decreasing in order from types 2–4. The presence of vegetation or topographic barriers at type 2 sites does not preclude aeolian sand from reaching a downwind site, but is interpreted to impede aeolian sand transport at least in part. We infer that vegetation or topographic barriers limit aeolian sand movement primarily by reducing the sand flux that moves by saltation or reptation (creep), transport mechanisms that rely on near-bed interactions among sand grains (for example, Nickling and McKenna Neuman, 2009, and references therein). Saltation and reptation can move substantial amounts of sand along a continuous sand bed (especially the coarser fraction of sand grains; Lancaster, 1995; Cheng and others, 2015), but where the ground surface contains, for example, cobble-bedded tributary channels or dense vegetation, sand entrainment and transport by saltation and reptation will be more limited. Alternatively, aeolian sand can travel in suspension higher above the bed, potentially

reaching sites that are downwind of vegetation or topographic barriers. Archeological sites are known to receive aeolian sand deposition in at least some cases from suspension transport. Aeolian sand deposition (inflation) on a type 2b site, separated by a tributary channel from the nearest upwind fluvial sandbar, has been documented previously during high-resolution lidar surveys in Marble Canyon (Collins and others, 2009). During strong wind events, we have also observed sand traveling in suspension from sandbars on one side of the river to the other (several hundred meters). Although aeolian transport in suspension across the river is a possible means of sand delivery to archeological sites, for the sake of assessing the most readily available sand sources we considered only sandbars directly adjacent to sites (on the same side of the river) and on the upwind side of the site with respect to the locally dominant wind direction.

Type 3 sites, which have upwind shorelines where no open sandbar formed during recent flooding, include sites that formerly may have been supplied by aeolian sand derived from eddy sandbars or channel-margin sand deposits. These former sand sources are now commonly covered and stabilized by postdam riparian vegetation (Sankey and others, 2015). Some new sand deposition may occur within the vegetation, but vegetation cover may not allow new deposition to be detected using aerial imagery. Places where riparian vegetation extends all the way to the river margin would be classified as type 3, whereas riparian vegetation

Figure 8. Examples of geomorphic features used to infer wind direction. Black arrows show inferred local prevailing wind directions. (*A*) and (*B*) Sand shadows formed as sand accumulated on the downwind, lee side of an obstacle such as a rock or vegetation. Sand shadows point downwind. Transverse wind ripples (which form perpendicular to wind direction) corroborate the wind direction inferred from orientations of the large sand shadows in the lee of shrubs. (*C*) Dune crest and slipface orientation indicate dune migration from right to left; this dune is a source-bordering dune formed from a 2012 controlled-flood sandbar. (*D*) A more complex situation in which two sets of wind ripples are superimposed on the stoss (upwind) side of an active dune; compass for scale. The superimposed bedforms indicate recent wind oriented slightly oblique to the dominant prevailing wind direction; the dominant direction was inferred from the orientation of the largest bedform present (the dune crest).

forming a border at the landward side of an open sand area, but with open sand remaining between vegetation and the river, would constitute a type 2a situation (fig. 9). Vegetation can alter fluvial depositional processes by increasing flow resistance, reducing water velocities and erosive power, increasing bank cohesion, and thus affecting fluvial sediment mobility, transport and deposition (Thorne, 1990; Nepf, 1999; Tal and Paola, 2010). The role that vegetation may play in impeding or enhancing future deposition is currently under study by others (Ralston and others, 2014; Mueller and others, 2015), and is not discussed further in this report. However, changes in vegetation conditions along shorelines that currently do not show evidence of having recent sand deposits could result in a reclassification of some type 3 sites in the future.

Type 4 sites do not receive sand transported by wind from recent flood deposits given the respective positions of flood deposits and locally dominant wind directions. Type 4 sites received river-derived sand (fluvial and aeolian) either from predam river flows (see Introduction) or from other, lower-elevation former source areas that are now covered by vegetation or are otherwise no longer evident in the modern postdam landscape. Many locations in the river corridor, including those with type 4 characteristics, would have received sand on or upwind of them only as a result of floods of 4,810 m^3/s and larger (Magirl and others, 2008). This interpretation is consistent with predam flood deposits having been identified at type 4 sites for which detailed stratigraphic analyses exist (for example, O'Connor and others, 1994; Hereford and others, 2000a; Draut and others, 2008; Anderson and Neff, 2011; Pederson and others, 2011; Museum of Northern Arizona, 2012); most type 4 sites also contain aeolian dunes. Therefore, although type 4 sites have

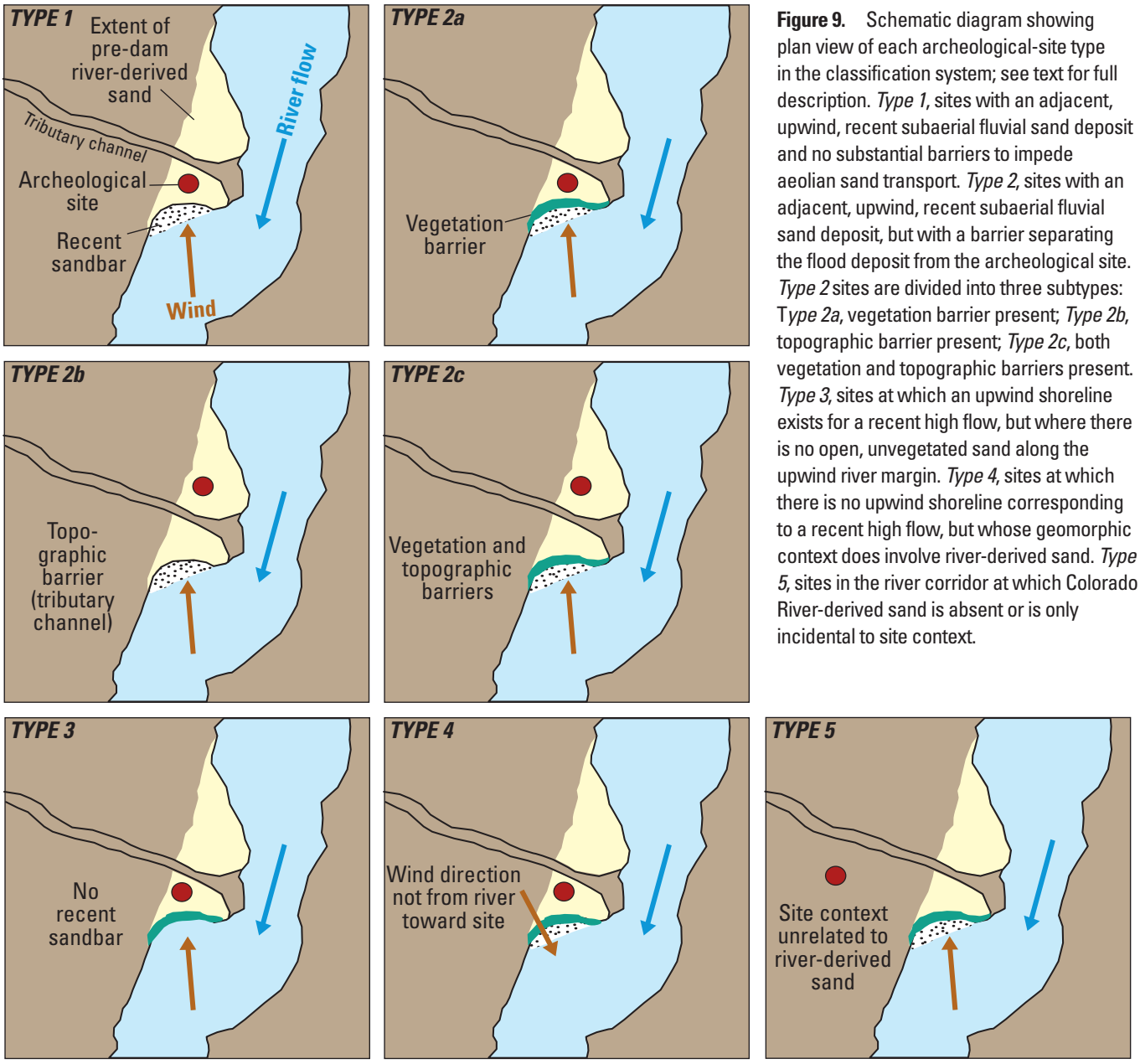

Figure 9. Schematic diagram showing plan view of each archeological-site type in the classification system; see text for full description. *Type 1*, sites with an adjacent, upwind, recent subaerial fluvial sand deposit and no substantial barriers to impede aeolian sand transport. *Type 2*, sites with an adjacent, upwind, recent subaerial fluvial sand deposit, but with a barrier separating the flood deposit from the archeological site. *Type 2* sites are divided into three subtypes: T*ype 2a*, vegetation barrier present; *Type 2b*, topographic barrier present; *Type 2c*, both vegetation and topographic barriers present. *Type 3*, sites at which an upwind shoreline exists for a recent high flow, but where there is no open, unvegetated sand along the upwind river margin. *Type 4*, sites at which there is no upwind shoreline corresponding to a recent high flow, but whose geomorphic context does involve river-derived sand. *Type 5*, sites in the river corridor at which Colorado River-derived sand is absent or is only incidental to site context.

river-derived sand as an integral part of their context, they would not receive substantial aeolian sand from 1,200-m³/s controlled-flood flows or, in many cases, even from deposits of larger postdam flows. Several type 4 sites do not appear to contain flood strata either, but appear to contain river-derived aeolian sediment as a cover despite not being downwind from any apparent flood shoreline nor near any substantial terrace deposit from which aeolian sand could have originated. In those cases (approximately 3–5 of the 358 sites we analyzed), aeolian sand may have reached those sites during occasional wind events whose direction deviated from the usual prevailing wind orientation.

Type 5 sites are unaffected by aeolian sand supply. They are included in this report for the sake of inventory completeness, in order to determine what proportion of river-corridor archeological sites potentially received aeolian sand supply.

Results

Fluvial sandbars and vegetation change substantially over time in Marble–Grand Canyon, thus the number and proportion of archeological sites in most of our defined categories changed over the intervals considered as well (fig. 10, appendix). The changing site classifications over time resulted from (1) changes in sandbar occurrence (whether fluvial sand deposits were present upwind of each site), (2) changes in vegetation—almost always growth, but in rare cases vegetation loss—and, less commonly, (3) tributary activity having changed local topography such that sandbar formation or aeolian sand movement (or both) was affected.

We determined that 266 of the 358 sites considered (74 percent) have Colorado River sand as an integral part of their geomorphic context. Among the sand-dependent sites, 232 fall into

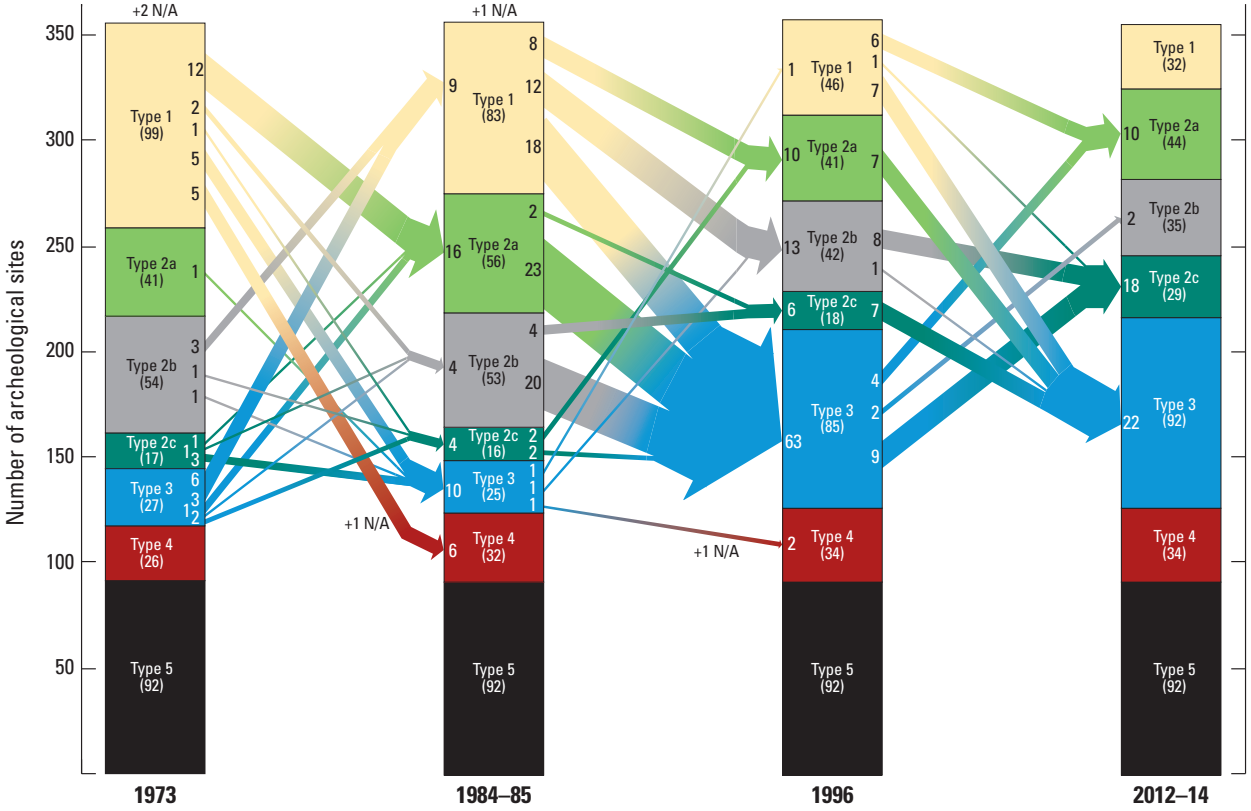

EXPLANATION

Types 1-4: river-derived sand integral to site context (fluvial or aeolian)

- 1 = Flood sediment deposition adjacent and upwind
- 2a = Vegetation barrier
- 2b = Topographic barrier
- 2c = Both vegetation and topographic barriers
- 3 = Flood shoreline upwind, but no deposition
- 4 = No flood shoreline upwind
- 5 = River-derived sand absent or only incidental to site context

1 **Number of archeological sites**

Figure 10. Results of archeological-site classification for each of four time intervals: 1973, the mid-1980s (1984 or 1985, depending on the availability of photographs), April 1996, and 2012–2014. Colored columns indicate number of sites, out of 358 sites analyzed, in each of the 7 categories defined by this study. Types 1–4 refer to sites in which river-derived sand forms an integral part of the geomorphic context. At Type 5 sites, river-derived sand is either absent or, if present, is merely incidental to site context. Arrows indicate sites that transitioned from one category to another between time steps; arrow width is proportional to number of sites that underwent transition. N/A, sites potentially inundated by recent flood flows, but with aerial view of possible deposition zone not visible due to overhanging bedrock. See text for details.

types 1–3 (65 percent of the sites, or 87 percent of sand-dependent sites)—those that are downwind of controlled-flood shorelines (of 1,200 m^3/s flows). The remaining 34 sand-dependent sites met the criteria for type 4, having locally dominant wind directions that would not supply sand to them from river shorelines reached by modern dam operations, even shorelines of 1,200-m^3/s controlled floods. Our documentation of spatial variations in local wind directions showed that although many regions of the canyon have persistent wind directions (most commonly toward upstream), wind direction can vary greatly around the mouths of large tributaries (fig. 11), with associated spatial variations in likely sand-transport paths.

The number and proportion of type 1 sites—those with the greatest potential to receive aeolian sand supply—decreased substantially over each time step (fig. 10). Whereas 98 cultural sites met the criteria for type 1 conditions in 1973, in the modern (2012–14) time step there were only 32 type 1 sites. Therefore, the proportion of type 1 river-corridor sites has decreased from

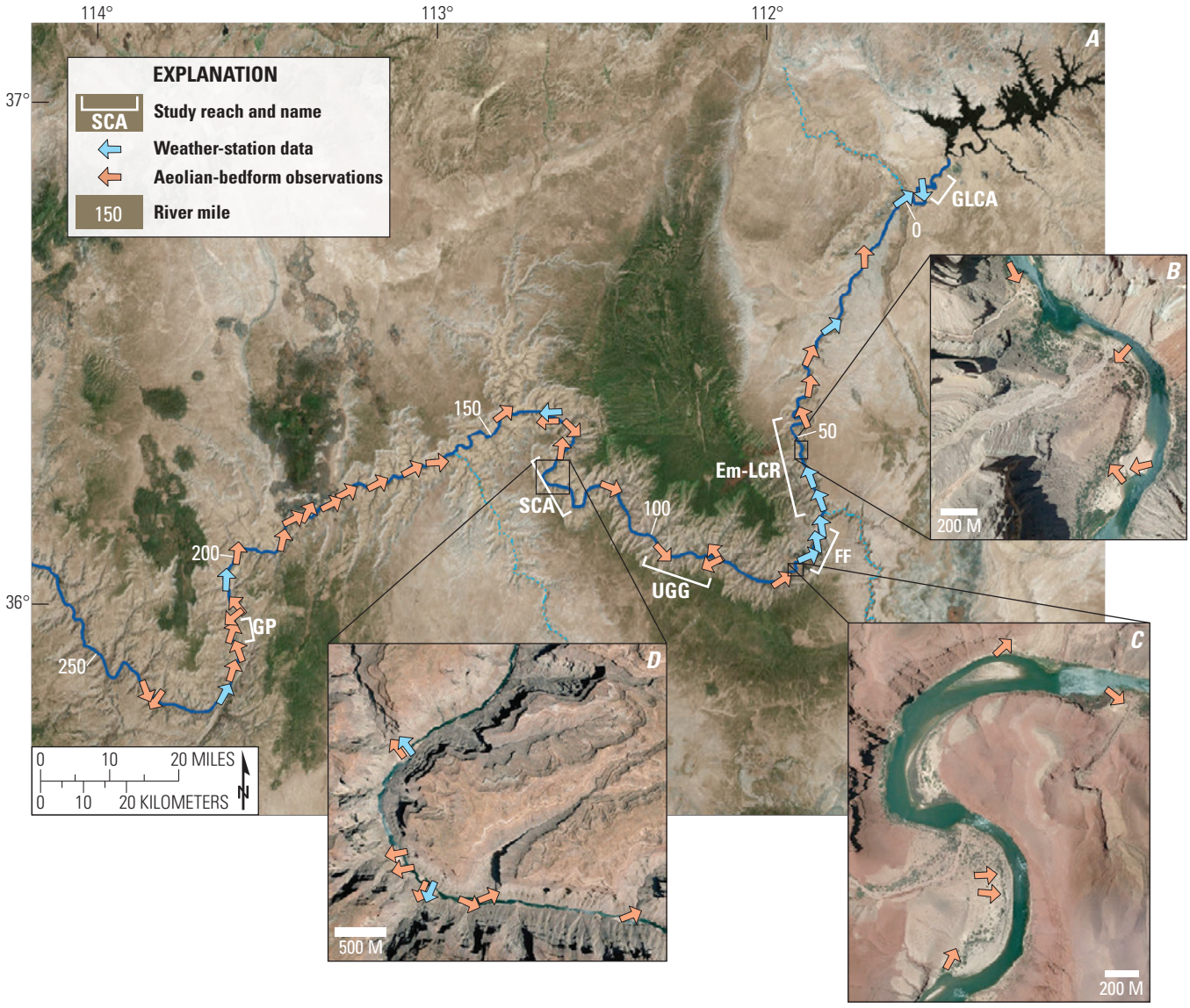

Figure 11. (*A*) Dominant wind directions inferred in Glen, Marble, and Grand Canyons from weather-station measurements (gray arrows) or geomorphic features (pink arrows). River miles (RM), measured downstream from Lees Ferry, in white text. Throughout most of the canyon a wind direction oriented toward upstream prevails, although with local variations around tributary confluences, particularly the large tributaries such as (*B*) Nankoweap and (*C*) Unkar, and also at (*D*) tight bends in canyon orientation. For clarity, additional observations that duplicated those shown in (*A*) were omitted, including approximately 40 locations between RM 65 and 71 and approximately 15 locations between RM 170 and 225. This graphic represents the current, most comprehensive understanding of dominant wind directions through the canyon and although local variations are illustrated, additional local variations also occur on smaller scales. Other situations of local variability probably exist that have not been observed to date. Six study reaches are indicated where aeolian sand activity and gully prevalence were mapped in detail (Section II): Glen Canyon (GLCA), Eminence to Little Colorado River (Em-LCR), Furnace Flats (FF), Upper Granite Gorge (UGG), Stevens-Conquistador Aisles (SCA), and Granite Park (GP).

27 percent in 1973 (37 percent of the 266 sites that depend on river-derived sand) to less than 9 percent today (12 percent of the sand-dependent sites). Moreover, the incidence of sites moving from some other category into type 1 decreased over each time step, from 9 sites that entered type 1 between 1973 and 1984–85 to only one site becoming type 1 in 1996, and none becoming type 1 between 1996 and 2012–14.

The decrease in type 1 sites since 1973 occurred partly by shoreline positional changes, such that open fluvial sand deposits occurred farther inland from the river margin in the 1973 and 1980s imagery, left by flows higher than those in the two later time steps (fig. 12). Positional changes of recent flood shorelines accounted for five sites having transitioned from type 1 to type 4 between 1973 and 1984—as of 1973, bright, apparently open fluvial sand deposits were visible in and upwind of five sites near each other that likely were deposits of the 3,540-m^3/s flood of 1957 (they correspond well with the modeled shoreline; Magirl and others, 2008). By 1984, those sites were judged to be type 4—given the local shoreline morphology and prevailing wind direction, the most recent high flows (including the 2,740-m^3/s flood peak of 1983) had no shoreline upwind of those sites. Shoreline positional differences between the 1980s high water and the 1996 controlled flood also accounted for 12 type 1 sites having become type 2b sites between 1984–85 and 1996 (fig. 10), and for 2 of the 8 sites that transitioned from type 1 to type 2a between 1984–85 and 1996.

Vegetation growth caused many sites to transition from type 1 to type 2, or from type 2b to type 2c (fig. 10). Even at some sites still apparently able to receive aeolian sand supply from fluvial sandbars today, vegetation encroachment appears to have reduced the sand supply or appears likely to necessitate a change in classification soon (fig. 13). In the most recent time step, 1996 to 2012–14, when the similar magnitude of recent controlled floods meant that there were no positional differences in shoreline extent, the loss of type 1 sites was equally attributable to vegetation growth (six type 1 sites becoming type 2a) and to sandbar nondeposition (becoming type 3). Other sites transitioned from type 1 to 2a to 3, as first vegetation growth overtook previously open fluvial sandbars and then either shoreline erosion removed the vegetation-covered sand (fig. 14) or, if the shoreline position did not change, vegetation overgrew the remaining part of the sandbar (Sankey and others, 2015). We observed vegetation loss in several places between 1973 and 1984–85, evidently from removal or overprinting of vegetation by flood deposits from the 2,740-m^3/s flow of 1983.

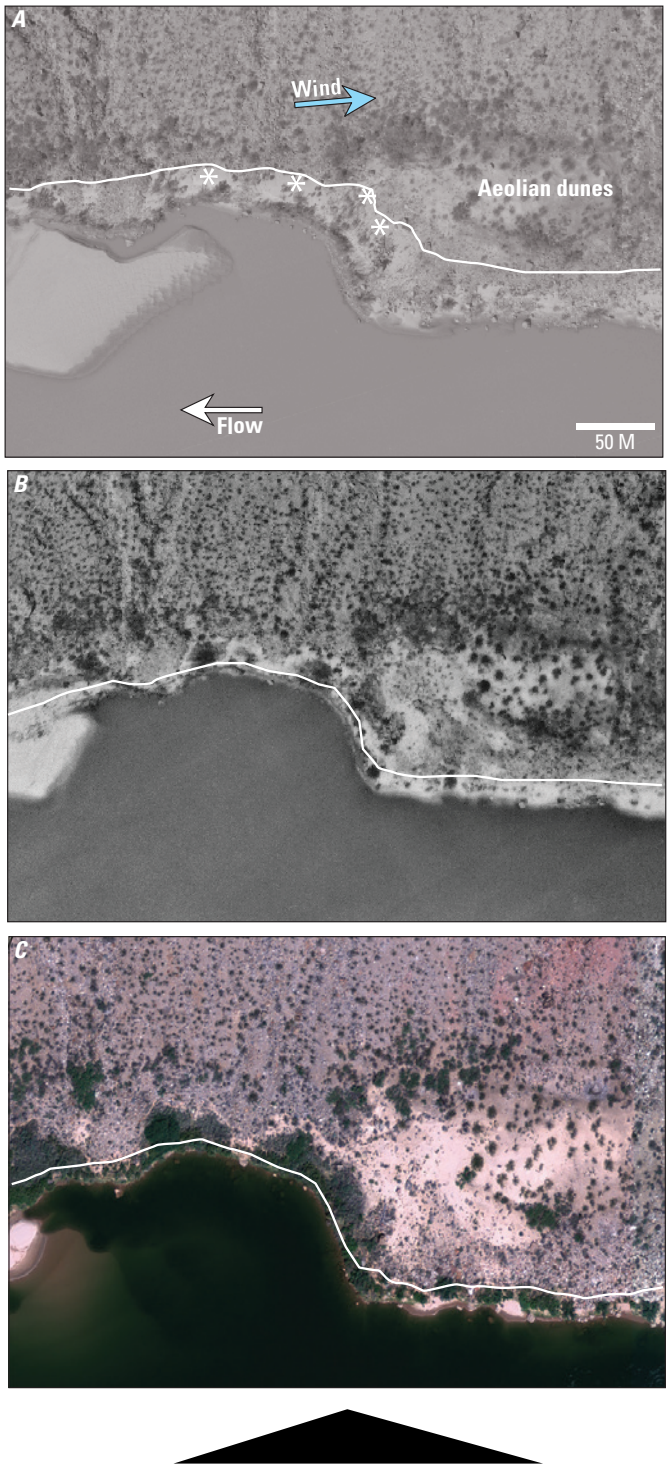

Figure 12. Example of a site that transitioned from type 1 to type 3 (see text for site-type descriptions). (*A*) Aerial photograph from 1984, showing fluvial sand deposits (asterisks) directly adjacent to and upwind of an aeolian dune field; river flow is approximately 140 m^3/s. White line shows approximate limit of the 1983 flood (Magirl and others, 2008; table 1). An archeological site in the aeolian dune field was ranked as type 1 because there were open fluvial sand deposits adjacent to the dune field on its upwind side. (*B*) April 1996, at a flow of 226 m^3/s. Black line shows approximate extent of the shoreline from the March 1996 controlled flood (Magirl and others, 2008; table 1). Although there was a small sandbar at the downstream end of the eddy, there were no recent fluvial sand deposits directly adjacent to and upwind of the dune field, indicating a type 3 ranking for 1996. (*C*) May 2013, at a flow of 226 m^3/s. Black line shows approximate extent of the recent controlled-flood shoreline; the lack of adjacent, upwind fluvial sand deposits indicated type 3 classification. Note abundant riparian vegetation growth on the sand deposits of the 1980s.

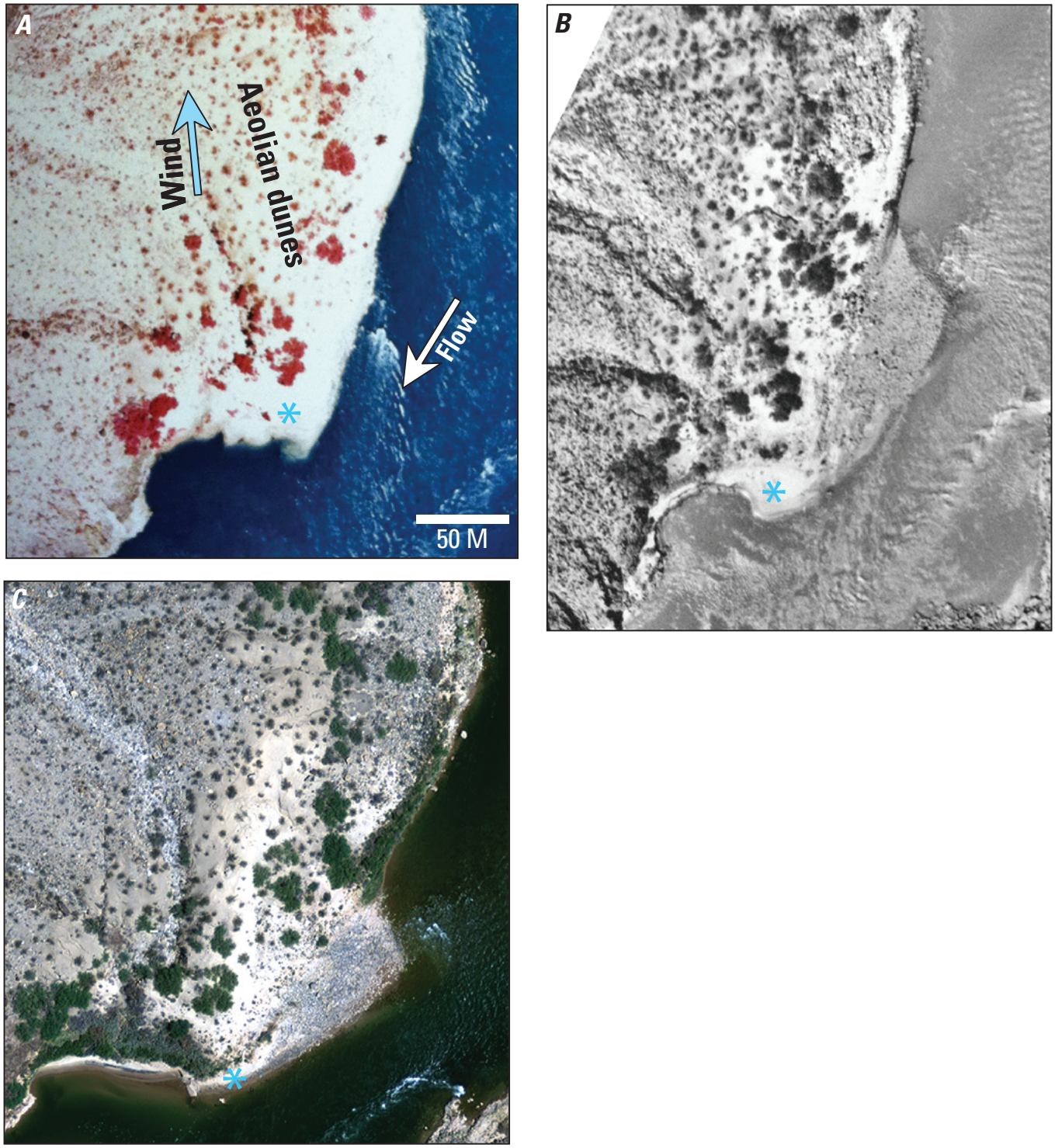

Figure 13. Example of a site transitioning from type 1 to type 2a because of riparian vegetation growth. (*A*) In June 1985 open, unvegetated fluvial sand deposits (blue asterisk) were directly upwind of, and adjacent to, a dune field, indicating type 1 conditions. River flow in (*A*) was between 850 and 1,020 m^3/s. (*B*) In June 1996, although fluvial sandbar area was less than in (A), the site(s) in the dune field still met criteria for type 1 classification; flow was 226 m^3/s. (*C*) As of May 2013, after substantial riparian vegetation growth in the preceding decade, the site barely qualified as type 1, with only a small expanse of fluvial sand (enlarged by the recent controlled flood) having nearly vegetation-free connectivity with the dune field; river flow in (*C*) was 226 m^3/s. This dune field contains archeological site AZ:G:03:0072, discussed in Section III.

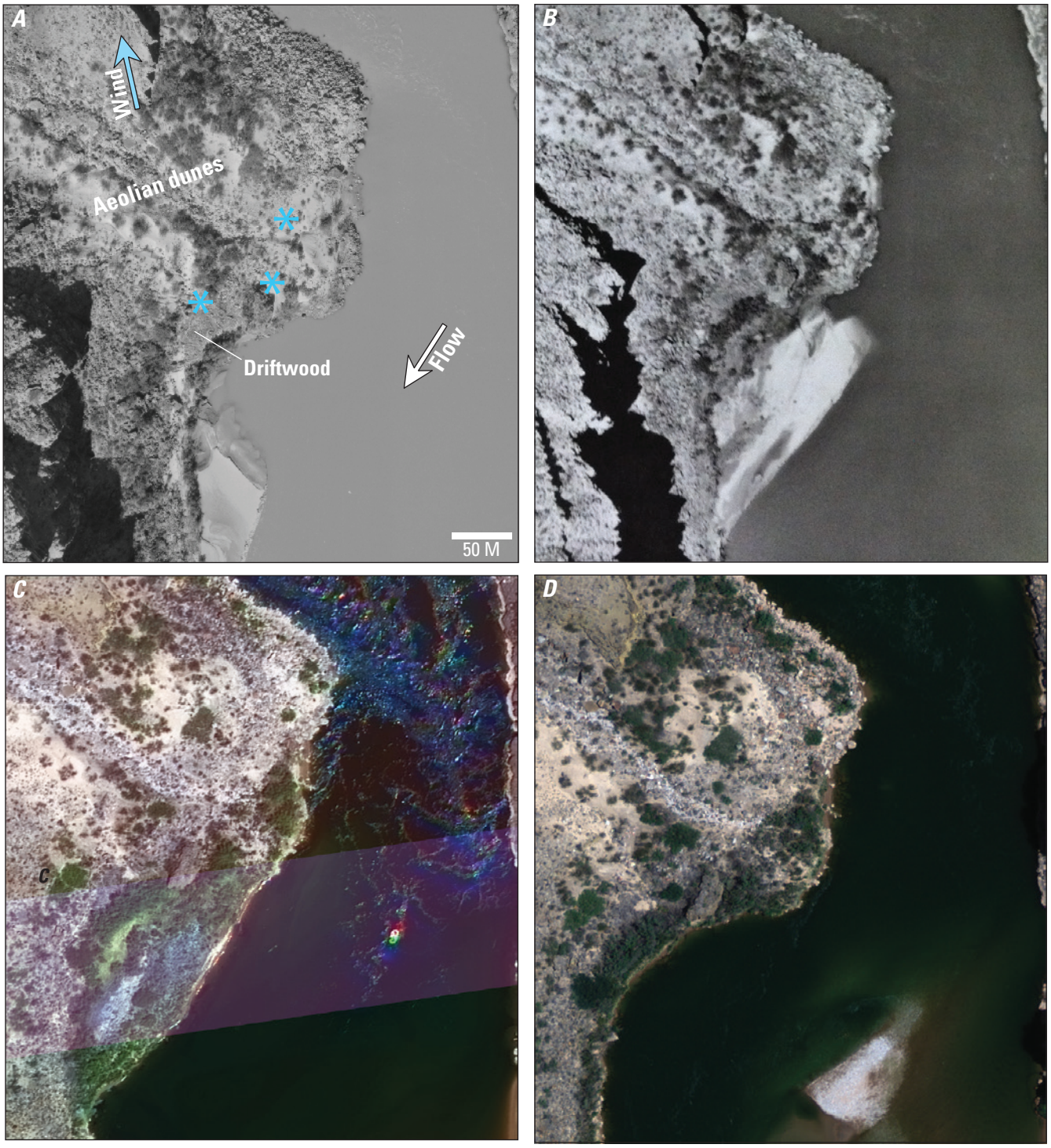

Figure 14. Example of a site that transitioned from type 1 to type 2a to type 3. (*A*) In October 1984 several open, unvegetated fluvial sand deposits (asterisks) were present upwind of this dune field (which is bisected by a tributary channel), presumably left by high flows in 1983 and 1984, indicating type 1 conditions. The 1983 flood (table 1) probably also deposited the large driftwood pile given that its peak stage was directly above that (Magirl and others, 2008). River flow in (*A*) was approximately 140 m^3/s. (*B*) In April 1996, just after a controlled flood, a sandbar filled most of the eddy. Riparian vegetation (and the driftwood pile) separated the sandbar from downwind aeolian dunes, indicating type 2a conditions. Flow was 226 m^3/s. (*C*) By May 2002, vegetation had covered most of the area that was open sand in 1996; flow was 226 m^3/s. (*D*) By May 2013 (shown at a flow of 226 m^3/s), the river had eroded the vegetated sandbar substantially. We observed no sandbar in that eddy after the 2012 or 2013 controlled floods, indicating type 3 conditions for the modern time step.

In general, over the latter two time steps we found a substantial increase in the number and proportion of type 3 sites—those with no fluvial sand deposit upwind. Although some sites that were nondepositional (type 3) in 1996 did have upwind sandbars after more recent controlled floods (15 sites that had been type 3 in 1996 became type 2 in 2012–14; fig. 10), there was still a net gain of type 3 sites over that time step. Type 3 sites included more than one fourth of all river-corridor archeological sites in the most recent time step (92 of 358), and more than one third of all sand-dependent sites (92 of 266 sites in types 1–4).

At several sites, tributary floods or debris flows influenced the local morphology enough to effect a transition from one category to another. Debris-flow deposition can change the morphology of a fan-eddy complex such that the eddy traps fluvial sand more readily; the clearest example of this in our dataset is shown in figure 15 (see also Yanites and others, 2006). We noted several other sites at which

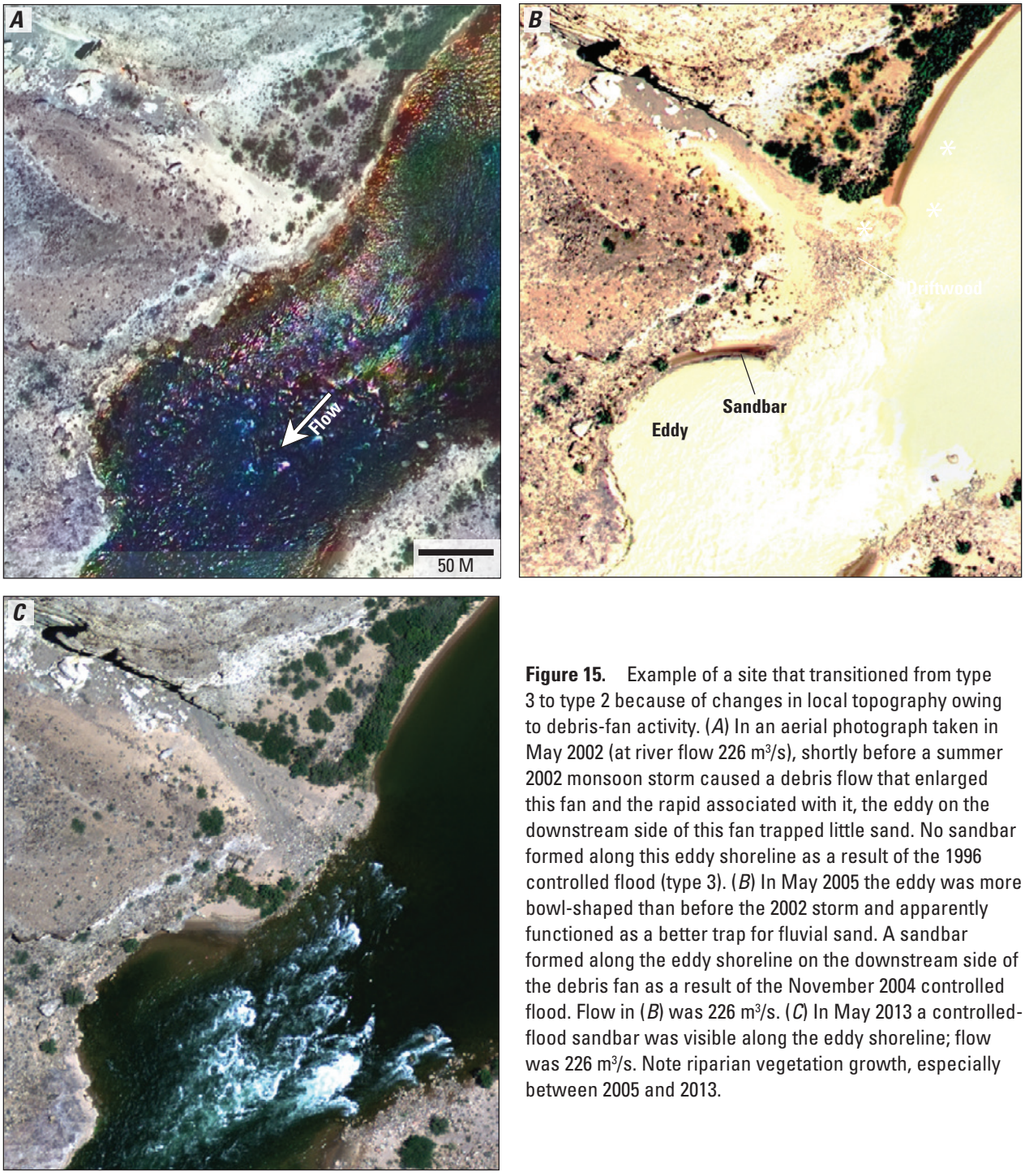

Figure 15. Example of a site that transitioned from type 3 to type 2 because of changes in local topography owing to debris-fan activity. (*A*) In an aerial photograph taken in May 2002 (at river flow 226 m^3/s), shortly before a summer 2002 monsoon storm caused a debris flow that enlarged this fan and the rapid associated with it, the eddy on the downstream side of this fan trapped little sand. No sandbar formed along this eddy shoreline as a result of the 1996 controlled flood (type 3). (*B*) In May 2005 the eddy was more bowl-shaped than before the 2002 storm and apparently functioned as a better trap for fluvial sand. A sandbar formed along the eddy shoreline on the downstream side of the debris fan as a result of the November 2004 controlled flood. Flow in (*B*) was 226 m^3/s. (*C*) In May 2013 a controlled-flood sandbar was visible along the eddy shoreline; flow was 226 m^3/s. Note riparian vegetation growth, especially between 2005 and 2013.

tributaries incised through formerly continuous fluvial or aeolian sand deposits (such as one site that transitioned from type 1 to type 2c between 1996 and 2012, fig. 10).

Site transitions from one category to another showed some noteworthy spatial patterns (figs. 16–19). The incidence of type 2a sites (those with vegetation barriers) has increased with time in the western canyon, particularly downstream from RM 190 (figs. 16–19). The aforementioned increase in type 3 occurrence is especially pronounced in the western canyon; 20 of the 22 sites that became type 3 in the most recent time step (1996 to 2012–14) were downstream from RM 175 (figs. 18, 19).

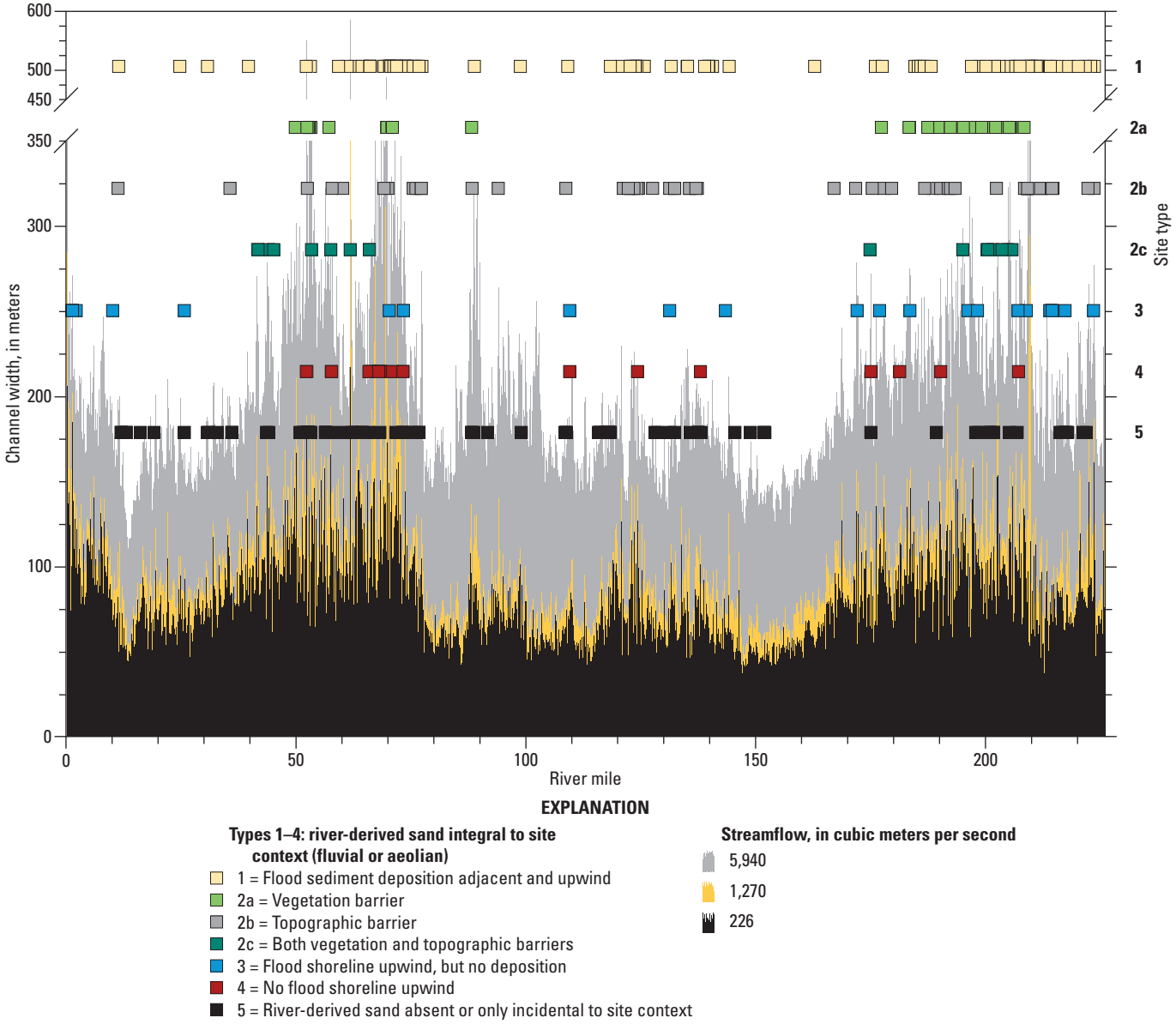

Figure 16. Distribution of river-corridor archeological sites by site type as of 1973, with distance along the river corridor, in river miles downstream from Lees Ferry (fig. 1). Gray-shaded and black regions indicate width of river flow (Magirl and others, 2008) for discharge of 226 m^3/s, 1,270 m^3/s (controlled-flood discharge), and the highest historical discharge, 5,947 m^3/s (in spring 1884). See text for full description of site types. Although the site-classification analysis continued to RM 239.8, the shoreline modeling by Magirl and others (2008) extended only to RM 226.

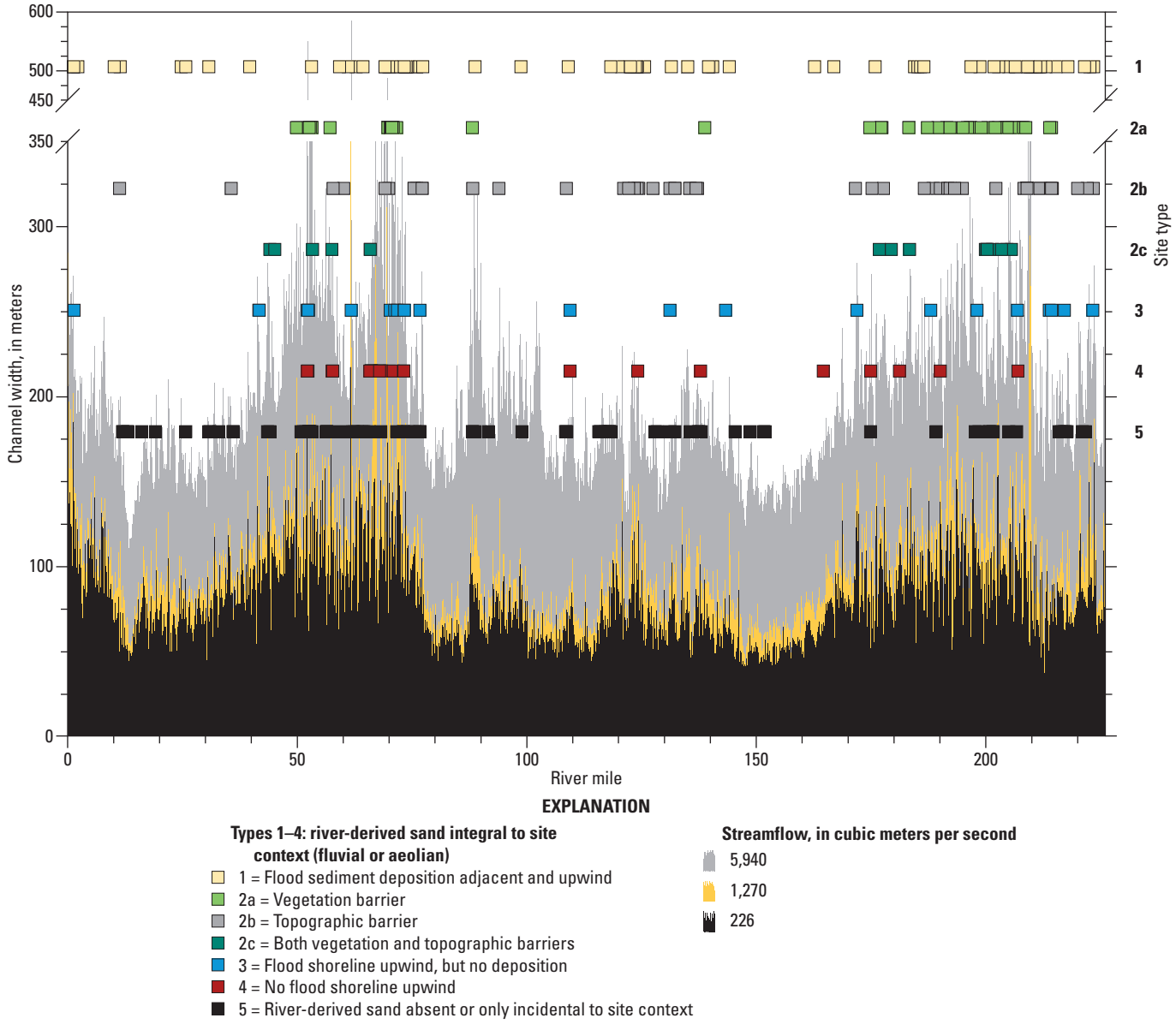

Figure 17. Distribution of river-corridor archeological sites, by site type in 1984 (in 1985 for sites downstream from river-mile 214), with distance along the river corridor, in river miles downstream from Lees Ferry (fig. 1). Gray-shaded and black regions indicate width of river flow (Magirl and others, 2008) for discharge of 226 m^3/s, 1,270 m^3/s (controlled-flood discharge), and the highest historical discharge, 5,947 m^3/s (in spring 1884).

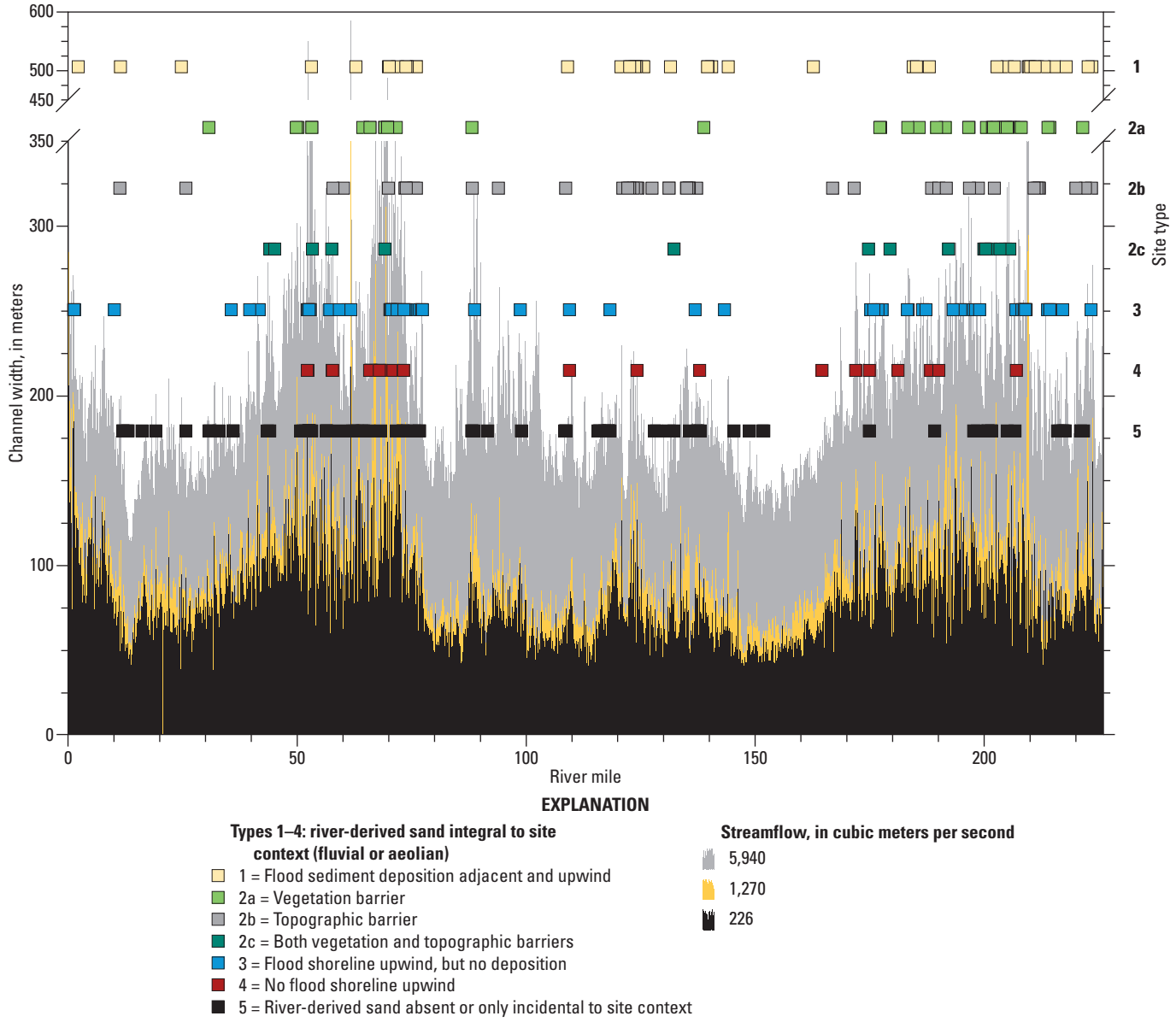

Figure 18. Distribution of river-corridor archeological sites, by site type in 1996 (immediately after the spring 1996 controlled flood), with distance along the river corridor, in river miles downstream from Lees Ferry (fig. 1). Gray-shaded and black regions indicate width of river flow (Magirl and others, 2008) for discharge of 226 m^3/s, 1,270 m^3/s (controlled-flood discharge), and the highest historical discharge, 5,947 m^3/s (in spring 1884).

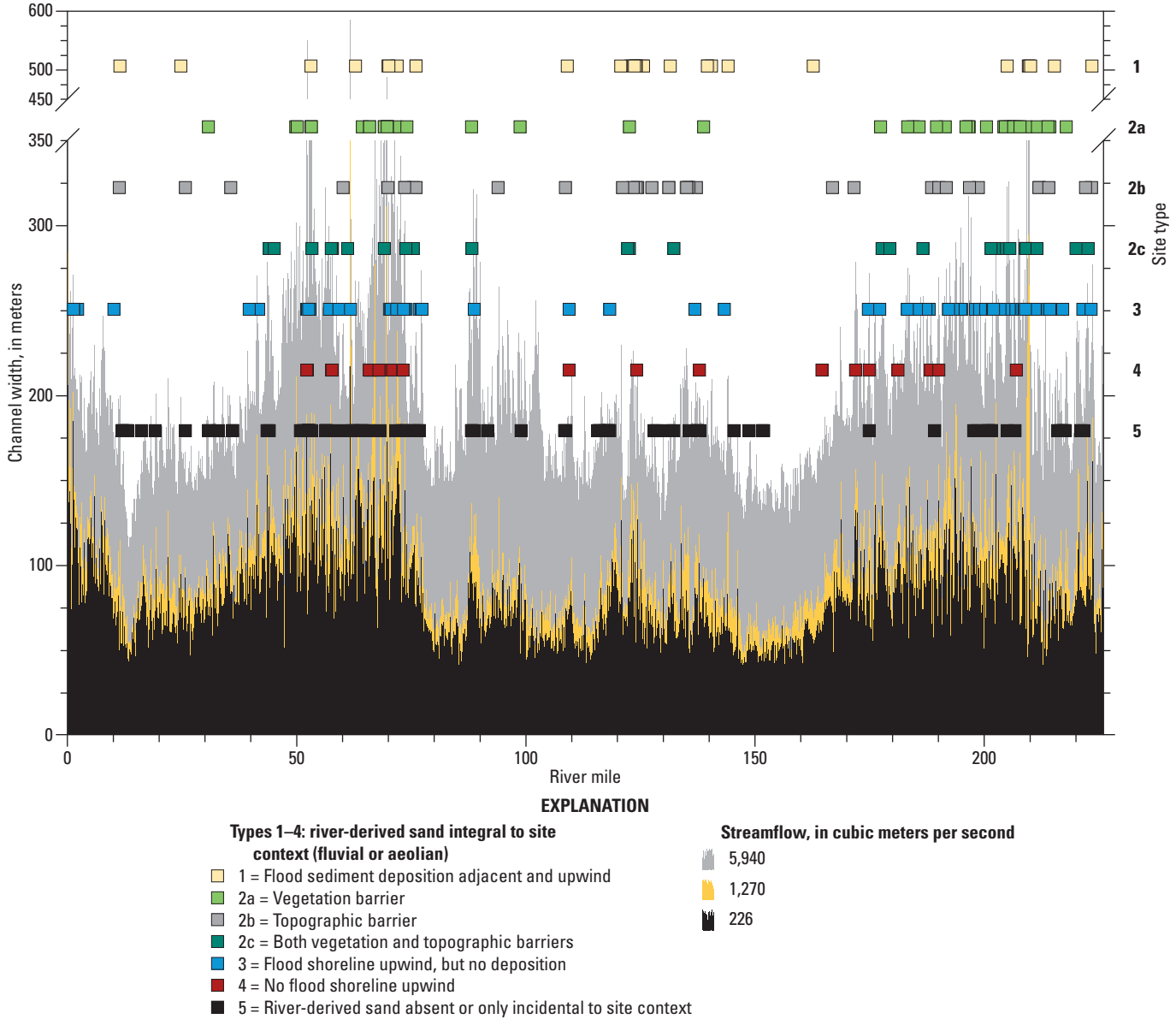

Figure 19. Distribution of river-corridor archeological sites, by site type in 2012–14, evaluated from field visits, with distance along the river corridor, in river miles downstream from Lees Ferry (fig. 1). Gray-shaded and black regions indicate width of river flow (Magirl and others, 2008) for discharge of 226 m^3/s, 1,270 m^3/s (controlled-flood discharge), and the highest historical discharge, 5,947 m^3/s (in spring 1884).

Discussion

We have used a classification system based on geomorphic and sedimentary context, local prevailing wind direction, fluvial sandbar occurrence, local vegetation, and topographic features to assess the relative potential for Colorado River sand supply to reach archaeological sites today and in the recent past. Our analysis shows a substantial decrease in sites with the greatest potential to receive sand supply, with the number and proportion of type 1 sites today being a third of what they were 40 years ago. This indicates that controlled flooding from Glen Canyon Dam, one goal of which is to increase sand supply to cultural sites, has had limited and decreasing influence on river-corridor archeological resources. Some of those limitations may be counteracted by deliberate vegetation removal in the future, a management action that potentially could reverse some of the transitions from type 1 to type 2a sites that we noted (or from type 2b to type 2c), or perhaps even transitions to type 3 that resulted from vegetation having completely overgrown sand deposits (Sankey and others, 2015; Mueller and others, 2015).

The recent increase in type 3 incidence (fig. 19) is consistent with other observations of generally decreasing size and number of fluvial sandbars in Grand Canyon National Park (Kearsley and others, 1994; Hazel and others, 2006, 2010), coupled with increased riparian vegetation (Turner and Karpiscak, 1980; Johnson, 1991; Webb and others, 2007; Sankey and others, 2015; Mueller and others, 2015). The abundance of type 3 sites may reflect the fact that although sand deposits tend to form in the same depositional zones repeatedly (most commonly in eddies; Schmidt, 1990; Hazel and others, 2006; Wright and Kaplinski, 2011; Grams and others, 2013), the exact response of any given eddy can vary from one flood to another. An eddy that contains a large subaerial sandbar after one controlled flood may have little or no subaerial sandbar after another flood of similar magnitude, depending on locally available fluvial sediment supply during each of the floods. Alternatively, the increase in type 3 sites may reflect the recent finding that in some locations, vegetation encroachment has narrowed the active river channel such that densely vegetated surfaces are not even inundated by controlled flooding (Mueller and others, 2015).

It is possible that the larger number of type 3 sites inferred in the 2012–14 time step is in part an artifact of our analysis methods, which may have been affected by slight differences in river flow at the time of photography. We relied on oblique photographs and field visits to rank sites in the 2012–14 time step, instead of using aerial photographs as we had in the earlier time steps; aerial photographs following the 2012–14 controlled floods were not available at the time of our analysis. The oblique photographs and field visits occurred at flows ranging from 181 to 375 m^3/s and generally greater than 226 m^3/s, thus the sandbars (or lack of sandbars) we detected using these data sources may have been less visible than those that would have appeared in aerial photographs, which, since the mid-1990s, typically are taken at a steady flow of 226 m^3/s. However, we do not believe that artifacts of analysis methods could explain our substantially greater inference of type 3 sites downstream from RM 175, as the daytime flows when we assessed sandbar occurrence in that part of the canyon were similar to those when we assessed sandbars farther upstream (by comparison of data from USGS stream gages at RM 0, RM 87, and RM 225). If, in the future, aerial photographs are taken at 226 m^3/s immediately following a controlled flood (within 3–4 weeks, as was the case for the April 1996 aerial photographs), we suggest conducting a similar analysis of sandbar presence and archeological-site classification based on postflood aerial photographs, to assess whether differences in analysis methods contribute to the spatial trends such as those evident in figures 18 and 19.

Several important caveats and limitations accompany this classification analysis. First, having high potential for recent sand supply (a type 1 situation) does not necessarily correspond to aeolian landscapes becoming or remaining very active (in the sense of Lancaster, 1994; fig. 7*A*,*B*). Although landscapes with modern sand supply generally have more active aeolian sand than do landscapes without modern sand sources (Draut, 2012), some type 1 landscapes are more active than others with respect to aeolian transport and dune migration. Even at some type 1 sites, the area or proportion of active aeolian sand may be fairly low, or the exposed archeological features may be within relatively inactive sand amid an otherwise active aeolian landscape. We have not analyzed the abundance of active aeolian sand relative to archeological-site occurrence because any such exercise would be complicated by a site-detection bias. Active dune migration repeatedly covers and exposes certain areas, and active aeolian deposition (inflation) can keep artifacts covered indefinitely; in inactive settings without those processes, archeological sites become preferentially exposed. Some archeological sites likely remain undetected because they exist in active aeolian sand, whereas sites on inactive sand surfaces (fig. 7*C*–*F*) or exposed in vertical gully cutbanks (more common in inactive sand landscapes; Section II) are more likely to be discovered.

Second, the inference that new windblown sand supply can reach archeological sites does not necessarily mean that sand will be deposited and remain on a site. Our analysis inferred the potential for sand transport to the site and its surroundings, but actual deposition and volumetric increase (inflation of the ground surface) often cannot be determined by examining photographs, visiting the sites, and measuring wind directions. To ascertain whether aeolian sand has been deposited on a site and caused volumetric inflation requires either repeated high-resolution topographic surveys or detailed examination of subsurface stratigraphy at repeated intervals. This study did include high-resolution topographic surveys at four type 1 sites (Section III).

Third, we did not attempt to quantify how effective sand replenishment might be given the relative source area or volume of upwind fluvial sand compared to the sand area

or volume in the landscape in and around archeological sites. Some of the upland aeolian landscapes have much greater areas and volumes than those of the modern sandbars upwind, surely limiting the ability of the sandbars to replenish those landscapes. Quantifying replenishment effectiveness would require detailed, repeated, high-resolution topographic mapping of both fluvial deposits and downwind landscapes (such as from airborne lidar), which is beyond the scope of this assessment.

A related problem concerns variations in potential aeolian sand supply as a function of longevity of the flood deposits, which is largely determined by (1) how quickly the flood deposits erode during normal, postflood dam operations, (2) by the relative timing of floods, and (3) the timing of the typically dry, windy spring season when most sand transport occurs (Draut and Rubin, 2008). All of these factors affect the amount and rate of aeolian sand transport from flood deposits toward downwind landscapes and archeological sites.

As described, these limitations mean it is not possible to predict the rate at which sand will accumulate at a specific site (if it accumulates at all) or to predict the relative rates of accumulation at sites classified as type 1 or 2. Some of these outstanding questions will be investigated through the 2015–17 GCDAMP triennial work plan.

This classification is intended to be an iterative process in which the site type for any of the type 1, 2, or 3 sites may be assigned differently after future flood flows. Although the cultural-site geomorphic context and locally dominant wind directions are presumably fairly constant, site classifications in any particular time step should not be considered a final determination. Type 4 sites would not be expected to change categories unless there was either a different evaluation of locally dominant wind direction or a substantial change in where a flood shoreline reaches topographically. Although wind directions are assumed to remain essentially constant through time, locally dominant wind directions can vary over small spatial scales, and so some sites may be reassigned to different classes if more precise information about local wind directions becomes available at a later date. A major shift in high-flow shorelines in response to topographic rearrangement after a tributary debris flow or rockfall could cause a type 4 site to convert to type 1, 2, or 3, but that had not occurred at any sites in the time intervals we considered. Type 5 sites are not expected to change categories.

How much sand supply reaches any of the 232 sand-dependent archeological sites in Marble–Grand Canyon today depends upon local sandbar response to any particular flow regime—whether open, dry, subaerial sandbars exist upwind of the sites—and whether vegetation or topographic barriers impede aeolian sand transport. The following sections will address whether modern aeolian sand activity reduces gully erosion in archaeologically rich upland sand deposits, and how modern sand supply and its influence on landscape evolution affect preservation of selected archeological sites.

Section II - Gullies and Aeolian Sand Activity in the Geomorphic Context of the Colorado River Corridor

Background

The role of gully erosion in landscape evolution is not unique to the Colorado River corridor, but is important in arid and semi-arid regions worldwide (Wainwright and others, 2011; Turnbull and others, 2012; D'Odorico and others, 2013). The causes of gully formation and enlargement have long interested geomorphologists, both from a theoretical standpoint of drainage development and because soil erosion and landscape degradation associated with gullies are major dryland-management concerns (Bryan, 1925; Antevs, 1952; Patton and Schumm, 1975; Ghimire and others, 2006; Zhu, 2012). Although many studies have investigated gully initiation and enlargement, which occurs largely from rainfall-runoff events and can include subsurface flow contribution (Faulkner and others, 2004; Tebebu and others, 2010; Svoray and others, 2012), there has been little research into mechanisms that limit gully formation or by which gullies anneal. In the Colorado River corridor and elsewhere, researchers have recognized that aeolian sand can fill gully channels (fig. 6) and have suggested that aeolian sand activity could counteract landscape erosion and cultural-site degradation. Gully development involves a competition between factors that cause incision, and those that limit erosion or that promote annealing or infilling after erosion has occurred. A more thorough understanding of this balance between gully incision and annealing today in Glen, Marble, and Grand Canyons is essential for evaluating the effects of dam operations on the landscape and cultural resources. In this section and in a companion publication (Sankey and Draut, 2014), we report on the first systematic, landscape-scale assessment of how extensively aeolian sand may mitigate gully erosion. Through this field and remote-sensing study we assessed the broader landscape context for geomorphic processes that we evaluate at the site scale in Sections III and IV.

Cultural sites in the river corridor, and particularly the sand-dependent sites (types 1–4; Section I), are concentrated in the widest reaches of the canyon, such as the Furnace Flats area (RM 66–73; fig. 19) and in some areas of the western canyon. In those widest reaches, the bedrock lithology and fault configuration form a particularly broad river corridor with ample accommodation space in which to store large fluvial terraces (see also Pederson and O'Brien, 2014). Those spatially extensive sediment deposits were conducive to prehistoric human occupation, providing substrate for farming and habitation sites (Fairley, 2003, 2005; Anderson and Neff, 2011). Multiple access routes there, typically along the faults, further facilitated human use of the inner canyon (Fairley and others, 1994). The large, relict, predam sand deposits (fluvial and reworked aeolian sand) in those wide reaches are now largely decoupled from modern aeolian sand supply, with vast

areas not situated downwind from modern, dam-influenced sandbars (RFS landscapes; Draut, 2012); much of their area is inactive with respect to aeolian transport, and also contains large gullies. Pederson and O'Brien (2014) confirmed that the Furnace Flats and western canyon areas, with their extensive Holocene fluvial terraces, contain a disproportionate number of archeological sites with acute gully erosion; their study did not include sites in Glen Canyon, where there are also extensive fluvial terraces with severely gullied sites. These findings—that the reaches with the richest archeological record seem most vulnerable to erosion—indicated a need to understand more fully the links between aeolian sand activity and gully prevalence, and to quantify the spatial distribution of both. Thus, we assessed how aeolian sand and gully occurrence vary spatially in canyon reaches of different widths. We also examined some of the links between aeolian and hillslope processes that are evident in most upland sand landscapes within the canyon, as gullies and aeolian sand activity often occur in spatial proximity. We evaluated whether gully prevalence is measurably greater in inactive sand than in active aeolian sand, and thus how gully erosion became so severe in those reaches of the canyon where the archeological record is most concentrated.

Research Questions

- How does the relative abundance of active and inactive aeolian sand vary in different segments of the Colorado River corridor?
  - Hypothesis 1: The proportion of active aeolian sand will be inversely related to river-corridor width, with a lower proportion of active sand in wide reaches (where accommodation space for sediment is greater) and a greater proportion in narrower reaches.
- How effective is aeolian sand activity as a gully-annealing mechanism—does gully prevalence differ measurably in sand deposits that are active versus inactive with respect to aeolian transport?
  - Hypothesis 2: Gullies are more evident in sand deposits that are inactive with respect to aeolian transport than in those with active aeolian transport.
  - Hypothesis 3: Gullies terminate more commonly in active aeolian sand than in inactive sand.

Methods

We combined field and remote-sensing analyses to address the science questions and test the hypotheses above. This analysis focused on aeolian sand activity and gully prevalence in six reaches of the river corridor (fig. 1): Glen Canyon (GLCA, RM -13 to -6), Eminence to the Little Colorado River (EmLCR, RM 44–61), Furnace Flats (FF, RM 66–72), Upper Granite Gorge (UGG, RM 87–99), Stevens-Conquistador Aisle (SCA, RM 116–128), and Granite Park (GP, RM 207–210).

In each of the six study reaches, we used the area of Colorado River-derived sediment above the direct effect zone (inundation zone) of contemporary dam operations as a means to quantify accommodation space for predam sediment storage. This terrestrial area was identified as the area above stage-elevation 1,270 m^3/s (the maximum elevation of controlled-flood releases, determined by the stage-discharge model of Magirl and others, 2008) and below the transition of river-derived and slopewash sediment to bedrock or talus. The landward boundary of terrestrial area (the transition to bedrock or talus) was identified by visual interpretation and delineation in a geographic information system (GIS) of 22-cm-resolution multispectral imagery acquired in 2009 (Davis, 2012).

For each reach, we evaluated the relative extent of modern aeolian sand activity by mapping the surfaces of river-derived (fluvial and reworked aeolian) sand deposits in the terrestrial (upland) area as being either active or inactive with respect to aeolian sand transport, as defined by Lancaster (1994; see our fig. 7). Because this analysis was concerned only with evidence for contemporary aeolian sand transport at the ground surface, we did not differentiate between fluvial, aeolian, and mixed fluvial-aeolian origins for the various sand deposits. Each deposit was delineated on the 22-cm-resolution imagery during field visits in 2011, 2012, or 2013; these data were transferred into a GIS as polygons with defined active/inactive attributes.

Hillslope flowpaths with concave across-slope shape with potential to channel overland flow ('potential gullies') were detected in each study reach using a novel combination of overland-flow accumulation and topographic modeling procedures commonly available in GIS and remote sensing software (ArcGIS, ENVI), and a 1-m-resolution digital elevation model (DEM) acquired in 2009 (Sankey and Draut, 2014). The DEM was derived from a 1-m-resolution digital surface model (DSM) derived from automated digital aerial photogrammetry with vertical accuracy within 0.30 m (Davis, 2012) and is the highest-resolution and most accurate digital topographic dataset available for all six study reaches. The first step of the potential-gully detection procedure entailed running an overland-flow accumulation model (ArcHydro Tools in ArcGIS) for the DEM to identify thalwegs of possible overland flow paths in terrestrial surfaces (Greenlee, 1987; Jenson and Domingue, 1988; Tarboton and others, 1991). The second step produced a plan convexity product and a root-mean-square error (RMSE)-roughness product for the DEM (see Sankey and Draut, 2014, for additional details). To detect gullies consistently, we applied thresholds to the flow-accumulation and plan-convexity raster products using heuristic values that we confirmed during field visits. We then used GIS to produce an intermediate dataset of individual polygons representing sections of hillslope flowpaths with concave across-slope shape (that is, potential gullies). We applied threshold values

of the RMSE-roughness product to the intermediate dataset to reduce the misclassification of topographically smooth interdune swales as potential gullies, resulting in a final dataset of individual potential-gully polygons (fig. 20). We analyzed only those potential-gully polygons that overlapped with the previously defined terrestrial area for each reach, thus limiting this consideration of potential gullies to those formed in river-derived fine sediment rather than through coarse talus. The average width of each potential gully polygon in the final dataset was measured in GIS to determine the distribution of potential gully sizes and estimate detection limits. We estimated the relative ability of these methods to detect real gullies by using a set of gullies that we identified independently in the field and surveyed with stadia rod and total station within three archeological sites in the GLCA reach (sites AZ:C:02:0035, AZ:C:02:0032, and AZ:C:02:0075); the surveyed gullies included segments with sub-meter widths.

We analyzed the resulting data in GIS to test the hypotheses above. After determining the terrestrial area and scaling it by reach length for each of the six reaches, we identified the ratio of potential gully area to terrestrial (sediment) area (the gully area ratio) and the ratio of active aeolian sand area to the sum of active and inactive sand area (the active sand ratio). We used a simple linear regression to examine the relationship between gully area ratio and active sand ratio. Using a paired t-test, we determined the gully area within active and inactive sand units and compared these values among reaches. To assess whether gullies terminate more commonly in active sand than in inactive sand, we determined the gully count, ratio of count to sand area, and ratio of potential gully area to sand area of all potential gullies that entered

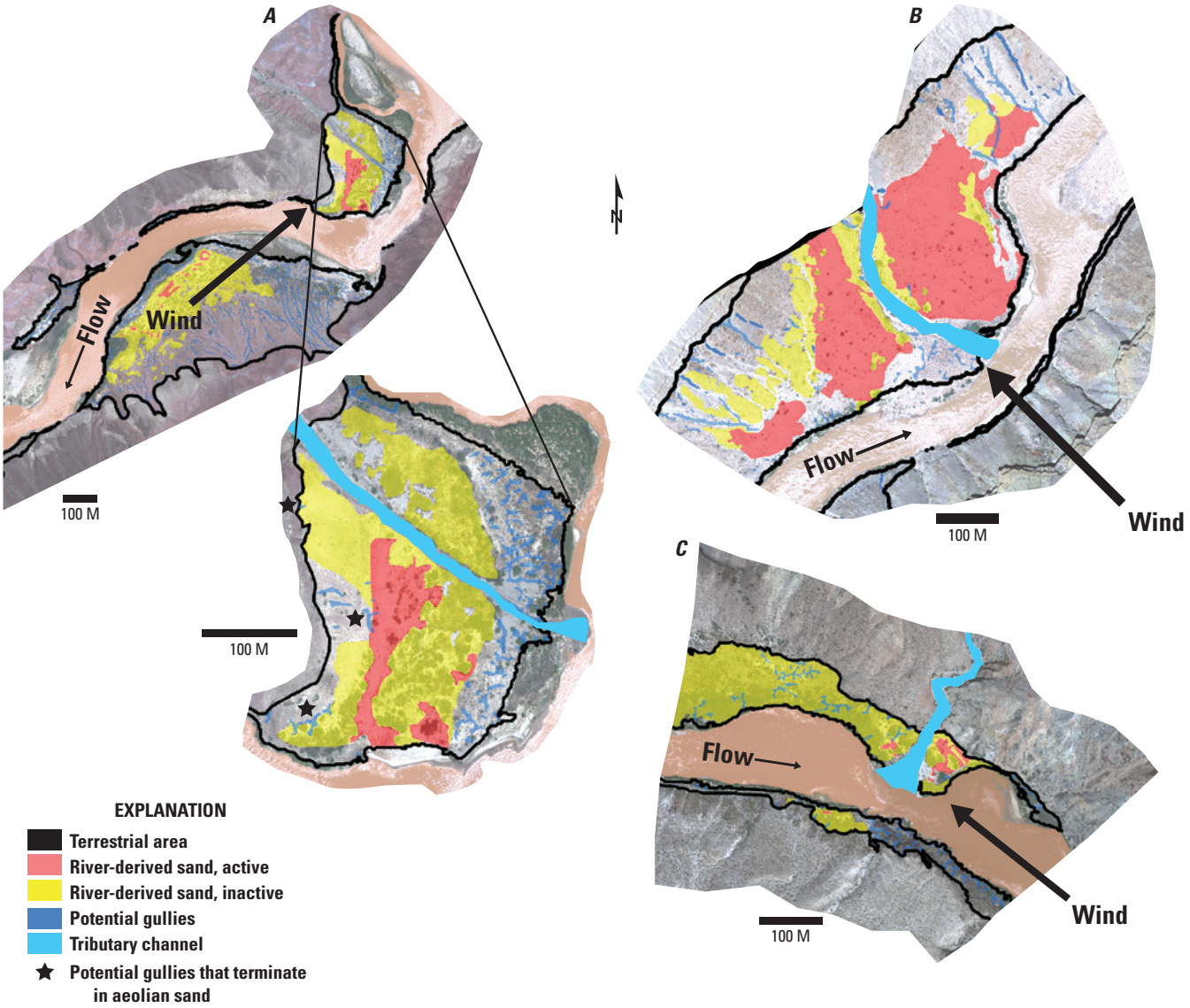

Figure 20. Examples from parts of three study reaches that show the aeolian sand and potential gullies detected with our remote-sensing algorithm. (*A*) a part of the Furnace Flats (FF) reach; (*B*) a part of the Stevens-Conquistador Aisles (SCA) reach; (*C*) a part of the Granite Park (GP) reach. Reach locations are shown in figure 1.

and terminated within river-derived sand units. Potential gullies were considered to terminate within sand units if they entered from outside (upslope) and dissipated before passing halfway through the unit. The rationale for considering dissipation that occurred before an individual gully travelled more than halfway through a sand unit was to use a criterion that was common among gullies and aeolian sediment units, and to provide spatially unambiguous evidence that a gully had entered a sand unit and also terminated within it. We compared gully termination in inactive and active sand among reaches using paired t-tests.

Finally, we examined the historical aerial photographic record for evidence of gullies that have, or have not, annealed over time and so are either still evident or are less so today than in the past. The entire set of potential gullies that terminate in active and inactive sand (detected in the 2009 imagery and DEM) were examined visually relative to aerial imagery from 2002 and 1984 to determine whether any gullies were more pronounced in the earlier imagery and (or) exhibited obvious infilling with aeolian sand as of 2009. In some cases, vegetation encroachment into gullies made it difficult to determine whether aeolian infilling had occurred; we recorded these ambiguous situations separately from examples of infilling with aeolian sand. Examples of vegetation encroachment in conjunction with aeolian infilling were recorded separately from examples where infilling with aeolian sand clearly was independent of vegetation growth.

Results

Terrestrial area, our proxy for river-corridor width, and the proportion of active aeolian sand varied greatly among the six study reaches (fig. 21). When scaled by reach length, terrestrial area is greatest in the EmLCR, FF, and SCA reaches, intermediate in the GLCA and GP reaches, and least in the UGG reach (fig. 21*A*). The active aeolian sand ratio in the UGG and SCA reaches (36 and 37 percent, respectively) was approximately 2–3 times that in the EmLCR and FF reaches, and nearly an order of magnitude greater than in the GLCA and GP reaches (fig. 21*B*). These proportions of active sand reflect not only the canyon morphology, but also local prevailing wind directions that vary among the six reaches. In places where the local wind direction blows at a high angle to the river (including much of the SCA reach), readily transporting sand from modern fluvial sandbars to inland aeolian dunes on the downwind side of the river, the source-bordering dunes contain more active aeolian sand than those in other reaches where the wind direction is nearly parallel to the river (fig. 11).

By comparing 14 gullies in the GLCA reach that we surveyed with rod and total station, as well as attempted to detect with our remote-sensing method, we determined that the algorithm was suitable for detecting some parts of real gullies, but not for delineating gully sections less than 1 m wide (Sankey and Draut, 2014). The remote-sensing algorithm identified 90 percent of the surveyed gully thalweg lengths in site AZ:C:02:0075, 50 percent in site AZ:C:02:0035, and 40 percent in site AZ:C:02:0032. The lower detection accuracies at sites AZ:C:02:0035 and AZ:C:02:0032 illustrate the relative limitations of 1-m-resolution

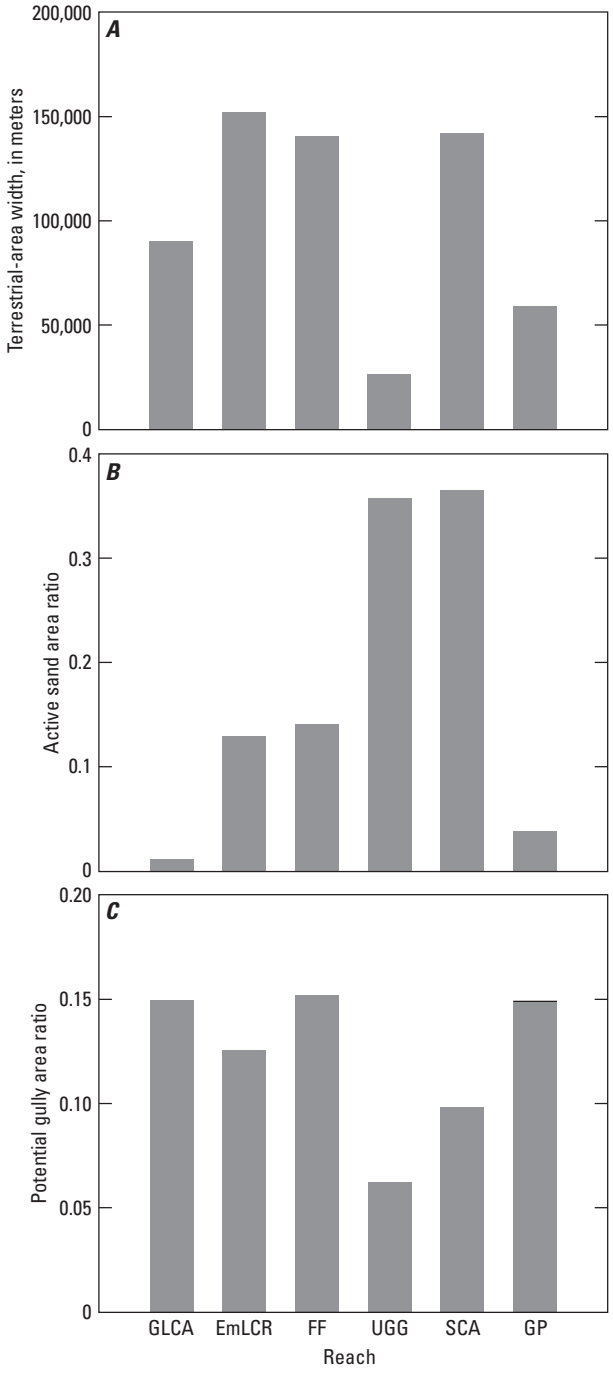

Figure 21. Terrestrial area and gully prevalence, by reach, in order from upstream (left) toward downstream (right); reach locations are shown in figure 1. Glen Canyon (GLCA), Eminence to Little Colorado River (Em-LCR), Furnace Flats (FF), Upper Granite Gorge (UGG), Stevens-Conquistador Aisles (SCA), and Granite Park (GP). (*A*) Average terrestrial-area width mapped in each reach of the Colorado River-derived sediment between the contemporary active channel of stage-elevation 1,270 m^3/s and the upslope transition to bedrock or talus. The width shown was calculated by dividing the total terrestrial area in each reach by the reach length; thus, terrestrial-area width is a proxy for total river-corridor width that excludes the part of the river corridor below the 1,270 m^3/s stage. (*B*) Active aeolian sand area ratio, by reach. (*C*) Potential gully area ratio, by reach.

DEM data for delineating the entire thalweg lengths of small (narrow, shallow) gullies and gully segments. In total, we detected 11,010 potential gullies in all six reaches, but the total number is probably much greater, in particular for gullies that are a few meters wide or narrower. The widest gullies that we detected were 30 m wide; most gullies were 1–4 m wide (fig. 22).

The inverse relationship of the potential gully area ratio (fig. 21*C*) to active sand area ratio (fig. 21*B*) was significant and strong, indicating lower gully prevalence in reaches with a greater proportion of active aeolian sand (p=0.02 in a Student's t-test; fig. 23). We identified significantly more potential gully area within inactive sand units than in active sand units (paired t-test p=0.03; fig. 24).

We identified 358 potential gullies that terminated in mapped (active and inactive) sand units, as opposed to potential gullies that travelled through sand units and (or) ultimately joined other potential gullies or the mainstem river. The number of terminating gullies scaled by sand-unit area was significantly greater in active aeolian sand than in inactive sand (paired t-test p=0.02; fig. 25). The total area of terminating gullies scaled by sand area was moderately significantly greater for active aeolian sand than for inactive sand (paired t-test p=0.06). It is necessary to scale by sand-unit area to make these comparisons of gully prevalence, because there is substantially less active sand area than inactive sand area in each reach (fig. 21*B*).

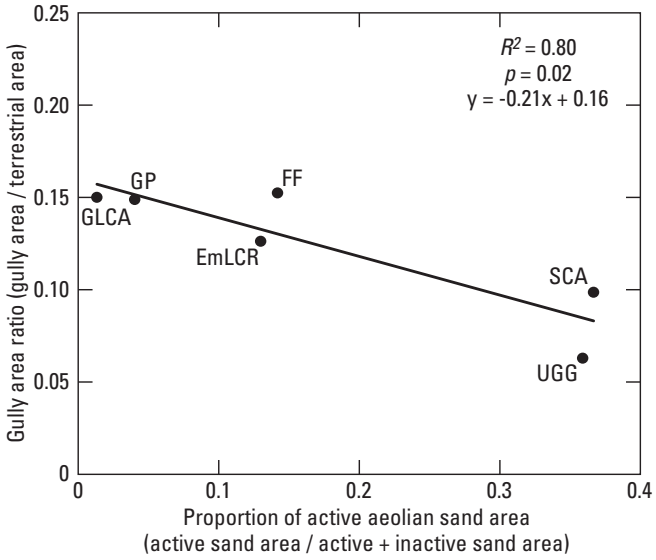

Figure 23. Relation of potential gully area ratio and active sand area ratio by reach. Glen Canyon (GLCA), Eminence to Little Colorado River (Em-LCR), Furnace Flats (FF), Upper Granite Gorge (UGG), Stevens-Conquistador Aisles (SCA), and Granite Park (GP).

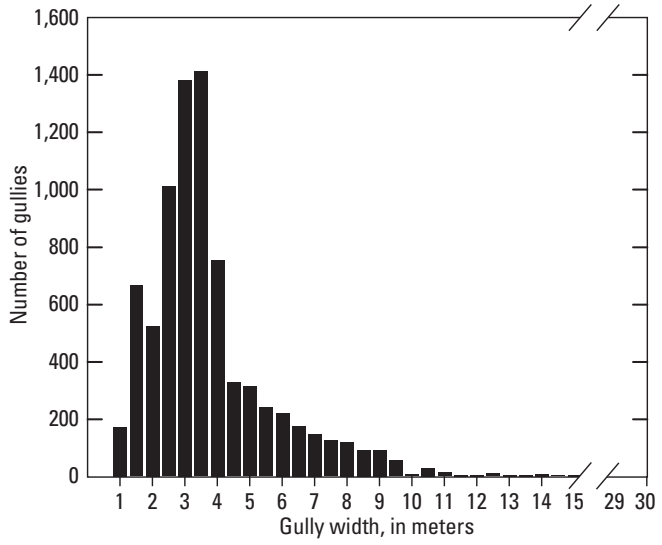

Figure 22. Distribution of average widths for all potential gullies (n=11,010) delineated by the remote-sensing algorithm described in the text.

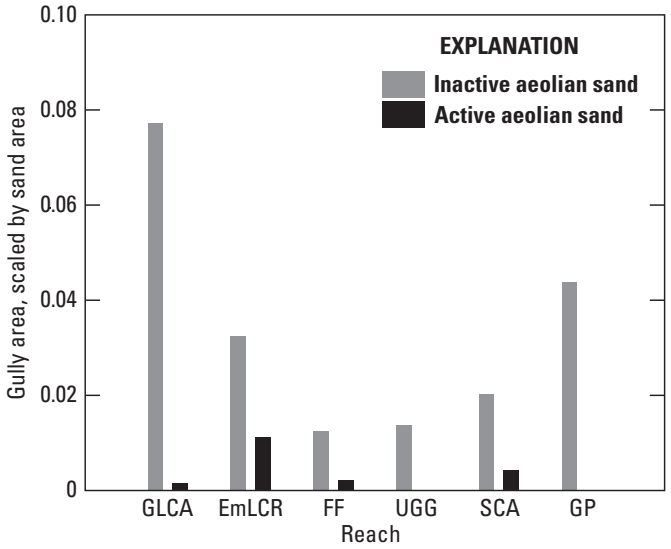

Figure 24. Potential gully area per mapped sand unit (active or inactive sand with respect to aeolian transport), summarized by reach. Vertical axis shows the dimensionless ratio obtained by dividing gully area by the terrestrial area occupied by active or inactive sand. Comparison of potential gully area within active and inactive sand indicated significantly more potential gully area within inactive sand units than in active sand units (p=0.03). Glen Canyon (GLCA), Eminence to Little Colorado River (Em-LCR), Furnace Flats (FF), Upper Granite Gorge (UGG), Stevens-Conquistador Aisles (SCA), and Granite Park (GP).

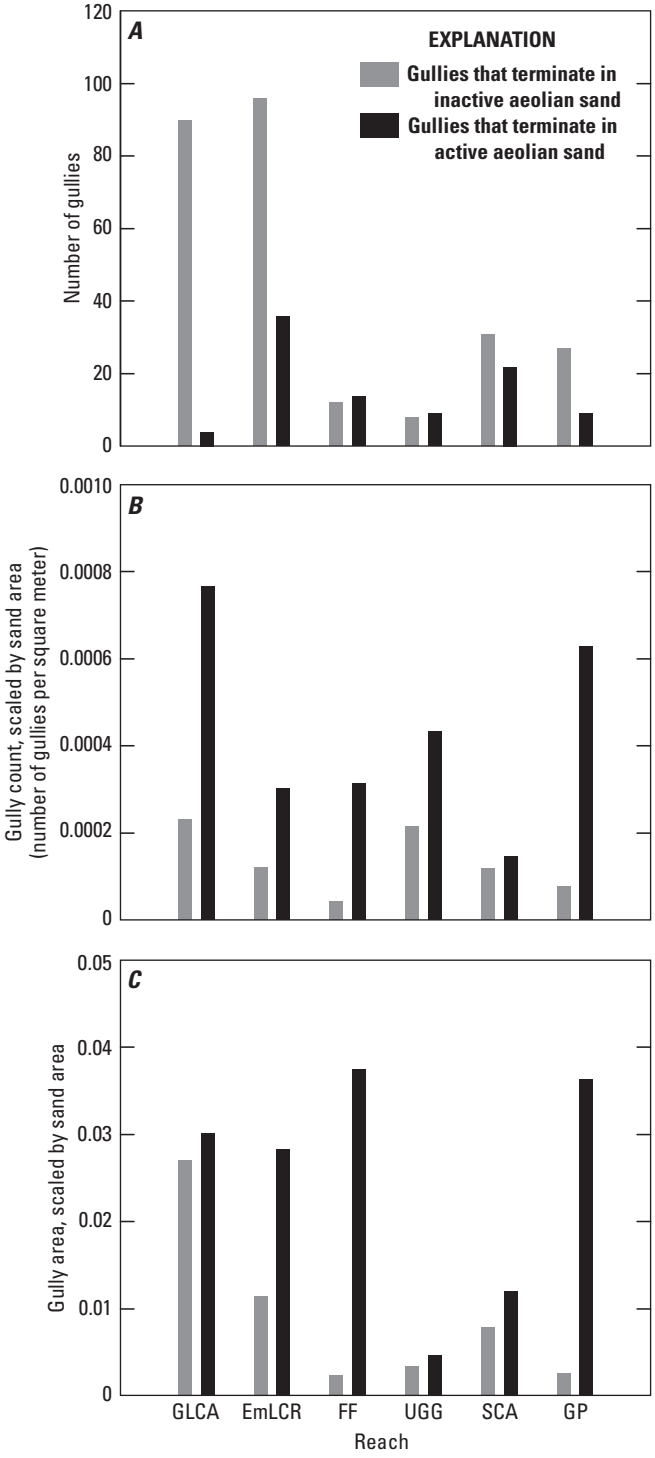

Figure 25. (*A*) The number of gullies, (*B*) number of gullies divided by sand area, and (*C*) area divided by sand area, for potential gullies that terminated in mapped sand units (active and inactive aeolian sand, respectively), summarized by reach. A total of 358 potential gullies were identified among all reaches that terminated in mapped (active and inactive) sand units. Simply comparing counts of terminating gullies in inactive versus active aeolian sand (*A*) indicated no significant difference (paired t-test p=0.11). However, there was more inactive than active aeolian sand in all reaches, and when the counts and areas of terminating gullies were normalized by the sand area (*B* and *C*, respectively), potential gullies evidently terminated more commonly in active aeolian sand (paired t-test p=0.02 and 0.06, respectively, for tests of results presented in *B* and *C*). Glen Canyon (GLCA), Eminence to Little Colorado River (Em-LCR), Furnace Flats (FF), Upper Granite Gorge (UGG), Stevens-Conquistador Aisles (SCA), and Granite Park (GP).

Comparison of historical imagery within our six study reaches from 1984 and 2002 with that from 2009 indicated that, as of 2009, a small proportion (1–3 percent, or as many as 11 gullies) of the gullies that terminated in aeolian sand showed clear indication of aeolian annealing (figs. 26, 27). An additional 1 percent (3 gullies) showed evidence of possible aeolian annealing in conjunction with vegetation encroachment (fig. 26). Approximately 2–10 percent of gullies showed evidence of vegetation encroachment within the terminus of the gully, but without clear evidence of aeolian infilling (fig. 26). The remaining fraction (approximately 85 percent of all gullies that occurred in 1984 and 2002) did not show evidence of annealing, and were similarly or more eroded as of 2009—our qualitative analysis did not have the topographic resolution to distinguish with certainty between those two outcomes in most cases.

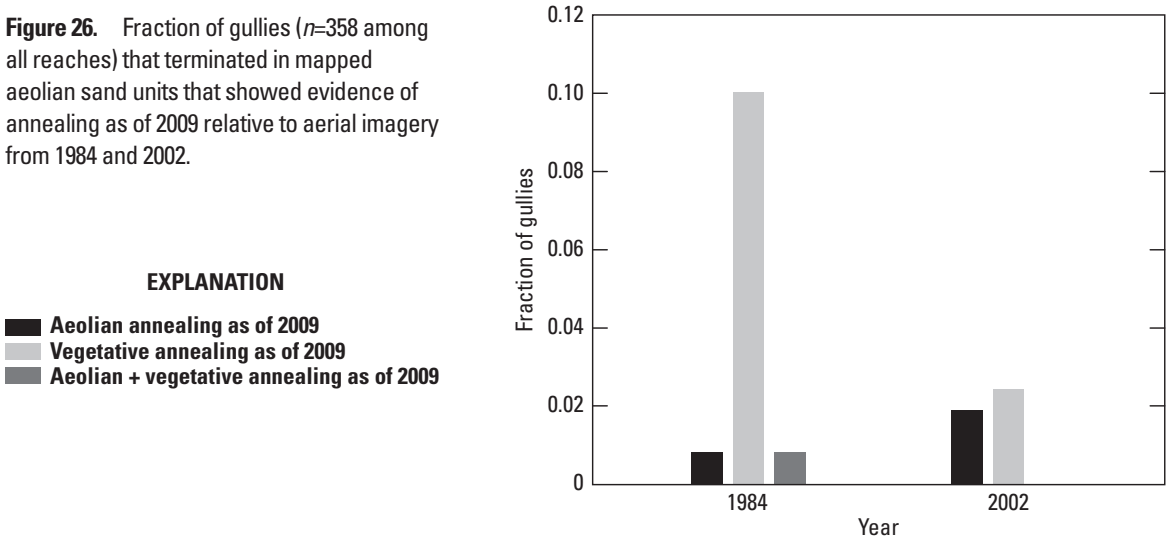

Figure 26. Fraction of gullies (*n*=358 among all reaches) that terminated in mapped aeolian sand units that showed evidence of annealing as of 2009 relative to aerial imagery from 1984 and 2002.

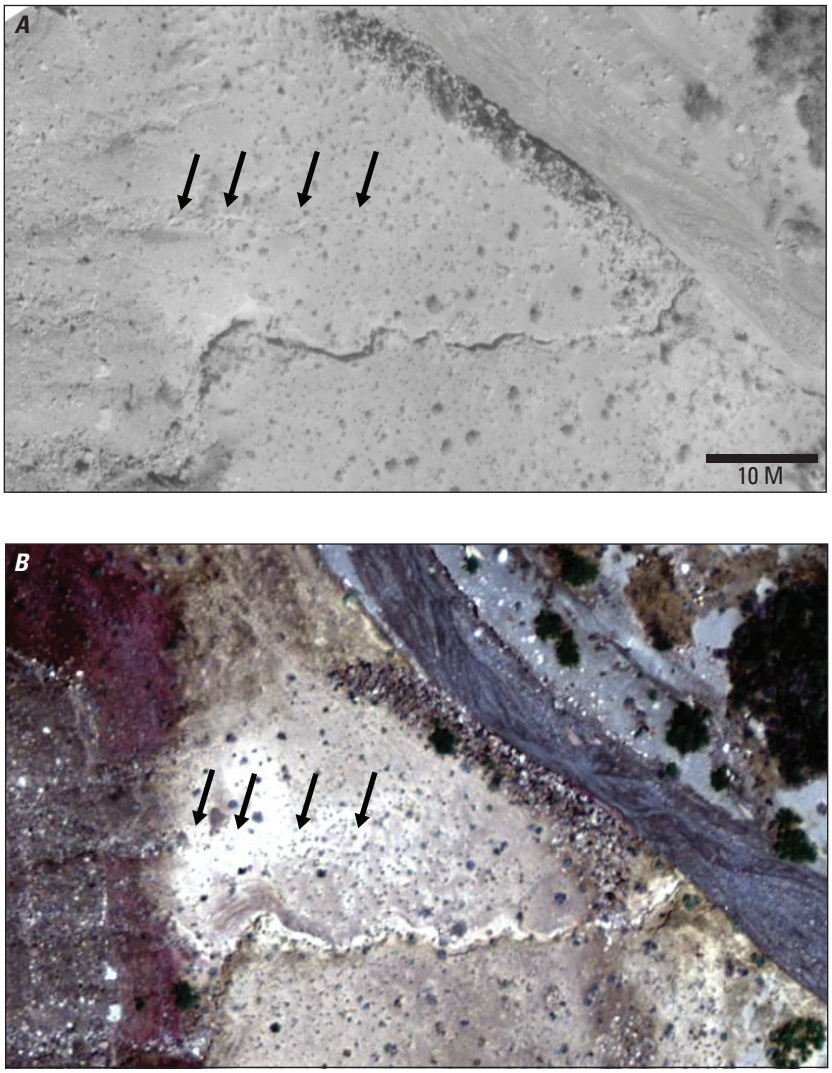

Figure 27. Example from the aerial photographic record of gully annealing by apparent aeolian-sand infilling between (*A*) October 1984 and (*B*) May 2009.

Discussion

Landscape evolution in the Colorado River corridor depends strongly on connectivity among fluvial, aeolian, and hillslope systems. Understanding factors that enhance or impede gully development depends on recognizing not only the roles of hillslope runoff, catchment size, and substrate parameters in gully formation, but also of aeolian sand transport in counteracting gully erosion. Our large-scale mapping work shows that aeolian sand can anneal and impede the expansion of gullies as a cumulative effect over time where aeolian sand is active; however, our study of temporal gully evolution in the recent aerial photographic record shows that seeing individual examples of aeolian annealing on short time scales is rare. There are large areas of the river corridor (including some of the most archeologically rich) where sand is too inactive to anneal gullies effectively. The second and third hypotheses of this part of our study—that gullies are less prevalent, and terminate more commonly, in active aeolian sand—are supported by the data. The first hypothesis—that aeolian sand activity is inversely related to accommodation space as determined by river-corridor width—was partly supported, but, as discussed below, we found that local wind directions as well as river-corridor morphology (width and other factors) play important roles in determining accommodation space, aeolian sand activity, and gully prevalence.

Spatial Variations in Aeolian Sand Activity

In testing hypothesis 1, which generally was not supported by our results, we identified additional factors that complicate links between river-corridor width and aeolian sand activity. In places where accommodation space—storage space for river-derived sediment—is a function of where large, predam floods could reach, there is indeed a relationship between width (terrestrial area) and the proportion of active aeolian sand, at least for the widest and narrowest end-member reaches. The Furnace Flats and Eminence–Little Colorado River reaches contain both a wide river corridor and a small proportion of active aeolian sand (fig. 21*A*,*B*). These are not true alluvial reaches (their hydraulic control is determined by bedrock and debris fans), but merely are wide enough to store large amounts of fluvial sediment, owing to bedrock lithology and fault configuration. Because much of that terrestrial area is decoupled from modern aeolian sand supply, those relict sediment deposits have become overgrown with biologic soil crust and have little aeolian sand activity (Draut, 2012). In some parts of the Furnace Flats (FF) reach, these relict sediment deposits contain abundant type 4 archeological sites (fig. 19). Sand-activity ratios for the FF reach are skewed by one large, low-elevation point bar at RM 69.6 that is situated directly downwind of modern sandbars, and so maintains an unusually high active sand ratio (82 percent). Without that dune field, the active sand area ratio for the FF reach as a whole would decrease from 14 percent (fig. 21*B*) to less than 11 percent. The narrowest reach, Upper Granite Gorge, where igneous and metamorphic bedrock walls confine the river more tightly than in the Em-LCR and FF reaches, stores little relict, predam flood sediment. The small amount of river-derived sand in the UGG reach is near the river and much of it receives aeolian sand supply from modern sandbars, resulting in a relatively large proportion of active aeolian sand (36 percent; fig. 21*B*).

However, spatial variations in wind direction and canyon morphology complicate the situation enough that it is not possible to generalize relations between aeolian sand activity (with potential for gully annealing) and river-corridor width. Accommodation space does not depend solely on where large, predam floods could deposit sediment. In parts of the canyon where the prevailing wind direction deviates from the usual river-parallel orientation, most notably in parts of the SCA reach where wind blows transverse to the river (fig. 11; see also Draut and Rubin, 2008, and Section III, below), windblown river-derived sand extends to a much higher elevation than even the largest prehistoric floods reached, forming sand ramps plastered against talus slopes (fig. 3*C*). Thus, in places where the wind direction is transverse to the river, accommodation space and sand storage are functions of wind conditions more than of river-corridor width and predam inundation zones. Transverse winds have brought so much river-derived sediment inland in parts of the SCA reach that the terrestrial area per unit river length in that reach is virtually identical to that of the FF reach (fig. 21*A*) even though the wall-to-wall width is narrower in the SCA reach (90–280 m) than in the FF reach (300–450 m). As a result of transverse-directed windblown sand transport and a history of eddy sandbars having enlarged substantially from controlled floods, the SCA reach has numerous active dune fields downwind of modern sandbars and a higher active-sand proportion than occurs in any other reach (37 percent; fig. 21*B*). The largest dune field in the SCA reach contains 70 percent active sand area; several other SCA locations have more than 60 percent active sand, although for the reach as a whole most of the sand-ramp area is currently inactive. Therefore, unlike the Em-LCR and FF reaches, where sediment storage is largely in predam fluvial terraces with little aeolian sand supply or activity today, the SCA reach stores large amounts of sand in active dune fields and sand ramps, maintaining high connectivity to modern fluvial sand supply and precluding a simple inverse relationship between river-corridor width and modern sand activity.

Results from the Glen Canyon (GLCA) and Granite Park (GP) reaches also do not support the first hypothesis, that river-corridor width would correspond inversely to aeolian sand inactivity, but we attribute this to local morphology rather than to wind direction. The GP reach, in which prevailing winds are oriented generally toward upstream (toward the northeast), contains a moderately low terrestrial area scaled by reach length (fig. 21*A*). Although the GP reach does not store a large amount of river-derived sand per unit length, much of the sand it does store is in two discrete expanses of predam fluvial terraces with aeolian-reworked surfaces that are now inactive (4 percent active aeolian sand for the reach overall; fig. 21*B*). One of the terraced areas is unusually broad, extending more than 300 m inland from the river margin, or 3–4 times the width that the river occupies at a nonflood flow of 226 m^3/s. The breadth of the GP terraces represents a unique situation in the canyon, and may be

related to predam Colorado River floods ponding upstream of the large Granite Park debris fan (RM 209.2) after debris flows temporarily increased the river-corridor constriction at the fan (see also Hereford and others, 2000a). In contrast, other reaches with sediment stored largely in predam flood deposits tend to have sand deposits that extend inland no more than 1–2 times the nonflood river width (although the aforementioned SCA aeolian sand ramps do extend inland by 3–4 times the nonflood river width). The combination of GP sand deposits extending unusually far inland from the river, such that they are exceptionally large relative to—and distant from—modern sandbars, along with the wind direction transporting sand obliquely rather than directly toward much of their area (unlike sand deposits in the SCA reach), makes it unusually difficult for modern sandbars to replenish the GP sand deposits—hence their low aeolian sand activity. In regions of the GP sand deposits that are downwind of modern sandbars, dense vegetation and several tributary channels also locally inhibit aeolian sand supply, constituting a type 2 situation for most archeological sites in this reach (fig. 19).

Geomorphic constraints also affect sand storage and aeolian sand supply in Glen Canyon, but in different ways than in the other study reaches (see also Section IV). Glen Canyon, or at least the part of it that is downstream from Glen Canyon Dam and Lake Powell (RM -15 to 0), differs from Marble and Grand Canyons in terms of bedrock lithology, topographic relief, tributary activity, and influence of dam operations. Glen Canyon bedrock is mechanically weak but fairly homogenous, and so erodes to form a wide river corridor with walls of massive-bedded Mesozoic sandstone (Wilson, 1965; Sprinkel and others, 2003; Bursztyn and others, 2015) stratigraphically above the Paleozoic sandstone, shale, and limestone of Marble and Grand Canyons (having been removed by erosion, the Mesozoic sandstones are not part of the Marble–Grand Canyon stratigraphy). The 300–400 m of topographic relief from rim to river in Glen Canyon is much less than in the reaches downstream (1,000–1,900 m in Marble Canyon, 1,200–2,000 m in Grand Canyon). The combination of uniform, clay-poor sandstone bedrock forming the canyon walls, and modest relief, means that there are no large debris fans in the Glen Canyon river corridor (in contrast to Marble–Grand Canyon; Melis and others, 1994; Webb and others, 2003; Griffiths and others, 2004). Without major debris fans, Glen Canyon not only lacks the fan-eddy complexes that form rapids and store eddy sandbars in Marble–Grand Canyon, but also has no major features to segment the hydraulic control on the mainstem river flow; the small riffles in Glen Canyon are not large enough to exert hydraulic control during flood flows. Whereas sediment-storage patterns in the pool-and-drop morphology of Marble–Grand Canyon largely depend on debris-fan controls (with secondary effects of local wind direction, as in the SCA reach), most relict sand in Glen Canyon is stored in thick (as much as 10 m), longitudinally extensive Holocene terraces atop point bars on the inside of meander bends. Some of these terrace deposits extend more than 1,200 m continuously along the river, and are located near the active river channel. These extensive, thick terrace deposits formed during predam high flows, as a function of reach-scale hydraulic control and grade changes (Tainer, 2010); this terrace morphology remains fairly continuous into uppermost Marble Canyon, around RM 4.

Because the GLCA reach is immediately downstream from Glen Canyon Dam, the sediment-supply-limiting effects of the dam and scouring potential of postdam high flows have been especially pronounced there. Postdam channel incision has lowered the riverbed in Glen Canyon by 2–4 m along most of the reach, and as much as 8 m locally; the water-surface elevation for a flow of approximately 150 m^3/s is as much as 2.3 m lower than in predam time (Grams and others, 2007). This reach is particularly sediment-starved, having essentially no upstream supply; the first major sediment-supplying tributary, the Paria River, joins the river corridor at the downstream end of Glen Canyon (Lees Ferry, RM 0; fig. 1). As a result of pronounced sediment deficit and bed winnowing, most fluvial sandbars in the contemporary active river channel have become gravel bars in postdam time (Grams and others, 2007).

The active sand area ratio in GLCA is notably lower than in any other study reach (1.3 percent; fig. 21*B*), with most sand area being heavily biocrusted. The terrestrial area (river-derived-sediment storage) per unit length in the GLCA reach is intermediate between that of the FF and GP reaches (fig. 21*A*). The Glen Canyon sediment deposits are gullied to a similar degree as those in the FF and GP reaches, with 15 percent of the terrestrial area occupied by gullies (fig. 21*C*). Aeolian dune activity may not have been very important in Glen Canyon even in predam time. Dune morphology is rare there, even though the predam terraces contain ample sediment supply (of similar grain sizes to terraces in Grand Canyon that have better-developed dune fields; fig. 28) and the wind in Glen Canyon is often strong enough to transport sand (Section IV). It is possible that local wind dynamics (zones of airflow convergence and divergence) simply were not conducive to dune formation, aeolian sand accumulation, or even to sand retention in many places; in fact, within our GLCA reach there are multiple locations where wind scour has eroded sediment from the predam fluvial terraces.

Today, the pronounced Colorado River sediment deficit, combined with the lack of fan-eddy complexes that would promote storage of any sand that enters the river from small tributaries, means that there is very little modern, subaerial, fluvial sandbar area to serve as a source for aeolian sand. The dearth of active aeolian sand in Glen Canyon today is not surprising in view of this lack of modern sandbars to supply aeolian sand, although even in the sediment-rich predam era this reach may have experienced little gully annealing from aeolian dune activity.

Gully Annealing by Aeolian Sand

Through our field and remote-sensing analyses, we determined that gullies are much more prevalent in inactive sand than in active aeolian sand (fig. 24). River-corridor reaches with a greater proportion of active aeolian sand also have a lower proportion of gully area (fig. 23), and gully terminations occur more commonly in active aeolian sand than in inactive sand deposits (fig. 25). This may be partly attributable to aeolian sand having infilled the gullies and annealed them, as

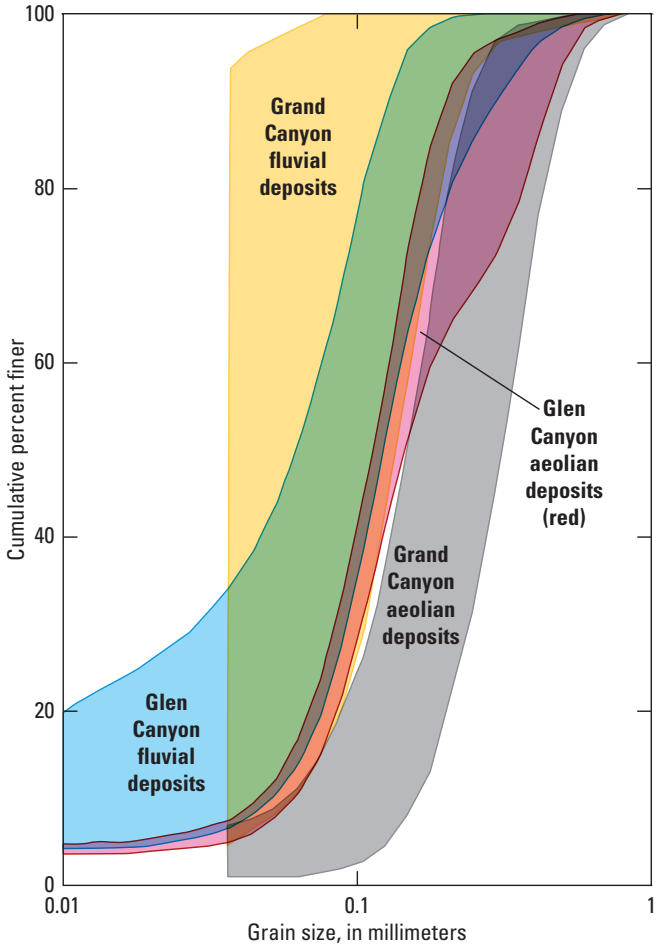

Figure 28. Grain-size distributions in predam flood deposits from Glen Canyon and Grand Canyon. Samples were analyzed with a Beckman Coulter LS 100Q laser particle-size analyzer at the U.S. Geological Survey Grand Canyon Monitoring and Research Center in Flagstaff, Ariz. Data from Glen Canyon include 12 fluvial sediment samples from predam flood deposits and 3 samples from reworked aeolian deposits on the terrace surfaces (this study); data from Grand Canyon include 19 fluvial sediment samples from predam flood deposits (terraces in the Furnace Flats and Granite Park reaches) and 10 samples from aeolian deposits (Draut and others, 2008). Values on vertical axis indicate the cumulative percent of the sediment sample that is finer than the corresponding grain diameter shown on the horizontal axis. Grand Canyon analyses were curtailed at the lower boundary of coarse silt (0.037 mm).

is commonly observed where topographic depressions act as sand traps (fig. 6), and partly attributable to gullies initially having formed more readily through inactive sand. Biocrusted, inactive sand has lower water-infiltration rates than does unconsolidated, uncrusted sand (Chamizo and others, 2012; Rodriguez-Caballeroa and others, 2012), promoting overland flow that could channelize into erosive gullies once it develops sufficient shear stress in a place where the crust is damaged or weak enough to erode. It is also possible that gullies, once formed, have less potential to continue propagating after they enter active sand, owing to the greater infiltration capacity.

Our field observations indicate that these latter processes (more difficult gully initiation and growth through active sand) are probably less important than aeolian annealing in this field setting because the great majority of gullies initiate outside (upslope) of the sand deposits rather than in them; overland flow commonly utilizes previously established channels across less-permeable bedrock or talus and then incises through (active and inactive) sand deposits. Our observations during intense rain events confirm that gullies through sand commonly form in this way rather than by initiating directly from rainfall on sand. Our field and aerial-photographic observations also confirm that aeolian annealing can erase gully paths. Thus, we infer that the lower gully prevalence in active sand, and the greater likelihood of gully termination in active sand, largely result from aeolian sand transport being an effective gully-annealing mechanism. Our field observations indicate that aeolian infilling occurs in conjunction with some backwasting of noncohesive sand in gully walls, which provides additional sand to infill gullies.

Our analysis of historical aerial imagery revealed that aeolian sand annealing had visibly affected a small but detectable proportion (1–3 percent) of the 358 terminating gullies we analyzed. Thus, aeolian infilling constituted a relatively uncommon fate for gullies in the river corridor, at least between 1984 and 2009. However, because gullies tend to form in the same place repeatedly from overland flow that follows persistent flow paths, it is likely that some gullies filled in, were excavated again by later overland flow, and then refilled between the relevant dates of analysis. We consider this likely, as previous work within our study reaches has measured rapid dune migration and aeolian inflation in close spatial and temporal proximity to gully erosion (Collins and others, 2009, 2012; Draut and others, 2010). Our work in Section III confirmed that gullying and aeolian sand movement are not rare, but rather are common processes measurably changing river-corridor landscapes over time scales of months to years.

Together with previous findings that modern sand supply from Colorado River sandbars promotes aeolian sand activity in downwind landscapes (Draut, 2012), results of this study imply that landscapes receiving aeolian sand supply from modern river sandbars are less likely to have advanced gully erosion than are biocrusted landscapes without modern sand supply or aeolian activity. Although gullies can erode both active and inactive sand landscapes—and some parts of the landscape will always be more vulnerable to gully formation than others are, given that overland flow tends to focus in the same places repeatedly—gully erosion evidently becomes less prevalent as gullies anneal in active aeolian sand. Thus, landscapes and archeological sites that receive modern sand supply from fluvial sandbars under the dam-controlled flow regime have less risk of developing advanced gully erosion, and a greater chance that gullies will anneal or have their growth impeded by aeolian sand.

The greatest distinguishing characteristic between active and inactive aeolian sand in the Colorado River corridor is biologic crust cover (fig. 7). Biologic crust, a community of lichen, mosses, fungi, algae, and cyanobacteria widespread on Southwest desert soils (Belnap and others, 2001; Belnap and Lange, 2003), tends to colonize sand deposits receiving little modern sand supply (Draut, 2012). Once a crust is established, it reduces aeolian sand entrainment and mobility by armoring the ground surface (Leys and Eldridge, 1998; Goossens, 2004; Zhang and others, 2008). Vegetation, too, inhibits aeolian sand transport once established (for example, Ash and Wasson, 1983; Buckley, 1987; Raupach and others, 1993). The growth of vegetation and biologic crust can enhance each other, both by virtue of stabilizing the sand surface, which facilitates plant recruitment, and because biologic crust fixes nitrogen that neighboring organisms use (MacGregor and Johnson, 1971; Harper and Belnap, 2001). As dam operations have reduced aeolian sand supply and sand activity in river-corridor landscapes, they have thereby promoted greater-than-natural biologic crust abundance (Draut, 2012). This has consequences not only for upland ecosystems, but also for how widespread gully erosion may become. In one sense, the unnaturally great abundance of biologic crust in the regulated Colorado River corridor stabilizes relict sand surfaces by preventing sand transport that otherwise would cause aeolian dunes to migrate over time. However, instead of destabilizing by dune migration (which affects the condition of some Marble–Grand Canyon archeological sites), biocrusted landscapes can destabilize by localized gully erosion instead, once the crust has been disturbed (fig. 24), substantially damaging archeological sites. Thus, the common perception that biocrusted sand deposits are stable is somewhat misleading in that it does not reflect the likely erosional trajectory of biocrusted landscapes and archeological sites once the crust is locally disturbed and gullying has been initiated.

While investigating the effectiveness of aeolian sand in gully annealing, we have not addressed other factors related to changes in local base level that may also influence gully development (Hereford and others, 1993). The potential for gully erosion likely depends not only on whether aeolian sand is available to infill the gullies, but also on the base level to which gully incision is graded—that of terrace surfaces higher than the mainstem river channel, tributary-channel elevations, or the mainstem river. We have focused on the role of aeolian sand in gully prevalence because of its relevance for the present management objectives of the GCDAMP—increasing the aeolian supply through sandbar growth from controlled floods is a realistic management option, whereas modifying the base level of the mainstem river through major flood flows is not currently under consideration. However, the influence of local base level on gully erosion in the Colorado River corridor warrants further investigation in subsequent studies.

Section III - Landscape Change at Archeological Sites Receiving Sand Supply After Controlled Floods, Grand Canyon National Park

Background

As we have shown in the preceding sections, river-corridor archeological sites in Grand Canyon National Park vary in their potential to receive aeolian sand supply from fluvial deposits under the modern, dam-controlled flow regime. Sites also vary in their inferred resilience to gully erosion, as a function of aeolian sand activity on the surrounding landscape (Section II). Type 1 sites (Section I) have the greatest connectivity between fluvial sand sources and upland sand-dominated landscapes, the greatest potential for modern aeolian sand supply, and thus the highest potential for natural mitigation of gully erosion. However, having high potential to receive modern aeolian sand supply does not necessarily mean that sites will be unaffected by gully erosion or other types of landscape degradation. Rain, wind, creep, and occasional rockfalls and debris flows continually reshape the river-corridor landscape, often altering the condition or integrity of cultural sites. Thus, even type 1 sites cannot be assumed to be stable and safe from erosive damage. To assess landscape change and stability at type 1 sites, we investigated the interplay of annealing and erosive forces on sites expected to receive additional aeolian sand supply owing to controlled floods.

We anticipated that type 1 sites, which receive aeolian sand from controlled-flood sandbars, would erode less rapidly than would other sites that lack windblown sand supply from modern (controlled-flood) sandbars. Thus, we quantified topographic change over several years at four type 1 sites in Grand Canyon National Park (Marble–Grand Canyon) that have substantial connectivity between fluvial sandbars and inland aeolian deposits, and compared these measurements to topographic change measured over a year at four sites in the Glen Canyon reach that do not receive modern sand supply (Section IV). We selected two groups of sites that represent end-member cases of modern sand supply. The four in Marble–Grand Canyon are within aeolian dune fields on top of debris fans that have sand-trapping eddies

on their downstream sides. Sand from those eddy sandbars blows downwind directly into the dune fields containing the type 1 sites, with no substantial vegetation or topographic barriers to limit sand movement. In contrast, the Glen Canyon sites in Section IV are in and on Holocene terraces with essentially no modern sand supply, and very little aeolian sand activity on the terrace surfaces. The differences in topographic evolution of these two groups thus likely represent end members of site evolution; landscape change at sites with intermediate modern sand-supply conditions will be evaluated during a subsequent study.

The four type 1 sites in Marble–Grand Canyon are located approximately 50 to 100 river miles (80 to 160 km) from one another (fig. 29), thereby capturing a broad spectrum of the regional conditions in the canyons. Herein, we refer to each of the sites by their archeological-site identification number (AZ:C:05:0031, AZ:C:13:0321, AZ:B:10:0225, and AZ:G:03:0072US – the suffix "US" indicates that we monitored only the upstream half of the large archeological site). We used high-resolution landscape-change detection and high-resolution records of weather events to assess the cumulative impacts of weather-related changes and the effects of controlled floods on archeological-site change over a four-year monitoring period. The monitoring period brackets two controlled floods, one each in November 2012 and November 2013 (table 1). Our work complements previous studies at three of the same sites (Collins and others, 2009, 2012), thereby extending our understanding of the detailed, short-term geomorphic response of these sites to varying weather and river flow conditions.

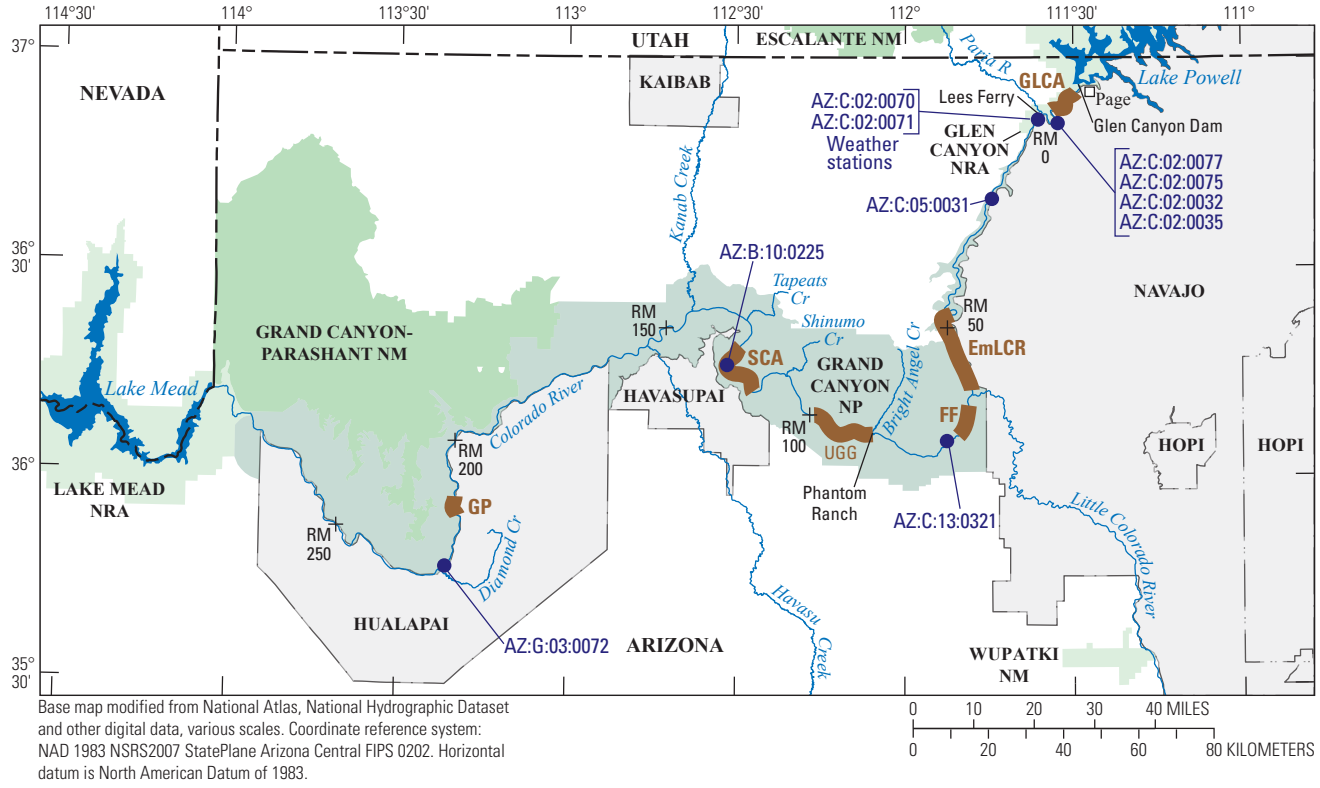

Figure 29. Location map (same area as in fig. 1*B*), showing approximate locations of archeological sites and weather stations discussed in Sections III and IV. The sites shown in Glen Canyon are near enough to each other not to be differentiable at this scale. Glen Canyon includes the canyon region from Lake Powell downstream to Lees Ferry (RM 0). Marble Canyon extends from RM 0–61 and Grand Canyon from RM 61–277.

Research Questions

We evaluated the four, abovementioned type 1 archeological sites by posing two questions:

- Does aeolian sand supply from controlled-flood sandbars to type 1 archeological sites cause enough deposition to offset erosion, and thereby protect the archeological resources?
- In areas with modern aeolian sand supply, and with land surfaces undergoing both gully erosion and active aeolian sand transport, is there net sediment loss and topographic lowering such that cultural resources are affected?

We investigated both questions quantitatively by measuring the sediment volume gain or loss at the selected archeological sites, and linking these findings to landscape-altering wind and rainfall processes.

Methods

We used a combination of site-specific topographic, meteorological, and time-series photographic monitoring to document changes at the four selected type 1 archeological sites in Marble–Grand Canyon over a 2- to 4-year interval (2010–13; exact dates of data collection varied among the sites). The topographic data revealed the nature and location of landscape change occurring at each site, whereas the meteorological data identified the magnitude and timing of processes that potentially caused landscape change; the photographic data constrained the timing of landscape change. Although we collected only two new topographic data sets as part of this work (in May 2013 and May 2014), we compared these topographic surfaces to those collected at the same four sites in September 2010 (Collins and others, 2012). Partial meteorological and photographic datasets are available from 2010 to 2012; we used these to try to constrain the cause and timing of detected changes. During intervals without meteorological or photographic data, we estimated the probable causes of change based on field observations made during our site visits (for example, active dunes indicating aeolian transport).

Topographic Change Detection

Our methods for identifying site-specific landscape change at archeological sites followed protocols previously developed for monitoring in Grand Canyon National Park (Collins and others, 2008, 2009, 2012). We used repeat, high-resolution, terrestrial (ground-based) lidar laser scanning to collect topographic data from each of the four archeological sites (fig. 30). The topographic data consist of millions of surveyed points (a point cloud) that capture the position and shape of any object within view of the laser instrument. In this study we used a Riegl Z420i scanner, in conjunction with a mounted and calibrated Nikon D300 digital camera, and a survey prism, to measure the x, y, z positions of each survey point, a red-green-blue-intensity determination of the pixel in which each point resides, and the x, y, z position of the laser instrument, respectively. By moving the laser scanner

Figure 30. Terrestrial lidar data-collection setup in Grand Canyon National Park; laser scanner is at right. Optimal surveying locations must be identified to capture the area of interest—here, the gully partly filled with aeolian sand. A total station and survey prism were used to georeference the instrument location, along with temporary reflector control points (one visible in the background, mounted on a tripod).

around each site and collecting data from several vantage points, we quantified the three-dimensional shape of the ground surface. The final result was a colored point cloud in which objects (gullies, cliffs, vegetation, etc.) are easily identified and distinguished from one another.

Uncertainties in the topographic data arise from three sources: the laser, the registration process of collating data from multiple vantage points, and the georeferencing procedure that assigns real-world coordinates to each survey point. We adopted previously calculated empirical error determinations for the datasets based on established error-analysis methods developed in prior topographic surveys at some of the same sites (Collins and others, 2012). Average vertical errors in each final point cloud collected in September 2010, May 2013, and May 2014 were determined to be 1.5 cm. Thus, we set a conservative change-detection threshold of 3 cm for each site, representing the limit of topographic change that can reasonably be detected and positively identified.

To calculate topographic differences from scans of the same site at different times, the point-cloud data were modeled by developing triangulated irregular network (TIN) surfaces and DEM grid surfaces. TINs typically represent terrain in better resolution, because the point data are used directly to form the corners of the triangular facets that define the surface. DEMs rely on extrapolation of the surface to the center of a grid cell, thereby introducing potential inaccuracies of the surface. However, DEMs also allow more robust change-detection algorithms, by computing the elevation difference between topographic surfaces resolved at different times. We used a minimum point density of 96 points/m^2 and a grid spacing of 5 cm to minimize potential errors in our surface modeling algorithms. For additional details of the data processing, see Collins and others (2009, 2012).

Meteorological Monitoring

To identify the role of weather, and the specific processes causing landscape change at the archeological sites, we installed remote weather stations at each site (fig. 29). The stations consisted of Vaisala™ WXT510/520 transmitters measuring wind direction, wind speed, maximum gust speed, air temperature, relative humidity, barometric pressure, and rainfall. Data loggers at each station recorded the parameters at 4-minute intervals, and were downloaded during field visits every few months. Full details of the weather stations and resulting data were provided by Dealy and others (2014) and Caster and others (2014); we refer here to general patterns and specific weather events recorded at these stations as necessary to interpret the landscape-change measurements discussed below.

Time-Series Photography

We collected high-resolution digital photographs of each archeological site and surrounding landscape to provide a means to verify and constrain the timing of the changes detected by the topographic monitoring. We used Cannon Rebel DSLR series T3/T4 cameras regulated with a Campbell Scientific CR200X data logger to take photographs every 2 hours during daylight. Where we were able to locate a camera in close proximity to a site, we were able to identify subtle landscape changes, such as the formation of incipient gullies. However, in cases where there was no suitable location for a camera deployment near the site, and cameras could only be located across the river from a site of interest, the photographs were useful only for identifying large-scale changes such as sandbar formation. We refer to these photographic records as necessary to document the timing of landscape changes discussed below; more detail about these records is available in Caster and Sankey (2016).

Results

AZ:C:05:0031

Site Description

Site AZ:C:05:0031 (figs. 31, 32) is an ancestral Puebloan camp site dating to the 11th or early 12th century. The site contains evidence of roasting features, pottery sherds, stone tool-making debris, and low stacked-stone walls (Fairley and others, 1994), and is located immediately below a steep outcrop of limestone. Aeolian dune sand forms a ramp from the Colorado River up to the base of the outcrop, and the site itself is primarily located in and on this dune sand. A prominent gully (G1) bisects the dune field and bounds the archeological site to the south. The site is covered mostly by sand, but large (1- to 2-m diameter) boulders and isolated vegetation cover parts of the site as well. Vegetation includes prickly-pear cactus (*Opuntia* sp., including beavertail cactus, *Opuntia basilaris*), Mormon tea (*Ephedra* sp.), dropseed (*Sporobolus* sp.), Indian ricegrass (*Achnatherum hymenoides*), asters (*Asteraceae* family), dicoria (*Dicoria canescens*), and nonnative Russian thistle (tumbleweed; *Salsola* sp.). O'Brien and Pederson (2009a) identified gullying, aeolian transport, piping, and creep affecting this site, and noted that whereas revegetation efforts and aeolian inflation have stabilized some parts of the site, the archeological resources continue to be affected by creep. This site and its surrounding dune field are directly downwind of a fluvial sandbar that enlarged during high flows in the 1980s and also during each of the subsequent controlled floods.

We analyzed landscape change in the area of the archeological site below the limestone outcrop and in three areas of dune sand located between the outcrop and the Colorado River (figs. 31, 32). Focusing on this part of the site allowed us to detect any potential aeolian aggradation in response to sand supply from the controlled-flood sandbar located immediately upwind of the dunes.

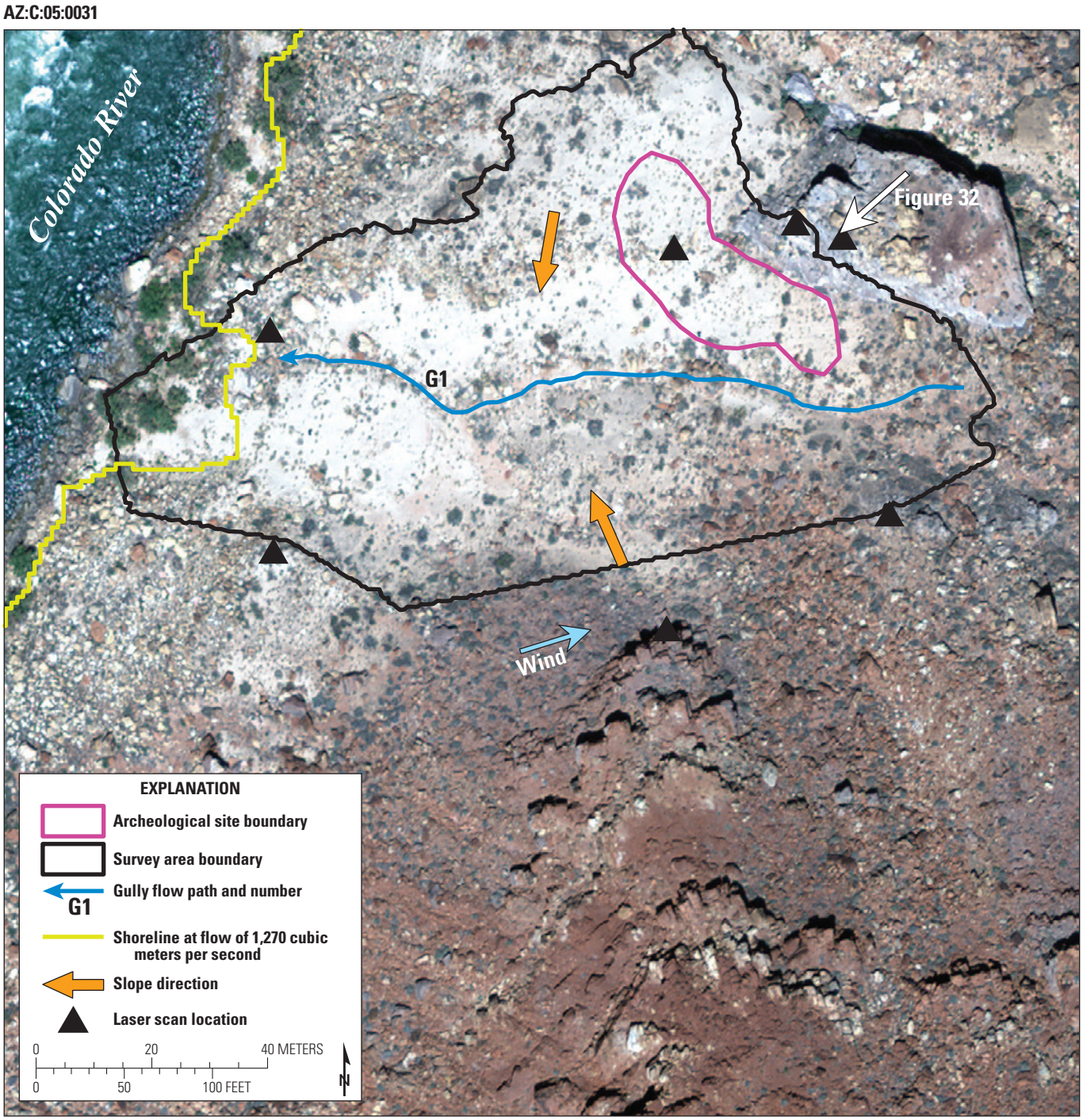

Figure 31. Site AZ:C:05:0031 survey-area map.

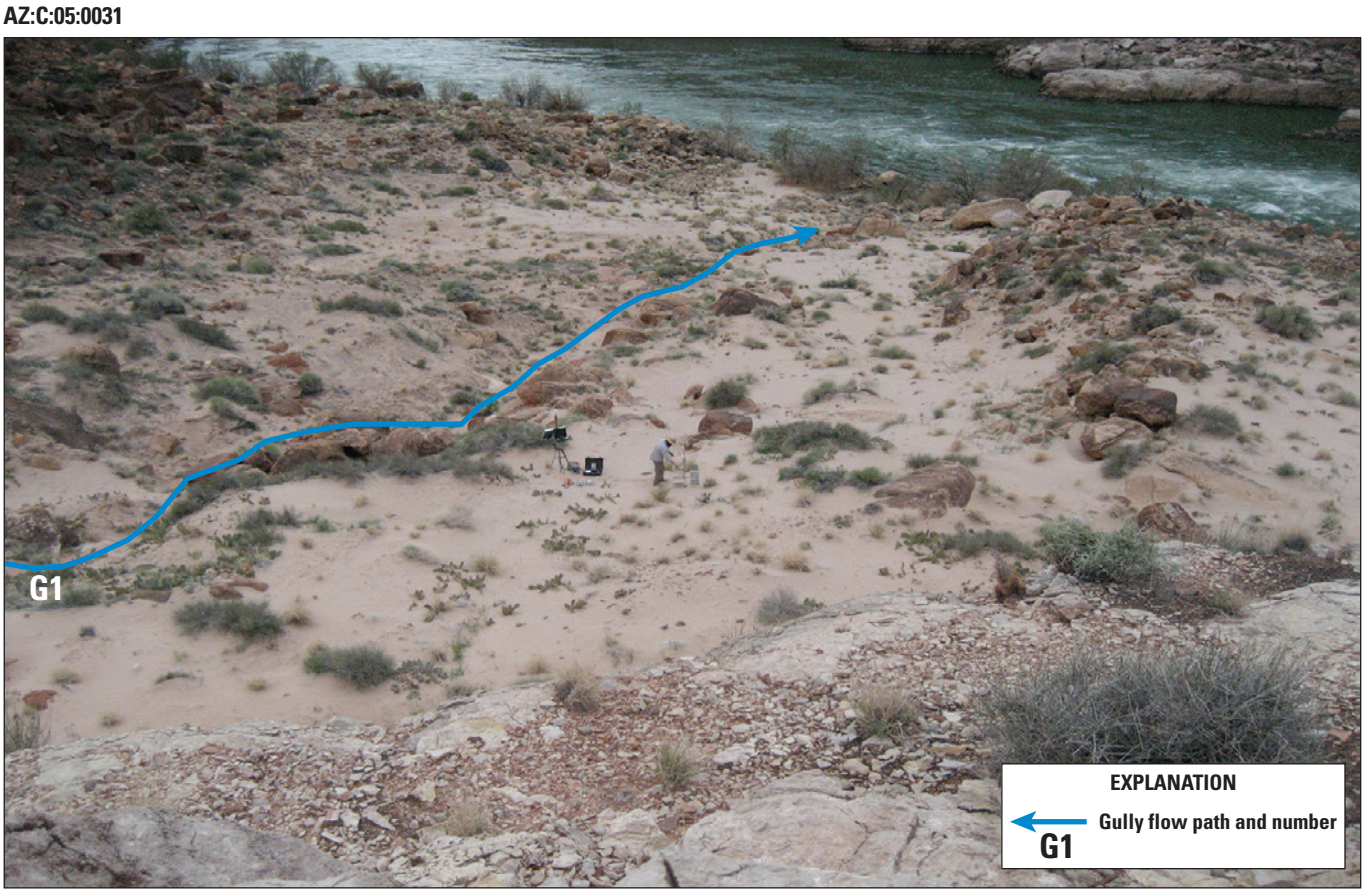

Figure 32. Site AZ:C:05:0031 survey-area photograph, showing flow path of gully G1 (blue). View is toward the southwest.

Topographic Change (2010–13)

Topographic changes at site AZ:C:05:0031 between 2010 and 2013 included both erosion and deposition, mainly related to aeolian sand transport (fig. 33*A*; table 2). The majority of change appears to have occurred from aeolian sand transport within the active inland dune field (as opposed to sand moving into the dune field from the fluvial sandbar). We infer sand transport from the southwest toward the northeast, coincident with the prevailing wind direction measured at this site (Draut and others, 2010). Erosion within the entire monitored area (that is, within the focused change-detection areas indicated by the green boundaries in fig. 33) totaled 27.72 m^3 and occurred over an area of 362.1 m^2; deposition totaled 12.54 m^3 and occurred over an area of 193.4 m^2, yielding net erosion of 15.18 m^3. The focused change-detection boundaries show where change is most likely to have occurred within areas of active aeolian sand deposits. The dominant erosional signal has a spatial pattern implying aeolian deflation, and indicates that sand is being transported by wind either into adjacent gullies (where it may partly offset overland-flow erosion) or out of the survey area entirely, where it has an unknown fate and unknown consequences for archeological-site stability. However, the deposition (aeolian inflation) that we detected within the archeological-site boundary indicates that active aeolian sand has likely increased site stability. In a previous monitoring campaign in 2010 (Collins and others, 2012), only erosion had been recorded at this site. Sand transport from the river margin toward the archeological site (toward the northeast) indicates that sandbar sediment, including some from controlled floods in 2008 and 2012, may be increasing site stability (that is, burying part of the archeological site in sand; fig. 33). One area of erosion (ER4) and two areas of deposition (DEP4, DEP5) were detected nearest to the Colorado River, at the westernmost side of the surveyed area (fig. 33*A*), and may be linked to direct fluvial sediment mobilization and redeposition during controlled floods.

Topographic Change (2013–14)

Topographic changes at site AZ:C:05:0031 between 2013 and 2014 showed similar patterns to those that occurred between 2010 and 2013, and included both erosion and deposition related to aeolian sand transport (fig. 33*B*; table 2) and also fluvial erosion and deposition in the westernmost part of the surveyed area, by the river (regions ER4, DEP4, and DEP5). Erosion within the surveyed area totaled 8.57 m^3 and occurred over an area of 135.7 m^2; deposition totaled 9.04 m^3 and occurred over an area

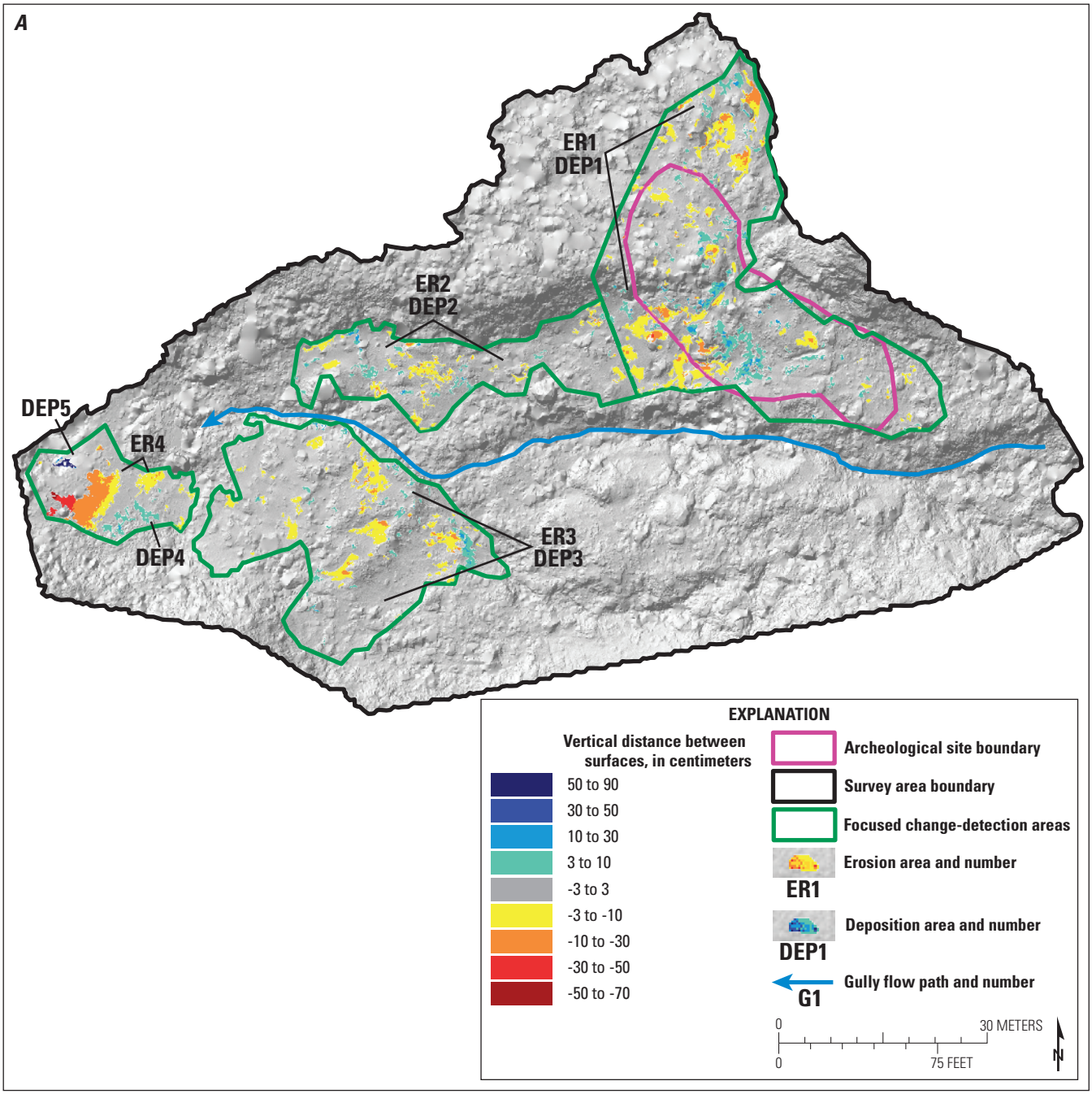

Figure 33. Landscape change at site AZ:C:05:0031. A 5-cm gridded topographic change output shows erosion (warm colors, negative) and deposition (cool colors, positive) from (*A*) September 2010 to April 2013, and (*B*) April 2013 to May 2014. Topographic change was calculated only in focused areas noted. Identified change is grouped by area labels (ER, erosion; DEP, deposition) that are cross-referenced with table 2. "IG#" denotes incipient gullies detected from landscape-change analyses.

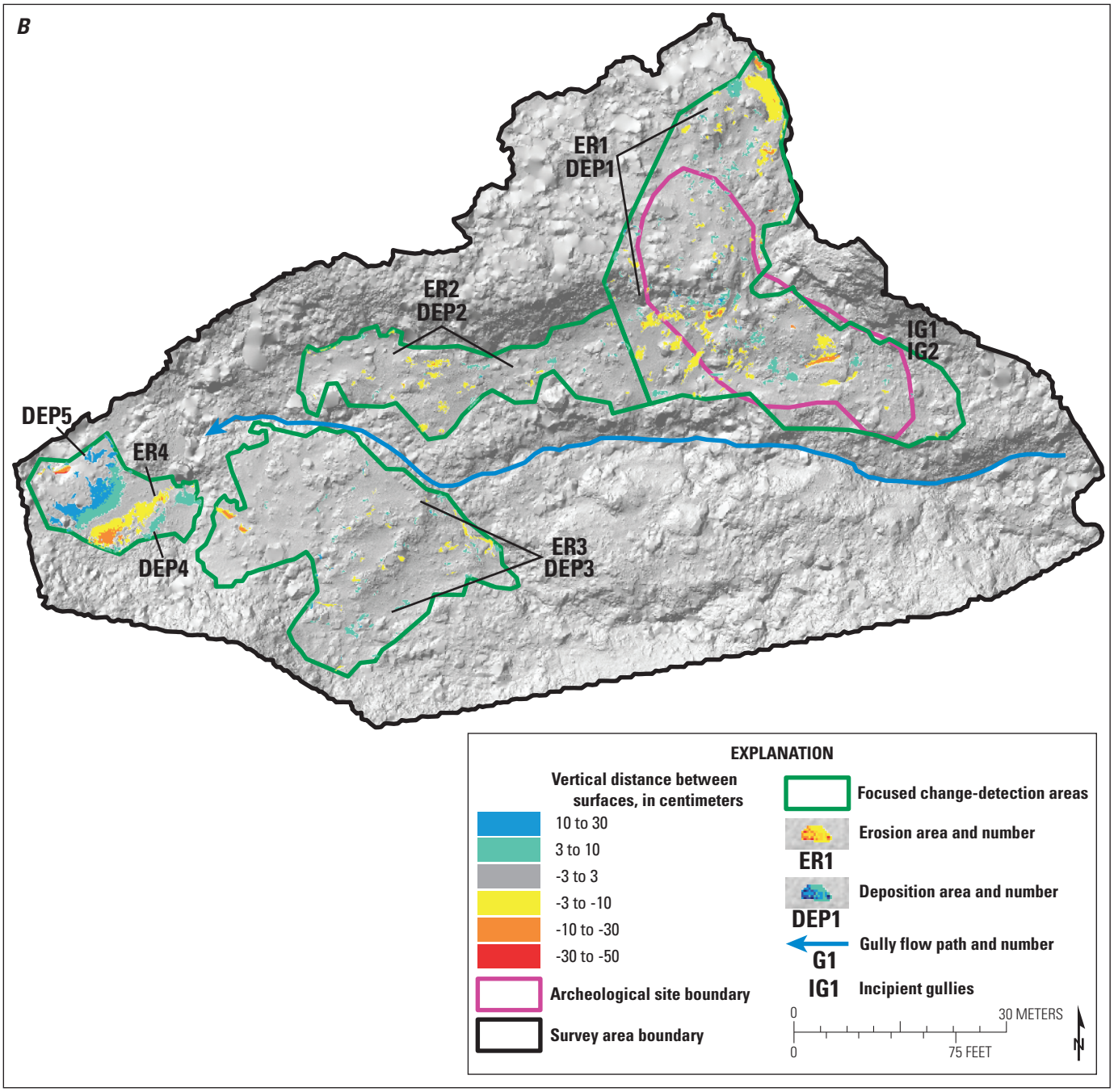

Figure 33.—Continued

Table 2. Summary of topographic change at site AZ:C:05:0031.

[m/yyyy, month/year; m^2, square meters; cm, centimeters; m^3, cubic meters]

Site number and region	Time period (m/yyyy)	Area (m^2)	Average depth (cm)	Volume (m^3)
AZ:C:05:0031 – ER1	9/2010–4/2013	169.2	-7	-11.72
AZ:C:05:0031 – ER2	9/2010–4/2013	50.6	-6	-2.85
AZ:C:05:0031 – ER3	9/2010–4/2013	85.4	-6	-4.78
AZ:C:05:0031 – ER4	9/2010–4/2013	56.9	-15	-8.37
AZ:C:05:0031 – DEP1	9/2010–4/2013	107.4	6	6.45
AZ:C:05:0031 – DEP2	9/2010–4/2013	25.8	6	1.51
AZ:C:05:0031 – DEP3	9/2010–4/2013	44.9	6	2.57
AZ:C:05:0031 – DEP4	9/2010–4/2013	12.7	5	0.62
AZ:C:05:0031 – DEP5	9/2010–4/2013	2.6	53	1.39
AZ:C:05:0031 – ER1	4/2013–5/2014	79.1	-6	-4.72
AZ:C:05:0031 – ER2	4/2013–5/2014	14.0	-5	-0.66
AZ:C:05:0031 – ER3	4/2013–5/2014	13.0	-6	-0.78
AZ:C:05:0031 – ER4	4/2013–5/2014	29.6	-8	-2.41
AZ:C:05:0031 – DEP1	4/2013–5/2014	43.6	5	2.19
AZ:C:05:0031 – DEP2	4/2013–5/2014	5.8	5	0.28
AZ:C:05:0031 – DEP3	4/2013–5/2014	16.0	5	0.84
AZ:C:05:0031 – DEP4	4/2013–5/2014	12.6	5	0.69
AZ:C:05:0031 – DEP5	4/2013–5/2014	43.6	12	5.04

of 121.6 m^2. Whereas the volume of erosion was substantially less (69 percent) than that recorded over the longer time interval between 2010 and 2013, and the net volume change was positive between 2013 and 2014 (by 0.47 m^3), the volume of deposition was similar (only 28 percent less over 2013–14), which may indicate positive short-term effects of the controlled floods in 2012 and 2013. Although most of the new deposition was in the form of a fluvial sandbar (region DEP5), aeolian transport of this sand inland toward the archeological site is likely, given the prevailing northeastward wind at this site.

Despite aeolian processes having dominated the site response, precipitation-induced runoff also played an important role within the archeological-site boundary. At site AZ:C:05:0031, two incipient gullies (IG1 and IG2, fig. 33*B*) formed as a result of storms in August and September 2013. These summer monsoonal storms had maximum 10-minute rainfall intensities of 75 and 61 mm/hr, respectively, both of which exceed the threshold for precipitation-induced runoff erosion identified to be important in this river-corridor environment (Collins and others, 2016). Lidar measurements in April 2014 indicated overall mean erosional depths of between 6 and 11 cm, with 0.57 m^3 of total erosion. Analysis of time-lapse photographs taken by the stationary camera at this site indicated that the magnitude of gullying was even greater initially—comparison of photographs from September 2013 with those from May 2014 showed that the incipient gullies partly annealed between September 2013 and May 2014, presumably by filling with aeolian sand (Caster and others, 2014).

AZ:C:13:0321

Site Description

Site AZ:C:13:0321 (figs. 34, 35) encompasses a large active dune field composed of source-bordering dunes directly inland from a Colorado River sandbar; the archeological-site boundary begins 30 m inland from the river. Because the dune field receives sand from an adjacent river sandbar enlarged by controlled floods, this site displays strong type 1 connectivity between fluvial and aeolian sand resources, burying and contributing to preservation of the archeological-site.

The site consists of a multi-component habitation area dating to the time period when ancestral Puebloan farmers occupied eastern Grand Canyon, approximately 700–1200 C.E. (Fairley and others, 1994; Fairley, 2003). Among the archeological remains are a rubble pile that appears to be a collapsed prehistoric masonry structure, at least four roasting features, several ceramic sherds, and fragments of ground stone. One of the roasting features (consisting of a circular mound of fire-cracked rocks, ash, and wood charcoal, encircled by upright stone slabs) is within the lowest part of the sand dunes adjacent to a channel-shaped swale formed by the dunes, and is intermittently buried by aeolian sand. Therefore, its protection and preservation are tied directly to the sandbar immediately upwind. The interdune swale slopes towards the river, but no indications of severe overland flow (that is, incised gullies) are readily evident (O'Brien and Pederson, 2009a)

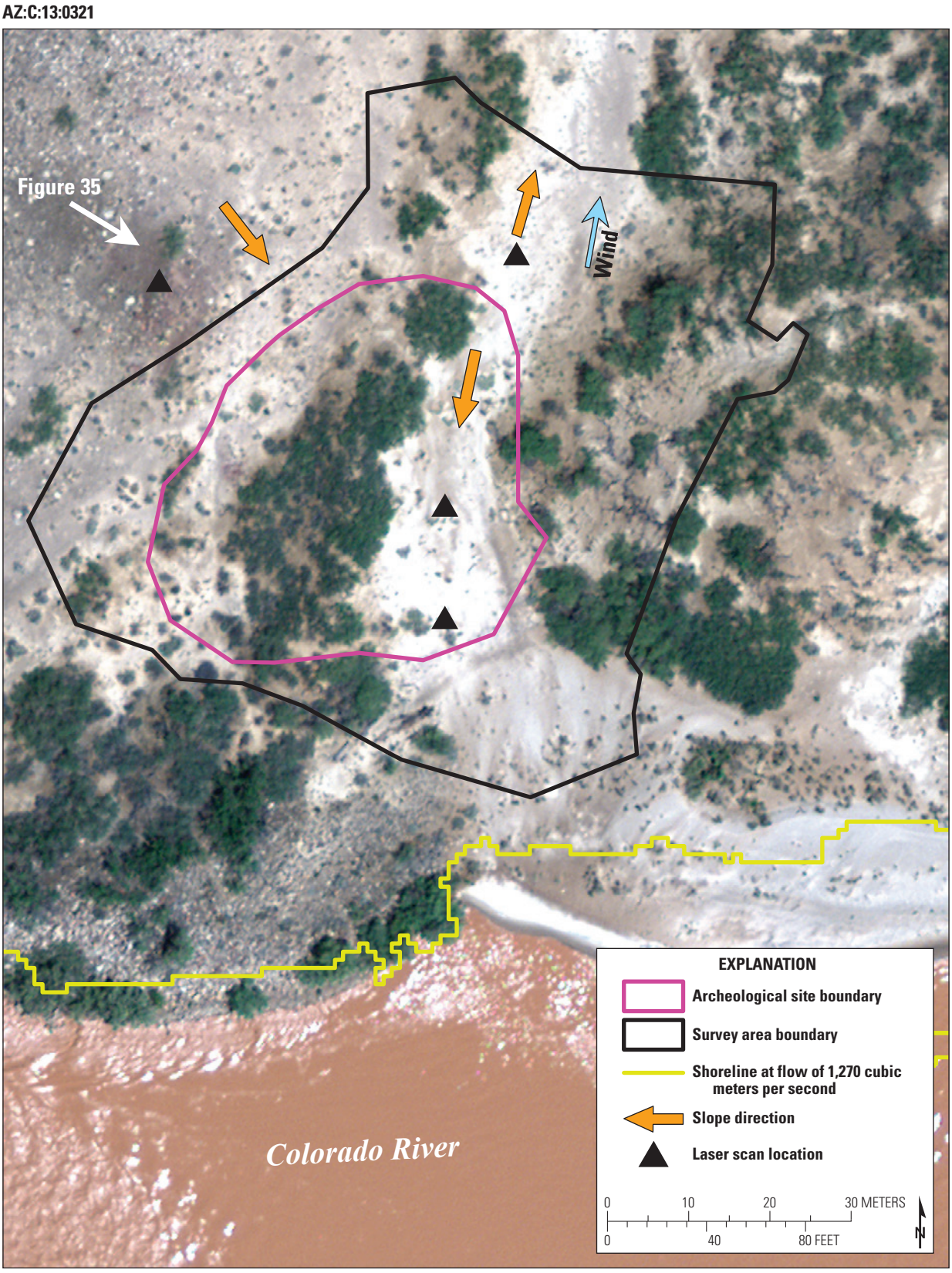

Figure 34. Site AZ:C:13:0321 survey-area map.

Figure 35. Site AZ:C:13:0321 survey area photograph. View is towards the north.

other than several areas of gravel-pebble slopewash located at the downslope end that we infer may be a lag deposit resulting from some past overland-flow episode. Honey mesquite trees (*Prosopis glandulosa,* some dead or dying, others healthy) surround the site. Within the site, a wide variety of isolated vegetation clusters are established within the dune sands and gravel substrate, including globemallow (*Sphaeralcea* sp.), arrowweed (*Pluchea sericea*), saltbush (*Atriplex* sp.), sand verbena (*Abronia elliptica*), and nonnative Russian thistle (*Salsola* sp.). O'Brien and Pederson (2009a) identified aeolian transport as the primary geomorphic process affecting this site. They noted that aeolian deflation can expose archeological artifacts there, making them vulnerable to anthropogenic impacts such as trampling.

We analyzed landscape change throughout the entire archeological site and adjacent sandbar to investigate potential linkages between site condition and the direction and quantity of windblown sand that the site receives. Dense vegetation at the top of the dunes prohibited detecting change in some areas; however, based on field observations over several years, we judged that it is unlikely that change greater than the uncertainty threshold (3 cm of vertical change) occurred beneath the vegetation in these areas.

Topographic Change (2010–13)

Topographic changes at site AZ:C:13:0321 between 2010 and 2013 included erosion and deposition related mainly to aeolian sand transport (fig. 36*A*; table 3). Erosion within the surveyed area (which included approximately half of the archeological-site area; fig. 36) totaled 27.15 m^3 and occurred over an area of 262.3 m^2; deposition totaled 25.32 m^3 and occurred over an area of 311.3 m^2. These values yielded net erosion of 1.83 m^3. The majority of change evidently occurred from aeolian transport of sand from an active fluvial sandbar (ER3) and associated inland dune deposits. Sand apparently was transported from the south-southeast toward the north-northwest, apparently, judging from the region of erosion (ER3) at the riverward, upwind side of the survey area and depositional areas north, or downwind, of the eroded region (fig. 36*A*). This is broadly consistent with the north- to northeastward prevailing wind direction in this area, measured at a weather station 700 m away (Draut and others, 2010; Caster and others, 2014) and inferred from dune slipface orientations immediately adjacent to the site. The volume of sand deposition within the archeological-site boundary (16.18 m^3 in region DEP1) was more than double that which exited (6.90 m^3 in region ER1), and the roasting feature in the lowest part of the dunes was buried increasingly by sand between 2010 and 2013 as a result of this new deposition. However, parts of the interdune swale eroded, indicating that the processes affecting the site (aeolian inflation and deflation) are not spatially uniform. Regardless, the overall depositional signal within the archeological site between 2010 and 2013 indicated that fluvial-sourced sand, potentially from controlled floods in 2008 and 2012 (floods that enlarged the sandbar upwind of this archeological site), may be reaching the archeological site downwind and thus achieving one objective of the controlled-flood management actions.

Topographic Change (2013–14)

Topographic changes at site AZ:C:13:0321 between 2013 and 2014 followed similar patterns to those detected between 2010 and 2013, and included both erosion and deposition related to aeolian sand-transport processes (fig. 36*B*; table 3). Erosion within the surveyed area (which included the entire archeological site) totaled 35.67 m^3 and occurred over an area of 503.8 m^2; deposition totaled 25.02 m^3 and occurred over an area of 360.2 m^2. These values yield net erosion of 10.65 m^3 within the entire survey area.

The survey area for 2013–14 was approximately twice as large as that surveyed for 2010–13; thus, only area-normalized change can be compared between the datasets for each time interval. The extended areal coverage in 2013–14 indicated that aeolian sand transport was widespread through the archeological site and neighboring areas. The overall pattern of sand transport remained unchanged from previous monitoring periods (see Collins and others, 2012, and results for 2010–13 reported herein), with broad patches of aeolian erosion and deposition (deflation and inflation)

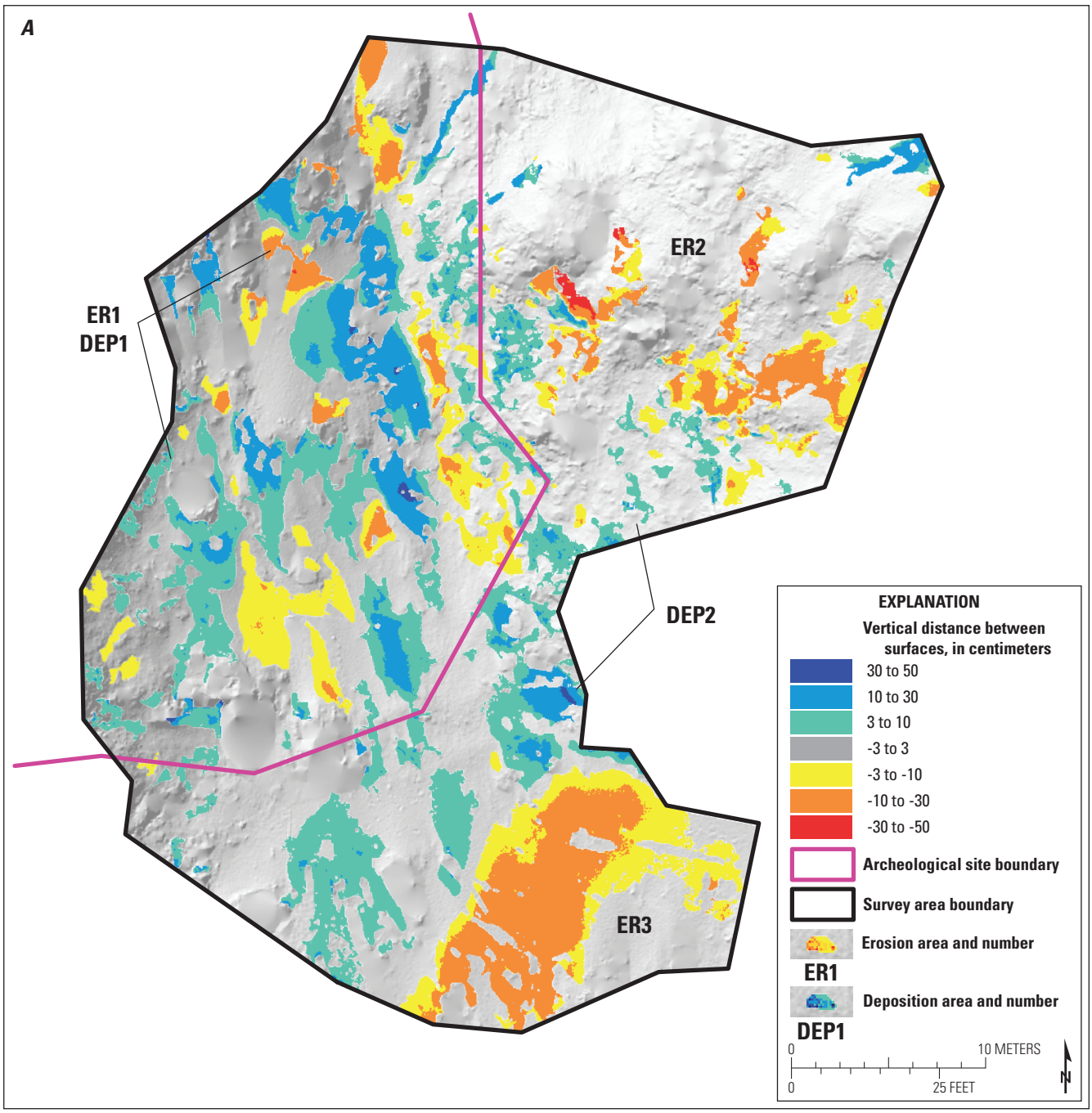

Figure 36. Landscape change at site AZ:C:13:0321. A 5-cm gridded topographic change output shows erosion (warm colors, negative) and deposition (cool colors, positive) from (*A*) September 2010 to May 2013, and (*B*) May 2013 to May 2014. Note difference in scales and area surveyed. Identified change is grouped by area labels (ER, erosion; DEP, deposition) that are cross-referenced with table 3.

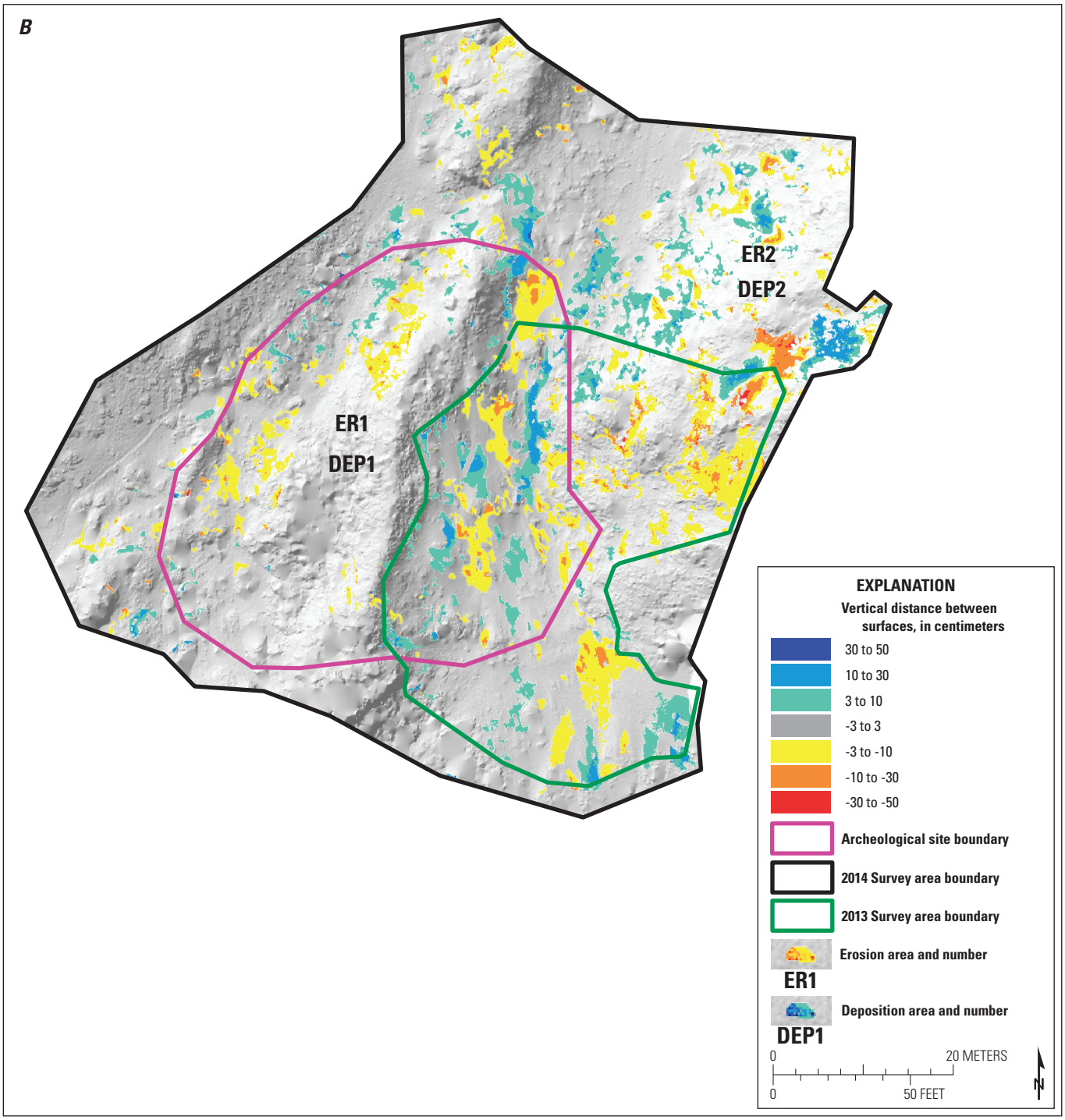

Figure 36.—Continued

Table 3. Summary of topographic change at site AZ:C:13:0321.

[m/yyyy, month/year; m^2, square meters; cm, centimeters; m^3, cubic meters]

Site number and region	Time period (m/yyyy)	Area (m^2)	Average depth (cm)	Volume (m^3)
AZ:C:13:0321 – ER1	9/2010–5/2013	85.2	-8	-6.90
AZ:C:13:0321 – ER2	9/2010–5/2013	84.1	-11	-8.87
AZ:C:13:0321 – ER3	9/2010–5/2013	93.0	-12	-11.38
AZ:C:13:0321 – DEP1	9/2010–5/2013	176.2	9	16.18
AZ:C:13:0321 – DEP2	9/2010–5/2013	135.1	7	9.14
AZ:C:13:0321 – ER1	5/2013–5/2014	193.9	-6	-12.11
AZ:C:13:0321 – ER2	5/2013–5/2014	309.9	-8	-23.56
AZ:C:13:0321 – DEP1	5/2013–5/2014	123.4	7	8.89
AZ:C:13:0321 – DEP2	5/2013–5/2014	236.8	7	16.13

adjacent to one another—indications of a tightly coupled fluvial–aeolian transport system. Notably, during the 2013–14 monitoring period, more sediment was eroded (12.11 m^3) than was transported into (8.89 m^3) the archeological site boundary. This pattern was opposite to that which occurred during the previous, but longer, monitoring period (2010–13; table 3). Whereas erosion rates were similar during these intervals (-0.69 cm/yr for 2010–13, compared to -0.72 cm/yr for 2013–2014), depositional rates varied, with the 2010–13 rate (0.64 cm/yr) being approximately 28 percent greater than that in 2013–14 (0.50 cm/yr). Considering the net volumetric effects normalized for variably sized survey areas and time scales, 0.05 cm/yr of sediment was eroded from the entire surveyed area between 2010 and 2013, and 0.21 cm/yr was eroded between 2013 and 2014. Owing to variability in weather conditions and the timing of controlled floods that enlarge the sandbar upwind of the site, such fluctuations are expected. However, the most important conclusion from this site is that significant changes can be related directly to aeolian sand supply from the adjacent fluvial sandbar.

AZ:B:10:0225

Site Description

Site AZ:B:10:0225 is located within a partly vegetated aeolian sand ramp that is backed by steep and sometimes overhanging sandstone ledges (figs. 37, 38). The ledges formed shelters for the prehistoric people who formerly inhabited the area, and the slope below these shelters is littered with pottery sherds, lithic debitage, fire-cracked rocks, and other artifacts (Fairley and others, 1994). Two large gullies (G1 and G2) traverse the edges of the site and fall steeply over sandstone ledges, terminating near the edge of the river in a deposit of large cobbles and boulders (20 cm to 1 m diameter). The gullies are filled with sand, presumably transported from active dunes immediately upwind. The 74,000-m^2 aeolian dune field surrounding site AZ:B:10:0225 is one of the most active in Grand Canyon, with as much as 70 percent active aeolian sand area; this site is within the Stevens-Conquistador Aisles (SCA) reach, where wind directions transverse to the main canyon orientation result in substantial sand transport inland from the river margins (Section II). Sand sources feeding this particular dune field include a fluvial sandbar upwind of the archeological site that has been enlarged by recent controlled floods. The site may also receive some windblown sand from patchy fluvial sand deposits covering a cobble bar across the river from the site. Vegetation in the area surrounding the archeological site includes catclaw acacia (*Senegalia greggii*) bushes, prickly pear (*Opuntia* sp.), alkali goldenbush (*Isocoma acradenia*), Mormon tea (*Ephedra* sp.), brittlebush (*Encelia* sp.), and perennial bunchgrasses such as Indian ricegrass (*Achnatherum hymenoides*). Tamarisk (*Tamarix ramosissima*) and arrowweed (*Pluchea sericea*) border the site near the edge of the river and lower dune areas. O'Brien and Pederson (2009a) identified gullying, overland flow, aeolian transport, and creep affecting this site, and noted that gullying and creep were incrementally eroding artifacts.

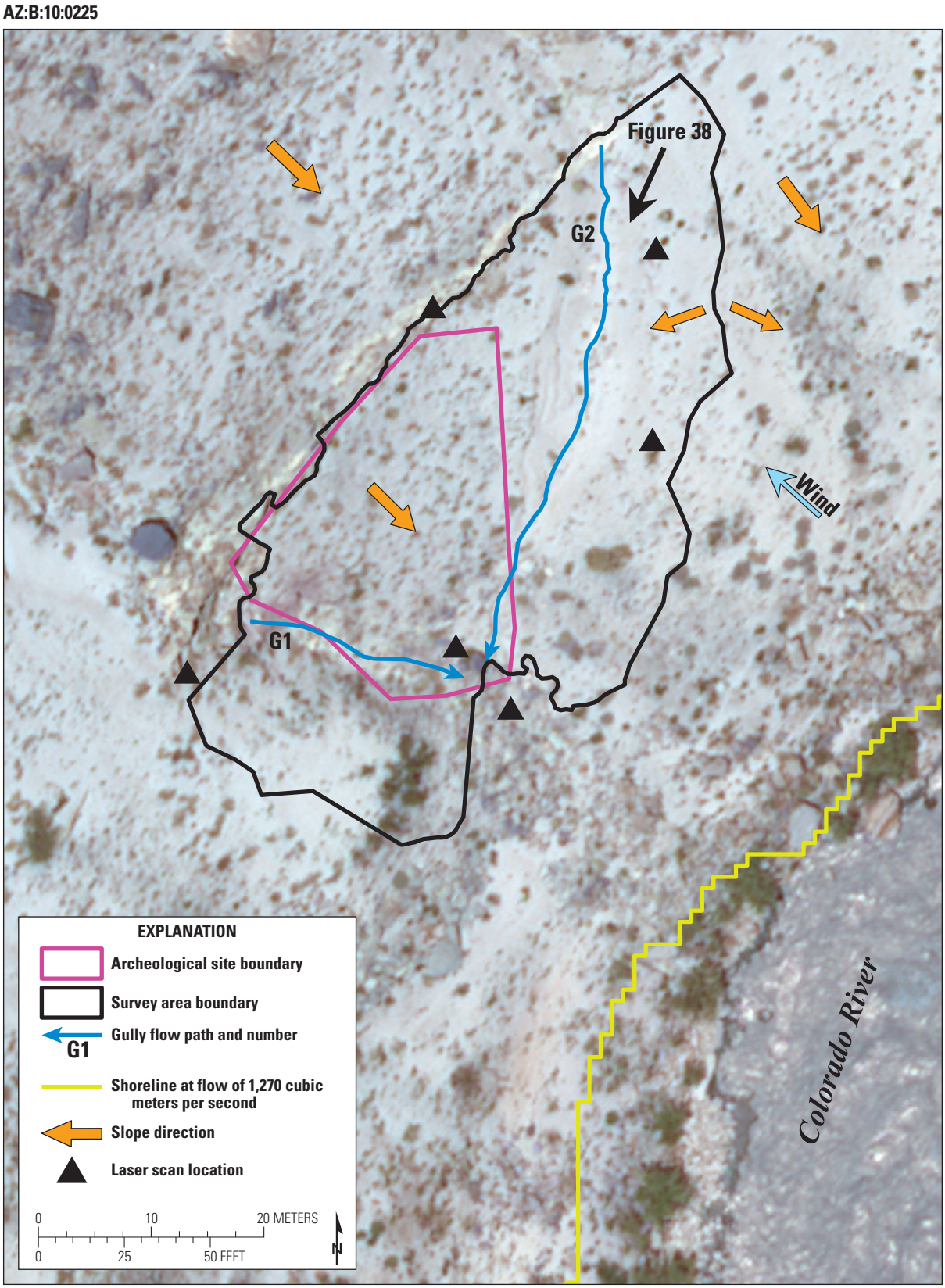

Figure 37. Site AZ:B:10:0225 survey-area map.

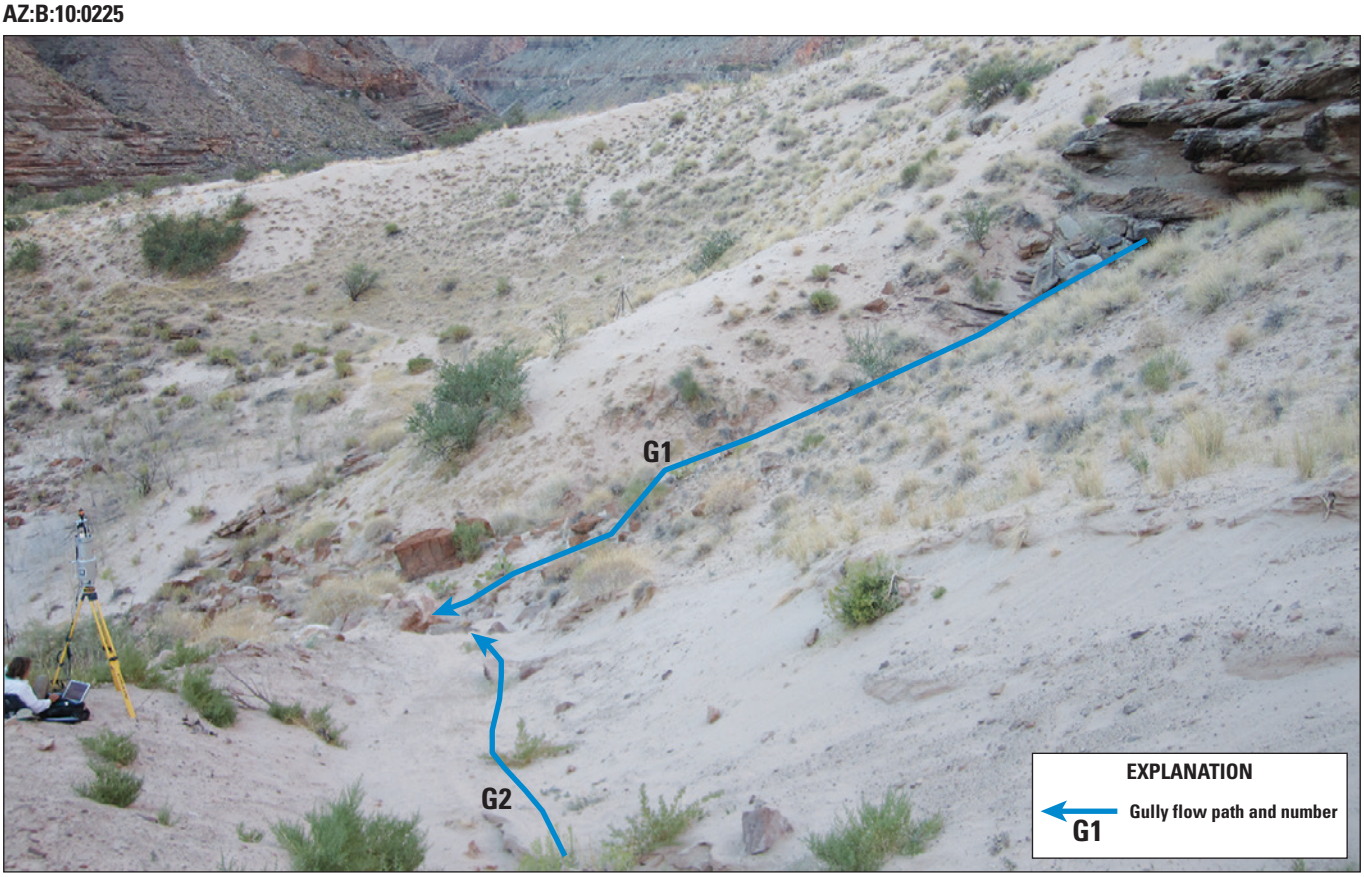

Figure 38. Site AZ:B:10:0225 survey-area photograph showing gully locations (G1 and G2). View is toward the southwest.

Topographic Change (2010–13)

Topographic changes at site AZ:B:10:0225 between 2010 and 2013 included massive gully-related erosion, and both erosion and deposition from aeolian sand-transport processes (fig. 39; table 4). Erosion within the surveyed area (which included nearly the entire archeological site) totaled 93.71 m^3 and occurred over an area of 275.5 m^2; deposition totaled 5.21 m^3 and occurred over an area of 72.5 m^2, yielding net erosion of 88.50 m^3. The vast majority of change occurred from overland-flow-induced erosion of gully G2. There, more than 90 percent of the volumetric erosion was associated with gully widening and deepening, including as much as 1.3 meters of new incision in region ER2. This area also had experienced extensive gullying previously, detected in surveys prior to 2010 (Collins and others, 2012), and the most recent episode of erosion continued to widen the gully to the east. Some effects of gullying during this time period affected the archeological site, to the west of the gully (figs. 37, 39*A*), but for the most part, we detected little change within the main part of the archeological site. Some minor aeolian and fluvial reworking of sediments also occurred in isolated patches within gully G2 (region DEP2), but the overall signal in and around that gully was erosional. We also identified apparent aeolian reworking of the sand surface in the vicinity of gully G1 (regions ER1, DEP1), but found little change to the archeological site itself.

Topographic Change (2013–14)

Topographic changes at site AZ:B:10:0225 between 2013 and 2014 provided evidence for continued widespread changes to the prominent gully (G2) located on the eastern edge of the site (figs. 37, 39*B*). Overall erosion within the surveyed area totaled 50.52 m^3 and occurred over an area of 313.7 m^2; deposition totaled 5.19 m^3 and occurred over an area of 61.1 m^2, yielding net erosion of 45.33 m^3. Aeolian reworking of sand near gully G1 (regions ER1 and DEP1; fig. 39*B*) occurred with a slightly greater erosional signal (in terms of volume change per unit time) compared to that measured between 2010 and 2013 (fig. 39*A*). We also detected some erosion within the archeological site boundary, inferred to have resulted from both gully-wall slope adjustment and aeolian transport. The area in and around gully G2, notable owing to the amount of erosional change documented in past monitoring periods (Collins and others, 2012, as well as documented herein for 2010–13) continued to experience widespread runoff-induced erosion. Gullying widened and deepened this area, removing nearly 43 m^3 of previously deposited sand that had likely infilled the gully through a combination of aeolian transport and backwasting of the unconsolidated sand walls of the gully. Weather-station data and time-lapse photographs indicated that storms in July and August 2013, with associated maximum

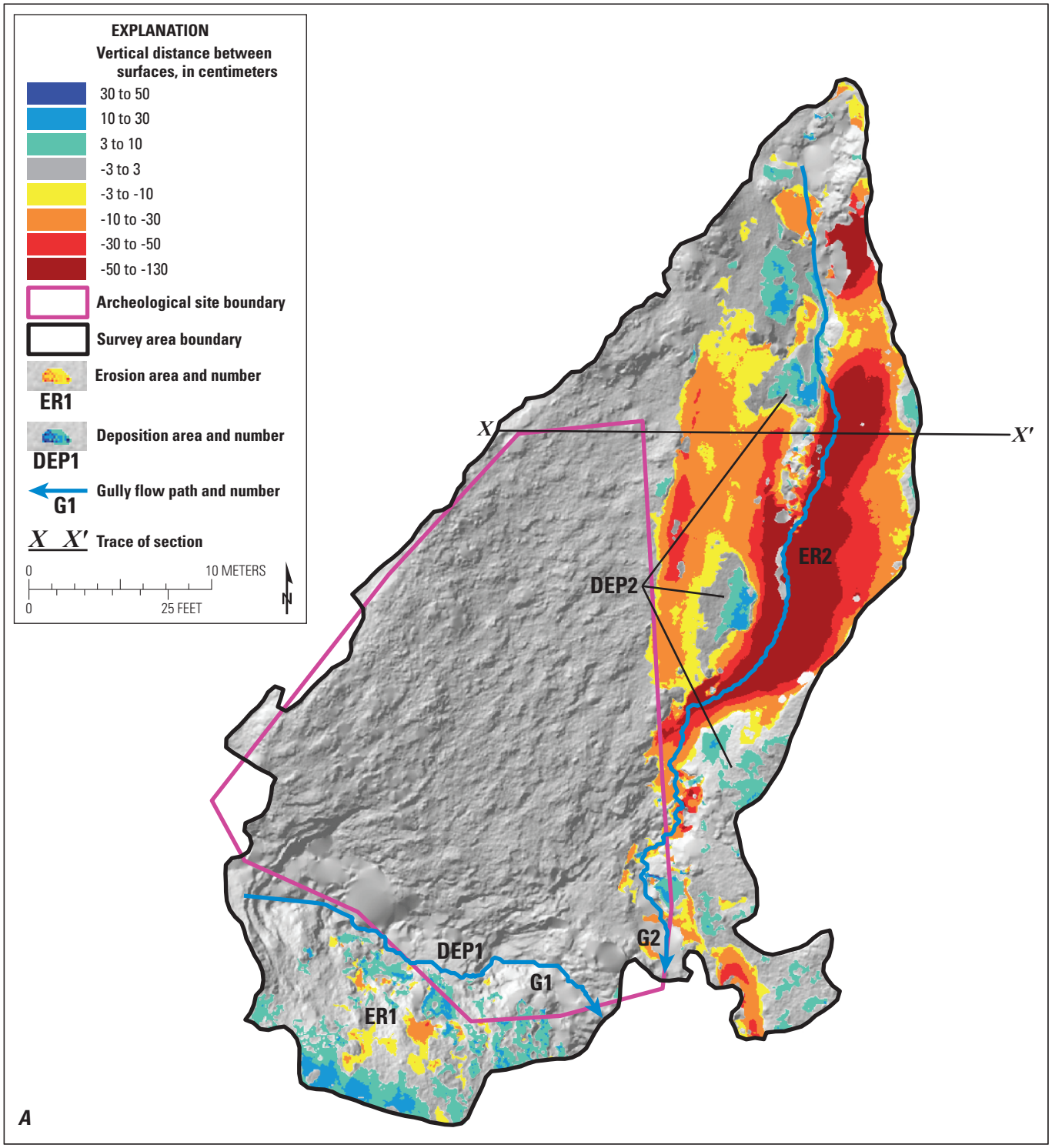

Figure 39. Landscape change at site AZ:B:10:0225. A 5-cm gridded topographic change output shows erosion (warm colors, negative) and deposition (cool colors, positive) from (*A*) September 2010 to May 2013, and (*B*) May 2013 to May 2014. Identified change is grouped by area labels (ER, erosion; DEP, deposition) that are cross-referenced with table 4. Line X–X′ shows location of cross sections in (*C*). (*C*) Cross-sections across gully G2, showing sequential topographic change between September 2007 and May 2014. Data for September 2007 and September 2010 sections are from Collins and others (2012).

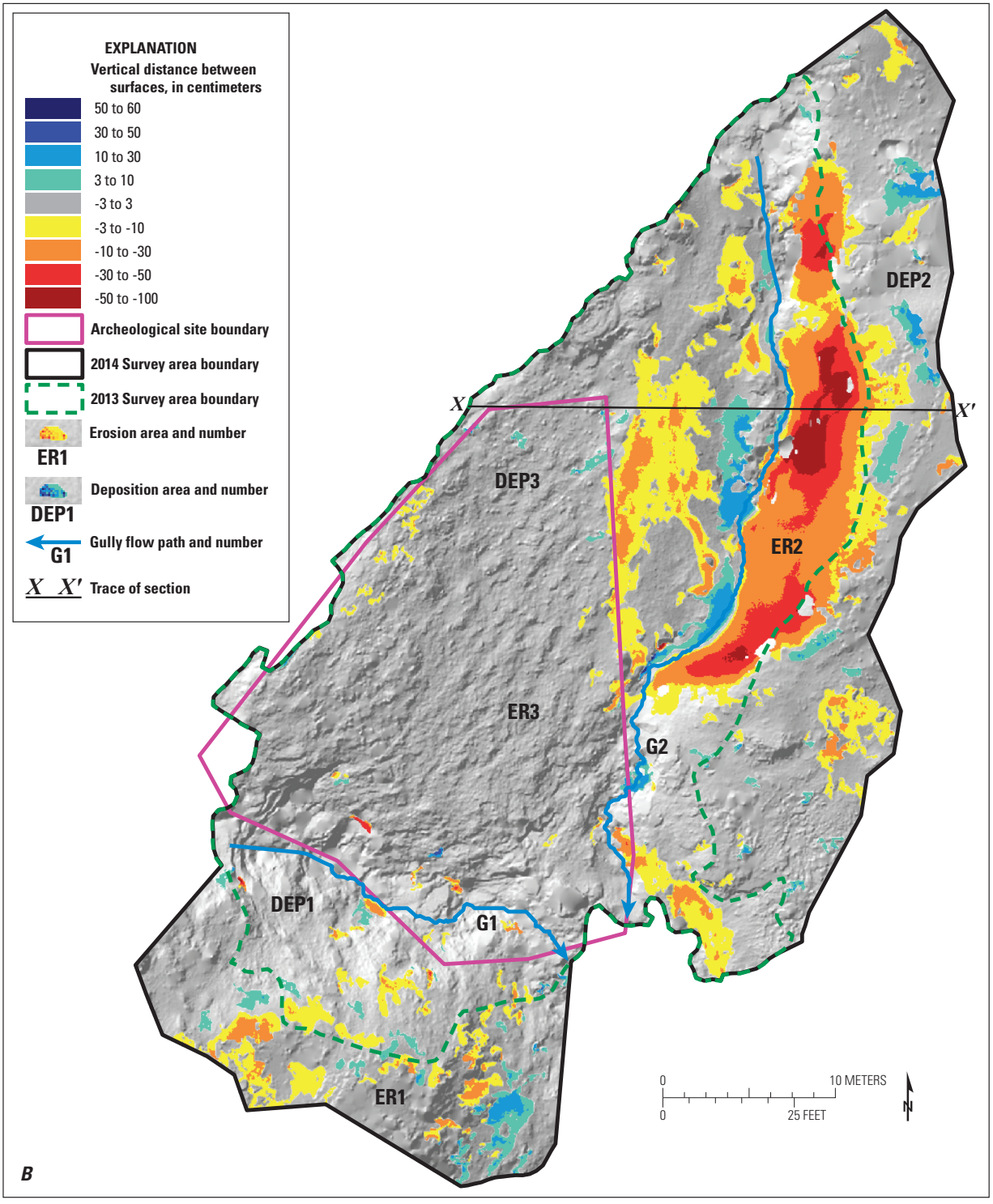

Figure 39.—Continued

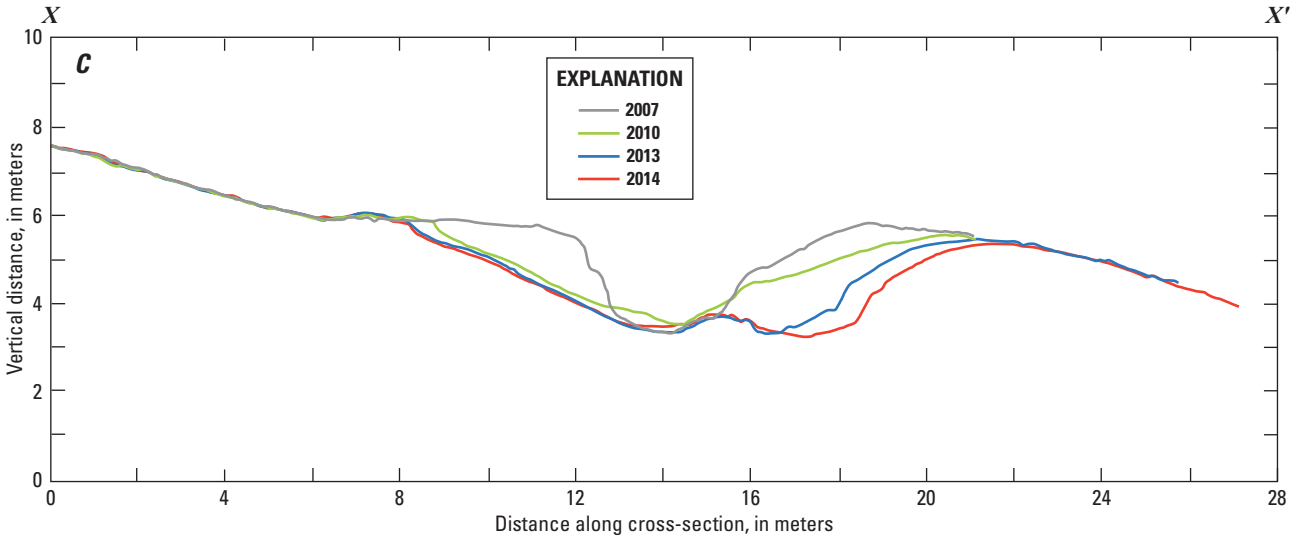

Figure 39.—Continued

Table 4. Summary of topographic change at site AZ:B:10:0225.

[m/yyyy, month/year; m^2, square meters; cm, centimeters; m^3, cubic meters]

Site number and region	Time period (m/yyyy)	Area (m^2)	Average depth (cm)	Volume (m^3)
AZ:B:10:0225 – ER1	9/2010–5/2013	10.6	-9	-0.90
AZ:B:10:0225 – ER2	9/2010–5/2013	264.9	-35	-92.81
AZ:B:10:0225 – DEP1	9/2010–5/2013	36.3	8	2.70
AZ:B:10:0225 – DEP2	9/2010–5/2013	36.2	7	2.51
AZ:B:10:0225 – ER1	5/2013–5/2014	35.3	-8	-2.73
AZ:B:10:0225 – ER2	5/2013–5/2014	264.3	-18	-46.52
AZ:B:10:0225 – ER3	5/2013–5/2014	14.1	-9	-1.27
AZ:B:10:0225 – DEP1	5/2013–5/2014	16.9	7	1.20
AZ:B:10:0225 – DEP2	5/2013–5/2014	40.8	9	3.71
AZ:B:10:0225 – DEP3	5/2013–5/2014	3.4	8	0.28

10-minute rainfall intensities of 35–42 mm/hr, likely generated overland flows that enhanced the gullying, and that strong (>2 m/s) winds in September and October 2013, and also during spring 2014, led to aeolian smoothing and reworking of the ground surface elsewhere at the site (Caster and Sankey, 2016).

Since the first lidar measurements at this site in September 2007 (Collins and others, 2012), more than 260 m^3 of sand have been lost from the G2 gully system. Whereas episodic storm-driven overland flow events have removed more than 1 m of sediment (vertically) in distinct locations throughout the gully, the overall result has been to shift the gully thalweg toward the east, away from the archeological-site boundary (fig. 39). The slope bordering the archeological site has remained at approximately 32° inclination (near the angle of repose for dune sand; West, 1995) as the gully has widened eastward. It is unclear whether this trend will continue, or whether the thalweg will avulse westward, in which case it could undermine the existing slope that forms the archeological-site boundary. However, it is clear that the area surrounding this site is undergoing rapid change and that aeolian infilling of gully G2 has not kept pace with runoff-induced erosion. New aeolian sand inputs from fluvial sandbars have not been detected definitively, and we infer that any new deposition has been a result of aeolian and runoff-generated reworking of existing sand at and near the site. Thus, although this type 1 site apparently has connectivity between an upwind fluvial sandbar and an active dune field downwind (containing the archeological site), and thus has the potential to receive aeolian sand supply that could increase the sand volume at the site itself, we have not resolved such a result at the site. The land surface within the archeological-site boundary, which contains moderate vegetation cover and biologic soil crust (fig. 38), has been unusually stable during the monitoring interval given its location in an otherwise relatively active dune field, which elsewhere contains well defined dune crests and slip faces of active, uncrusted, and unvegetated aeolian sand. This may represent an example of the site-detection bias mentioned in Section II, in that the exposure of archeological artifacts at the land surface is probably greater, and thus sites are more likely to be documented, in relatively inactive sand landscapes.

AZ:G:03:0072

Site Description

Site AZ:G:03:0072 is located within Colorado River sand deposits, approximately 30 m inland from the river (figs. 40, 41). The site is a prehistoric and protohistoric habitation area that contains sparse surface artifacts and numerous large mounds of fire-cracked rocks representing the remains of agave-roasting pits (Fairley and others, 1994). The upstream part of the archeological site (the focus of our analysis, herein named AZ:G:03:0072 US) consists of a convex hillslope situated between an alluvial terrace and the Colorado River. The hillslope is further bounded on one side by a boulder-choked overland-flow channel, and on the other side by steep talus slopes and basalt cliffs. Three gullies traverse this part of the site; two (G1 and G2) are founded on cobbles and boulders, whereas the other (G3) cuts through an active aeolian dune field. The dune field extends from gully G2 to the west edge of the site near the boulder-choked channel. Brush check dams were installed in gully G2 in May 2006 in an attempt to slow erosion (O'Brien and Pederson, 2009b). Vegetation in and around the site consists of native bunchgrasses, shrubs, and prickly pear cactus (*Opuntia basilaris*), along with taller groups of ocotillo (*Fouquieria splendens*), buckhorn cholla cactus (*Cylindropuntia acanthocarpa*), and creosote bush (*Larrea tridentata*) and catclaw acacia trees (*Acacia greggii*) several meters high. O'Brien and Pederson (2009a,b) identified gullying, creep, aeolian transport, and overland flow as the geomorphic processes affecting this site, and they noted that archeological features were actively being eroded by these processes.

Although the position of site AZ:G:03:0072 relative to an adjacent, upwind fluvial sandbar indicates type 1 classification presently, the riparian zone upwind of this site has experienced rapid vegetation growth over recent years (fig. 13). If the vegetation expansion continues, the site soon will need to be reclassified as type 2a, in which vegetation barriers are assumed to reduce the connectivity between fluvial and aeolian sedimentary systems, or type 3 if no open sand exists riverward of the vegetation.

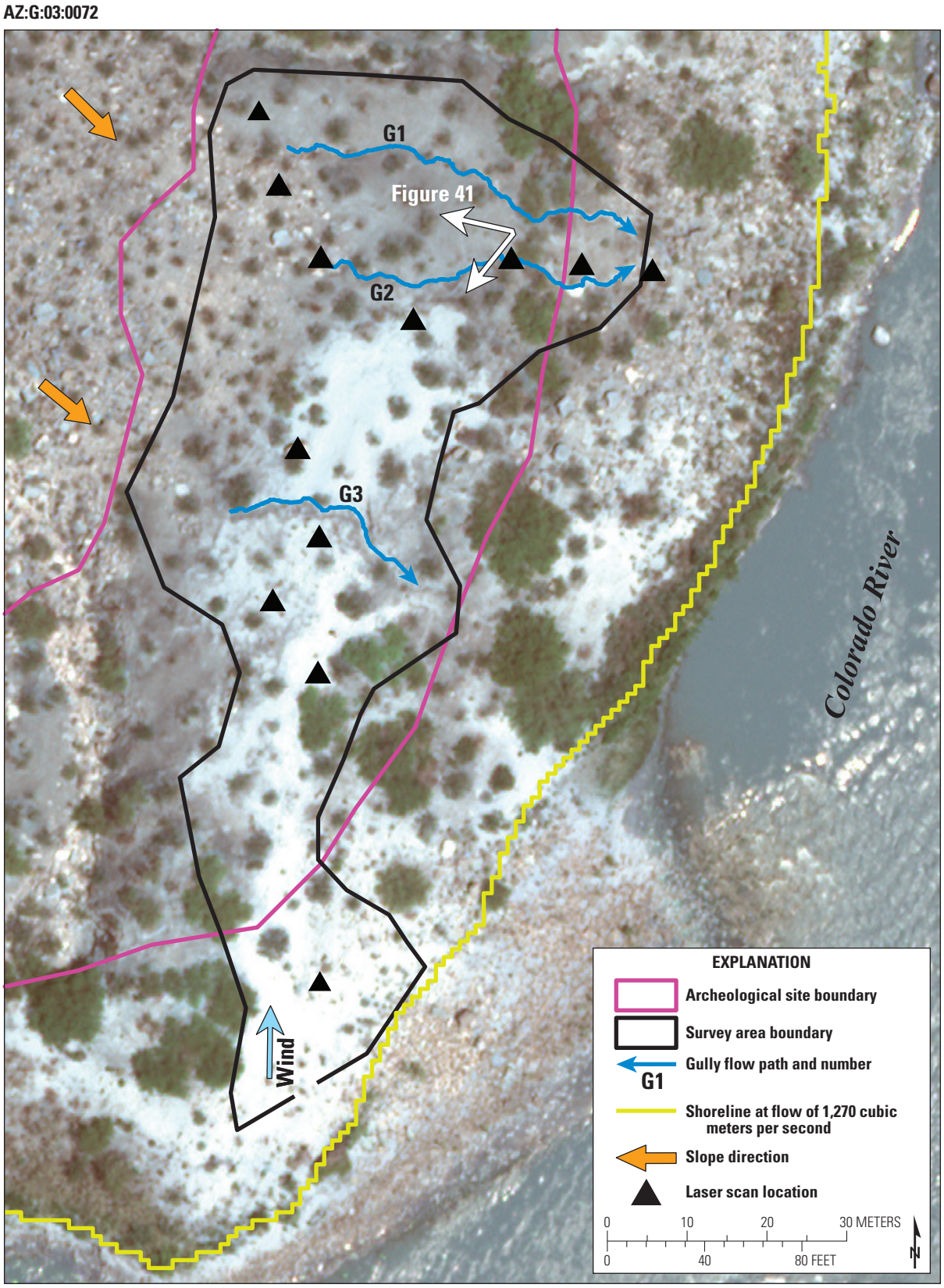

Figure 40. Site AZ:G:03:0072 survey-area map.

Figure 41. Site AZ:G:03:0072 US survey-area photograph, showing gully locations (G1–G3). View is toward the west.

Topographic Change (2010–13)

Topographic changes at site AZ:G:03:0072US between 2010 and 2013 included erosion and deposition related to both aeolian and overland flow processes (fig. 42*A*; table 5). Erosion within the entire surveyed area (which includes only the upstream part of the archeological site; figs. 40, 42) totaled 6.27 m^3 and occurred over an area of 78.2 m^2. Deposition within this 2010–13 survey area totaled 5.86 m^3 and occurred over an area of 99.6 m^2, yielding net erosion of 0.41 m^3. Widespread gully erosion had been documented previously at this site (Collins and others, 2009, 2012), and the volume loss measured over the 2010–13 interval was consistent with those previous observations. However, only one gully (G3, regions ER2 and DEP2) changed between 2010 and 2013, suggesting that storms during this time interval did not cause widespread runoff. Instead, inspection of topographic change along the gully walls revealed that topographic smoothing (backwasting) of the previously formed near-vertical sidewalls (see Collins and others, 2012) probably caused the wall erosion and deposition within the thalweg.

We detected widespread aeolian sand transport signals in two regions (ER1-DEP1 and ER3-DEP3), indicating deflation and inflation of the land surface. Comparison of the shapes, locations, and associated volumetric change between patches of erosion and deposition indicates that net sand transport was toward the northeast, coincident with the predominant wind direction measured here (Draut and others, 2010; Caster and others, 2014). Sand from region ER1 likely was deposited exclusively in region DEP1, and sand from region ER3 was transported to region DEP3. However, whereas the volumetric change in regions ER1 and DEP1 were nearly the same (within 10 percent; table 5), suggesting simple aeolian erosion from region ER1 and redeposition immediately downwind in region DEP1, the deposition in region DEP3 was approximately 25 percent greater than the erosion detected within the ER3 patches. This indicates that sand from outside the survey boundary (from a location southward, upwind and closer to the river, presumably the fluvial sandbar that receives new deposition during controlled floods) may have been introduced to the site area during this time interval.

Topographic Change (2013–14)

Topographic changes at site AZ:G:03:0072US between 2013 and 2014 were similar to those detected during 2010–2013, but with indications that precipitation-induced runoff was more active. Erosion within the entire surveyed area (a larger area than that surveyed in 2010) totaled 6.89 m^3 and occurred over an area of 123.7 m^2. Deposition within the 2013–14 survey area totaled 5.11 m^3 and occurred over an area of 102.0 m^2, yielding net erosion of 1.78 m^3. Erosion and deposition in all three gullies was detected and in gully G3, the volume of sediment eroded (from region ER4) was nearly three times as great as the volume deposited (in region DEP4). In gullies G1 and G2, small areas of deposition may indicate sediment storage above check dams that were installed in the early 2000s to slow archeological-site erosion (Pederson and others, 2006), or from natural landscape features providing temporary storage behind boulders or vegetation. We inferred aeolian reworking in the mid-site area (regions ER3 and DEP4) and south of gully G1 (regions ER5 and DEP5). Only in the far southern, upwind part of the site (regions ER6 and DEP6) were the volumes of mobilized sediment dissimilar, with three times as much erosion as deposition (table 5). Overall, the results suggest that little new sand came into the site (for example, from the upwind fluvial sandbar), despite the wind conditions having been favorable for aeolian transport from river level toward the archeological site (Caster and others, 2014).

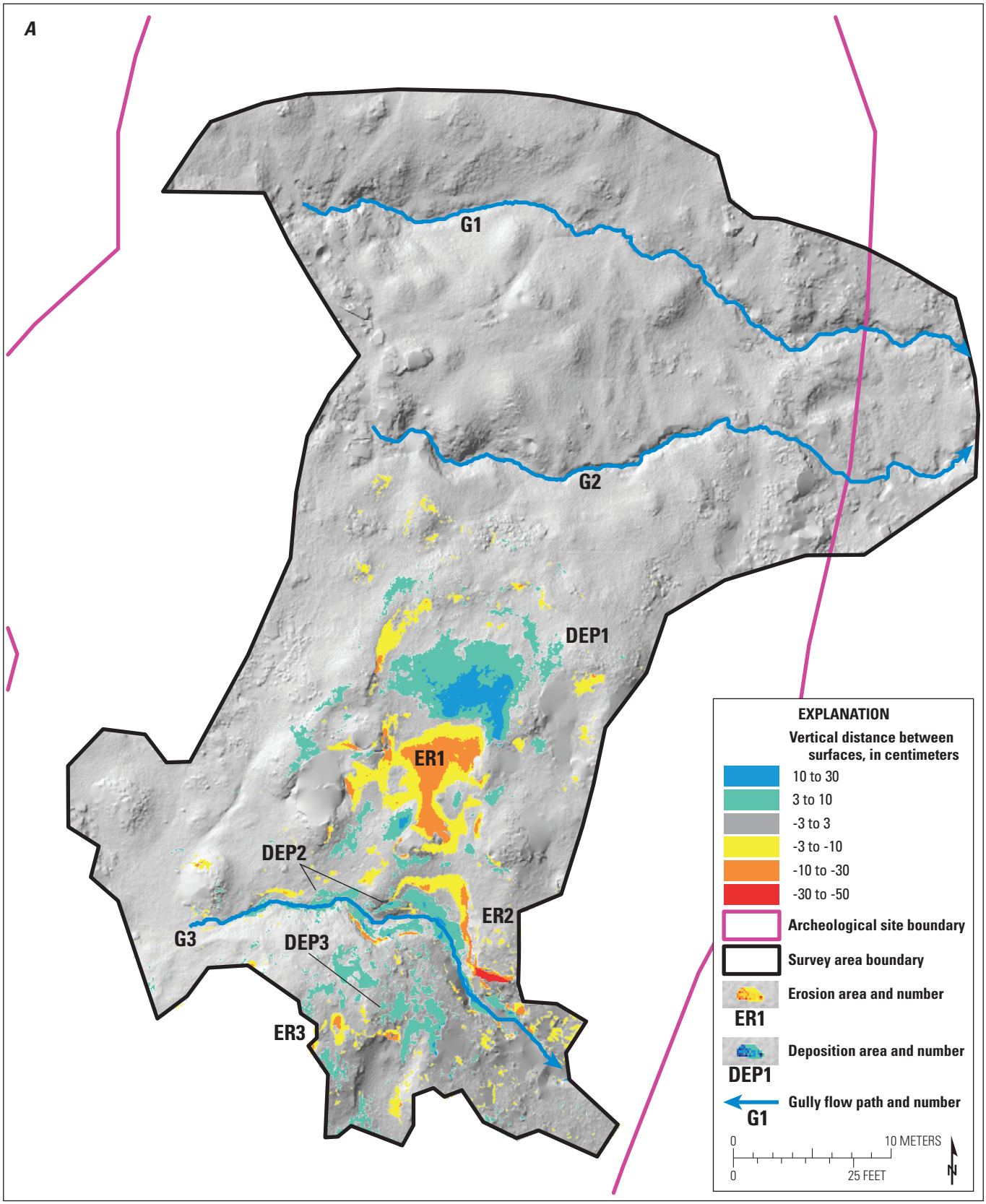

Figure 42. Landscape change at site AZ:G:03:0072US. A 5-cm gridded topographic change output shows erosion (warm colors, negative) and deposition (cool colors, positive) from (*A*) October 2010 to May 2013, and (*B*) May 2013 to May 2014. Note difference in scales and area surveyed. Identified change is grouped by area labels (ER, erosion; DEP, deposition) that are cross-referenced with table 5.

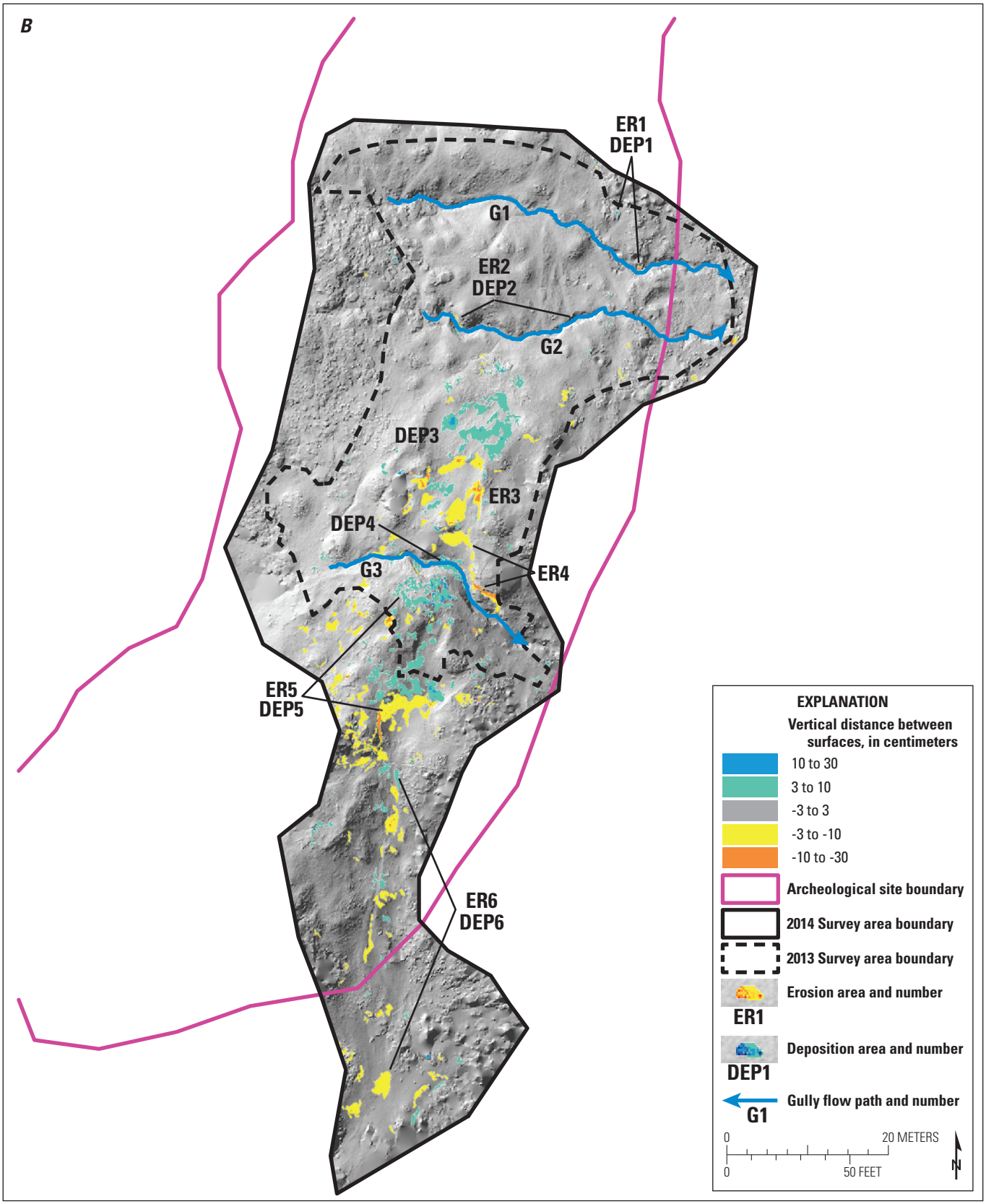

Figure 42.—Continued

Table 5. Summary of topographic change at site AZ:G:03:0072US.

[m/yyyy, month/year; m^2, square meters; cm, centimeters; m^3, cubic meters]

Site number and region	Time period (m/yyyy)	Area (m^2)	Average depth (cm)	Volume (m^3)
AZ:G:03:0072US – ER1	10/2010–5/2013	52.6	-8	-4.15
AZ:G:03:0072US – ER2	10/2010–5/2013	10.3	-12	-1.25
AZ:G:03:0072US – ER3	10/2010–5/2013	15.3	-6	-0.87
AZ:G:03:0072US – DEP1	10/2010–5/2013	58.9	6	3.78
AZ:G:03:0072US – DEP2	10/2010–5/2013	16.2	6	0.99
AZ:G:03:0072US – DEP3	10/2010–5/2013	24.5	4	1.09
AZ:G:03:0072US – ER1	5/2013–5/2014	0.6	-8	-0.05
AZ:G:03:0072US – ER2	5/2013–5/2014	3.6	-6	-0.23
AZ:G:03:0072US – ER3	5/2013–5/2014	27.3	-6	-1.57
AZ:G:03:0072US – ER4	5/2013–5/2014	15.7	-7	-1.13
AZ:G:03:0072US – ER5	5/2013–5/2014	47.2	-5	-2.49
AZ:G:03:0072US – ER6	5/2013–5/2014	29.3	-5	-1.42
AZ:G:03:0072US – DEP1	5/2013–5/2014	0.5	6	0.03
AZ:G:03:0072US – DEP2	5/2013–5/2014	2.0	6	0.12
AZ:G:03:0072US – DEP3	5/2013–5/2014	40.9	5	1.96
AZ:G:03:0072US – DEP4	5/2013–5/2014	7.3	6	0.41
AZ:G:03:0072US – DEP5	5/2013–5/2014	40.9	5	2.10
AZ:G:03:0072US – DEP6	5/2013–5/2014	10.4	5	0.49

Discussion: Landscape Change and Response to Controlled Floods

The dominant landscape-change signal in the four type 1 sites that we analyzed in Marble–Grand Canyon has been that of erosion (fig. 43). Since monitoring began at these sites between 2006 and 2010 (depending on the particular site), 74 percent of the detected change (as measured by the percent surface area per year) has been from erosion. Even at these type 1 sites, which represent 'best-case scenarios' for maintaining sediment cover through potential aeolian sand supply from fluvial sources, overall, more site area underwent erosion than deposition over any given monitoring interval (fig. 43). Over nearly a decade of landscape-change detection, our research group has documented only two instances when sand deposition slightly outpaced erosion (by area) in any site-monitoring interval (at site AZ:C:13:0321 between 2010 and 2013, and at site AZ:G:03:0072US between 2010 and 2013; fig. 43). During the interval reported herein (2010–14), the volume of upland landscape erosion (245.72 m^3, which excludes probable fluvial erosion that occurred within the AZ:C:05:0031 survey area but not within or near the archeological site boundary; areas ER4, DEP4, and DEP5 in fig. 33), was nearly three times the volume of deposition (85.55 m^3). The finding that volumetric change from aeolian inflation and deflation (193.07 m^3) was 40 percent greater than that from overland flow (138.19 m^3) indicates the importance of aeolian transport in shaping landscapes in which archeological sites have high connectivity to fluvial sand sources. This conclusion is supported by the areal landscape-change data (the percent of the total changed area per year, again not including apparently fluvial changes at AZ:C:05:0031). These data indicate that the proportion of area influenced by aeolian processes since monitoring began is more than double that influenced by runoff processes (70 percent compared to 30 percent; fig. 43). This difference reflects the fact that changes caused by runoff generally are focused on isolated, narrow gully channels, whereas aeolian inflation and deflation act across wider regions and greater area overall.

We can use the detailed topographic changes detected at these four type 1 archeological sites in Marble–Grand Canyon to address the science questions posed at the beginning of this section. Regarding the potential for the aeolian sand supply from controlled-flood sandbars to reach type 1 sites, we found conclusive evidence at one site (AZ:C:13:0321), and potential linkages at the three others (AZ:C:05:0031, AZ:B:10:0225, and AZ:G:03:0072), that direct aeolian transport pathways between fluvial sandbars and downwind dune fields can provide archeological sites with

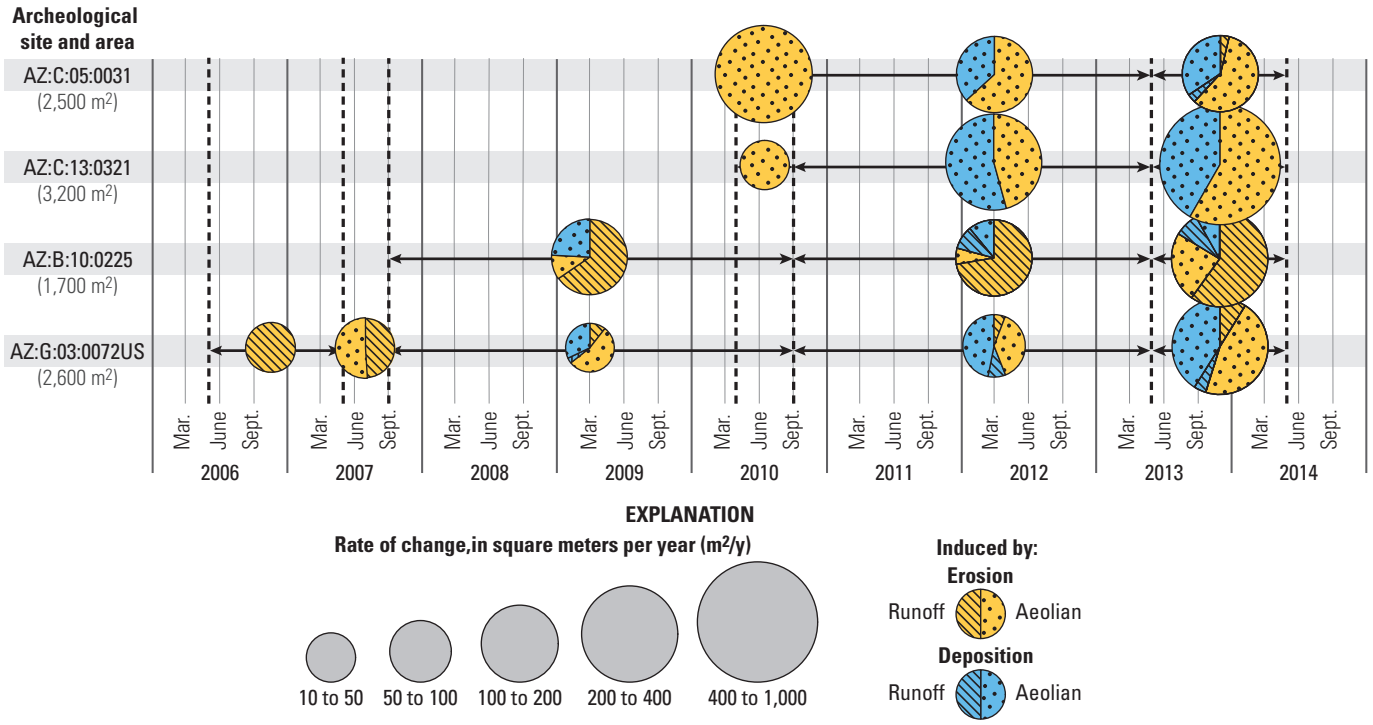

Figure 43. Summary of landscape change at four type 1 archeological sites in the Colorado River corridor of Marble–Grand Canyon over various monitoring intervals (data for 2006–10 from Collins and others, 2009, 2012). Pie size indicates the total area of erosion and deposition, normalized by the length of time between measured changes. Hatching pattern indicates the primary geomorphic process inferred to have caused the change. Values in parentheses indicate average total area where change detection was investigated. Dashed lines are dates of data collection; pie locations indicate measured change between times represented by adjacent dashed lines.

new sand. At site AZ:C:13:0321, direct effects of the recent controlled floods in building a fluvial sandbar adjacent to the site, combined with a near-optimal prevailing wind direction, resulted in net sediment influx to the site between 2010 and 2013 (fig. 36*A*, table 3). Although that site lost sand volume overall between 2013 and 2014, our results indicate that at least some sand continued to move into the site (fig. 36*B*). At the other three sites some aeolian deposition also occurred, but it was unclear whether, during these time intervals, deposition resulted from reworking of existing aeolian sand at the sites (which ultimately derives from fluvial deposits), or whether sand from newly formed sandbars was transported into the site area. Regardless, we identified transport evidence with wind directions indicating that sand could be transported to these sites from fluvial sandbars formed during controlled floods. Examples of this are most clear at sites AZ:C:05:0031 and AZ:G:03:0072 (figs. 33*A*,*B*, 42*B*).

However, our measurements indicate that the presence of a recent controlled-flood sandbar upwind of a type 1 site does not necessarily lead immediately to net depositional conditions at the downwind archeological site (our first science question of Section III), although we have shown that situation to be possible at some sites over some time intervals (fig. 43). Only one site (AZ:C:13:0321) shows clear evidence that new sand coming from outside the site, sourced from a controlled-flood sandbar, has deposited in such a way that it covered previously exposed archeological features over our measurement time scales. At the other sites, cultural features may have been protected by new aeolian sand deposition, but there is insufficient data to determine whether this is from aeolian reworking of existing sand sourced at or near the site (which ultimately originated from fluvial sandbars, but took longer than our annual measurement interval to travel from the sandbar to the downwind site) or a direct result of recent controlled-flood sandbar growth. Answering this part of the question may require either longer-term monitoring, or additional controlled floods at different flow conditions and seasons to maximize sandbar building and subsequent aeolian sand transport.

Our second science question of Section III, whether sites with active aeolian deposition and substantial gully incision undergo net sediment loss and topographic lowering such that archeological features degrade, can be answered using the two sites that experienced extensive gullying over the monitoring period—AZ:B:10:0225 and AZ:G:03:0072. At site AZ:B:10:0225, repeated overland flow events in gully G2 removed more than 260 m^3 of sediment over approximately 7 years, lowering the surface elevation immediately east of the archeological site by as much as 2.2 m in some places

(fig. 39*C*). That gully drains a steep bedrock watershed, and pours over sandstone ledges before forming a gully through active dune sand, thereby representing a landscape likely to undergo repeated overland-flow incision. Despite the large magnitude of erosion in the gully itself, we detected relatively little change within the boundaries of the adjacent archeological site, which underwent only minor erosion along its west boundary related to gully bank slumping (fig. 39*A*) and minor aeolian reworking of the surface (fig. 39*B*). Instead, most erosion focused on the side of the gully located away from the archeological-site boundary (fig. 39*C*), which could be related either to the presence of weaker, more erosive substrate that underwent backwasting or to slight realignment of the incoming source of overland flow. Depending on variations in these processes, topographic lowering eventually could affect the archeological site (for example, if the gully flowpath changes orientation again). At site AZ:G:03:0072, repeated erosion and incision have occurred in gully G3 over 8 years (this study and Collins and others, 2009, 2012). Recent monitoring (fig. 42) indicates that incision has lowered the thalweg elevation by 30 cm locally and consequent bank slumping has widened the active gully channel by several meters since the initial survey in 2006. Thus, site AZ:G:03:0072 provides an example of repeated gully incision causing overall topographic lowering of parts of the archeological site.

At both sites AZ:B:10:0225 and AZ:G:03:0072, our observations imply that without enhanced aeolian sand input to the gully areas, overland flow erosion and gully backwasting will continue to cause net sediment loss, likely with eventual negative effects for the integrity of the archeological sites. Thus, to answer our second question—site erosion in and adjacent to gullies is tied to a complex set of factors including substrate erosive susceptibility and the tendency of gullies to avulse or meander away from a static channel alignment in one direction or another, processes with some degree of stochasticity that makes detailed site-scale assessments or predictions difficult.

Section IV - Landscape Change at Archeological Sites in a Sediment-Starved Reach: Glen Canyon

Background

In Section III, we showed that in some cases the erosion of river-corridor archeological sites in sand-dominated landscapes can be counteracted partly by deposition of aeolian sand supplied from fluvial sandbars. The sites where we measured landscape change in Grand Canyon National Park were identified as best-case scenarios for site preservation—sites that maintain high connectivity with active fluvial sand sources (type 1 sites in our classification system; Section I) and with active aeolian sand movement (Section II). However, we also showed that landscape change at type 1 sites can include erosion by overland flow and gullying, aeolian deflation, or both, and that erosion and sediment loss exceeded deposition and sediment gain at most sites over most intervals. The interplay between erosion and annealing processes is paramount to identifying why, where, and how rapidly archeological sites erode.

In this section, we investigated topographic change to infer landscape processes at archeological sites in a sediment-starved section of the Colorado River, where aeolian inflation is expected to be minimal or absent—in Glen Canyon, the Colorado River reach immediately downstream from Glen Canyon Dam. We studied four sites in Holocene terrace deposits of Glen Canyon, in which mainstem fluvial sediment interbeds with slopewash material (for example, Pederson and others, 2011). The geomorphic setting of the Glen Canyon sites forms an end-member case to contrast with the type-1 sites in Marble–Grand Canyon, in terms of the likelihood of gully annealing by aeolian sand activity. We contrasted sites in these two end-member settings to evaluate whether the type 1 sites would erode less rapidly than would the Glen Canyon sites, which are essentially disconnected from sediment supply from modern sandbars—sites exhibiting the best- and worst-case scenarios for modern preservation potential, respectively.

The Glen Canyon reach appears particularly prone to widespread gully erosion, owing to a combination of inherent geomorphic conditions and pronounced sediment starvation in postdam time (Section II). The geomorphic setting of Glen Canyon (including a lack of large debris fans, and thus no strong segmenting of hydraulic control) resulted in deposition of extensive Holocene fluvial terraces. The terraces, which are close to the river and contain a high concentration of archeological sites, are vulnerable to gully erosion and today have extremely low potential for either aeolian inflation of the terrace surfaces or gully annealing by aeolian sand transport, because this reach has almost no modern aeolian sand supply (with very few modern fluvial sandbars) and a low proportion of active aeolian sand area (Section II; figs. 23, 24). The inactive sand within the Glen Canyon reach contains more gully area per unit sand area than do any of the reaches we studied in Marble–Grand Canyon (fig. 24). Gullies in Glen Canyon have grown very large locally, and in some places have incised entirely through the sedimentary terraces to bedrock, degrading and removing archeological material. This is generally consistent with the findings of Pederson and O'Brien (2014) in Marble–Grand Canyon that wide Holocene terrace deposits tend to host cultural sites with acute gully erosion.

In this section we report our findings from high-resolution landscape-change detection at four archeological sites in Glen Canyon, and concurrent measurements of weather events to which landscape changes can be linked. The four sites, numbered AZ:C:02:0032, AZ:C:02:0035, AZ:C:02:0075, and AZ:C:02:0077 (fig. 29), all exhibit representative landscape processes occurring commonly in the Glen Canyon reach. The sites were monitored twice with terrestrial lidar, once in mid-September 2012 and again in early November 2013, thereby bracketing the November 2012 controlled flood (table 1). Our methods were similar to those in Section III for landscape-change detection and examination

of possible controlled-flood effects. We analyzed geomorphic factors that might influence comparison of site responses between Glen Canyon and Marble–Grand Canyon. We also analyzed and compared historical rainfall records from Glen Canyon and Marble–Grand Canyon, to investigate whether the intensive gullying in Glen Canyon may relate to regional precipitation trends. Understanding climatic and geomorphic process potential more fully will allow for future development of site-monitoring and mitigation plans that best address the unique geomorphic setting and likely trajectory for river-corridor cultural sites in Glen Canyon National Recreation Area.

Research Questions

- How do rates and processes of landscape change at Glen Canyon archeological sites compare to those measured in Marble–Grand Canyon, where the modern sand supply is greater?
- Are weather conditions in Glen Canyon more conducive to causing gully erosion than in Marble–Grand Canyon?

Methods

Similar to the methods outlined in Section III, we used a combination of site-specific topographic, meteorological, and time-series photographic monitoring to document changes at the four selected archeological sites in Glen Canyon. In contrast to the multi-year time interval analyzed in Marble–Grand Canyon, our Glen Canyon data-collection interval spanned just longer than one year (September 2012 to November 2013).

Topographic Change Detection

Our methods for identifying site-specific landscape change at Glen Canyon used identical terrestrial-lidar data collection, processing, and analysis protocols as described in Section III. We also collected airborne lidar data of the Glen Canyon sites in July 2013 as part of an effort to analyze the geomorphology of a longer section of Glen Canyon. Those results are presented by Collins and others (2014) and are not included here. However, we rely on the geomorphologic interpretations in that report to infer likely causes of change that we detected during the present study.

Geomorphologic Analysis

We conducted comparative qualitative and quantitative geomorphic assessments at the four type-1 archeological sites studied in Marble–Grand Canyon (Section III) and the four Glen Canyon sites investigated herein. We compared site substrates, gully geometry, site topography, and the watershed area draining into each of these sites. Using these parameters, we assessed whether site geomorphic setting, taken as a whole, could explain any differences in net topographic change between our best-case (type 1) and worst-case (Glen Canyon terrace) study areas.

Lacking consistent infiltration measurements, we assessed substrate differences qualitatively through observations of generalized surface sediment. We compared gully geometry quantitatively by using gully width and depth measurements from our terrestrial-lidar data. Similarly, we compared topographic slope and drainage area quantitatively among the sites by analyzing available lidar data, including 1-m digital elevation models (DEMs) of the Colorado River corridor (for example, Kaplinski and others, 2014) and 10-m DEMs for watershed areas outside the river corridor (http://nationalmap.gov/elevation.html). After calculating flow direction and accumulation using the 10-m-resolution data, we defined pour points at each of the survey-area boundaries and calculated watershed area upslope from those points. Using the 1-m DEM data, we then calculated flow direction and accumulation within the river-corridor area of each site. We integrated the watershed polygons based on these accumulations with those previously obtained for the 10-m data to calculate an up-watershed area for each site boundary. We finalized these watershed areas by using Google Earth™ imagery and high-resolution orthoimagery (http://earthexplorer.usgs.gov/) to define apparent drainage pathways above the river corridor. Where apparent drainage paths differed in distance or direction from the 10-m-DEM estimates, the watershed was modified to match the most probable contributing area; this final step allowed inclusion of rock fractures that were visible in aerial imagery but not adequately represented in the 10-m DEM. This analysis yielded conservative estimates of contributing watershed area, while representing the clearest flow paths from upper watersheds to the site boundaries.

Meteorological Monitoring

We deployed one weather station in Glen Canyon and one near Lees Ferry in 2013 with identical characteristics to those described earlier (Section III; Caster and others, 2014). Although incomplete records exist from these stations for the time bracketing the landscape-change data collection, we used the available weather data to identify wind and rain events that might have caused landscape change.

In addition to relating weather events to specific topographic changes, we analyzed spatial variability in weather by using data from the stations deployed in Glen and Marble–Grand Canyons (hereafter referred to as USGS inner-canyon stations; Draut and others, 2009a,b, 2010; Caster and others, 2014; Dealy and others, 2014), and three National Weather Service Cooperative Observer Program (COOP) stations located in and near the canyon (fig. 1; National Oceanic and Atmospheric Administration, 2014). We analyzed rainfall data for three time intervals: 2013–2014, to overlap with the landscape-change analyses of this study; October 2007 to October 2010, the interval from which USGS inner-canyon records are most extensive; and 1952–2012, the most complete COOP regional climate record.

This analysis focused specifically on wind speed and rainfall. We analyzed rainfall amount and intensity, factors that contribute to overland-flow erosion (Collins and others, 2016). Although daily rain accumulation (depth) can be calculated directly from USGS inner-canyon stations and COOP stations, only the USGS inner-canyon data has sufficient resolution to permit calculation of subdaily rainfall intensity. To estimate rainfall intensity at COOP stations for the purpose of understanding long-term rainfall variability, we developed regression relations between daily rain depth and maximum daily 10-minute intensity, for each rain season recorded at the USGS inner-canyon stations (Caster and Sankey, 2016). Rain seasons follow the definitions of Hereford and others (2014) for Grand Canyon, with the so-called cool season from October 8 to March 31, dry season from April 1 to June 31, and warm (monsoon) season from July 1 to October 7. The seasonal depth-intensity regression equations were applied to long-term National Weather Service COOP daily rainfall records to estimate maximum daily 10-minute intensities from 1952 to 2012. Additional details of methods that we used to estimate the relationships at the USGS inner-canyon stations and apply them to the COOP records are presented by Caster and Sankey (2016).

Maximum wind-gust speed was compared for 92,355 4-minute intervals concurrently recorded during approximately one year (February 13, 2014 to February 5, 2015), at six USGS inner-canyon stations within Glen and Marble–Grand Canyon. In addition to comparing these parameters, we assessed aeolian sand-transport potential by calculating the amount of time that maximum gust speed exceeded three possible sand-transport thresholds: 2 m/s (Draut and Rubin, 2005, 2008), 5 m/s (Stout, 2004; Liu and others, 2015), and 8 m/s (Baudat and Breed, 1999), with the lowest examined wind speed (2 m/s) representing the typical threshold for dry sand transport within Grand Canyon (assuming a grain size of fine sand and Bagnold-type entrainment; Bagnold, 1941; Draut and Rubin, 2005, 2008).

Time-Series Photography

Although we did not initiate time-series photographic monitoring in Glen Canyon, we did utilize a pre-existing dataset of the AZ:C:02:0032 archeological-site area dating back to 1992, provided by the Aquatics Program and Cultural Resources Program staff at Glen Canyon National Recreation Area. The dataset includes images (at varying temporal intervals, often daily) showing most of the archeological site and the steep riverbank that forms one of the boundaries of the site. We used these photographs to examine the effects of fluvial inundation on the toe of the river cutbank during previous controlled floods.

Topographic Change Detection

AZ:C:02:0077

Site Description

Site AZ:C:02:0077 consists of a sparse scatter of flaked stone distributed on the surfaces of two adjoining fluvial terraces, with an erosional cutbank (terrace scarp) separating the two terrace surfaces (figs. 44, 45). The site also contains buried archeological features, particularly in the upper terrace, and may contain some of the oldest cultural remains in Glen Canyon (Anderson, 2006; Spurr and Collette, 2007; Collins and others, 2014). The terraces are covered mainly with inactive, biocrusted river-derived sand and some gravel, with active aeolian sand patches to the north of the site. Previous archeological investigations mentioned active aeolian processes at the site, as well as rodent burrowing and social trailing from a nearby campground (Neff and Wilson, 2002). Aeolian dune forms are not well developed on the terrace surfaces, however. Owing to the upwind presence of a Colorado River shoreline that has received controlled-flood sand deposition in the past, one of the few such places in Glen Canyon, as well as a dense band of vegetation between the shoreline and the site, we considered this to be a type 2a site (upwind fluvial sand source but with vegetation barrier; fig. 9). The upper terrace edge is approximately 100 m landward from the edge of the river, and vegetation covers the riverward 75 percent of the lower terrace. The vegetation is differentiated qualitatively by the two terrace surfaces, with Tamarisk trees (*Tamarix ramosissima*), Drummond's goldenbush (*Isocoma drummondii*), and fourwing saltbush (*Atriplex canescens*) found predominantly on the lower terrace. Fourwing saltbush (*Atriplex canescens*) is also found on the upper terrace, along with grasses, Mormon tea (*Ephedra* sp.), and snakeweed (*Gutierrezia* sp.) shrubs, puncture vine (*Tribulus terrestris*), and Engelmann's hedgehog cacti (*Echinocereus engelmannii*).

Several gullies are incised into the upper (presumably older) terrace scarp, and sediment from these gullies forms small alluvial fans on the lower, younger terrace surface. Collins and others (2014) found recent gully incision to be minor over the majority of the terrace with the exception of the deeper gully (G3) located to the south of the site, which drains a larger watershed emanating from two deep clefts in the adjacent bedrock cliffs. The smaller gullies, G1 and G2, originate in terrace sediment, not in bedrock catchments. The lack of severe gully incision at this site, especially given the position of G3 at the outlet of bedrock catchments, was attributed to high soil infiltration capacity in the lower terrace (Collins and others, 2014).

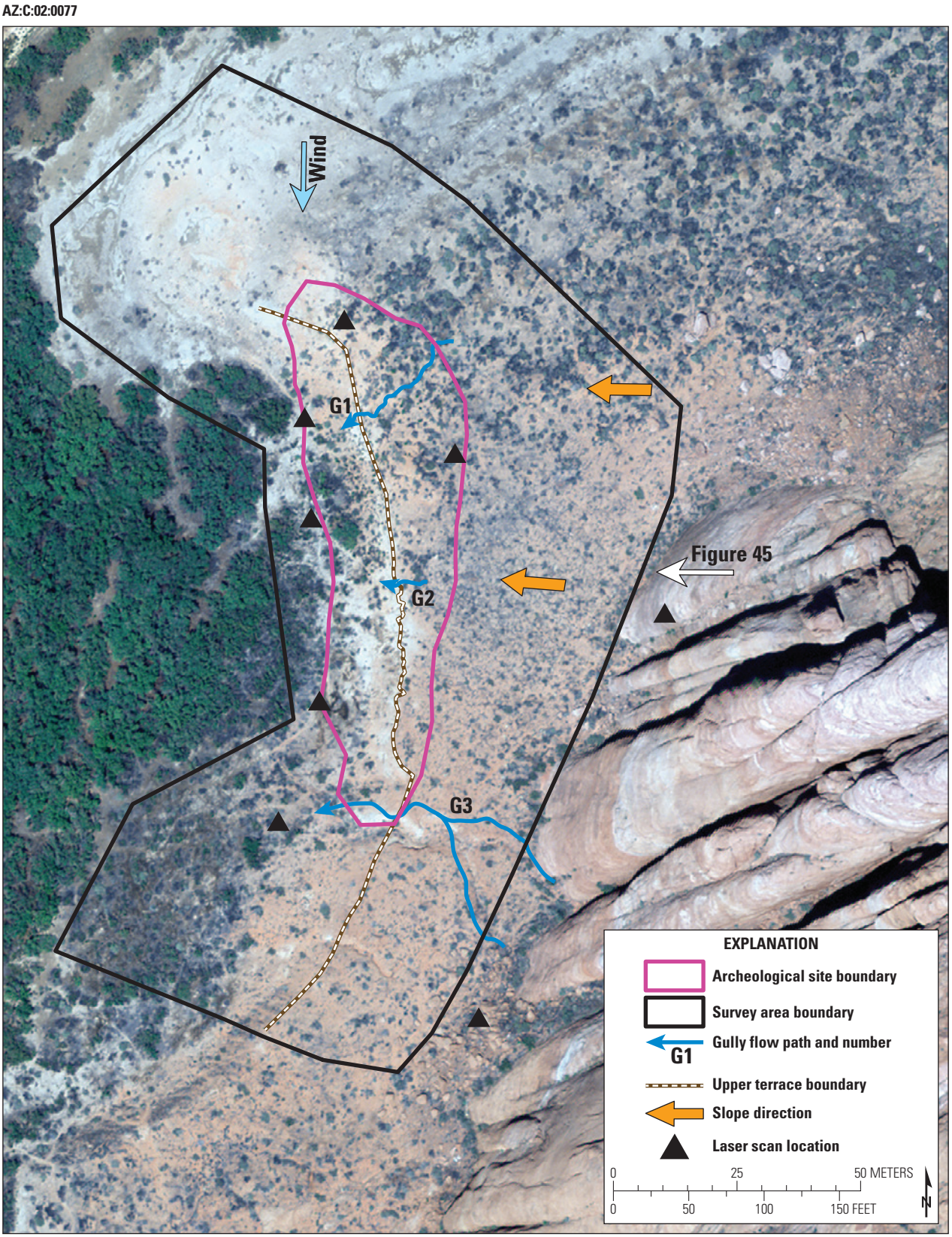

Figure 44. Site AZ:C:02:0077 survey-area map.

Figure 45. Site AZ:C:02:0077 survey-area photograph, showing gully locations (G1–G3). View is toward the west.

Topographic Change (2012–13)

We analyzed landscape change at site AZ:C:02:0077, spanning the entire archeological-site boundary and adjacent terrace areas (fig. 46) including an apparently active aeolian sand area northwest of the site, to assess the potential for aeolian sand transport to the site (the dominant wind direction being generally toward the south; fig. 44). Overall, less than 0.1 percent of the archeological-site area underwent change that exceeded our detection threshold (3 cm). Topographic changes observed between 2012 and 2013 consisted of small (<1 m^2) erosional areas within the archeological-site boundary (regions ER3, ER4, ER5) and a larger area of aeolian erosion and deposition at the north boundary of the site (regions ER1, DEP1; table 6).

The somewhat large magnitude of erosional downcutting (9 to 19 cm) compared to the small gully area over which we detected change (limited to a few square meters in unnamed gullies; fig. 46) suggests that downcutting by overland flow was limited to surficial erosion of the steeper areas of the terrace edge, at least over this measurement interval. Moreover, neither the ER3 nor the ER4 erosion area connects to a larger upstream gully, and neither the G1 nor the G2 gully is incised; these gullies are subtle, shallow, ephemeral features (Collins and others, 2014). These observations, together with a lack of substantial gullying below the terrace edge separating the lower and upper terraces, indicate that precipitation-induced gullying is not a prevalent geomorphic process at this site, with the exception of flow paths directly fed by bedrock-sourced overland flow (gully G3, which did not change during this monitoring interval).

The spatial pattern of the larger areas of change identified in the northwestern part of the survey area (ER1 and DEP1; fig. 46) suggests aeolian processes, with change having occurred over 422.8 m^2. Areas of change consist of neighboring patches of erosion and deposition (deflation and inflation), and the volume of aeolian erosion (in region ER1) and deposition (in region DEP1) are nearly identical (approximately 17 m^3 each; table 6). The spatial distribution of deposition in an arcuate zone south of the main area of erosion suggests a generally north-to-south wind direction, consistent with that measured by a nearby meteorological station during fall and winter 2013 (Caster and others, 2014), which indicates a wind vector-sum direction from due north. This area is part of a broad, active aeolian sand region that extends approximately 250 m north of the site. However, this area of inferred aeolian sand activity is entirely above the inundation stage of controlled floods (approximately 1,200 m^3/s), and there are no geomorphic indications that controlled-flood sand has been transported through the vegetation into the area that neighbors the archeological site. Thus, we infer no connectivity between modern fluvial sand deposits and the downwind aeolian sand landscape in the vicinity of the archeological site. Instead, the aeolian sand activity likely reflects reworking of a predam flood deposit, and indeed wind-scour features that we observed on the terrace surface around region ER1 imply that the wind is removing predam flood sediment there and redepositing it downwind.

Table 6. Summary of topographic change at site AZ:C:02:0077.

[m/yyyy, month/year; m^2, square meters; cm, centimeters; m^3, cubic meters]

Site number and region	Time period (m/yyyy)	Area (m^2)	Average depth (cm)	Volume (m^3)
AZ:C:02:0077 – ER1	9/2012–11/2013	168.0	-10	-16.97
AZ:C:02:0077 – ER2	9/2012–11/2013	0.6	-19	-0.11
AZ:C:02:0077 – ER3	9/2012–11/2013	0.6	-15	-0.09
AZ:C:02:0077 – ER4	9/2012–11/2013	2.7	-9	-0.25
AZ:C:02:0077 – DEP1	9/2012–11/2013	254.8	7	17.33

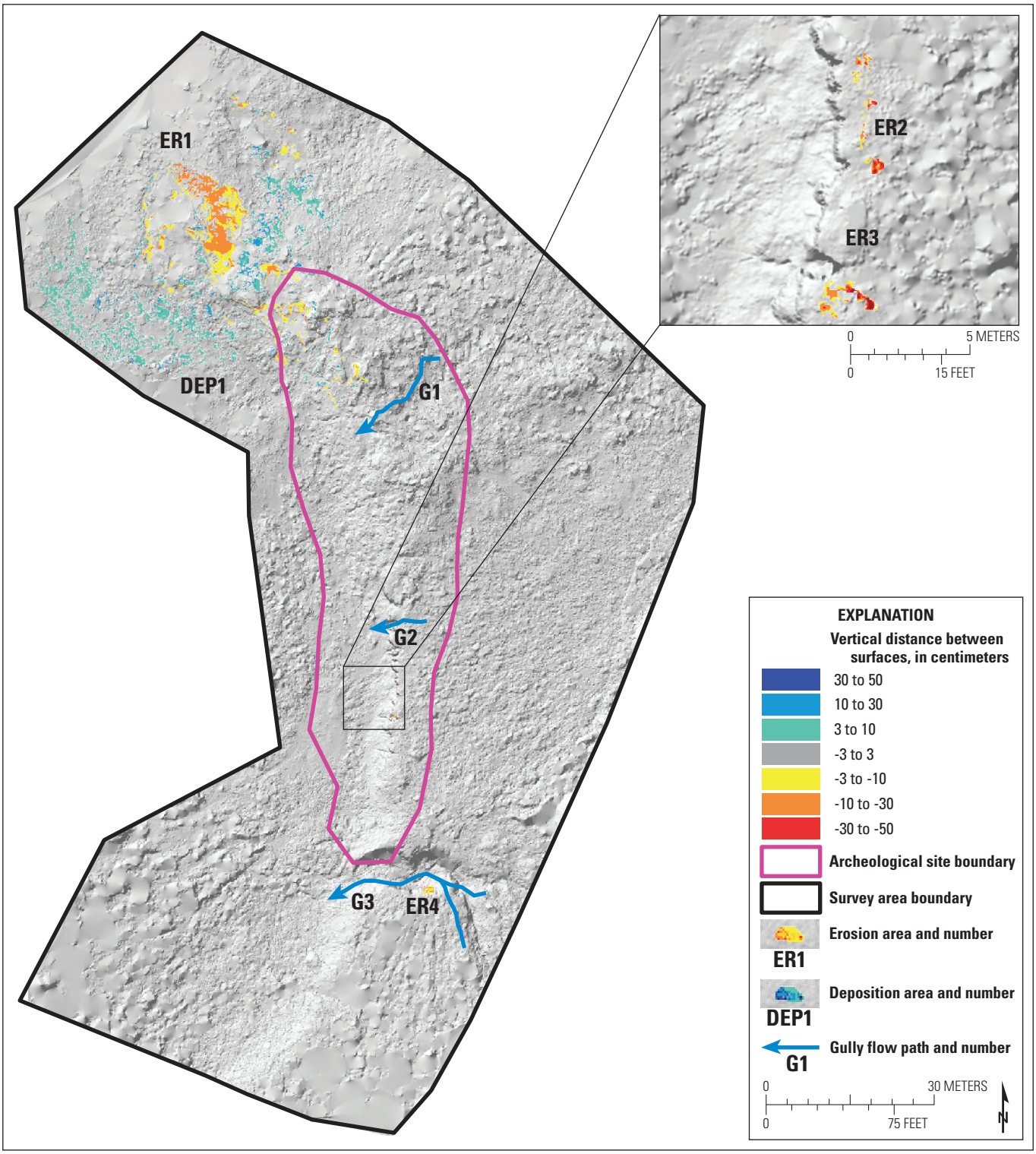

Figure 46. Landscape change at site AZ:C:02:0077. A 5-cm gridded topographic change output showing erosion (warm colors, negative) and deposition (cool colors, positive) between September 2012 and November 2013. Identified change is grouped by area labels (ER, erosion; DEP, deposition) and cross-referenced with table 6.

AZ:C:02:0075

Site Description

Site AZ:C:02:0075 is just downstream from site AZ:C:02:0077 in an area where the lower and upper terraces narrow to form a 20-m-wide zone between the Colorado River and adjacent bedrock cliffs (figs. 47, 48). Two areas of artifacts and buried cultural features are located within the terrace deposits, separated by a deeply incised gully (G3), and erosion probably has removed a substantial amount of archeological material from the site. The terrace surface is similar in composition to that at site AZ:C:02:0077, and near the river margin the terrace surface includes inactive, as well as possibly active, aeolian sand deposits. Terrace vegetation is similar to that at site AZ:C:02:0077, and includes taller (1 to 2 m) Tamarisk trees (*Tamarix ramosissima*) near the river on the remnants of the lower terrace and irregularly spaced grasses, Mormon tea (*Ephedra* sp.) shrubs, and Engelmann's hedgehog cacti (*Echinocereus engelmannii*) on the upper terrace.

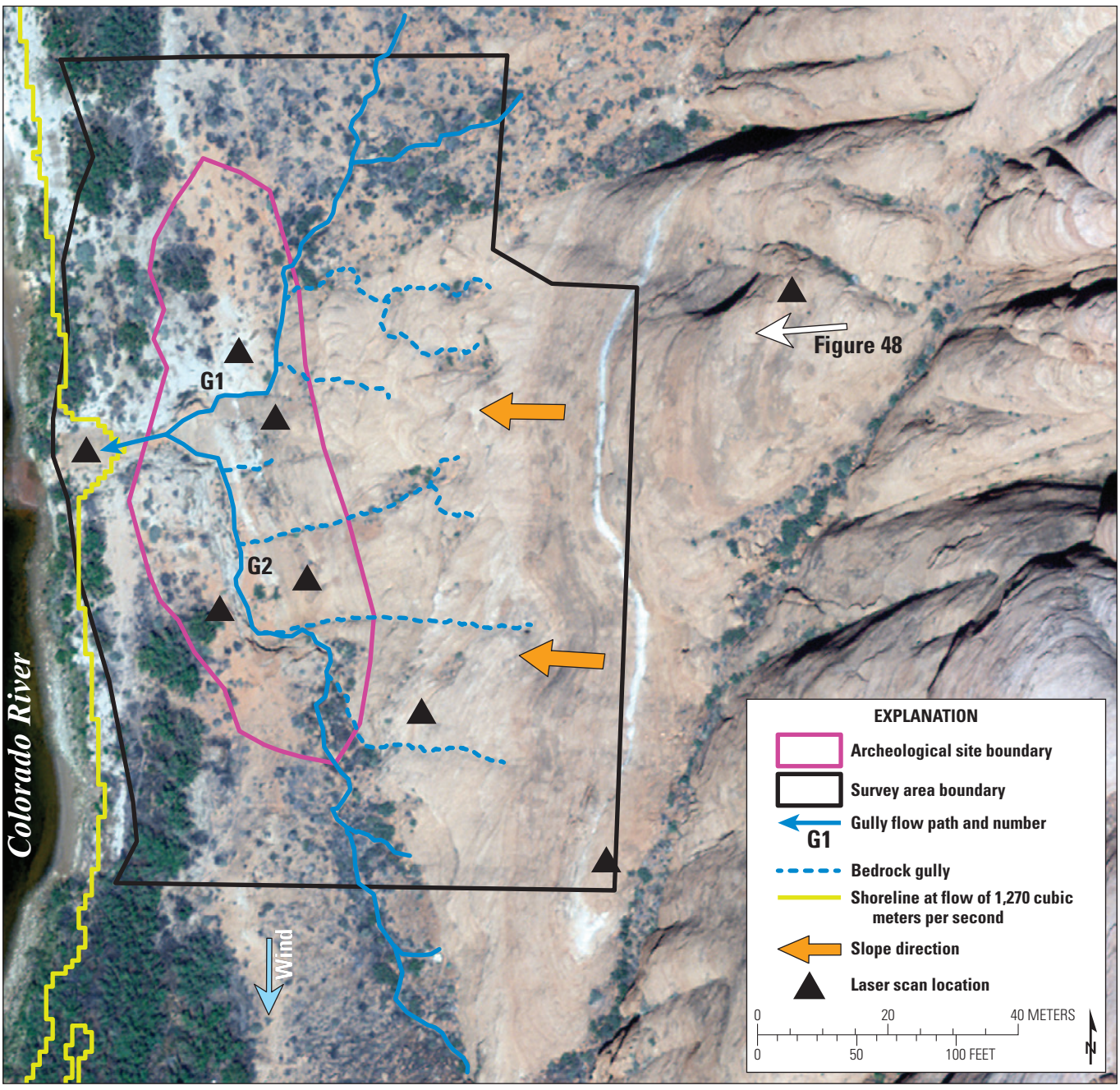

Figure 47. Site AZ:C:02:0075 survey-area map.

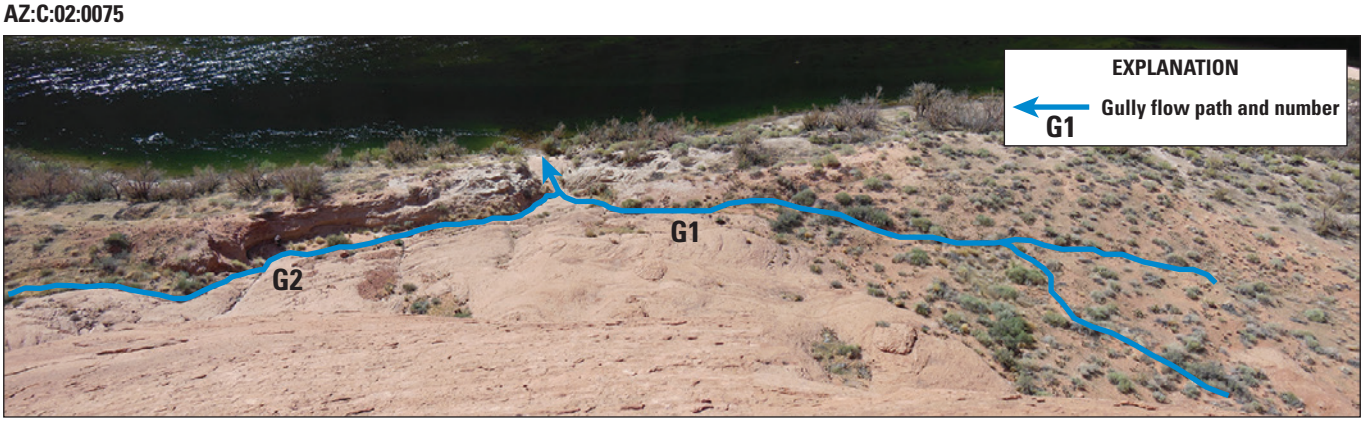

Figure 48. Site AZ:C:02:0075 survey-area photograph showing gully locations (G1, G2). View is toward the west.

A deep (approximately 3 m) gully traverses much of the site, and is incised entirely through the terrace sediment to bedrock in the lower parts of gullies G1 and G2; the upper parts of these gullies traverse the terrace surfaces but do not incise all the way to bedrock. Previous investigations identified widespread gullying as the predominant geomorphic process active at the site, but also mentioned aeolian processes, bedrock-sourced overland flow, rodent burrowing, and visitor impacts by way of social trails from a nearby campground (Neff and Wilson, 2002; Collins and others, 2014). Although a narrow sandbar is sometimes subaerially exposed upwind of the site, we have not observed modern controlled-flood sand deposition there. Thus, we classify this site as type 3 (having an upwind shoreline but no recently deposited fluvial sand; fig. 9). Fluvial erosion by the Colorado River is also possible here at high flows; water would have pooled in the bedrock-floored part of the gullies during the high flows of 1983, based on our observations at this site during the 2012 controlled flood.

Topographic Change (2012–13)

We analyzed topographic change over the entire archeological site and adjacent terrace area (fig. 49), focusing especially on the steep sidewalls of the gullies that traverse the site. Over this monitoring interval, nearly 10 percent of the archeological-site area underwent change greater than 3 cm. Measured topographic changes between 2012 and 2013 were all erosional and occurred over 211.5 m^2 of surface area.

The majority of erosion (in region ER3) occurred as a result of channelized gullying in gully G2, where 25.74 m^3 of the 2-m-tall vertical gully cut bank fell away. We measured no deposition at this site, indicating that gully flow transported all of the newly eroded material directly into the Colorado River. Although rainfall data are incomplete at the station closest to the site for the September 2012 to November 2013 timeframe in which this gullying occurred, the partial record (Caster and others, 2014) and unpublished data from local rain gages (D.J. Topping, USGS Grand Canyon Monitoring and Research Center, written commun., 2015) indicate that several large, high-intensity storms occurred in summer 2013. The 10-minute maximum rainfall intensities exceeded 30 mm/hr on at least 4 days during this time and reached 72 mm/hr during one event in late August (Caster and others, 2014). This intensity exceeds the threshold (64 mm/hr) determined by Collins and others (2016) to cause gullying at other archeological sites in Grand Canyon that have river-derived sediment as the substrate. In addition, a storm on August 2, 2013, caused the largest flooding documented in 14 years (2001–14) in Water Holes Canyon, a tributary that joins the Colorado River approximately 5 km from site AZ:C:02:0075 (D.J. Topping, written commun., 2015), suggesting that flow depths may have been substantial in the bedrock-incised gullies during that August 2013 event.

The two other areas of erosion (regions ER1 and ER2) were immediately adjacent to the gullies, but on the terrace surface rather than in the gully bottom. The spatial pattern of erosion indicated that it occurred by aeolian reworking of on-site sediment. Erosion removed 13.52 m^3 of sediment, with mean erosion depths of 7 and 11 cm for regions ER1 and ER2, respectively (table 7). Given the prevailing wind direction from the north (Caster and others, 2014), we might have expected deposition south of the site, but detected no new deposition anywhere within the surveyed area. Therefore, we assume that aeolian deflation exported sand from the survey area, possibly with some blown into the gullies and then removed by overland flow into the Colorado River.

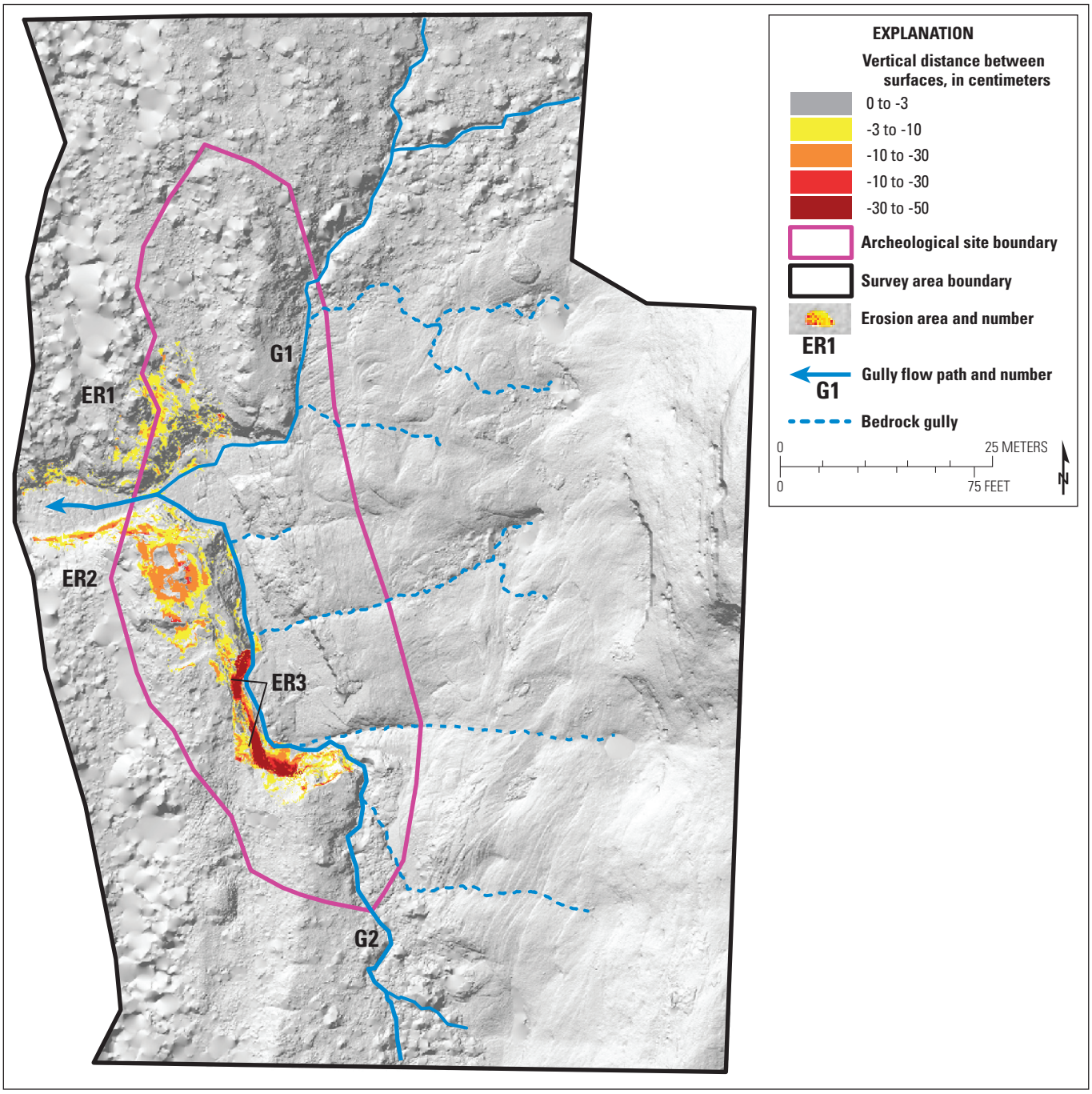

Figure 49. Landscape change at site AZ:C:02:0075. A 5-cm gridded topographic change output showing erosion (warm colors, negative) from September 2012 to November 2013. No deposition was detected. Identified change is grouped by area labels (ER, erosion) and cross-referenced with table 7.

Table 7. Summary of topographic change at site AZ:C:02:0075.

[m/yyyy, month/year; m^2, square meters; cm, centimeters; m^3, cubic meters]

Site number and region	Time period (m/yyyy)	Area (m^2)	Average depth (cm)	Volume (m^3)
AZ:C:02:0075 – ER1	9/2012–11/2013	56.5	-7	-3.79
AZ:C:02:0075 – ER2	9/2012–11/2013	85.4	-11	-9.73
AZ:C:02:0075 – ER3	9/2012–11/2013	69.6	-37	-25.74

AZ:C:02:0032

Site Description

Site AZ:C:02:0032 is located along and at the top of a terrace adjacent to an approximately 11-m-tall cutbank (height measured while river flow was 226 m^3/s) bordering the Colorado River (figs. 50, 51). Archeological material includes several lenses of charcoal-stain deposits at the site, along with grinding slabs, ceramics, and a probable hearth (Anderson, 2006; Spurr and Collette, 2007; Pederson and others, 2011). These cultural features, together with geoarcheological analyses (Pederson and others, 2011), indicate that the site has undergone at least three different cut-and-fill episodes, with each set of fill preserving different periods of human occupation—the oldest dates to approximately 500 B.C.E. and possibly as old as around 1500 B.C.E. (Pederson and others, 2011). The terrace is composed of interbedded slopewash and mainstem Colorado River fluvial deposits, with the top 30 cm indicating aeolian reworking (Pederson and others, 2011). However, our mapping showed little evidence of modern aeolian

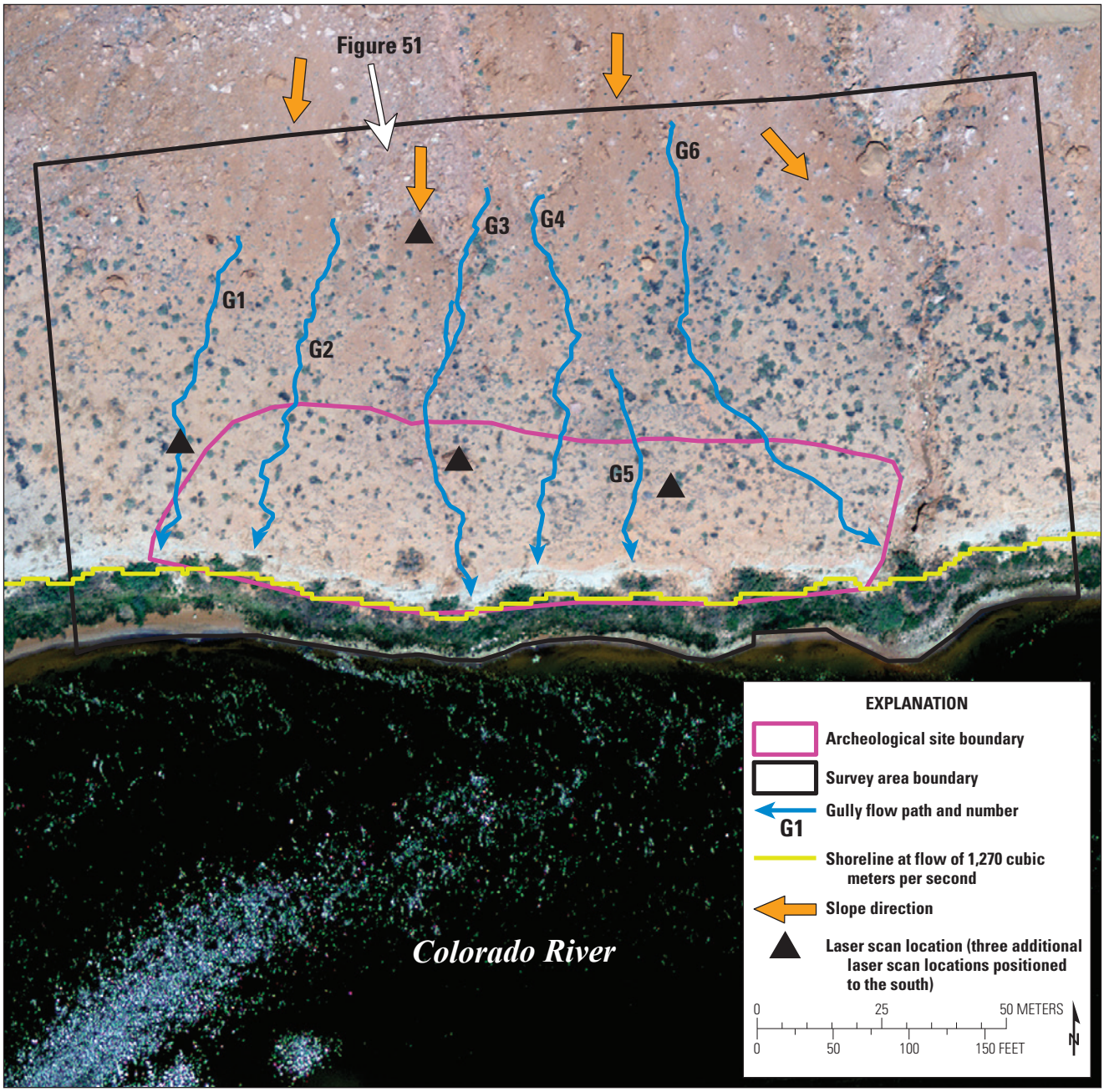

Figure 50. Site AZ:C:02:0032 survey-area map. Prevailing wind direction is not shown on this site map because this region is in a transition zone between dominantly upstream and dominantly downstream winds (inferred from weather stations in fig. 29); we observed no geomorphic features that indicated a clear prevailing wind direction at this site.

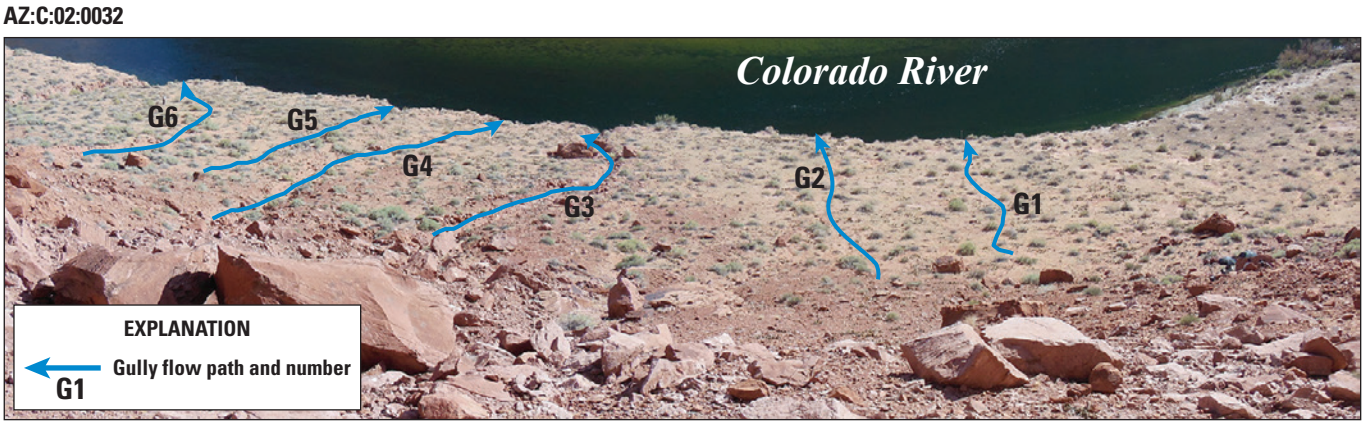

Figure 51. Site AZ:C:02:0032 survey-area photograph, showing gully locations (G1–G6). View is toward the south.

sand activity in this area, and dune forms are not present on the terrace surface. The major erosional processes affecting the site are overland-flow gully erosion across the terrace surface, and terrace bank collapse associated with high flows of the Colorado River. Terrace bank erosion at this site has been severe in the past (Burchett, 1996; Grams and others, 2007) and continues to threaten archeological-site stability (Pederson and others, 2011). We categorized the site as type 4, having no upwind shoreline corresponding to a recent controlled flood (fig. 9).

Six gullies traverse this terrace, incised to varying degrees (fig. 51; Collins and others, 2014). Four are shallow swales (<40 cm deep) as they cross the terrace; the other two have incised 40–60 cm. This geomorphology is similar to what was mapped in Marble–Grand Canyon by Hereford and others (1993), with some gullies being terrace-based (that is, thalwegs that do not reach the Colorado River) and others river-based, with a clear drainage path to the river. The two river-based gullies at site AZ:C:02:0032 have incised notches in the terrace bank edge, with one incising through nearly half of the terrace thickness (the gully incises through 5.2 m of the 11-m-thick terrace). Site vegetation consists of grasses, fourwing saltbush (*Atriplex canescens*), puncture vine (*Tribulus terrestris*), Mormon tea (*Ephedra* sp.) shrubs, and prickly pear cacti (*Opuntia polyacantha* var. *erinacea*); vegetation appears to offer only minor erosional resistance to the overland flow generated on the neighboring talus slope. The severity of gully erosion is related to episodic runoff from the talus slope, but fluvial bank erosion also might determine the incision rate near the terrace edge (Collins and others, 2014). Additional site details, including a more in-depth examination of gullying processes at this site, are included in Collins and others (2014).

Topographic Change (2012–13)

We focused our change-detection analyses on both the terrace surface and terrace cutbank (fig. 52), analyzing the terrace cutbank in three-dimensional space (as opposed to plan view). The results for this area are shown in a rotated view to assist with visualization, using a 45-degree oblique view (fig. 52). We identified 18 areas of erosion over the entire survey area (fig. 52, table 8), encompassing 115.6 m^2, which account for 1.3 percent of the plan-view surface area within the archeological-site boundary. We found no areas where deposition was evident at site AZ:C:02:0032 over this monitoring interval.

Whereas overland-flow-induced erosion was active in the deepest, most incised gully crossing the terrace (G3; regions ER14 through ER18), the total sediment volume eroded from the terrace surface (0.85 m^3) was much less than the erosion that occurred along the terrace cutbank. There, along a 200-m length of the terrace edge, 13 generalized areas of erosion (regions ER1 through ER13) totaled 20.23 m^3 of erosion. The average plan-view depth of erosion among all erosional areas was 15 cm; terrace erosion was confined to distinct parts of the terrace cutbank rather than whole-height collapses (fig. 52). Although the cause of the terrace-edge erosion cannot be identified with certainty, we consider the November 2012 controlled flood the most likely agent because erosion was widespread along the cutbank and appeared not to be directly related to particular spillover points from the gullies on the terrace surface. Time-lapse photographic documentation by National Park Service (NPS) staff (T. Baker, written commun., 2013) shows that during other controlled floods, the toe of the cutbank has been inundated by rising water levels. After saturation of the cutbank toe, and upon water levels subsequently dropping as controlled floods recede, soil piping likely occurs, wherein water seeps out of the cutbank and destabilizes its toe. This mechanism is akin to a rapid drawdown effect that must be designed for, or restricted by all means, in earthen-dam operations. Destabilization by seepage forces may undercut the cutbank and (or) alter the stress condition of overlying exposed areas of the cutbank, wherein discrete areas of the cutbank fall away. If erosion occurs during recession of a controlled flood, the river flow may export the eroded material. If erosion occurs at some time soon after, piles of debris (that is, deposition) may accumulate at the toe of the cutbank. Because vegetation obscures most of the cutbank toe at this site, our lidar measurements could not resolve whether such deposits remain there.

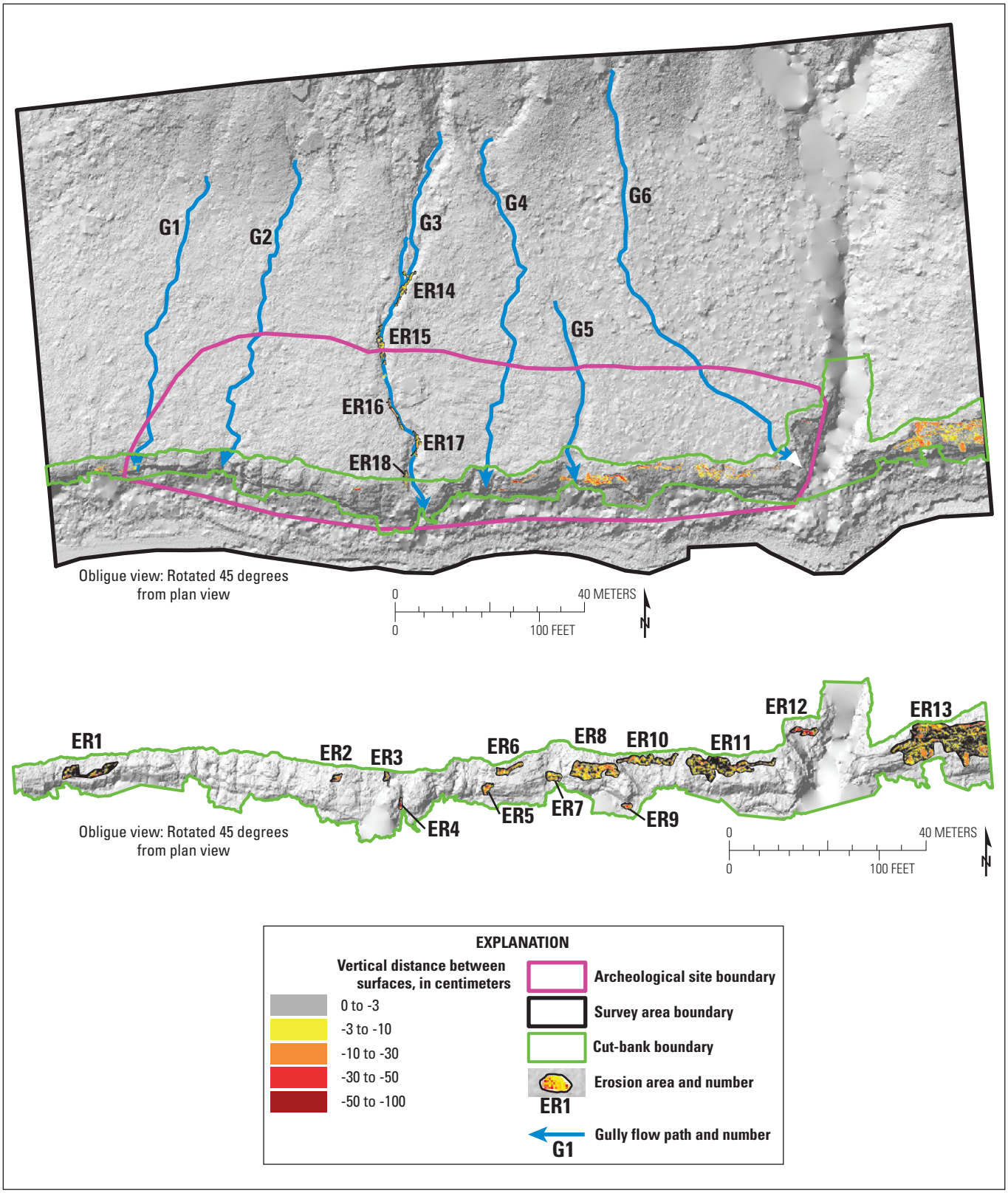

Figure 52. Landscape change at site AZ:C:02:0032. A 5-cm gridded topographic change output showing erosion (warm colors, negative) from September 2012 to November 2013. No deposition was detected. Identified change is grouped by area labels (ER, erosion) and cross-referenced with table 8.

Table 8. Summary of topographic change at site AZ:C:02:0032.

[m/yyyy, month/year; m^2, square meters; cm, centimeters; m^3, cubic meters]

Site number and region	Time period (m/yyyy)	Area (m^2)	Average depth (cm)	Volume (m^3)
AZ:C:02:0032 – ER1	9/2012–11/2013	3.6	-12	-3.13
AZ:C:02:0032 – ER2	9/2012–11/2013	1.0	-18	-0.56
AZ:C:02:0032 – ER3	9/2012–11/2013	0.7	-16	-0.45
AZ:C:02:0032 – ER4	9/2012–11/2013	0.6	-29	-0.20
AZ:C:02:0032 – ER5	9/2012–11/2013	1.9	-13	-0.30
AZ:C:02:0032 – ER6	9/2012–11/2013	3.1	-12	-0.50
AZ:C:02:0032 – ER7	9/2012–11/2013	2.9	-9	-0.31
AZ:C:02:0032 – ER8	9/2012–11/2013	16.6	-9	-2.00
AZ:C:02:0032 – ER9	9/2012–11/2013	1.2	-15	-0.18
AZ:C:02:0032 – ER10	9/2012–11/2013	7.5	-9	-1.09
AZ:C:02:0032 – ER11	9/2012–11/2013	16.2	-9	-3.02
AZ:C:02:0032 – ER12	9/2012–11/2013	3.1	-33	-1.10
AZ:C:02:0032 – ER13	9/2012–11/2013	47.5	-10	-7.39
AZ:C:02:0032 – ER14	9/2012–11/2013	3.2	-6	-0.21
AZ:C:02:0032 – ER15	9/2012–11/2013	2.9	-6	-0.18
AZ:C:02:0032 – ER16	9/2012–11/2013	1.4	-18	-0.24
AZ:C:02:0032 – ER17	9/2012–11/2013	1.9	-9	-0.18
AZ:C:02:0032 – ER18	9/2012–11/2013	0.3	-13	-0.04

By dividing the volumes of erosion (table 8) by the three-dimensional surface area of the erosion regions at the site (approximately three times the plan view area reported in table 8), we calculated the average erosion into the cutbank to be 10 cm (ranging between 5 and 24 cm) at the areas undergoing change. This calculation is not an overall indication of average terrace retreat, which must be calculated using the entire areal extent of the cutbank. Using the surveyed cutbank height (7.6 m) and length (200 m), and over the 1.1-year time frame bracketing the repeat topographic surveys, this volume of erosion yields a short-term terrace-retreat rate of 0.01 m/yr. This rate is an order of magnitude less than that documented by NPS staff (0.11 m/yr, the mean of four surveyed control points with one showing no erosion and the others showing between 10 and 25 cm of erosion) at the site between 1991 and 2003 (Wulf and Moss, 2004). However, our retreat rate is based on a shorter measurement interval (1.1 years). Compared to long-term retreat rates measured in other nearby areas of the same terrace, our calculated bank-retreat rates are low. Grams and others (2007) showed that the terrace in the vicinity of this same archeological site eroded approximately 90 m between 1952 and 1984 (2.8 m/yr). At a location <1 km downriver, repeat measurements at surveyed cross-sections indicate that the terrace eroded 34 m horizontally between 1959 and 1965 (5.8 m/yr) and that another 12 m eroded between 1990 and 2000 (1.3 m/yr; Grams and others, 2007). Although Grams and others (2007) noted that this area of Glen Canyon may have undergone anomalously high rates of erosion compared to other sections, the recent measurements of ongoing terrace erosion are a reminder that the terrace bank at this site is dynamic, and has not achieved a stable configuration with respect to ongoing dam operations.

AZ:C:02:0035

Site Description

Site AZ:C:02:0035 is located just downriver from site AZ:C:02:0032 on a continuation of the predam fluvial terrace that borders the river in this stretch of Glen Canyon. The terrace at site AZ:C:02:0035 narrows to the east (downstream), and large boulders from rockfalls are situated on and immediately adjacent to the terrace surface, which grades into a talus slope (figs. 53, 54). The area is archeologically important as a prehistoric ancestral Puebloan site with two concentrations of artifacts. Previous fluvial geomorphological research (R. Hereford, unpub. data; Anderson, 2006) indicates that the deposits were emplaced during and prior to the Puebloan period (700–1200 C.E.) and that higher, older terraces are preserved by the talus deposits that cover part of the site. The main terrace is similar to that forming site AZ:C:02:0032 and is composed of interbedded slopewash and mainstem Colorado River fluvial sediment, although at the toe

AZ:C:02:0035

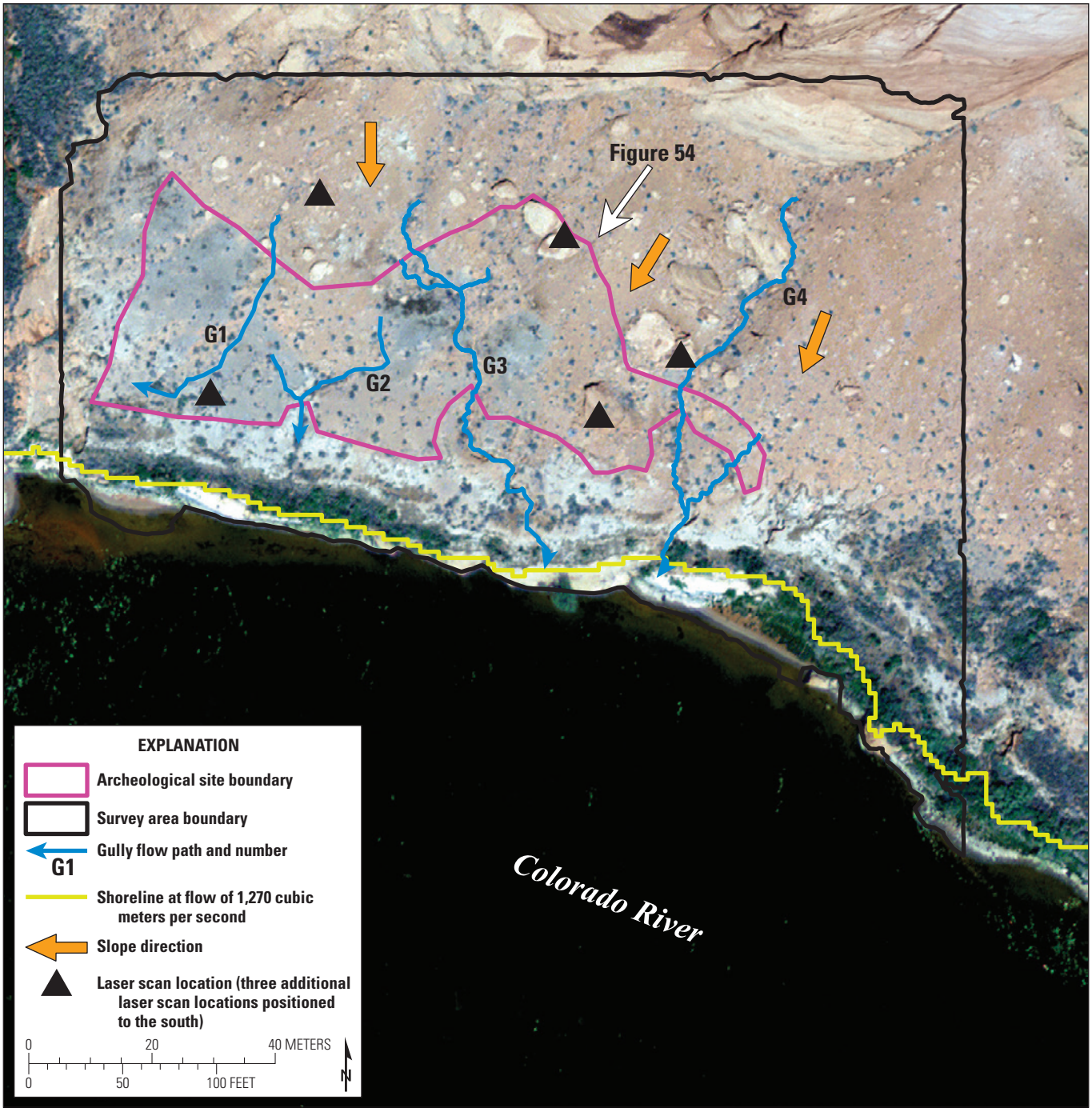

Figure 53. Site AZ:C:02:0035 survey-area map. Wind direction is not indicated because this region is in a transition zone between dominantly upstream and dominantly downstream winds (inferrered from weather stations in fig. 29); we observed no geomorphic features that indicated a clear prevailing wind direction at this site.

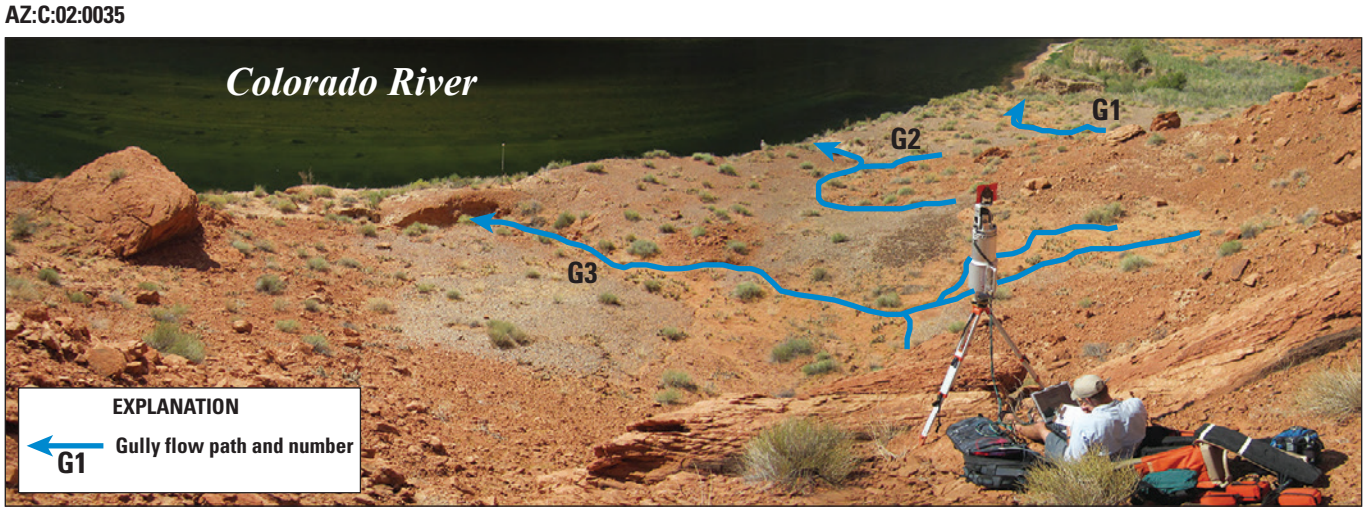

Figure 54. Site AZ:C:02:0035 survey-area photograph showing gully locations (G1–G3). View is toward the southwest.

of the cutbank that forms the river-side of the terrace, these deposits are underlain by a 3-m-tall bedrock outcrop that was likely exposed during previous high flows released from Glen Canyon Dam (Grams and others, 2007). No active aeolian sand presently exists at this site; similar to site AZ:C:02:0032, gullying erosion is the dominant erosional process. Unlike the situation near site AZ:C:02:0032, the terrace area riverward of site AZ:C:02:0035 has not undergone as extensive cutbank collapse during recent controlled floods, owing to the erosional protection offered by the bedrock outcrop at the terrace toe. However, the terrace at this site retreated approximately 100 m between 1952 and 1984 (Grams and others, 2007), and the cross-section-based rapid retreat rates mentioned previously (5.8 m/yr between 1959 and 1965, and 1.3 m/yr between 1990 and 2000) were obtained even closer to this site than to site AZ:C:02:0032. We categorized site AZ:C:02:0035 as type 4 (no upwind shoreline corresponds with a recent high flow); there is no active aeolian sand source upwind of this site.

Four gullies traverse the terrace, incised to varying degrees (figs. 53, 54; Collins and others, 2014). The two gullies with the deepest incision (G3 and G4) begin high on the talus slopes inland and upslope of the terrace, and have larger contributing drainage area than do the four less-incised gullies, potentially linked to overland flow inputs from the cliffs and cliff-top areas. Vegetation is similar to, but sparser than, site AZ:C:02:0032, with grasses, fourwing saltbush (*Atriplex canescens*), Mormon tea (*Ephedra* sp.) shrubs, and prickly pear cacti (*Opuntia polyacantha* var. *erinacea*) interspersed on the terrace surface.

Topographic Change (2012–13)

We analyzed topographic change over the entire archeological site and adjacent terrace area (fig. 55), including the cutbank that forms the south edge of the site. Within the archeological-site boundary we documented only 0.1 percent of surface area change, all caused by precipitation-induced erosion in gully G3 (erosion areas ER1 and ER2). Substantial gullying also occurred outside the archeological-site boundary, farther downstream along gully G3 and within the other deeply incised gully (G4). In these locations, between 21 and 33 cm of vertical downcutting occurred (regions ER3, ER4, ER5; table 9). Over the entire survey area, the eroded volume totaled 1.53 m^3 and occurred over an area of 8.4 m^2. We did not detect evidence for aeolian inflation or deflation of the land surface, nor for any gully filling by aeolian sand.

The most notable erosion occurred in gully G3, where we measured mean erosion depths of between 28 and 33 cm (regions ER3 and ER4; table 9) and from which more than 1 m^3 in sediment volume was lost. Detailed analysis of these erosion areas revealed that the gully widened (as opposed to merely downcutting), with some parts of the gully sidewalls having been undercut by as much as 38 cm and forming overhanging sections that are likely to collapse. We detected no deposition in any part of the site, suggesting that all eroded sediment was exported downstream by the Colorado River. The same storms identified to have caused gullying at sites AZ:C:02:0075 and AZ:C:02:0032 likely were responsible for the erosion here. Storms with high rainfall intensity (10-minute intensity > 60 mm/hr) likely exceeded the soil infiltration capacity threshold at this site (Collins and others, 2016). Because erosion occurred only in the largest, most deeply incised gullies (G3 and G4), the erosion observed at AZ:C:02:0035 could have been a result of the potentially larger catchment area of these gullies (with consequently greater overland flow), the steeper gradient (because these gullies are already deeply incised, and grade to river level; Collins and others, 2014), or possibly the lower infiltration capacity of the gully bottoms. In all regards, it should come as no surprise that erosion occurred in locations where gullies had formed in the past.

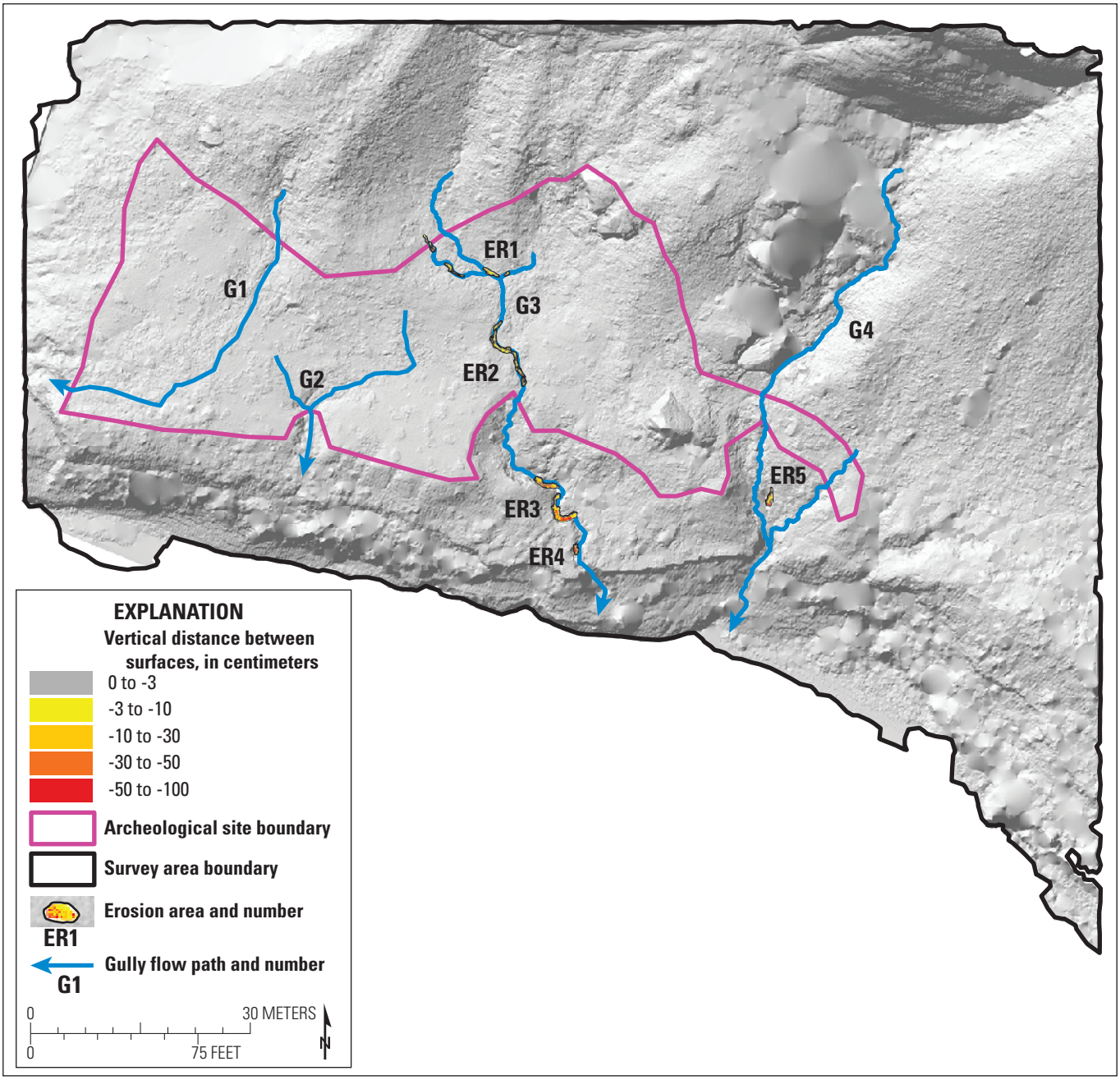

Figure 55. Landscape change at site AZ:C:02:0035. A 5-cm gridded topographic change output showing erosion (warm colors, negative) from September 2012 to November 2013. No deposition was detected. Identified change is grouped by area labels (ER, erosion) and cross-referenced with table 9.

Table 9. Summary of topographic change at site AZ:C:02:0035.

[m/yyyy, month/year; m^2, square meters; cm, centimeters; m^3, cubic meters]

Site number and region	Time period (m/yyyy)	Area (m^2)	Average depth (cm)	Volume (m^3)
AZ:C:02:0035 – ER1	9/2012–11/2013	1.3	-5	-0.06
AZ:C:02:0035 – ER2	9/2012–11/2013	2.0	-4	-0.09
AZ:C:02:0035 – ER3	9/2012–11/2013	3.9	-28	-1.09
AZ:C:02:0035 – ER4	9/2012–11/2013	0.4	-33	-0.13
AZ:C:02:0035 – ER5	9/2012–11/2013	0.8	-21	-0.16

Landscape Change in Glen Canyon

Topographic-change analyses indicate that erosion processes dominated strongly over depositional processes at our four study sites in Glen Canyon (fig. 56). At all four sites overland-flow erosion incised gullies, in some cases lowering the land surface by more than 2 m over 14 months. Topographic changes included gully-wall undercutting and widening, in addition to some gully downcutting—particularly at gradient changes and knickpoints at terrace edges. Direct effects of Colorado River flows caused terrace-bank erosion at one site (AZ:C:02:0032)—a process which has been ongoing over the past five decades since construction of Glen Canyon Dam and now appears to be slowing, but is still indicative of a system that has not reached a stable configuration. At only one site did we detect any deposition (AZ:C:02:0077; fig. 46). Although the spatial pattern of that deposition suggested aeolian inflation (fig. 46), it could not be linked to any fluvial sand source formed under the current flow regime, and we inferred redistribution by wind of local, relict terrace sediment as the most likely process. Aeolian transport at the other sites was not entirely absent, but where present (AZ:C:02:0075; fig. 49), resulted only in erosion and net sand loss.

The four Glen Canyon sites showed a greater dominance of erosional processes compared to depositional processes than did our four Marble–Grand Canyon study sites over the temporal intervals measured (compare fig. 43 with fig. 56). Whereas gross erosion rates (the area of change per year per site) were actually higher at the Marble–Grand Canyon sites (an average of 143 m^2/yr/site during 2010–14) than at the Glen Canyon sites (117 m^2/yr/site during 2012–13), deposition offset some of that erosion in Marble–Grand Canyon such that net erosion rates were higher at the Glen Canyon sites (58 m^2/yr/site) than at the Marble–Grand Canyon sites (51 m^2/yr/site). Comparing volumetric change for eroding regions yields similar results. Whereas gross erosion volumes (the volume of change per year per site, using the same time periods as for the area-based calculations) were similar between the Marble–Grand Canyon sites (average of 17.9 m^3/yr/site) and Glen Canyon sites (18.3 m^3/yr/site), net erosional volumes were again higher in Glen Canyon (14.3 m^3/yr/site) than in Marble–Grand Canyon (11.4 m^3/yr/site). Moreover, whereas some aeolian deposition occurred at all four study sites in Marble–Grand Canyon during both monitoring intervals (2010–13 and 2013–14; fig. 43), aeolian deposition occurred at only one site in Glen Canyon (AZ:C:02:0077; fig 46), and that deposition was apparently caused by reworking of relict (predam) rather than newly supplied sediment.

This type of direct comparison between landscape evolution in Glen and Marble–Grand Canyons is undoubtedly limited because the processes responsible for changes are different, the measurements spanned different time intervals, and the total surveyed area varied among sites. In addition, geomorphic setting varied somewhat from site to site. The first three factors (landscape process, measurement timing, and surveyed area) arguably will have limited impact on inferred differences between the two groups of sites: the process types are similar, the temporal intervals were not vastly different—1.1 yr and 3.6 yr, respectively, for Glen Canyon and Marble–Grand Canyon—and although the total surveyed area is 83 percent greater in Glen Canyon, that is unlikely to affect interpretations substantially because the areas where we detected landscape change are smaller and spatially isolated compared to the total area surveyed. However, the geomorphic settings must be closely compared to determine whether the Glen Canyon sites may be more predisposed (by factors other than their lack of aeolian-sand activity) to erosion.

We identified similarities and differences in geomorphic parameters between the two groups of sites. Topographic slope at the Glen Canyon sites compares favorably to that at the Marble–Grand Canyon sites (average values of 15° and 13°, respectively; fig. 57*A*) and up-watershed substrates are generally composed of talus slopes with likely similar infiltration capacity. Watershed area, on the other hand, is roughly double at the sites in Glen Canyon compared to those in Marble–Grand Canyon (averages of approximately 29,000 m^2 and 14,400 m^2, respectively; fig. 57*B*). Whereas this could lead to either more

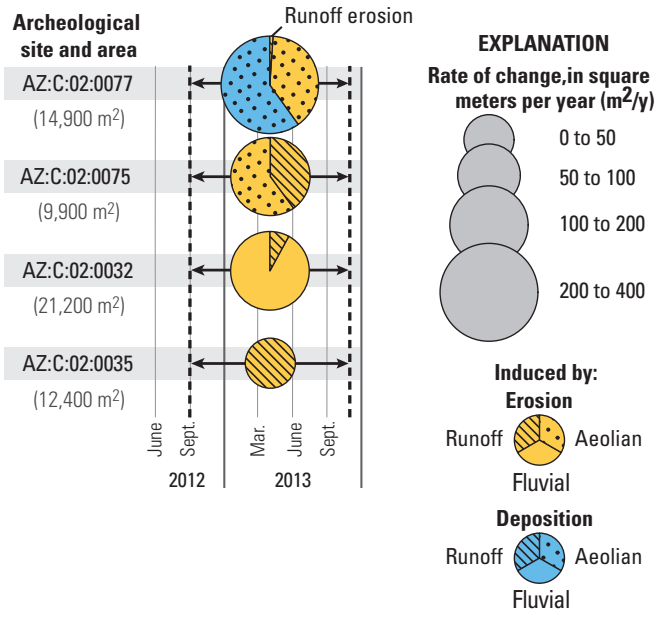

Figure 56. Summary of landscape change measured at four archeological sites in the Colorado River corridor through the Glen Canyon reach, by area, over the 2012–2013 monitoring interval. Pie size indicates the total area of erosion and deposition, normalized by the length of time between measured changes. Hatching pattern indicates the primary geomorphic process inferred to have caused the change. At site AZ:C:02:0032, fluvial-related change occurred in the form of terrace cutbank erosion likely related to toe inundation from a controlled flood in 2012. Values in parentheses indicate average total area where change detection was investigated. Dashed lines are dates of data collection; pie locations indicate measured change between times represented by adjacent dashed lines.

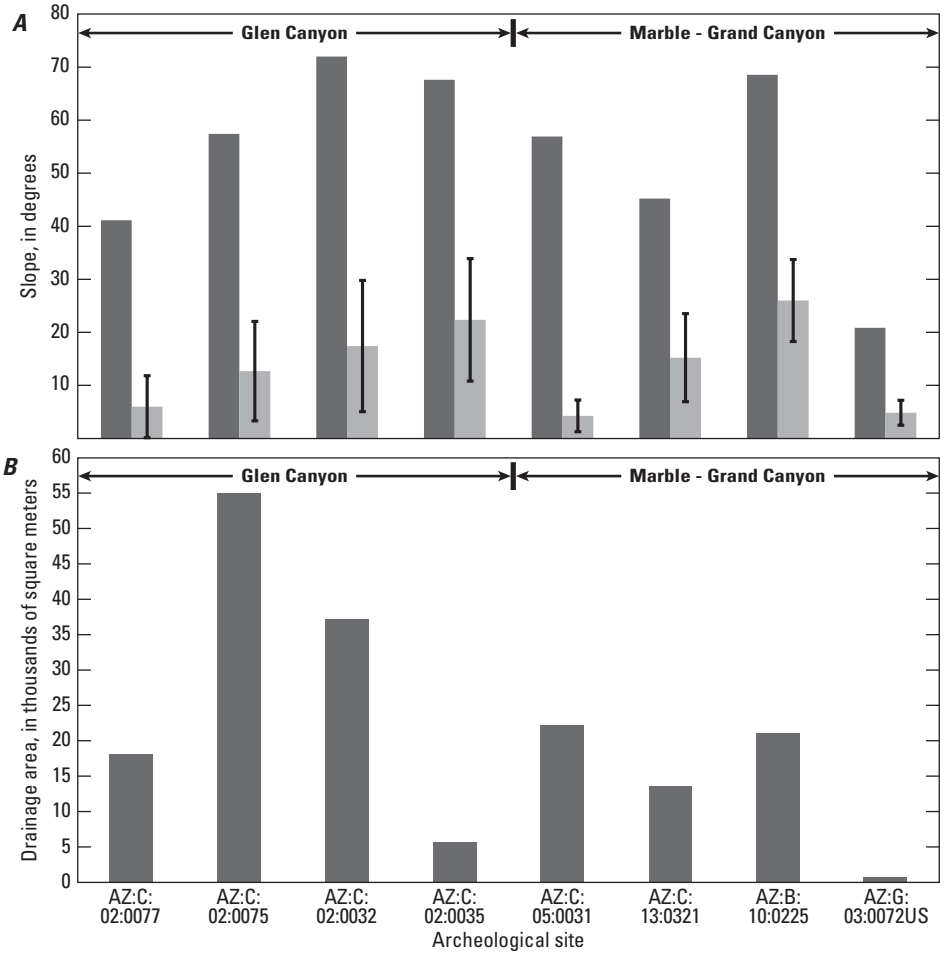

Figure 57. (*A*) Maximum and mean slope calculated within the survey area of each of the eight archaeological sites investigated in Sections III and IV. Error bars represent the standard deviation of the mean slope. (*B*) Contributing drainage area upslope of the survey boundary for each site.

frequent or more deeply incised gullies through greater overland flow, a closer look at the data raises doubts that this is the only relevant factor. The sites with the largest and smallest overland-flow erosion volume per year—AZ:B:10:0225, in Grand Canyon, with 37.4 m^3/yr, and AZ:C:02:0077, in Glen Canyon, with 0.4 m^3/yr during the total monitoring period at each site—have similar contributing watershed area—the area draining into those sites is within 3,000 m^2 (20 percent of the standard deviation between all watershed-area measurements) of each other. Thus, although two of the Glen Canyon sites have the largest watershed areas (fig. 57*B*), it is unclear to what extent this contributes to the observed differences in surface change between Glen and Marble–Grand Canyons.

Factors such as site substrate and gully-incision magnitude are not helpful in identifying parameters that might be responsible for the observed differences in erosion rates among the study sites. Aeolian sand is a more common substrate at the Marble–Grand Canyon sites than in the Holocene terraces of Glen Canyon, but this is expected given the design of the study (in Marble-Grand Canyon, we purposefully selected type 1 sites, whereas in Glen Canyon, none of the sites has apparent connectivity to modern aeolian sand supply). Similarly, there are more (3.8 versus 2.0 gullies/site) and deeper (1.4 m versus 0.9 m) gullies in the Glen Canyon sites compared to the Marble-Grand Canyon sites, but again, these differences existed before our study (and were factored into the study design), and it is unclear whether these pre-existing differences affected erosion rates measured during the study.

The contrast between landscape change measured at the Marble–Grand Canyon sites and that measured at the Glen Canyon sites illustrates the best- and worst-case scenarios for site-preservation trajectory in the Colorado River corridor, given the range in connectivity to modern sand supply and geomorphic context in this system. Sand deposition at the type 1 Marble–Grand Canyon archeological sites increases the potential for erosion to be counteracted either by aeolian inflation or gully annealing, as discussed in Section III. With little or no deposition at Glen Canyon sites, in contrast, there is less possibility for inflation and volume gain on terrace surfaces, or for gullies to anneal. Thus, even undergoing nearly the same event-scale or annual-scale erosion rates as in Marble–Grand Canyon, archeological sites in Glen Canyon are more likely to become more highly dissected and degraded. These process links are perhaps best exemplified by the changes measured at site AZ:C:02:0035 in Glen Canyon, where the most-incised gullies also showed the most erosion during the study period. No substantial net aeolian inflation or aeolian gully annealing is likely to occur in Glen Canyon owing to the lack of connectivity to modern fluvial sand sources; therefore, erosion is likely to continue there essentially unabated if present conditions and processes persist.

Climatologic Comparison of Glen and Marble–Grand Canyons

We investigated whether the extensive gully erosion in Glen Canyon could be caused or exacerbated by a subregional climate that might include substantially more precipitation, and more intense storms capable of causing overland flow. Below, we address the second science question of Section IV with regard to whether weather patterns could cause substantially different landscape-change trajectories in Glen Canyon than in Marble–Grand Canyon.

Glen Canyon received less annual rainfall than did most of Marble–Grand Canyon over the 3-year interval when the greatest number of USGS inner-canyon weather stations operated concurrently and from which we also have National Weather Service COOP-station records (October 2007 to October 2010; fig. 58). Long-term, 60-year mean annual rainfall records from COOP stations at Phantom Ranch (Grand Canyon), Lees Ferry (boundary of Marble and Glen Canyons), and Page (on the southeast rim, above Glen Canyon) similarly indicate that the Glen Canyon region receives less annual rainfall, on average, compared to farther downriver in Grand Canyon (fig. 59*A*). During the drought year of 2014, however, below-average annual rainfall was observed at all locations, and rainfall in Glen Canyon and at Lees Ferry was slightly greater than at the Phantom Ranch COOP station (fig. 59*B*), a situation that appears atypical in the context of longer-term records (Hereford and others, 2014).

Decadal-scale records (1958–2012) show that rainfall intensity and the frequency of days with high-intensity rainfall in Glen Canyon appear to be typically less, and certainly not greater, than in Grand Canyon (fig. 60). When compared to the Phantom Ranch COOP station (at RM 87, Grand Canyon), the estimated maximum daily 10-minute rainfall intensity values at Lees Ferry and Page generally have been lower—less than 85 mm/hr at Lees Ferry and Page (although one event in 1964 exceeded 90 mm/hr at Page), compared to more than 116 mm/hr at Phantom Ranch (fig. 60). Moreover, approximately half as many moderate to strong storms (defined as individual days having 10-minute maximum rainfall intensity >32 mm/hr; Collins and others, 2016) occurred at Lees Ferry (35) and Page (32) compared to Phantom Ranch (65) during 1958–2012. Long-term records from three stations surely do not represent conditions over the entire, vast canyon area, especially given that a 60-year record exists from only one point in Grand Canyon (Phantom Ranch), and that spatial variations in rainfall amount and intensity often are substantial in this river corridor (for example, Draut and Rubin, 2008; Caster and others, 2014). However, the available long-term data imply that storms capable of gully erosion have been less frequent in Glen Canyon since 1958.

Wind speeds within Glen Canyon did not differ substantially from those recorded in Marble–Grand Canyon between February 2014 and February 2015 (the interval from which data are available for all USGS inner-canyon stations). Thus, the wind data we analyzed did not explain differences in the prevalence of aeolian geomorphic processes between the two study areas—rarity of active aeolian sand in Glen Canyon (Section II), and less aeolian inflation or deflation measured at the four sites there compared to those in Marble–Grand

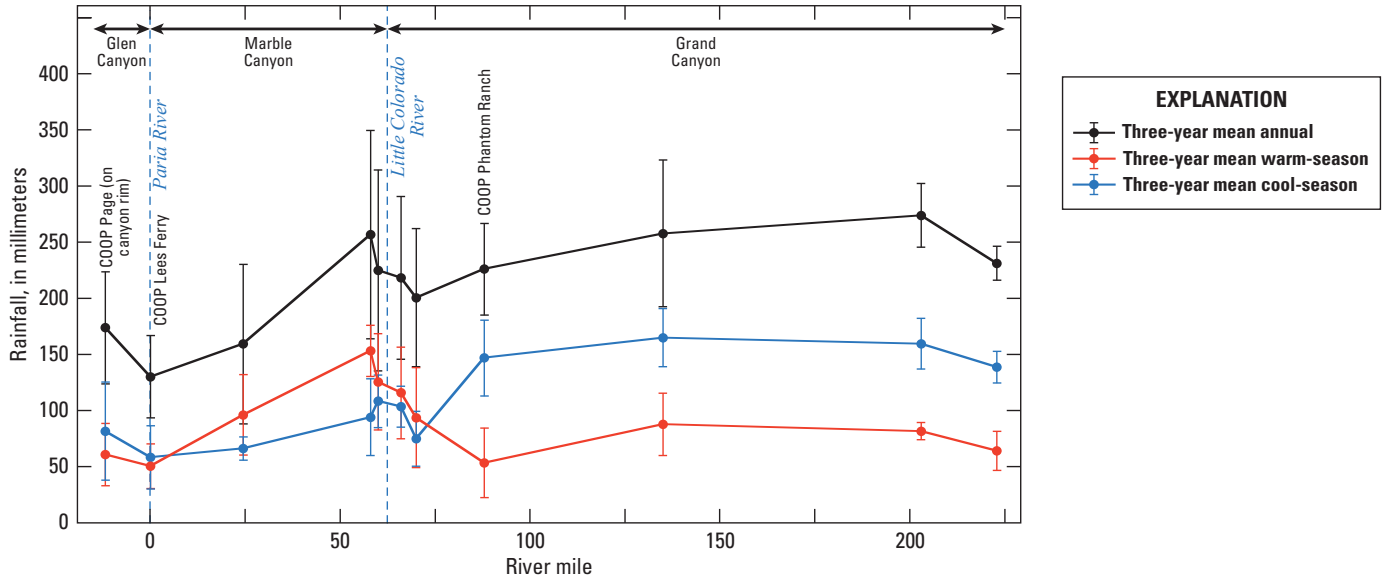

Figure 58. Spatial distribution of annual and seasonal rainfall within the Colorado River corridor and an adjacent rim location. Mean values were calculated from data collected between October 8, 2007, and October 7, 2010, the period with greatest number of concurrently operating stations, at 8 U.S. Geological Survey inner-canyon stations and 3 National Weather Service Cooperative Observer Program (COOP) stations (Phantom Ranch, Grand Canyon; Lees Ferry, at the boundary of Glen and Marble Canyons; and Page, on the southeast rim above Glen Canyon). Major tributary confluences are shown for reference. Error bars represent standard error of the 3-year mean.

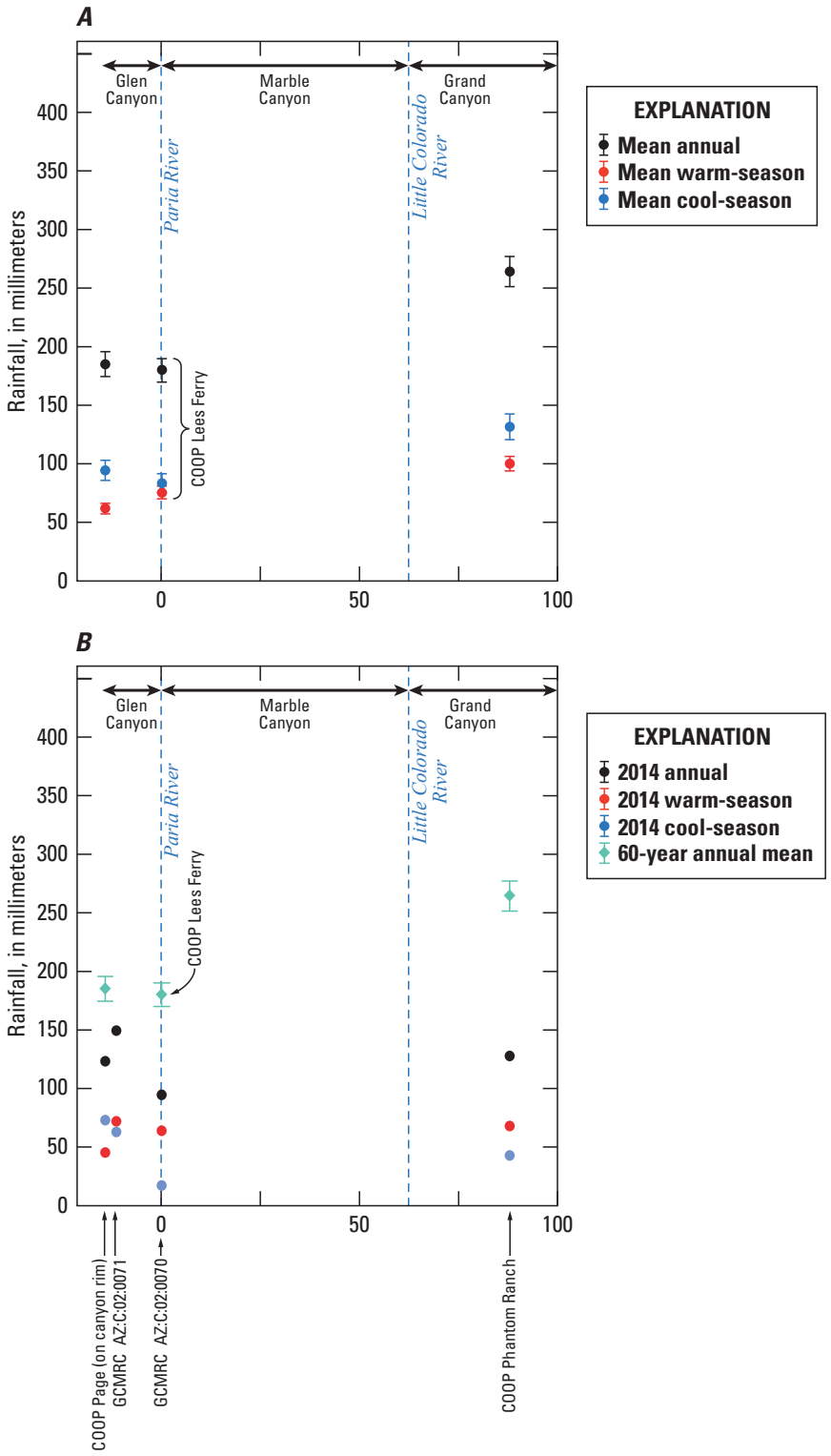

Figure 59. Temporal summaries of mean seasonal and annual rainfall measured at National Weather Service Cooperative Observer Program (COOP) stations Phantom Ranch (Grand Canyon), Lees Ferry (boundary of Glen and Marble Canyons), and Page (on the southeast rim, above Glen Canyon) by distance downstream from Glen Canyon Dam. (*A*) 60-year (1952–2012) annual and seasonal mean rainfall. Major tributary confluences are shown for reference. Error bars represent standard error of the 60-year mean. (*B*) Seasonal and annual rainfall totals from October 8, 2013, through October 7, 2014, for U.S. Geological Survey inner-canyon weather stations AZ:C:02:0070 and AZ:C:02:0071 (locations on fig. 29; Caster and others, 2014) and COOP stations at Phantom Ranch and Page. The COOP station at Lees Ferry was removed in 2012. The 60-year annual means are provided for reference.

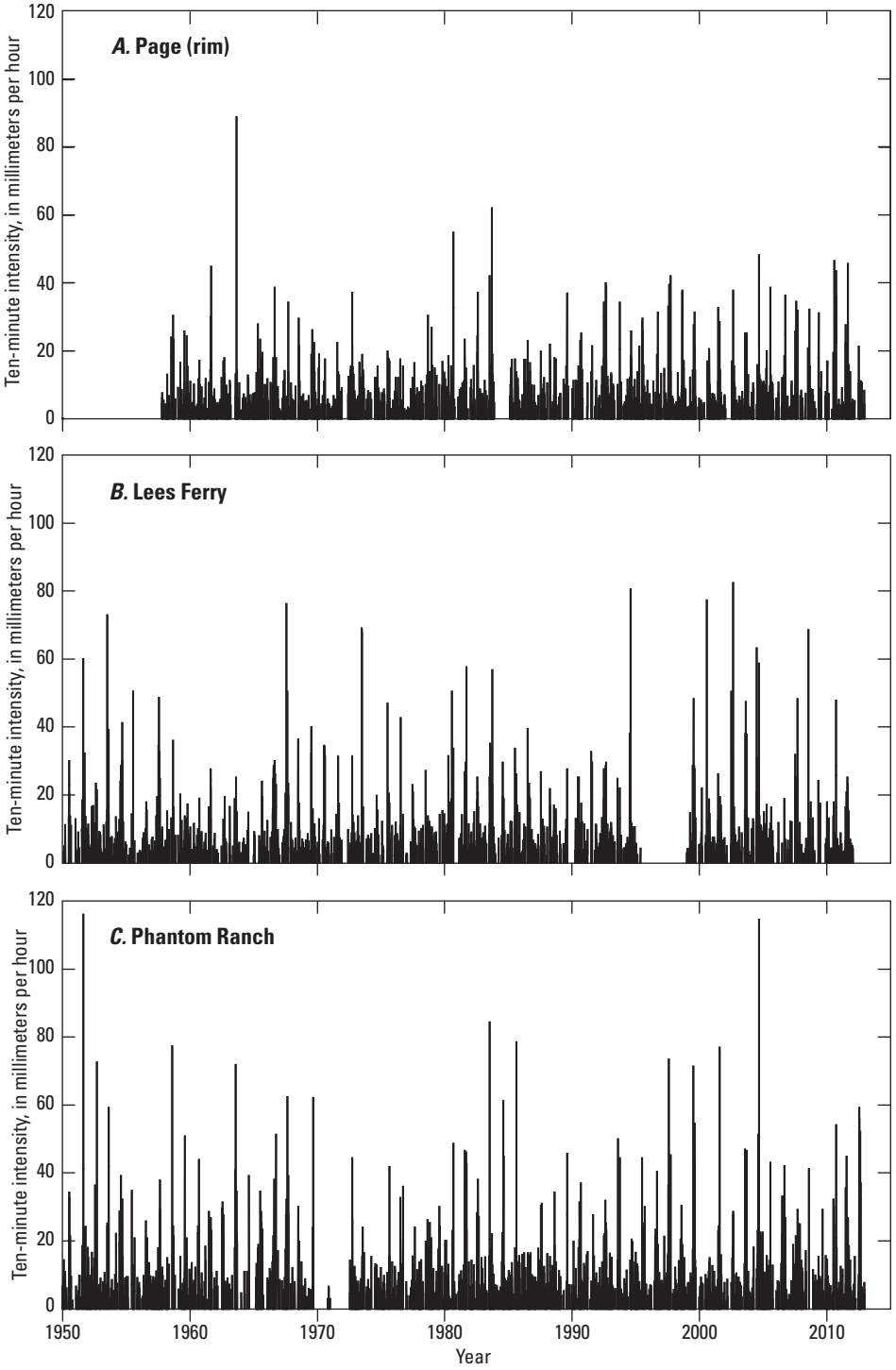

Figure 60. Estimated maximum daily 10-minute rainfall intensities (in millimeters per hour) measured by National Weather Service Cooperative Observer Program (COOP) weather stations at (*A*) Page (on the southeast rim above Glen Canyon), (*B*) Lees Ferry (boundary of Glen and Marble Canyons, RM 0) and (*C*) Phantom Ranch (within Grand Canyon). Daily maximum intensity estimates were based on seasonal equations (Caster and Sankey, 2016).

Canyon (Sections III, IV). In this discussion we focus on 4-minute maximum gust speeds rather than on 4-minute-averaged wind speeds because the former provide more information about aeolian sand-transport potential (4-minute average speed being low or near zero much of the time). The maximum 4-minute gust speed recorded in Marble–Grand Canyon was 16.2 m/s, at site AZ:B:10:0225, slightly lower than the maximum gust speed of 17.1 m/s recorded in Glen Canyon (fig. 61*A*). Mean and median 4-minute-maximum gust speeds in Glen Canyon were similar to those in Marble–Grand Canyon (1.9–2.1 m/s and 1.6–1.8 m/s, respectively; fig. 61*A*). The proportion of time when maximum 4-minute gusts exceeded the assumed sand-transport threshold of 2 m/s was also similar, being only 5 percent greater, on average, at the Marble–Grand Canyon stations compared to those at Glen Canyon or Lees Ferry (fig. 61*B*; station AZ:C:05:0031, in Marble Canyon, recorded substantially lower wind speeds than did any other station). The longest continuous measurement of maximum gusts >2 m/s was recorded in Grand Canyon (at site AZ:C:13:0345; Caster and others, 2014) and exceeded one full day (386 consecutive 4-minute records). The longest interval with wind gusts >2 m/s at all other stations (including Glen Canyon) ranged from 170 to 200 consecutive records. Wind gusts >5 m/s occurred 6.5 percent of the time in Marble–Grand Canyon and 5.4 percent of the time in Glen Canyon, on average (fig. 61*B*). Finally, wind gusts >8 m/s were uncommon, occurring less than 1 percent of the time at all stations (fig. 61*B*).

Based on the available data, we infer that Glen Canyon and Marble–Grand Canyon have similar wind conditions. Wind and aeolian sand transport are, however, highly variable and dynamic processes, such that detecting and quantifying spatial and temporal patterns is notoriously difficult, even with much greater measurement resolution than was available in this study (Bauer and others, 1996). Long-term wind records from within Glen Canyon do not exist, so it is not possible to assess whether the comparison of wind conditions in these regions over 2014–15 is representative of other years.

Thus, our climatologic analysis did not indicate that rainfall or wind conditions differ sufficiently to produce

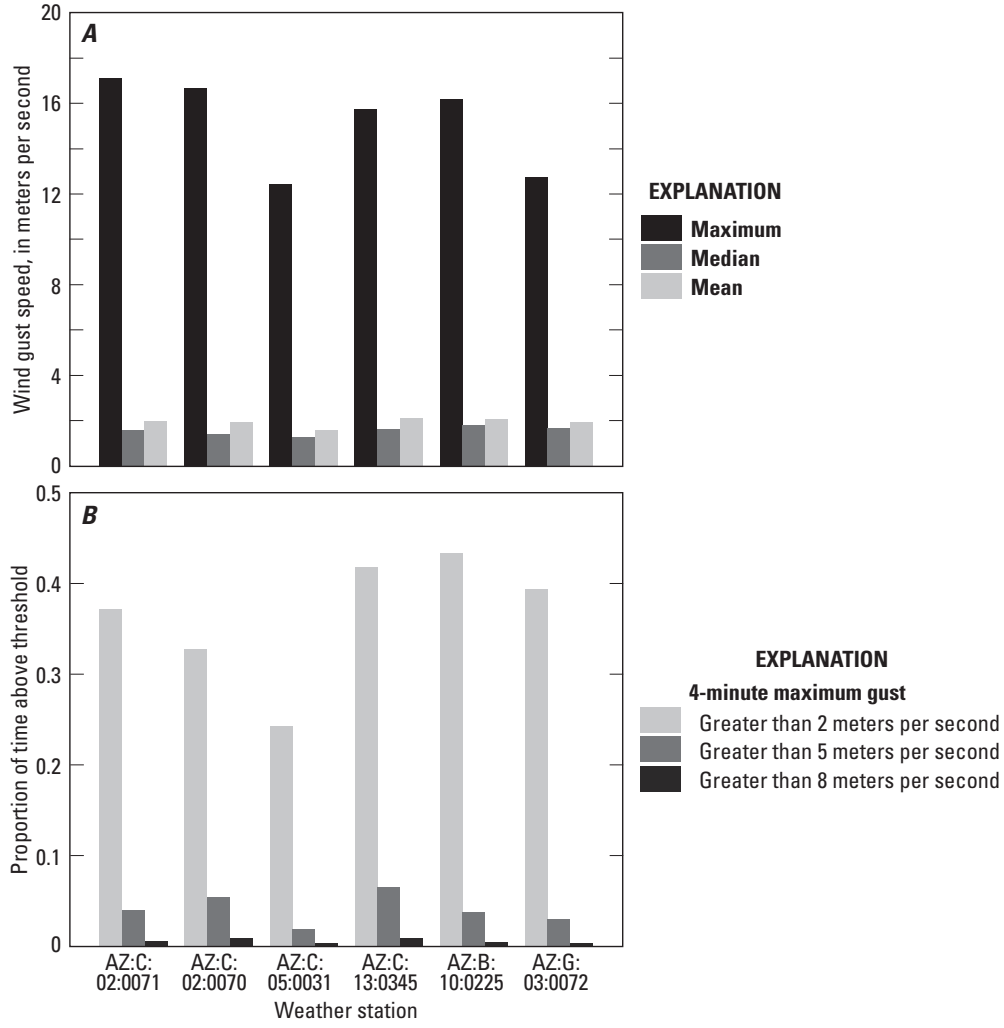

Figure 61. Summary statistics for wind-speed measurements at U.S. Geological Survey inner-canyon weather stations. (*A*) Maximum, mean, and median values, calculated from 92,355 concurrent 4-minute maximum-gust-speed records collected between February 13, 2014, and February 5, 2015. (*B*) Proportion of time that maximum gust speed was above the 2, 5, and 8 m/s thresholds for sand transport. See text for explanation of threshold choice.

consistently more erosive conditions in Glen Canyon compared to Marble–Grand Canyon. The available records indicate that conditions are typically drier, with fewer high-intensity storms, in Glen Canyon than in Marble–Grand Canyon. Wind conditions within Glen Canyon, including the frequency and duration of wind speeds with potential to transport sand, were not notably different from those in Marble–Grand Canyon during the assessment period. Therefore, we see no indication that climatic differences would have caused the greater prevalence of gully erosion and lack of aeolian sand activity in Glen Canyon. Rather, we infer that these differences in landscape processes and topographic evolution result from inherent geomorphic characteristics (the large terraces in Glen Canyon, and lack of eddy sand deposits) combined with especially pronounced effects of sediment starvation there in the postdam era.

Section V - Synthesis and Conclusions

Landscape evolution in the Colorado River corridor demonstrates not only the importance of connectivity among fluvial, aeolian, and hillslope processes, but also the relative roles of common geomorphic processes and extreme events in shaping landscapes—a balance that scientists have long sought to understand in various geomorphic contexts. Sedimentary terraces of the Colorado River corridor formed largely from episodic flood deposition over thousands of years, and were modified by wind and hillslope runoff (overland flow) between large, landscape-resetting floods. Fluvial, aeolian, and hillslope processes all occur with a range of magnitudes and frequencies; of those three, fluvial processes have been altered the most by dam operations. In the postdam river, hillslope runoff and wind action occur with presumably natural or near-natural magnitude and frequency, such that gullying and aeolian sand transport alter the landscape on seasonal to annual time scales. Major wind events move sand (in places with active, mobile sand surfaces) on seasonal or shorter time scales, and rainfall runoff erodes gullies commonly every 2–3 years at most sites. Thus, hillslope and aeolian processes modify the landscape much as they did in predam time, albeit with reduced sediment supply to the landscapes they affect. In contrast, the magnitude and frequency of river flows have changed profoundly as a function of dam operations. The loss of decadal- to centennial-scale sediment-rich floods, which provided a large-scale mechanism to anneal gullies and resupply upland dunes, together with the loss of low flows that exposed much fluvial sand area to wind, and substantial riparian-vegetation encroachment, have left aeolian and hillslope processes as disproportionately important factors modifying river-corridor landscapes and archeological sites.

Modern controlled floods (flows of around 1,200 m^3/s, lasting several days), which are relatively small and brief compared to even the annual predam spring flood, and much smaller than decadal-scale predam floods, cannot be expected to restore natural geomorphic evolution of river-corridor sedimentary deposits. Nevertheless, because controlled floods do form or enlarge some sandbars, controlled flooding does provide some modern aeolian sand supply to some upland areas. In our evaluation of how this modern sand supply affects archeological resources, we have shown that only a small minority of river-corridor archeological sites are ideally situated to receive aeolian sand supply from sandbars of recent controlled floods. Whereas three-fourths of the 358 river-corridor archeological sites we examined include Colorado River-derived sand as an integral component of their geomorphic context, only 32 sites—9 percent of the total number, or just under 12 percent of the sand-dependent sites—appear to have a high degree of connectivity between modern fluvial sandbars and a downwind aeolian sand landscape (type 1 sites in our classification system). In total, we identified 232 sand-dependent sites that we consider to be potentially influenced by dam operations, because they are downwind from river shorelines reached by flows of 1,270-m^3/s (site types 1–3). A site need not necessarily be type 1 to receive some aeolian sand supply from controlled-flood sandbars; for example, such connectivity has been documented previously for a type 2b site, where aeolian sand crossed a topographic barrier and deposited at an archeological site.

The number and proportion of type 1 archeological sites, which have the greatest potential to receive windblown sand from modern fluvial sand sources, decreased over each time step we evaluated (1973, 1984–85, 1996, and 2012–14), and now constitute one-third the number evident in 1973. Therefore, controlled floods have had a limited, and decreasing, influence on aeolian sand supply to archeological sites in the river corridor. We infer that the decrease in type 1 sites resulted from (1) a lack of sediment-rich flows large enough to both deposit sandbars at elevations above the controlled-flood stage and to remove riparian vegetation, (2) vegetation growth having covered formerly open sand sources and impeded sand entrainment and transport, and (3) fluvial erosion of some formerly open (as well as some vegetated) sand deposits.

Aeolian sand activity in the Colorado River corridor varies substantially as a function of reach morphology and dominant wind direction relative to the river-corridor orientation, factors that control accommodation space for river-derived sand and the modern aeolian sand supply to source-bordering dunes in the absence of large floods. The active aeolian sand ratio in the Upper Granite Gorge and Stevens-Conquistador Aisle reaches is 2–3 times greater than that in the Eminence–Little Colorado River and Furnace Flats reaches, and nearly an order of magnitude greater than in the Glen Canyon and Granite Park reaches. In places where the wind blows at an angle orthogonal to the river, source-bordering dunes and sand ramps generally have more active aeolian sand than in other reaches where the wind direction is nearly parallel to the river. These attributes, together with a negative correlation between aeolian sand activity and gully occurrence, imply substantial variation in net long-term gully-erosion risk for sediment deposits and associated archeological sites in different regions of the river corridor.

Gully erosion is less severe in active aeolian sand landscapes than in those that are inactive with respect to aeolian transport; gullies terminate more commonly in active sand. We infer that these characteristics largely result from aeolian

sand transport being an effective gully-annealing mechanism, and active aeolian sand being a poor retainer of gully-channel morphology. Aeolian infilling occurs in conjunction with backwasting of noncohesive sand in gully walls, which provides an additional mechanism leading to the obliteration of gully morphology in active aeolian areas. Seasonal- to annual-scale topographic-change detection, and limited examples of annealed gullies in the aerial photographic record, indicate that both gullying and infilling of gullies are not rare (though gully formation is much more common than annealing), but rather are common processes altering river-corridor landscapes.

The prevalence of inactive sand landscapes in Marble–Grand Canyons indicates that aeolian annealing is likely to occur over only spatially limited regions—currently 5–35 percent of the sand landscape area in Marble–Grand Canyon has active aeolian surfaces where gully annealing likely could occur (the proportion varies spatially, for reasons of geomorphology and wind direction). Thus, over most of the Colorado River corridor, including some of the archeologically richest regions, there is too little aeolian sand activity to anneal gullies effectively.

At archeological sites where landscape change has been measured at high resolution, sand loss by overland flow (gully erosion) and aeolian deflation generally exceeds deposition, such that erosional signals typically dominate landscape change over most monitoring intervals—even at type 1 sites with modern connectivity to new sand supply. The rate of landscape degradation in places having both active aeolian transport and gully erosion is a complex result of gully meandering, incision, and aeolian sand flux, processes with enough stochasticity, or randomness, to make site-specific predictions difficult.

The Glen Canyon reach of the river corridor appears especially vulnerable to gully erosion. Gully prevalence in the large terrace deposits of Glen Canyon is comparable to the most-intensively gullied parts of Grand Canyon (large, predam flood deposits of the Furnace Flats or Granite Park reaches). Glen Canyon also has proportionally less active aeolian sand area than in any of the five reaches we studied in Marble–Grand Canyon, indicating extremely low potential for aeolian sand to anneal gullies. Within the sample of archeological sites that we monitored in detail, and over the temporal change-detection intervals we used, erosional processes dominated over depositional processes to a greater degree at Glen Canyon sites than at Marble–Grand Canyon sites. A relative lack of depositional processes led to greater net erosion at the Glen Canyon sites compared to those in Marble–Grand Canyon. Having found no differences in weather patterns to suggest greater erosive forcing in Glen Canyon, we attribute the greater erosion observed there to a combination of (1) inherent geomorphic context, which includes extensive predam fluvial terraces, and precludes retention of eddy sandbars that could serve as aeolian sand sources; and (2) pronounced effects of postdam sediment-supply limitation (sand deficit and base-level lowering).

In this study, we sought to determine whether archeological sites in the Colorado River corridor through Glen, Marble, and Grand Canyons are eroding or changing faster or in a substantially different manner than they would if Glen Canyon Dam were operated differently than it has been. We conclude that most river-corridor archeological sites are subject to increased risk of net gully erosion under present dam operations. For the more than 260 archeological sites that have river-derived sand as an integral part of their geomorphic context, we infer elevated erosion risk owing to a combination of reduced sand supply (both fluvial and aeolian) through (1) the lower-than-natural flood magnitude, frequency, and sediment supply of the controlled-flooding protocol; (2) reduction of open, dry sand area available for wind redistribution under current normal (nonflood) dam operations, which do not include flows as low as natural seasonal low flows; and (3) impeded aeolian sand entrainment and transport owing to increased riparian vegetation growth in the absence of larger, more-frequent floods.

If dam operations were to increase the supply of sand available for windblown transport—for example, through larger floods, sediment augmentation, or increased fluvial sandbar exposure by low flows—and also decrease riparian vegetation, the prevalence of active aeolian sand landscapes likely would increase over time. We suggest that in such a situation, the prevalence of gully development through those landscapes and associated archeological sites would be less than will occur if management of flow, sediment, and riparian vegetation remains unchanged. Ultimately, the river-corridor landscape context of many cultural sites is altered fundamentally by the lack of large, sediment-rich floods (flows on the order of 5,000 m^3/s, with decadal-scale return intervals). Although structural considerations of Glen Canyon Dam preclude designing such large controlled floods, some combination of sediment-rich flows above 1,270 m^3/s, seasonal flows below 226 m^3/s, and riparian-vegetation removal likely would increase the preservation potential for sand-dependent archeological resources in the Colorado River corridor.

References Cited

Anderson, K.C., 2006, Geoarcheological investigations of 53 sites between Glen Canyon Dam and Paria Riffle: Navajo Nation Archaeology Department Report No. 05–229, submitted to Bureau of Reclamation, Upper Colorado Region, Salt Lake City, Utah, report on file at Bureau of Reclamation.

Anderson, K.C., and Neff, T., 2011, Geomorphic interpretation of Pueblo II to Early Pueblo III (A.D. 1050–1170) period settlement patterns along the Colorado River in Grand Canyon, Arizona: Catena, v. 85, p. 168–186.

Antevs, E., 1952, Arroyo-cutting and filling: Journal of Geology, v. 60, p. 375–385.

Ash, J.E., and Wasson, R.J., 1983, Vegetation and sand mobility in the Australian desert dunefield: Zeitschrift für Geomorphologie, supplement 45, p. 7–25.

Bagnold, R.A., 1941, The physics of blown sand and desert dunes (4th ed.): London, Chapman and Hall, 265 p.

Balsom, J.R., Ellis, J.G., Horn, A., and Leap, L.M., 2005, Using cultural resources as part of the plan—Grand Canyon management and implications for resource preservation, *in* van Riper, C., III, and Mattson, D.J., eds., The Colorado Plateau II—biophysical, socioeconomic, and cultural research: Tucson, University of Arizona Press, p. 367–377.

Baudat, M.R., and Breed, C.S., 1999, Meteorological influences on eolian activity at the Yuma Desert Geomet Site, Arizona, 1988–1993, *in* Breed, C.S., and Reheis, M.C., eds., Desert winds—monitoring wind-related surface processes in Arizona, New Mexico, and California: U.S. Geological Survey Professional Paper 1598, p. 87–104.

Bauer, B.O., Davidson-Arnott, R.G.D., Nordstrom, K.F., Ollerhead, J., and Jackson, N.L., 1996, Indeterminacy in aeolian sediment transport across beaches: Journal of Coastal Research, v. 12, p. 641–653.

Belnap, J., Kaltenecker, J.H., Rosentreter, R., Williams, J., Leonard, S., and Eldridge, D., 2001, Biological soil crusts—ecology and management: U.S. Department of the Interior, Bureau of Land Management Technical Reference 1730-2, 110 p.

Belnap, J., and Lange, O.L., eds., 2003, Biological soil crusts and wind erosion, *in* Belnap, J., and Lange, O.L., eds., Biological soil crusts—structure, function, and management (2d edition): Ecological Studies series, v. 150, Berlin, Springer-Verlag, p. 339–347.

Belnap, J., Munson, S.M., and Field, J.P., 2011, Aeolian and fluvial processes in dryland regions—the need for integrated studies: Ecohydrology, v. 4, p. 615–622.

Beus, S.S., Carothers, S.W., and Avery, C.C., 1985, Topographic changes in fluvial terrace deposits used as campsite beaches along the Colorado River in Grand Canyon: Arizona-Nevada Academy of Sciences Journal, v. 20, p. 111–120.

Boyer, D.E., and Webb, R.H., 2007, Damming Grand Canyon—the 1923 USGS Colorado River expedition: Logan, Utah State University Press, 289 p.

Bryan, K., 1925, Date of channel trenching (arroyo cutting) in the arid southwest: Science, v. 62, p. 338–344.

Buckley, R., 1987, The effect of sparse vegetation on the transport of dune sand by wind: Nature, v. 325, p. 426–428.

Bullard, J.E., and Livingstone, I., 2002, Interactions between aeolian and fluvial systems in dryland environments: Area, v. 34, p. 8–16.

Bullard, J.E., and McTainsh, G.H., 2003, Aeolian-fluvial interactions in dryland environments—examples, concepts, and Australia case study: Progress in Physical Geography, v. 27, p. 471–501.

Burchett, T.W., 1996, Glen Canyon environmental studies fiscal year 1996 trip report: Glen Canyon National Recreation Area, National Park Service, Page, Ariz., 43 p., accessed January 17, 2014, at http://www.riversimulator.org/Resources/GCMRC/GCES/Cultural/Burchett1996.pdf.

Burke, K.J., Fairley, H.C., Hereford, R., and Thompson, K.S., 2003, Holocene terraces, sand dunes, and debris fans along the Colorado River in Grand Canyon, *in* Beus, S.S., and Morales, M., eds., Grand Canyon Geology (2d edition): New York, Oxford University Press, p. 352–370.

Bursztyn, N., Pederson, J.L., Tressler, C., Mackley, R.D., and Mitchell, K.J., 2015, Rock strength along a fluvial transect of the Colorado Plateau—quantifying a fundamental control on geomorphology: Earth and Planetary Science Letters, v. 429, p. 90–100.

Caster, J., Dealy, T., Andrews, T., Fairley, H., Draut, A., and Sankey, J., 2014, Meteorological data for selected sites along the Colorado River corridor, Arizona, 2011–13: U.S. Geological Survey Open-File Report 2014–1247, 56 p., http://dx.doi.org/10.3133/ofr20141247.

Caster, J., and Sankey, J.B., 2016, Variability in rainfall at monitoring stations and derivation of a long-term rainfall intensity record in the Grand Canyon region, Arizona, USA: U.S. Geological Survey Scientific Investigations Report 2016–5012, 38 p., http://dx.doi.org/10.3133/sir20165012.

Chamizo, S., Cantón, Y., Lázaro, R., Solé-Benet, A., and Domingo, F., 2012, Crust composition and disturbance drive infiltration through biological soil crusts in semiarid ecosystems: Ecosystems, v. 15, p. 148–161.

Cheng, H., He, J., Zou, X., Li, J., Liu, C., Liu, B., Zhang, C., Wu, Y., and Kang, L., 2015, Characteristics of particle size for creeping and saltating sand grains in aeolian transport: Sedimentology, v. 62, p. 1497–1511.

Chien, N., 1985, Changes in river regime after the construction of upstream reservoirs: Earth Surface Processes and Landforms, v. 10, p. 143–159.

Collier, M., Webb, R.H., and Schmidt, J.C., 1996, Dams and rivers—a primer on the downstream effects of dams: U.S. Geological Survey Circular 1126, 94 p.

Collins, B.D., Bedford, D.R., Corbett, S.C., Cronkite-Ratcliff, C., and Fairley, H.C., 2016, Relations between rainfall–runoff-induced erosion and aeolian deposition at archaeological sites in a semi-arid dam-controlled river corridor: Earth Surface Processes and Landforms, doi:10.1002/esp.3874.

Collins, B.D., Brown, K.M., and Fairley, H.C., 2008, Evaluation of terrestrial LIDAR for monitoring geomorphic change at archeological sites in Grand Canyon National Park, Arizona: U.S. Geological Survey Open-File Report 2008–1384, 60 p., http://pubs.usgs.gov/of/2008/1384/.

Collins, B.D., Corbett, S.C., Fairley, H.C., Minasian, D., Kayen, R., Dealy, T.P., and Bedford, D.R., 2012, Topographic change detection at select archeological sites in Grand Canyon National Park, Arizona, 2007–2010: U.S. Geological Survey Scientific Investigations Report 2012–5133, 77 p., http://pubs.usgs/gov/sir/2012/5133/.

Collins, B.D., Corbett, S.C., Sankey, J.B., and Fairley, H.C., 2014, High-resolution topography and geomorphology of select archeological sites in Glen Canyon National Recreation Area, Arizona: U.S. Geological Survey Scientific Investigations Report 2014–5126, 31 p., http://dx.doi.org/10.3133/sir20145126.

Collins, B.D., Minasian, D., and Kayen, R., 2009, Topographic change detection at select archeological sites in Grand Canyon National Park, Arizona, 2006-2007: U.S. Geological Survey Scientific Investigations Report 2009–5116, 68 p., http://pubs.usgs.gov/sir/2009/5116/.

Davis, P.A., 2012, Airborne digital-image data for monitoring the Colorado River corridor below Glen Canyon Dam, Arizona, 2009—image-mosaic production and comparison with 2002 and 2005 image mosaics: U.S. Geological Survey Open-File Report 2012–1139, 82 p., http://pubs.usgs.gov/of/2012/1139/.

Dealy, T., East, A.E., and Fairley, H.C., 2014, 2010 weather and aeolian sand-transport data from the Colorado River corridor, Grand Canyon, Arizona: U.S. Geological Survey Open-File Report 2014–1135, 90 p., http://dx.doi.org/10.3133/ofr20141135.

D'Odorico, P., Bhattachan, A., Davis, K.F., Ravi, S., and Runyan, C.W., 2013, Global desertification—drivers and feedbacks: Advances in Water Resources, v. 51, p. 326–344.

Dong, Z., Lu, J., Man, D., Lv, P., Qian, G., Zhang, Z., and Luo, W., 2011, Equations for the near-surface mass flux density profile of wind-blown sediments: Earth Surface Processes and Landforms, v. 36, p. 1292–1299.

Draut, A., 2012, Effects of river regulation on aeolian landscapes, Colorado River, southwestern USA: Journal of Geophysical Research—Earth Surface, v. 117, F02022, doi:10.1029/2011JF002329.

Draut, A.E., Andrews, T., Fairley, H.C., and Brown, C.R., 2009a, 2007 weather and aeolian sand-transport data from the Colorado River corridor, Grand Canyon, Arizona: U.S. Geological Survey Open-File Report 2009–1098, 110 p., http://pubs.usgs.gov/of/2009/1098/.

Draut, A.E., Hazel, J.E., Jr., Fairley, H.C., and Brown, C.R., 2010, Aeolian reworking of sandbars from the March 2008 Glen Canyon Dam high flow experiment in Grand Canyon, *in* Melis, T.S., Hamill, J.F., Coggins, L.G., Jr., Grams, P.E., Kennedy, T.A., Kubly, D.M., and Ralston, B.E., (eds.), Proceedings of the Colorado River Basin Science and Resource Management Symposium, November 18–20, 2008, Scottsdale, Ariz.: U.S. Geological Survey Scientific Investigations Report 2010–5135, p. 325–331.

Draut, A.E., and Rubin, D.M., 2005, Measurements of wind, aeolian sand transport, and precipitation in the Colorado River corridor, Grand Canyon, Arizona—November 2003 to December 2004: U.S. Geological Survey Open-File Report 2005–1309, 70 p., http://pubs.usgs.gov/of/2005/1309/.

Draut, A.E., and Rubin, D.M., 2006, Measurements of wind, aeolian sand transport, and precipitation in the Colorado River corridor, Grand Canyon, Arizona—January 2005 to January 2006: U.S. Geological Survey Open-File Report 2006–1188, 88 p., http://pubs.usgs.gov/of/2006/1188/.

Draut, A.E., and Rubin, D.M., 2008, The role of eolian sediment in the preservation of archeologic sites along the Colorado River corridor in Grand Canyon National Park, Arizona: U.S. Geological Survey Professional Paper 1756, http://pubs.usgs.gov/pp/1756/.

Draut, A.E., and Rubin, D.M., 2013, Assessing grain-size correspondence between flow and deposits of controlled floods in the Colorado River, USA: Journal of Sedimentary Research, v. 83, p. 962–973.

Draut, A.E., Rubin, D.M., Dierker, J.L., Fairley, H.C., Griffiths, R.E., Hazel, J.E., Jr., Hunter, R.E., Kohl, K., Leap, L.M., Nials, F.L., Topping, D.J., and Yeatts, M., 2005, Sedimentology and stratigraphy of the Palisades, Lower Comanche, and Arroyo Grande areas of the Colorado River corridor, Grand Canyon, Arizona: U.S. Geological Survey Scientific Investigations Report 2005–5072, 68 p., http://pubs.usgs.gov/sir/2005/5072/.

Draut, A.E., Rubin, D.M., Dierker, J.L., Fairley, H.C., Griffiths, R.E., Hazel, J.E., Jr., Hunter, R.E., Kohl, K., Leap, L.M., Nials, F.L., Topping, D.J., and Yeatts, M., 2008, Application of sedimentary-structure interpretation to geoarcheological investigations in the Colorado River corridor, Grand Canyon, Arizona: Geomorphology, v. 101, p. 497–509.

Draut, A.E., Sondossi, H.A., Hazel, J.E., Jr., Fairley, H.C., Andrews, T., Brown, C.R., and Vanaman, K.M., 2009b, 2008 weather and aeolian sand-transport data from the Colorado River corridor, Grand Canyon, Arizona: U.S. Geological Survey Open-File Report 2009–1190, 98 p., http://pubs.usgs.gov/of/2009/1190/.

Fairley, H.C., 2003, Changing river; time, culture, and the transformation of landscape in the Grand Canyon—a regional research design for the study of cultural resources along the Colorado River in lower Glen Canyon and Grand Canyon National Park, Arizona: Flagstaff, Ariz., U.S. Geological Survey, Grand Canyon Monitoring and Research Center, Technical Series 79, 179 p.

Fairley, H.C., 2005, Cultural resources in the Colorado River corridor, *in* Gloss, S.P., Lovich, J.E., and Melis, T.S., eds., The state of the Colorado River ecosystem in Grand Canyon: U.S. Geological Survey Circular 1282, p. 177–192.

Fairley, H.C., Bungart, P.W., Coder, C.M., Huffman, J., Samples, T.L., and Balsom, J.R., 1994, The Grand Canyon river corridor survey project—archeological survey along the Colorado River between Glen Canyon Dam and Separation Canyon: Flagstaff, Ariz., Grand Canyon National Park, prepared in cooperation with the Bureau of Reclamation, Glen Canyon Environmental Studies, cooperative agreement no. 9AA–40–07920, 276 p.

Fairley, H.C., and Hereford, R., 2002, Geoarchaeology of the Colorado River in Grand Canyon, *in* Phillps, D.A., Jr., and Ware, J.A., eds., Culture and environment in the American Southwest—essays in honor of Robert C. Euler: Phoenix, Ariz., SWCA Environmental Consultants, Anthropological Research Paper no. 8, p. 39–48.

Faulkner, H., Alexander, R., Teeuw, R., and Zukowskyj, P., 2004, Variations in soil dispersivity across a gully head displaying shallow sub-surface pipes, and the role of shallow pipes in rill initiation: Earth Surface Processes and Landforms, v. 29, p. 1143–1160.

Field, J.P., Breshears, D.D., and Whicker, J.J., 2009, Toward a more holistic perspective of soil erosion—why aeolian research needs to explicitly consider fluvial processes and interactions: Aeolian Research, v. 1, p. 9–17.

Ghimire, S.K., Higaki, D., and Bhattarai, T.P., 2006, Gully erosion in the Siwalik Hills, Nepal—estimation of sediment production from active ephemeral gullies: Earth Surface Processes and Landforms, v. 31, p. 155–165.

Gibling, M.R., Sinha, R., Roy, N.G., Tandon, S.K., and Jain, M., 2008, Quaternary fluvial and eolian deposits on the Belan river, India—paleoclimatic setting of Paleolithic to Neolithic archeological sites over the past 85,000 years: Quaternary Science Reviews, v. 27, p. 391–410.

Gilbert, G.K., 1899, Sand dunes, Biggs, Oregon: U.S. Geological Survey Photographic Library, ID ggk00503–515, http://libraryphoto.cr.usgs.gov/.

Goossens, D., 2004, Effect of soil crusting on the emission and transport of wind-eroded sediment—field measurements on loamy sandy soil: Geomorphology, v. 58, p. 145–160.

Grams, P.E., Schmidt, J.C., and Topping, D.J., 2007, The rate and pattern of bed incision and bank adjustment on the Colorado River in Glen Canyon downstream from Glen Canyon Dam, 1956–2000: Geological Society of America Bulletin, v. 119, p. 556–575.

Grams, P.E., Schmidt, J.C., Wright, S.A., Topping, D.J., Melis, T.S., and Rubin, D.M., 2015, Building sandbars in the Grand Canyon: Eos, Transactions, American Geophysical Union, v. 96, doi:10.1029/2015EO030349.

Grams, P.E., Topping, D.J., Schmidt, J.C., Hazel, J.E., Jr., and Kaplinski, M., 2013, Linking morphodynamic response with sediment mass balance on the Colorado River in Marble Canyon— issues of scale, geomorphic setting, and sampling design: Journal of Geophysical Research—Earth Surface, v. 118, p. 361–381.

Greenbaum, N., Harden, T.M., Baker, V.R., Weisheit, J., Cline, M.L., Porat, N., Halevi, R., and Dohrenwend, J., 2014, A 2000 year natural record of magnitudes and frequencies for the largest Upper Colorado River floods near Moab, Utah: Water Resources Research, v. 50, no. 6, p. 5249–5269, doi:10.1002/2013WR014835.

Greenlee, D.D., 1987, Raster and vector processing for scanned linework: Photogrammetric Engineering and Remote Sensing, v. 53, p. 1383–1387.

Griffiths, P.G., Webb, R.H., and Melis, T.S., 2004, Frequency and initiation of debris flows in Grand Canyon, Arizona: Journal of Geophysical Research, v. 109, F04002, doi:10.1029/2003JF000077.

Han, G., Zhang, G., and Dong, Y., 2007, A model for the active origin and development of source-bordering dunefields on a semiarid fluvial plan—a case study from the Xiliaohe Plain, Northeast China: Geomorphology, v. 86, p. 512–524.

Harper, K.T., and Belnap, J., 2001, The influence of biological soil crusts on mineral uptake by associated vascular plants: Journal of Arid Environments, v. 47, p. 347–357.

Harvey, J.E., and Pederson, J.L., 2011, Reconciling arroyo cycle and paleoflood approaches to late Holocene alluvial records in dryland streams: Quaternary Science Reviews, v. 30, p. 855–866.

Hazel, J.E., Jr., Grams, P.E., Schmidt, J.C., and Kaplinski, M., 2010, Sandbar response in Marble and Grand Canyons, Arizona, following the 2008 high-flow experiment on the Colorado River: U.S. Geological Survey Scientific Investigations Report 2010–5015, 52 p., http://pubs.usgs.gov/sir/2010/5015/.

Hazel, J.E., Jr., Kaplinski, M., Parnell, R.A., and Fairley, H.C., 2008, Aggradation and degradation of the Palisades gully network, 1996 to 2005, with emphasis on the November 2004 high-flow experiment, Grand Canyon National Park, Arizona: U.S. Geological Survey Open-File Report 2008–1264, 14 p., http://pubs.usgs.gov/of/2008/1264/.

Hazel, J.E., Jr., Topping, D.J., Schmidt, J.C., and Kaplinski, M., 2006, Influence of a dam on fine-sediment storage in a canyon river: Journal of Geophysical Research, v. 111, F01025, doi: 10.1029/2004JF000193.

Hereford, R., 1996, Surficial geology and geomorphology of the Palisades Creek area, Grand Canyon National Park, Arizona: U.S. Geological Survey Miscellaneous Investigations Series Map I-2449, scale 1:2,000.

Hereford, R., Bennett, G.E., and Fairley, H.C., 2014, Precipitation variability of the Grand Canyon region, 1893 through 2009, and its implications for studying effects of gullying of Holocene terraces and associated archeological sites in Grand Canyon, Arizona: U.S. Geological Survey Open-File Report 2014–1006, 23 p., http://dx.doi.org/10.3133/ofr20141006.

Hereford, R., Burke, K.J., and Thompson, K.S., 1998, Quaternary geology and geomorphology of the Nankoweap Rapids area, Marble Canyon, Arizona: U.S. Geological Survey Geologic Investigations Series Map I-2608, scale 1:4,600.

Hereford, R., Burke, K.J., and Thompson, K.S., 2000a, Quaternary geology and geomorphology of the Granite Park area, Grand Canyon, Arizona: U.S. Geological Survey Geologic Investigations Series Map I-2662, scale 1:2,000.

Hereford, R., Burke, K.J., and Thompson, K.S., 2000b, Map showing Quaternary geology and geomorphology of the Lees Ferry area, Glen Canyon, Arizona: U.S. Geological Survey Geologic Investigations Series Map I-2663, scale 2,000.

Hereford, R., Fairley, H.C., Thompson, K.S., and Balsom, J.R., 1993, Surficial geology, geomorphology, and erosion of archeologic sites along the Colorado River, eastern Grand Canyon, Grand Canyon National Park, Arizona: U.S. Geological Survey Open-File Report 93–517, 46 p.

Hereford, R., Thompson, K.S., Burke, K.J., and Fairley, H.C., 1996, Tributary debris fans and the late Holocene alluvial chronology of the Colorado River, eastern Grand Canyon, Arizona: Geological Society of America Bulletin, v. 108, p. 3–19.

Holliday, V.T., Hoffecker, J.F., Goldberg, P., Macphail, R.I., Forman, S.L., Anikovich, M., and Sinitsyn, A., 2007, Geoarchaeology of the Kostenki–Borshchevo sites, Don River Valley, Russia: Geoarchaeology, v. 22, p. 181–228.

Howard, A., and Dolan, R., 1981, Geomorphology of the Colorado River in the Grand Canyon: Journal of Geology, v. 89, p. 269–298.

Jenson, S.K., and Domingue, J.O., 1988, Extracting topographic structure from digital elevation data for geographic information system analysis: Photogrammetric Engineering and Remote Sensing, v. 54, p. 1593–1600.

Johnson, R.R., 1991, Historic changes in vegetation along the Colorado River in Grand Canyon, *in* Colorado River Ecology and Dam Management—Proceedings of a Symposium, May 24–25, 1990, Santa Fe, New Mexico: Washington, D.C., National Academy Press, p. 178–206.

Kaplinski, M., Hazel, J.E., Jr., Grams, P.E., Davis, P.A., 2014, Monitoring fine-sediment volume in the Colorado River ecosystem, Arizona—construction and analysis of digital elevation models: U.S. Geological Survey Open-File Report 2014–1052, 29 p., http://dx.doi.org/10.3133/ofr20141052.

Kearsley, L.H., Schmidt, J.C., and Warren, K.D., 1994, Effects of Glen Canyon Dam on Colorado River sand deposits used as campsites in Grand Canyon National Park, USA: Regulated Rivers Research and Management, v. 9, p. 137–149.

Kocurek, G., 1998, Aeolian system response to external forcing factors—a sequence stratigraphic view of the Saharan region, *in* Alsharhan, A.S., Glennie, K.W., Whittle, G.L., and St.C. Kendall, C.G., eds., Quaternary deserts and climatic change: Rotterdam, Balkema, p. 327–349.

Lancaster, N., 1994, Controls on aeolian activity—some new perspectives from the Kelso Dunes, Mojave Desert, California: Journal of Arid Environments, v. 27, p. 113–125.

Lancaster, N., 1995, Geomorphology of desert dunes: London, Routledge, 290 p.

Le Roux, J.J., and Sumner, P.D., 2012, Factors controlling gully development—comparing continuous and discontinuous gullies: Land Degredation and Development, v. 23, p. 440–449.

Leschin, M.F., and Schmidt, J.C., 1995, Description of map units to accompany maps showing surficial geology and geomorphology of the Point Hansbrough and Little Colorado River confluence reaches of the Colorado River, Grand Canyon National Park, Arizona: Flagstaff, Ariz., Bureau of Reclamation Glen Canyon Environmental Studies Report, 6 p.

Leys, J.F., and Eldridge, D.J., 1998, Influence of cryptogamic crust disturbance to wind erosion on sand and loam rangeland soils: Earth Surface Processes and Landforms, v. 23, p. 963–974.

Liu, L., Yang, Y., Shi, P., Zhang, G., and Qu, Z., 2015, The role of maximum wind speed in sand-transporting events: Geomorphology, v. 238, p. 177–186.

Loope, D.B., Swinehart, J.B., and Mason, J.P., 1995, Dune-dammed paleovalleys of the Nebraska Sand Hills—intrinsic versus climatic controls on the accumulation of lake and marsh sediments: Geological Society of America Bulletin, v. 107, p. 396–406.

Lucchitta, I., 1991, Quaternary geology, geomorphology, and erosional processes, eastern Grand Canyon, Arizona: U.S. Geological Survey administrative report, submitted to Bureau of Reclamation, Upper Colorado Region, Salt Lake City, Utah, report on file at Bureau of Reclamation.

Lucchitta, I., and Leopold, L.B., 1999, Floods and sandbars in the Grand Canyon: GSA Today, Geological Society of America, v. 9. no. 4, p. 1–7.

MacGregor, A.N., and Johnson, D.E., 1971, Capacity of desert algal crusts to fix atmospheric nitrogen: Soil Science Society of America Proceedings, v. 35, p. 843–844.

Magirl, C.S., Breedlove, M.J., Webb, R.H., and Griffiths, P.G., 2008, Modeling water-surface elevations and virtual shorelines for the Colorado River in Grand Canyon, Arizona: U.S. Geological Survey Scientific Investigations Report 2008–5075, 40 p., http://pubs.usgs.gov/sir/2008/5075/.

Magirl, C.S., Webb, R.H., and Griffiths, P.G., 2005, Long-term change in the water-surface profile of the Colorado River in Grand Canyon, Arizona: Water Resources Research, v. 41, W05021, doi:10.1029/2003WR002519.

Martínez, G., and Martínez, G.A., 2011, Late Holocene environmental dynamics in fluvial and aeolian depositional settings—archeological record variability at the lower basin of the Colorado river (Argentina): Quaternary International, v. 245, p. 89–102.

Mazaeva, O., Kaczmarek, H., Khak, V.A., and Kozyreva, E.A., 2011, The short-term changes of gully erosion forms in the context of the water level fluctuations in the Bratsk reservoir (Russia): Landform Analysis, v. 17, p. 117–123.

McIntosh, P.D., Kiernan, K., and Price, D.M., 2004, An aeolian sediment pulse at c. 28 kyr BP in southern Tasmania: Journal of the Royal Society of New Zealand, v. 34, p. 369–379.

McKee, E.D., 1938, Original structures in Colorado River flood deposits of Grand Canyon: Journal of Sedimentary Petrology, v. 8, p. 77–83.

Melis, T.S., ed., 2011, Effects of three high-flow experiments on the Colorado River ecosystem downstream from Glen Canyon Dam, Arizona: U.S. Geological Survey Circular 1366, 147 p., http://pubs.usgs.gov/circ/1366/.

Melis, T.S., Webb, R.H., Griffiths, P.G., and Wise, T.J., 1994, Magnitude and frequency data for historic debris flows in Grand Canyon National Park and vicinity, Arizona: U.S. Geological Survey Water Resources Investigations Report 94-4214, 285 p.

Melis, T.S., Webb, R.H., Griffiths, P.G., and Wise, T.J., 1995, Magnitude and frequency data for historic debris flows in Grand Canyon National Park and vicinity, Arizona: U.S. Geological Survey Water Resources Investigations Report 94-4214, 285 p.

Museum of Northern Arizona, 2012, Grand archaeology—excavation and discovery along the Colorado River: Plateau, v. 7, no. 1, 56 p.

National Oceanic and Atmospheric Administration [2014], National Weather Service, archive of the National Climate Data Center for Cooperate Observer Stations 26471, 24849, and 26180: National Oceanic and Atmospheric Administration Web page, accessed May 5, 2015, at https://www.ncdc.noaa.gov/cdo-web/.

Neal, L.A., Gilpin, D., Jonas, L., and Ballagh, J.H., 2000, Cultural resources data synthesis within the Colorado River corridor, Grand Canyon National Park and Glen Canyon National Recreation Area, Arizona: SWCA, Inc., Cultural Resources Report 98-85, 198 p. plus appendices.

Neff, L.C., and Wilson, M.A., 2002, Archeological Investigations at Ferry Swale Bench—Glen Canyon National Recreation Area, Arizona: Western Archeological and Conservation Center (tDAR ID: 4342), Publications in Anthropology, v. 81, doi:10.6067/XCV8513WZJ.

Neff, T., and Anderson, K., 2012, Layers of time—Axehandle Alcove chronostratigraphy, *in* Grand Archaeology—Excavation and discovery along the Colorado River: Plateau, Museum of Northern Arizona, Flagstaff, Ariz., v. 7, no. 1, p. 44–45.

Nepf, H.M., 1999, Drag, turbulence, and diffusion in flow through emergent vegetation: Water Resources Research, v. 35, p. 479–489.

Nickling, W.G., and McKenna Neuman, C., 2009, Aeolian sediment transport, *in* Parsons, A.J., and Abrahams, A.D., eds., Geomorphology of desert environments (2d ed.): Dordrecht, Netherlands, Springer, p. 517–555.

O'Brien, G., and Pederson, J., 2009a, Geomorphic attributes of 232 cultural sites along the Colorado River in Grand Canyon National Park, Arizona: Final report, Department of Geology, Utah State University, Logan, Utah, to U.S. Geological Survey, Grand Canyon Monitoring and Research Center, Flagstaff, Ariz., under cooperative agreement 04HQAG0122, sub-agreement 04122HS010, 195 p.

O'Brien, G., and Pederson, J., 2009b, Gully erosion processes and parameters and six cultural sites along the Colorado River in Grand Canyon National Park, Arizona: Final report, cooperative agreement 04HQAG0122 and subagreement 04122HS010, Utah State University and U.S. Geological Survey, Grand Canyon Monitoring and Research Center, 129 p.

O'Connor, J.E., Ely, L.L., Wohl, E.E., Stevens, L.E., Melis, T.S., Kale, V.S., and Baker, V.R., 1994, A 4500-year record of large floods on the Colorado River in the Grand Canyon, Arizona: Journal of Geology, v. 102, p. 1–9.

Okin, G.S., Gillette, D.A., and Herrick, J.E., 2006, Multi-scale controls on and consequences of aeolian processes in landscape change in arid and semi-arid environments: Journal of Arid Environments, v. 65, p. 253–275.

Patton, P.C., and Schumm, S.A., 1975, Gully erosion, northwestern Colorado—a threshold phenomenon: Geology, v. 3, p. 88–90.

Pederson, J.L., 2012, A review of the geomorphology of eastern Grand Canyon, *in* Timmons, J.M., and Karlstrom, K.E., eds., Grand Canyon geology—two billion years of Earth's history: Geological Society of America Special Paper 489, p. 119–129.

Pederson, J.L., and O'Brien, G.R., 2014, Patterns in the landscape and erosion of cultural sites along the Colorado River corridor in Grand Canyon, USA: Geoarchaeology, v. 29, p. 431–447.

Pederson, J.L., O'Brien, G.R., Neff, T., and Spurr, K., 2011, Grand Canyon geoarchaeology project—report on data recovery at nine cultural sites in Grand Canyon and Lower Glen Canyon, 2008–2010: Utah State University report submitted to Bureau of Reclamation, Upper Colorado Region, Salt Lake City, Utah, report on file at Bureau of Reclamation.

Pederson, J.L., Petersen, P.A., and Dierker, J.L., 2006, Gullying and erosion control at archeological sites in Grand Canyon, Arizona: Earth Surface Processes and Landforms, v. 31, p. 507–525.

Pederson, J.L., Petersen, P.A., Macfarlane, W.W., Gonzales, M.F., and Kohl, K., 2003, Mitigation, monitoring, and geomorphology related to gully erosion of cultural sites in Grand Canyon: Utah State University report submitted to USGS Grand Canyon Monitoring and Research Center, 243 p., http://www.gcmrc.gov/library/reports/cultural/Archaeology/Pederson2003.pdf.

Ralston, B.E., Sarr, D., Sankey, J.B., Grams, P.E., Yackulic, C.B., Kennedy, T.A., Muehlbauer, J., Merritt, D.M., Shaforth, P., Hazel, J.E., Plamquist, E., Cagney, L., Chaudry, T., Perkins, D.W., and Spence, J., 2014, Project II—Riparian vegetation monitoring and analysis of riparian vegetation, landform change, and aquatic-terrestrial linkages to faunal communities, *in* Glen Canyon Dam adaptive management program triennial budget and work plan, fiscal years 2015–2017: Prepared by Bureau of Reclamation Upper Colorado Regional Office and U.S. Geological Survey Grand Canyon Monitoring and Research Center, 533 p., at http://www.usbr.gov/uc/rm/amp/twg/mtgs/14jun24/TWP_rev_14aug01.pdf.

Raupach, M.R., Gillette, D.A., and Leys, J.F., 1993, The effect of roughness elements on wind erosion threshold: Journal of Geophysical Research, v. 98, D2, p. 3023–3029.

Rodríguez-Caballeroa, E., Cantón, Y., Chamizo, S., Afana, A., and Solé-Benet, A., 2012, Effects of biological soil crusts on surface roughness and implications for runoff and erosion: Geomorphology, v. 145–146, p. 81–89.

Roskin, J., Katra, I., Agha, N., Goring-Morris, A.N., Porat, N., and Barzilai, O., 2014, Rapid anthropogenic response to short-term aeolian-fluvial palaeoenvironmental changes during the Late Pleistocene–Holocene transition in the northern Negev Desert, Israel: Quaternary Science Reviews, v. 99, p. 176–192.

Rubin, D.M., Topping, D.J., Schmidt, J.C., Hazel, J., Kaplinski, M., and Melis, T.S., 2002, Recent sediment studies refute Glen Canyon Dam hypothesis: Eos, Transactions, American Geophysical Union, v. 83, p. 273, 277–278.

Sankey, J.B., and Draut, A., 2014, Gully annealing by aeolian sediment—Field and remote-sensing investigation of aeolian-hillslope-fluvial interactions, Colorado River corridor, Arizona, USA: Geomorphology, v. 220, p. 68–80, doi: 10.1016/j.geomorph.2014.05.028.

Sankey, J.B., Ralston, B.E., Grams, P.E., Schmidt, J.C., and Cagney, L.E., 2015, Riparian vegetation, Colorado River, and climate—five decades of spatiotemporal dynamics in the Grand Canyon with river regulation: Journal of Geophysical Research–Biogeosciences, v. 120, p. 1532–1547.

Schmidt, J.C., 1990, Recirculating flow and sedimentation in the Colorado River in Grand Canyon, Arizona: Journal of Geology, v. 98, p. 709–724.

Schmidt, J.C., and Graf, J.B., 1987, Aggradation and degradation of alluvial sand deposits, 1965 to 1986, Colorado River, Grand Canyon National Park, Arizona: U.S. Geological Survey Open-File Report 87–555, 120 p.

Schmidt, J.C., and Graf, J.B., 1990, Aggradation and degradation of alluvial sand deposits, 1965 to 1986, Colorado River, Grand Canyon National Park, Arizona: U.S. Geological Survey Professional Paper 1493, 74 p.

Schmidt, J.C., and Rubin, D.M., 1995, Regulated streamflow, fine-grained deposits, and effective discharge in canyons with abundant debris fans, *in* Costa, J.E., Miller, A.J., Potter, K.W., and Wilcock, P.R., eds., Natural and anthropogenic influences in fluvial geomorphology: American Geophysical Union Geophysical Monograph 89, p. 177–195.

Schmidt, J.C., Topping, D.J., Grams, P.E., and Hazel, J.E., 2004, System-wide changes in the distribution of fine sediment in the Colorado River corridor between Glen Canyon Dam and Bright Angel Creek, Arizona: Logan, Utah State University, Department of Aquatic, Watershed, and Earth Resources report, 107 p.

Schmidt, J.C., and Wilcock, P.R., 2008, Metrics for assessing the downstream effects of dams: Water Resources Research, v. 44, W04404, doi:10.1029/2006WR005092.

Sprinkel, D.A., Chidsey, T.C., Jr., and Anderson, P.B., eds., 2003, Geology of Utah's parks and monuments (2d ed.): Utah Geological Association Publication 28, 562 p.

Spurr, K., and Collette, J.H., 2007, Condition assessment and significance evaluation for cultural resources between Glen Canyon Dam and Paria Riffle, Glen Canyon National Recreation Area, Arizona: Navajo Nation Archaeology Department Report No. 05–123, submitted to Bureau of Reclamation, Upper Colorado Region, Salt Lake City, Utah, report on file at Bureau of Reclamation.

Stout, J.E., 2004, A method for establishing the critical threshold for aeolian transport in the field: Earth Surface Processes and Landforms, v. 29, p. 87–104.

Svoray, T., Michailov, E., Cohen, A., Rokah, L., and Sturm, A., 2012, Predicting gully initiation—comparing data mining techniques, analytical hierarchy processes and the topographic threshold: Earth Surface Processes and Landforms, v. 37, p. 607–619.

Tainer, E.M., 2010, High-resolution Holocene alluvial stratigraphy at archaeological sites in eastern Grand Canyon, Arizona: Logan, Utah State University, M.S. Thesis, 165 p.

Tal, M., and Paola, C., 2010, Effects of vegetation on channel morphodynamics—results and insights from laboratory experiments: Earth Surface Processes and Landforms, v. 35, p. 1014–1028.

Tarboton, D.G., Bras, R.L., and Rodriguez-Iturbe, I., 1991, On the extraction of channel networks from digital elevation data: Hydrological Processes, v. 5, p. 81–100.

Tebebu, T.Y., Abiy, A.Z., Dahlke, H.E., Easton, Z.M., Zegeye, A.D., Tilahun, S.A., Collick, A.S., Kidnau, S., Moges, S., Dadgari, F., and Steenhuis, T.S., 2010, Surface and subsurface flow effect on permanent gully formation and upland erosion near Lake Tana in the northern highlands of Ethiopia: Hydrology and Earth System Sciences, v. 7, p. 5235–5265.

Telfer, M.W., Mills, S.C., and Mather, A.E., 2014, Extensive Quaternary aeolian deposits in the Drakensberg foothills, Rooiberge, South Africa: Geomorphology, v. 219, p. 161–175.

Thompson, K.S., and Potochnik, A.R., 2000, Development of a geomorphic model to predict erosion of pre-dam Colorado River terraces containing archeological resources: Flagstaff, Ariz., SWCA Environmental Consultants, Inc. Cultural Resources Report 99-257, 225 p., accessed May 28, 2015, at http://www.riversimulator.org/Resources/GCMRC/Cultural/Thompson2000b.pdf.

Thorne, C.R., 1990, Effects of vegetation on riverbank erosion and stability, *in* Thornes, J.B., ed., Vegetation and erosion: Chichester, U.K., John Wiley and Sons, p. 125–144.

Topping, D.J., Rubin, D.M., Grams, P.E., Griffiths, R.E., Sabol, T.A., Voichick, N., Tusso, R.B., Vanaman, K.M., and McDonald, R.R., 2010, Sediment transport during three controlled-flood experiments on the Colorado River downstream from Glen Canyon Dam, with implications for eddy-sandbar deposition in Grand Canyon National Park: U.S. Geological Survey Open-File Report 2010–1128, 111 p., http://pubs.usgs.gov/of/2010/1128/.

Topping, D.J., Rubin, D.M., Schmidt, J.C., Hazel, J.E., Jr., Wright, S.A., Kaplinski, M., Draut, A.E., and Breedlove, M.J., 2006, Comparison of sediment-transport and bar-response results from the 1996 and 2004 controlled-flood experiments on the Colorado River in Grand Canyon: Proceedings of the 8th Federal Interagency Sediment Conference, Reno, Nevada, April 2006, ISBN 0-9779007-1-1.

Topping, D.J., Rubin, D.M., and Vierra, L.E. Jr., 2000, Colorado River sediment transport 1—natural sediment supply limitation and the influence of Glen Canyon Dam: Water Resources Research, v. 36, p. 515–542.

Topping, D.J., Schmidt, J.C., and Vierra, L.E., Jr., 2003, Computation and analysis of the instantaneous-discharge record for the Colorado River at Lees Ferry, Arizona—May 8, 1921, through September 30, 2000: U.S. Geological Survey Professional Paper 1677, 118 p.

Turnbull, L., Wilcox, B.P., Belnap, J., Ravi, S., D'Odorico, P., Childers, D., Gwenzi, W., Okin, G., Wainwright, J., Caylor, K.K., and Sankey, J., 2012, Understanding the role of ecohydrological feedbacks in ecosystem state change in drylands: Ecohydrology, v. 5, p. 174–183.

Turner, R.M., and Karpiscak, M.M., 1980, Recent vegetation changes along the Colorado River between Glen Canyon Dam and Lake Mead, Arizona: U.S. Geological Survey Professional Paper 1132, 125 p.

U.S. Geological Survey, 2015, Stream-gaging station 09402500 (Colorado River near Grand Canyon, Arizona): National Water Information System (NWIS), accessed May 18, 2015, at http://nwis.waterdata.usgs.gov/az/nwis/peak?site_no=09402500&agency_cd=USGS&format=html..

Wainwright, J., Turnbull, L., Ibrahim, T.G., Lexartza-Artza, I., Thornton, S.F., and Brazier, R.E., 2011, Linking environmental regimes, space and time—interpretations of structural and functional connectivity: Geomorphology, v. 126, p. 387–404.

Webb, R.H., Leake, S.A., and Turner, R.M., 2007, The ribbon of green—change in riparian vegetation in the southwestern United States: Tucson, University of Arizona Press, 403 p.

Webb, R.H., Melis, T.S., and Griffiths, P.G., 2003, Debris flows and the Colorado River, *in* Beus, S.S., and Morales, M., Grand Canyon Geology (2d ed.): New York, Oxford University Press, p. 371–390.

Webb, R.H., Schmidt, J.C., Marzolf, G.R., and Valdez, R.A., eds., 1999, The controlled flood in Grand Canyon: Washington, D.C., American Geophysical Union Geophysical Monograph 110, 367 p.

West, T.R., 1995, Geology applied to engineering: Prentice Hall, New Jersey, 541 p.

Williams, G.P., and Wolman, M.G., 1984, Effects of dams and reservoirs on surface-water hydrology; changes in rivers downstream from dams: U.S. Geological Survey Professional Paper 1286, 83 p.

Wilson, R.F., 1965, Triassic and Jurassic strata of southwestern Utah, *in* Goode, H.D., and Robison, R.A., eds., Geology and resources of south-central Utah—resources for power: Utah Geological Society Guidebook, v. 19, p. 88–90.

Wright, S.A., and Kaplinski, M., 2011, Flow structures and sandbar dynamics in a canyon river during a controlled flood, Colorado River, Arizona: Journal of Geophysical Research—Earth Surface, v. 116, F01019, doi:10.1029/2009JF001442.

Wright, S.A., Melis, T.S., Topping, D.J., and Rubin, D.M., 2005, Influence of Glen Canyon Dam operations on downstream sand resources of the Colorado River in Grand Canyon, *in* Gloss, S.P., Lovich, J.E., and Melis, T.S., eds., The state of the Colorado River ecosystem in Grand Canyon: U.S. Geological Survey, Circular 1282, p. 17–31, http://pubs.usgs.gov/circ/1282/.

Wright, S.A., Schmidt, J.C., Melis, T.S., Topping, D.J., and Rubin, D.M., 2008, Is there enough sand? Evaluating the fate of Grand Canyon sandbars: GSA Today, v. 18, no. 8, p. 4–10, doi: 10.1130/GSATG12A.1.

Wulf, L., and Moss, J., 2004, Archeological site monitoring and management along the Colorado River corridor below Glen Canyon Dam: National Park Service FY2004 Annual Monitoring Report, 120 p.

Xu, J., Yang, J., and Yan, Y., 2006, Erosion and sediment yields as influenced by coupled eolian and fluvial processes—the Yellow River, China: Geomorphology, v. 73, p. 1–15.

Yanites, B.J., Webb, R.H., Griffiths, P.G., and Magirl, C.S., 2006, Debris-flow deposition and reworking by the Colorado River in Grand Canyon, Arizona: Water Resources Research, v. 42, W11411, doi:10.1029/2005WR004847.

Yeatts, M., 1996, High elevation sand deposition and retention from the 1996 spike flow—An assessment for cultural resources stabilization, *in* Balsom, J.R., and Larralde, S., eds., Mitigation and monitoring of cultural resources in response to the experimental habitat building flow in Glen and Grand Canyons, Spring 1996: Flagstaff, Ariz., Report to Bureau of Reclamation and U.S. Geological Survey Grand Canyon Monitoring and Research Center, p. 124–158.

Zhang, Z., Dong, Z., Zhao, A., Yuan, W., and Han, L., 2008, The effect of restored microbiotic crusts on erosion of soil from a desert area in China: Journal of Arid Environments, v. 72, p. 710–721.

Zhu, T.X., 2012, Gully and tunnel erosion in the hilly Loess Plateau region, China: Geomorphology, v. 153–154, p. 144–155.

Appendix

Appendix. Classification of 358 river-corridor archaeological sites in Grand Canyon National Park with respect to potential for aeolian sand supply. Sites are listed in order from upstream to downstream. Two sites (AZ:B:09:0314 and AZ:A:16:0159) were not classified for time intervals when recent high flows potentially could have inundated the site area, according to the modeled flood shorelines of Magirl and others (2008), but for which sand deposition could not be confirmed; those two sites are beneath bedrock overhangs and so are not visible in aerial imagery.

Site number	1973	1984–85	1996	2012–14
C:02:0098	3	1	3	3
C:02:0097	3	1	3	3
C:02:0094	3	1	3	3
C:02:0092	3	3	3	3
C:02:0096	3	1	1	3
C:02:0101	3	1	3	3
C:06:0003-1	2b	2b	2b	2b
C:06:0003-2	1	1	1	1
C:06:0002	5	5	5	5
C:06:0005	5	5	5	5
C:06:0008	5	5	5	5
C:06:0010	5	5	5	5
C:06:0004	5	5	5	5
C:05:0005	5	5	5	5
C:05:0031	1	1	1	1
C:05:0004	3	1	2b	2b
C:05:0033	5	5	5	5
C:05:0037	1	1	2a	2a
C:05:0009	5	5	5	5
C:05:0039	5	5	5	5
C:09:0065	5	5	5	5
C:09:0064	2b	2b	3	2b
C:09:0004	5	5	5	5
C:09:0005	5	5	5	5
C:09:0088	1	1	3	3
C:09:0034	2c	3	3	3
C:09:0083	2c	3	3	3
C:09:0032	5	5	5	5
C:09:0030	5	5	5	5
C:09:0030	2c	2c	2c	2c
C:09:0031	2c	2c	2c	2c
Unassigned	2a	2a	2a	2a
C:09:0068	2a	2a	2a	2a
C:09:0056	5	5	5	5
C:09:0058	5	5	5	5
C:09:0085	5	5	5	5
C:09:0050	4	4	4	4
C:09:0053	1	3	3	3
C:09:0033	4	4	4	4
C:09:0069	2a	3	3	3
C:09:0062	2b	3	3	3
C:09:0080	5	5	5	5
C:09:0186	5	5	5	5
C:09:0059	2a	2a	3	3
C:09:0061	2a	2a	3	3
C:09:0051	2a	2a	3	3
C:09:0082	2a	2a	3	3
C:09:0060	5	5	5	5
C:09:0184	5	5	5	5
C:09:0188	5	5	5	5
C:09:0189	5	5	5	5
C:09:0187	5	5	5	5
C:09:0001	5	5	5	5
C:09:0052	2a	2a	3	3
C:09:0071	2a	2a	2a	2a
C:09:0185	1	1	1	1
C:09:0072	2a	2a	2a	2a
C:09:0073	2a	2a	2a	2a

Appendix.—Continued

Site number	1973	1984–85	1996	2012–14
C:09:0054	2c	2c	2c	2c
C:09:0070	5	5	5	5
C:09:0075	5	5	5	5
C:09:0074	5	5	5	5
C:09:0076	5	5	5	5
C:09:0067	5	5	5	5
C:09:0084	2a	2a	3	3
C:13:0368	2c	2c	2c	2c
C:13:0370	4	4	4	4
C:13:0372	4	4	4	4
C:13:0365	2b	2b	2b	2c
C:13:0329	1	1	3	3
C:13:0331	5	5	5	5
C:13:0006	2b	2b	2b	2b
C:13:0353	1	1	3	2c
C:13:0374	2c	3	3	3
C:13:0376	5	5	5	5
C:13:0380	5	5	5	5
C:13:0371	1	1	1	1
C:13:0375	5	5	5	5
C:13:0360	5	5	5	5
C:13:0003	1	1	2a	2a
C:13:0486	5	5	5	5
C:13:0033	5	5	5	5
C:13:0007	2c	2c	2a	2a
C:13:0384	2c	2c	2a	2a
C:13:0355	4	4	4	4
C:13:0098	4	4	4	4
C:13:0099	1	4	4	4
C:13:0100	1	4	4	4
C:13:0101	1	4	4	4
C:13:0272	1	4	4	4
C:13:0334	4	4	4	4
C:13:0336	1	4	4	4
C:13:0332	4	4	4	4
C:13:0337	4	4	4	4
C:13:0335	4	4	4	4
C:13:0373	4	4	4	4
C:13:0333	4	4	4	4
C:13:0274	5	5	5	5
C:13:0273	4	4	4	4
C:13:0339	4	4	4	4
C:13:0341	2b	2b	2c	2c
C:13:0323	1	1	2a	2a
C:13:0324	1	1	2a	2a
C:13:0340	2a	2a	2a	2a
C:13:0327	2a	2a	2a	2a
C:13:0008	2a	2a	2a	2a
C:13:0338	2a	2a	2a	2a
C:13:0009-1	2b	2b	2b	2b
C:13:0009-2	1	1	1	1
C:13:0321	1	1	1	1
C:13:0092	3	3	3	3
C:13:0325	4	4	4	4
C:13:0342	1	2a	3	3
C:13:0344	1	2a	3	3
C:13:0346	1	2a	3	3
C:13:0348	1	2a	3	3
C:13:0350	1	2a	3	3
C:13:0352	1	2a	3	3
C:13:0349	1	2a	3	3
C:13:0345	2a	2a	3	3

Appendix.—Continued

Site number	1973	1984–85	1996	2012–14
C:13:0351	2a	2a	3	3
C:13:0343	4	4	4	4
C:13:0347	1	3	3	3
C:13:0069	1	2a	2a	2a
C:13:0322	5	5	5	5
C:13:0364	1	3	3	3
C:13:0010	1	1	1	1
C:13:0291	1	1	3	3
C:13:0776	5	5	5	5
C:13:0001	5	5	5	5
C:13:0787	4	4	4	4
C:13:0377	4	4	4	4
C:13:0786	4	4	4	4
C:13:0788	3	3	3	3
C:13:0790	3	3	3	3
C:13:0779	1	1	3	3
C:13:0780	1	1	2b	2b
C:13:0379	1	1	2b	2b
C:13:0070	1	1	3	3
C:13:0385	1	1	1	3
C:13:0386	1	1	2b	2c
C:13:0387	1	1	1	2a
C:13:0354	5	5	5	5
C:13:0359	1	2b	3	2c
C:13:0381	2b	2b	2b	2b
C:13:0361	5	5	5	5
C:13:0389	1	1	1	1
C:13:0390	1	1	1	1
C:13:0391	2b	2b	2b	2b
C:13:0363	1	3	3	3
C:13:0382	5	5	5	5
C:13:0383	5	5	5	5
C:13:0005	2b	2b	3	3
C:13:0392	2b	2b	3	3
C:13:0393	1	1	3	3
B:16:0001	2a	2a	2a	2a
B:16:0257	5	5	5	5
B:16:0365	5	5	5	5
B:16:0364	2b	2b	2b	2c
B:16:0258	5	5	5	5
B:16:0259	1	1	3	3
B:16:0170	5	5	5	5
B:16:0911	2b	2b	2b	2b
B:16:0261	1	1	3	2a
B:16:0003	5	5	5	5
B:15:0096	5	5	5	5
B:15:0124	5	5	5	5
B:15:0128	2b	2b	2b	2b
B:15:0097	5	5	5	5
B:15:0001	1	1	1	1
B:15:0139	3	3	3	3
B:15:0132	4	4	4	4
B:15:0133	5	5	5	5
B:15:0134	5	5	5	5
B:15:0125	5	5	5	5
B:15:0118	5	5	5	5
B:15:0119	5	5	5	5
B:15:0073	5	5	5	5
B:15:0123	5	5	5	5
B:15:0143	5	5	5	5
B:15:0126	1	1	3	3
B:15:0138	1	1	1	1

Appendix.—Continued

Site number	1973	1984–85	1996	2012–14
B:15:0127	2b	2b	2b	2b
B:15:0135	2b	2b	2b	2c
B:14:0107	2b	1	2b	2c
B:14:0105	1	1	1	2a
B:14:0093	1	1	1	1
B:14:0094	1	1	1	1
B:14:0095	1	1	1	1
B:14:0108	1	1	1	1
B:10:0261	1	1	1	1
B:10:0263	1	1	1	1
B:10:0260	2b	2b	2b	2b
B:10:0253	4	4	4	4
B:10:0111	2b	2b	2b	2b
B:10:0224	1	1	1	1
B:10:0225	1	1	1	1
B:11:0280	2b	2b	2b	2b
B:11:0283	5	5	5	5
B:11:0273	5	5	5	5
B:11:0279	2b	2b	2b	2b
B:11:0284	5	5	5	5
B:11:0278	3	3	2b	2b
B:11:0282	1	1	1	1
B:11:0272	2b	2b	2c	2c
B:11:0359	5	5	5	5
B:11:0276	2b	2b	2c	2c
B:11:0277	1	1	2b	2b
B:11:0281	1	1	2b	2b
B:11:0275	2b	2b	2b	2b
B:11:0271	2b	2b	2b	2b
B:11:0002	5	5	5	5
B:10:0004	2b	2b	3	3
B:10:0252	2b	2b	2b	2b
B:10:0229	5	5	5	5
B:10:0231	5	5	5	5
B:10:0001	4	4	4	4
B:10:0250	5	5	5	5
B:10:0226	1	2a	2a	2a
B:10:0237	1	1	1	1
B:10:0238	1	1	1	1
B:10:0121	1	1	1	1
B:10:0249	3	3	3	3
B:10:0264	1	1	1	1
B:10:0227	5	5	5	5
B:10:0266	5	5	5	5
B:10:0228	5	5	5	5
B:10:0223	5	5	5	5
B:09:0316	1	1	1	1
B:09:0314	N/A	4	4	4
B:09:0317	2b	1	2b	2b
B:13:0001	2b	2b	2b	2b
B:13:0002	3	3	4	4
A:16:0160	2c	2a	2c	3
A:16:0168	5	5	5	5
A:16:0223	4	4	4	4
A:16:0149	2b	2b	3	3
A:16:0153	1	1	3	3
A:16:0150	3	2c	3	3
A:16:0162	2a	2a	2a	3
A:16:0154	1	2a	2a	2a
A:16:0151	2b	2b	3	2c
A:16:0163	2b	2c	2c	2c
A:16:0157	4	4	4	4

Appendix.—Continued

Site number	1973	1984–85	1996	2012–14
A:16:0180	2a	2a	3	3
A:16:0173	2a	2a	2a	2a
A:16:0167	3	2c	3	3
A:16:0158	1	1	1	2a
A:16:0174	1	1	1	3
A:16:0161	1	1	2a	2a
A:16:0148	1	1	3	3
A:16:0164	2b	2b	3	2c
A:16:0155	2a	2a	3	3
A:16:0001	1	3	1	3
A:16:0159	N/A	N/A	4	4
A:16:0003	2b	2b	2b	2b
A:16:0177	5	5	5	5
A:16:0184	2a	2a	2a	2a
A:16:0165	4	4	4	4
A:16:0004	2b	2b	2b	2b
A:16:0176	2a	2a	2a	2a
A:16:0169	2b	2b	2b	2b
A:16:0175	2a	2a	2c	3
A:16:0185	2b	2b	2c	3
A:16:0171	2b	2b	3	3
A:15:0026	2c	2b	3	3
A:15:0022	2a	2a	3	3
A:15:0044	3	2a	3	2a
A:15:0035	2a	2a	2a	2a
A:15:0031	2a	2a	2a	2a
A:15:0020	1	1	2b	2b
A:15:0019	5	5	5	5
A:15:0023	5	5	5	5
A:15:0018	3	3	3	3
A:15:0003	1	1	2b	2b
A:15:0027	2a	2a	3	3
A:15:0021	1	2c	2c	3
A:15:0024	2c	2c	2c	3
A:15:0028	2c	2c	2c	3
A:15:0032	2a	2a	2a	2a
A:15:0025	5	5	5	5
A:15:0034	5	5	5	5
A:15:0048	2c	2c	2c	2c
A:15:0052	5	5	5	5
A:15:0056	5	5	5	5
A:15:0036	1	1	2a	3
A:15:0040	2a	2a	2a	3
A:15:0005	2b	2b	2b	2c
A:15:0029	2a	2a	2a	3
A:15:0033	1	1	1	3
A:15:0039	2c	2c	2c	3
A:15:0037	2a	2a	2a	2a
A:15:0043	2a	2a	2a	2a
A:15:0001	2c	2c	2c	2c
A:15:0042	2a	2a	2a	2a
A:15:0038	2a	2a	2a	3
A:15:0055	5	5	5	5
A:15:0047	1	1	1	1
A:15:0051	2c	2c	2c	2c
A:15:0004	2a	2a	2a	2a
G:03:0056	1	1	2a	2a
G:03:0038	1	1	1	2a
G:03:0042	5	5	5	5
G:03:0004	3	3	3	3
G:03:0037	4	4	4	4
G:03:0046	1	2a	3	2a

Appendix.—Continued

Site number	1973	1984–85	1996	2012–14
G:03:0060	2a	2a	2a	2a
G:03:0040	2a	2a	2a	3
G:03:0064	2a	2a	3	3
G:03:0041	2b	2b	3	3
G:03:0071	3	2a	3	3
G:03:0002	2b	2b	3	2c
G:03:0024	2b	2b	3	2c
G:03:0081	2b	2b	3	3
G:03:0025	2b	2b	3	2c
G:03:0028	2b	2b	3	2c
G:03:0026	2b	2b	3	2c
G:03:0003	1	1	3	2a
G:03:0043	1	1	3	3
G:03:0055	1	1	1	1
G:03:0059	1	1	1	1
G:03:0063	1	1	1	1
G:03:0034	1	1	2b	3
G:03:0076	1	1	1	3
G:03:0032	2b	2b	2b	2c
G:03:0044	1	1	1	2a
G:03:0020-1	2b	1	2b	2b
G:03:0020-2	2b	2b	2b	2b
G:03:0030	1	1	1	3
G:03:0045	3	3	3	3
G:03:0049	1	2a	2a	2a
G:03:0029	3	2b	3	2b
G:03:0036	3	2a	2a	2a
G:03:0053	3	3	3	3
G:03:0073	2b	2b	3	3
G:03:0052	2b	2b	3	3
G:03:0066	1	1	1	1
G:03:0077	5	5	5	5
G:03:0082	5	5	5	5
G:03:0057	5	5	5	5
G:03:0061	3	3	3	3
G:03:0065	5	5	5	5
G:03:0048	5	5	5	5
G:03:0006	1	1	1	2a
G:03:0067	1	2b	2b	2c
G:03:0083	5	5	5	5
G:03:0058	1	1	2a	3
G:03:0062	5	5	5	5
G:03:0080	2b	2b	2b	2b
G:03:0054	1	1	1	2c
G:03:0085	3	3	3	3
G:03:0023	2b	2b	2b	2b
G:03:0072	1	1	1	1
G:02:0102	2b	2b	2b	2b
G:02:0101	5	5	5	5
G:02:0106	3	3	3	3
G:02:0100	1	1	1	1
G:02:0105	5	5	5	5

Menlo Park Publishing Service Center
Manuscript approved for publication March 29, 2016
Edited by Katherine Jacques
Cartography and graphics by Jeanne DiLeo and Jacqueline Olson
Layout by Cory D. Hurd

ISSN 2330-7102 (online)
http://dx.doi.org/10.3133/pp1825